



EeFarm II

Description, testing and application

J.T.G. Pierik
(ECN Wind Energy)

U. Axelsson
E. Eriksson
D. Salomonsson
(Vattenfall)

ECN-E--09-051

Abstract: In this project, a user friendly computer program, EeFarm-II, for wind farm electrical and economic evaluation has been developed. EeFarm-II has been built as a Simulink Library in the graphical interface of Matlab-Simulink. The EeFarm-II Library consists of wind farm component models, such as models of wind turbines, generators, transformers, AC cables, inductors, nodes, splitters, PWM converters, thyristor converters, DC cables, choppers and Statcoms.

Each EeFarm-II component model calculates the output voltage and current phasor (AC) or voltage and current value (DC) based on the input voltage and current and the component parameters. This is repeated for the complete operation range of the wind farm, i.e. the range of input wind speed. Secondly, the total price of the electrical system (if wind turbine prices are not included) or of the wind farm (if wind turbine prices are included) is determined. Based on the output power for each wind speed bin and the wind speed distribution, the annual produced energy is determined. The final step is the calculation of the Levelised Production Costs (LPC).

After EeFarm-II testing at ECN, the program has been made available to Vattenfall for testing and application.

EeFarm-II has also been used to re-evaluate the thirteen electrical systems of the Erao-1 study of 2001.

Keywords: offshore wind farm electrical systems, offshore wind farm design, offshore wind farm economics.

Acknowledgement

The EeFarm-II project has been financially supported by the BSIK Program, executed by the we@sea consortium, by Vattenfall and by the ECN Programmafinanciering of the Ministry of Economic Affairs of the Netherlands.

The original EeFarm program was developed by ECN and TU Delft (Michiel Damen and Paul Bauer). The GCL model used in section 2.2 was developed by Gunnar Larson (Risoe National Laboratory). The Hagg model used in section 2.3 was developed by Frank Hagg (Stork SPE).

We@sea project number: 2007-010
Project title: EeFarm-II
Project coordinator: ECN
Project partners: Vattenfall
Period: 1 januari 2008 - 31 may 2009
ECN project number: 7.9514

Contents

1	Introduction	9
1.1	Wind farm layout and electrical system optimization	10
2	Wind farm wake effects on wind farm power	11
2.1	FyndFarm and Fluxfarm	11
2.2	GCL wind farm wake model	11
2.2.1	GCL model results	13
2.2.2	GCL model implementation in EeFarm 2	14
2.3	Hagg model	19
3	EeFarm II description	21
3.1	Turbine models	24
3.1.1	P(V) curve, FluxFarm or FyndFarm input	24
3.1.2	Compounded turbine model	24
3.1.3	Turbine internal curve	25
3.1.4	Turbine WF eff	25
3.1.5	VSP turbine	25
3.2	Generator models	26
3.2.1	Generic generator model	26
3.2.2	Constant speed induction machine	27
3.2.3	DFIG	29
3.2.4	FCIM	34
3.2.5	FCSM	37
3.3	AC cable models	41
3.3.1	Constant temperature AC cable model	41
3.3.2	AC cable model with temperature dependent resistance	42
3.4	Transformer model	43
3.4.1	Transformer without reactive power consumption	43
3.4.2	Transformer with reactive power consumption	44
3.5	Inductor model	47
3.6	AC and DC node model	48
3.7	DC cable model	50
3.8	Diode and thyristor rectifier, inverter and back-to-back converter models	52
3.8.1	Diode rectifier and thyristor rectifier	52
3.8.2	Thyristor inverter	57
3.8.3	Thyristor back-to-back converter	59
3.9	PWM rectifier, inverter and back-to-back converter models	59
3.9.1	PWM rectifier (Infineon)	59
3.9.2	PWM inverter (Infineon)	62
3.9.3	PWM rectifier (Kazmierkowski)	64
3.9.4	PWM inverter model (Kazmierkowski)	69
3.9.5	PWM back-to-back converter (Kazmierkowski)	72
3.9.6	PWM rectifier (TUD)	72

3.9.7	PWM inverter (TUD)	76
3.10	Statcom	78
3.11	Step-up chopper	79
4	Availability	83
5	Power performance and Economic calculation	87
5.1	Annual energy production	87
5.2	Economic calculation	88
6	EeFarm-II parameter database	91
6.1	Component parameter list	91
6.2	Database implementation	93
7	Component model testing	95
7.1	Turbine models	96
7.2	Generator models	98
7.2.1	Generic Generator	98
7.2.2	Constant speed induction machine	99
7.2.3	DFIG	100
7.2.4	FCIM	101
7.2.5	FCSM	103
7.3	AC cable models	105
7.4	Transformer model	106
7.5	Inductor model	107
7.6	TUD-PWM rectifier, inverter and DC cable model	108
7.7	Kaz-PWM rectifier and inverter model	112
7.8	Inf-PWM rectifier and inverter model	114
7.9	Thyristor rectifier and inverter model	115
7.10	Statcom	117
7.11	Step-up chopper	118
8	EeFarm-II application to Erao-1 system evaluation	119
8.1	System description	119
8.2	Results	122
9	Conclusions	127
A	Vattenfall EeFarm-II validation and application to Lillgrund case	131
B	Wind farm wake program input for EeFarm II	154
C	EeFarm II questions and answers	157
D	Electrical modelling aspects	159
D.1	Conventions	159
D.2	Reactive power of shore cable	161

D.3	Effect of temperature on cable resistance	164
E	EeFarm 1 database	167
E.1	Transformer data	167
E.2	PWM converter data	168
E.3	THY converter data	169
E.4	AC cable data	171
E.5	DC cable data	171
F	Differences between the EeFarm and EeFarm-II program	173
G	Summary Erao 1 (EeFarm model version 1)	175

EXECUTIVE SUMMARY

INTRODUCTION

In 2001, ECN and TU Delft have developed the EeFarm programme for the electrical and economic evaluation of different electrical layouts and concepts for Offshore Wind Farms [17]. EeFarm calculates the voltages, currents, powers, reactive powers and electric losses for each node of a given wind farm and for each wind speed and wind direction. It uses these to determine the annually produced energy and the costs per generated MWh. Since voltages and currents are calculated for each component in the wind farm and for each wind speed and wind direction bin, an accurate calculation of electrical performance of the farm is possible. The programme can be used to make an estimate of the production cost of a proposed wind farm and to study the effect of different electrical system layouts and concepts on these production costs.

The version of EeFarm made in 2001 consists of a number of Matlab routines, one or more for each type of electrical component. For each wind farm concept, a wind farm layout dependent program has to be written by the user that calls the component routines. Matlab command lines have to be programmed for each individual component, the in- and output signals have to be connected in the correct way and the correct component parameters have to be loaded. The creation or modification of the calling program has to be repeated each time the wind farm layout or components are changed. This is a time consuming process and a cause of errors. The major drawback of the 2001 version of EeFarm is its user-unfriendly-ness.

To solve this problem, the EeFarm II project was defined as part of the we@sea consortium.

OBJECTIVE

The main objective of the *EeFarm-II* project is to develop a user friendly version of the EeFarm program. The second objective of the project is to demonstrate and evaluate the program in two case studies: one for the thirteen Erao-1 electrical systems and a second one for the Lillgrund wind farm.

METHOD

For electrical and economic calculations for wind farms a computer program based on a component model library and a database with component parameters is very useful. The component models and database have been developed in a previous project (Erao-1), but it is very user-unfriendly. In the *EeFarm-II* project the component model library will be reprogrammed to make it easy to use and the database will be updated. The original EeFarm consisted of a number of Matlab routines. The new EeFarm consists of a set of component models in a Simulink Library. Each component model has a single input and a single output, which consists of same set of variables for each AC component or each DC component. This makes building and modifying of a wind farm model very easy.

The EeFarm program calculates the voltages and currents at the output of each component in the wind farm. Since the wind turbine power and the grid voltage are known, an exact calculation would either require iteration or linearisation and solution of a set of linear equations. Since wind farm models are large, i.e. consist of many often nonlinear equations, a method has to be chosen which limits computer time. Since the objective is to include DC components, such as PWM converters and DC cables, in the wind farm electrical system, this further complicates an exact solution of the load flow. Therefore, an approximate calculation was chosen without iteration. Since the voltage drops and voltage angle shifts in a wind farm are expected to be relatively small, this does not have a big effect on the produced electrical energy.

EEFARM-II MODEL DEVELOPMENT RESULTS

The following new wind farm component models have been developed:

1. two simple wind farm wake implementations, which can be used if no input from a wind farm wake program is available;
2. generator models for a constant speed induction machine, a doubly fed induction machine, a full converter induction machine and a full converter synchronous machine;
3. a transformer model which includes reactive power consumption;
4. AC and DC node and splitter models;
5. two PWM converter models, based on literature by Kazmierkowski and Infineon;

-
6. a statcom model;
 7. a reactive power controller, which enables a desired reactive power value at the point of connection of the wind farm to the grid.

A second improvement is the introduction of an availability block to calculate the effect of component failure and maintenance on wind farm energy production.

The EeFarm database was reprogrammed and filled with 2009 component data.

EEFARM-II VERIFICATION AND TESTING RESULTS

EeFarm-II was verified and tested in two steps. First a component test program was made for each component in the library. Secondly, the EeFarm-II component library was independently verified and tested by Vattenfall. Both steps resulted in the correction of a number of errors and some modifications to improve the program.

EEFARM-II CASE STUDY RESULTS

Two case studies have been performed. In the first case, the thirteen Erao-1 electrical systems are re-evaluated with EeFarm-II and the updated database. Since 2001 prices and performance of some of the components have changed. A wind farm size of 200 MW has been chosen and a distance to shore of 100 km. In the Erao-1 study (with two system sizes, 100 and 500 MW and two distances to shore, 20 and 60 km), the AC connected systems are the most cost effective (lowest LPC). In the present study, the difference in LPC between the AC connected systems and the Park Variable (PV) DC connected systems is too small to be significant. This can partly be explained by the longer distance to shore. The investment costs of the AC and PV-DC systems are about the same, due to the high AC cable costs. The losses in the PV-DC systems are a bit higher than in the AC case.

In the second case study two electrical systems for the Lillgrund wind farm have been evaluated, an AC and a DC system.

CONCLUSIONS

A versatile library of electrical component models for steady state and economic evaluations of offshore wind farm is now fully operational. Full control can be exerted over all modeling aspects: nothing is hidden behind a user interface. The models have proven their usefulness in designing and evaluating wind farm electrical systems.

LIST OF DELIVERABLES

The deliverables of the EeFarm-II project are:

1. the EeFarm-II program consisting of a component model library and the pre- and post-processor files;
2. the component database (confidential);
3. a detailed report describing the EeFarm-II program, the component models and the case study results;
4. a journal paper.

COMPARING PROJECT RESULTS TO PROJECT OBJECTIVES:

All project objectives have been met. All project tasks have been completed:

- Determination of method and program language;
- Model conversion;
- Development of missing component models;
- Implementation of location dependent turbine data;
- Database update and extension;
- Demonstration of EeFarm-II for a number of wind farm lay-outs;

- Delivery of EeFarm-II to Vattenfall
- Preparation of final report;
- Journal paper (optional);

CONTEXT OF THE PROJECT

This project is a continuation of the model development of the Erao-projects. In the Erao-1 project steady state (load flow) models have been developed and used in combination with a component price database to estimate the contribution of the electrical system to the cost of electricity. In the Erao-2 project dynamic models for four different ITWF have been developed and demonstrated [21, 22]. A partial verification of the developed wind farm models has been executed in the Erao-3 project [19, 18, 20].

1 Introduction

In 2001, ECN and TU Delft have developed the EeFarm programme for the electrical and economic evaluation of different electrical layouts and concepts for Offshore Wind Farms [17]. EeFarm calculates the voltages, currents, powers, reactive powers and electric losses for each node of a given wind farm and for each wind speed and wind direction. It uses these to determine the annually produced energy and the costs per generated MWh. Since voltages and currents are calculated for each component in the wind farm and for each wind speed and wind direction bin, an accurate calculation of electrical performance of the farm is possible. The programme can be used to make an estimate of the production cost of a proposed wind farm and to study the effect of different electrical system layouts and concepts on these production costs.

The version of EeFarm made in 2001 consists of a number of Matlab routines, one or more for each type of electrical component. For each wind farm concept, a wind farm layout dependent program has to be written by the user that calls the component routines. Matlab command lines have to be programmed for each individual component, the in- and output signals have to be connected in the correct way and the correct component parameters have to be loaded. The creation or modification of the calling program has to be repeated each time the wind farm layout or components are changed. This is a time consuming process and a cause of errors. The major drawback of the 2001 version of EeFarm is its user-unfriendly-ness.

To solve this problem, the EeFarm II project was defined as part of the we@sea consortium. The main project objective is [16]:

Development and demonstration of a user friendly second version of the EeFarm computer program for wind farm electrical layout and optimization.

EeFarm has been re-program entirely, resulting in a user friendly, easy to use analysis and optimisation tool for wind farm developers. This was achieved by converting EeFarm to a graphically based user interface, viz. Simulink. In the process, EeFarm has been extended with missing component models and updated and improved where needed. EeFarm II has been tested and evaluated by ECN and Vattenfall. This report describes the results.

The EeFarm program incorporates the following aspects:

- wind speed (and wind direction) dependent calculation of:
 - turbine power production, including the effect of the location of the turbine in the farm (wind speed deficit in wake);
 - voltage and current phasor at each wind farm component input and output (turbine, transformer, cable, converter);
 - electric losses per component;
 - wind farm power production;
- estimation of the effect of component failure on the power production, based on component failure rates and repair time;
- a database with component electrical parameters and component costs;
- wind farm annual energy production, based on the wind speed distribution;
- wind farm production cost (Euro/kWh).

The voltages and currents will not be calculated iteratively to reduce the simulation time (one run includes hundreds of components and hundreds of wind speed and wind direction bins). The effect of this approximation on the currents, voltages and electrical losses is relatively small. The amplitude and rotation of the voltage phasor at the grid connection can be used to as a check. Under normal circumstances the maximum voltage difference the wind farm (from wind turbine to point of grid connection) is expected to be a few percent. The difference between the exact and the approximated voltage and current will be a fraction of this value. Therefore, the error in the power losses due to the non-iterative solution is expected to be less than one percent.

1.1 Wind farm layout and electrical system optimization

The EeFarm II programme can be used to investigate the effect of wind farm component choice, layout and component control on the voltages, currents, electrical losses and production costs. Aspects of an investigation can be:

- different cable routing and location of transformer platforms;
- different component types and ratings, especially the effect of different cable choices;
- reactive power control by variable speed wind turbine generators;
- settings of transformer taps;
- AC versus DC connections;
- redundancy, especially the effect of multiple cables to shore.

2 Wind farm wake effects on wind farm power

In the electrical and economic evaluation of a wind farm, the electric power of each turbine produces is an important aspect. The produced power depends on the aerodynamic power, which depends on the current wind speed, the location of the turbine and the wind direction. Wind farm wake programs calculate the wind speed and wind direction dependent power production. Examples are the FyndFarm and FluxFarm programs, developed by ECN. The wake and wind speed deficit are calculated at each turbine positions for each wind speed and wind direction bin. The turbine parameters, the turbine locations and the wind rose (wind speed and direction distribution) have to be known. The use of a detailed wind farm wake model like FyndFarm and FluxFarm is time consuming and may not always be necessary. In EeFarm-II the following options are available:

1. EeFarm-II uses FyndFarm or Fluxfarm input: the electric power for each wind speed and wind direction for each turbine in the wind farm;
2. EeFarm II uses an internal approximation:
 - the GCL model (single wake turbine wind speed deficit);
 - the Hagg model (rule of thumb approximation of the average turbine wind speed deficit);
3. EeFarm II uses the manufacturer supplied power curve for all turbines in the farm, i.e. no wind farm wake correction is applied.

2.1 FyndFarm and Fluxfarm

FyndFarm and Fluxfarm are computer programs to optimise the aerodynamic performance of wind farms [5]. Both programs generate the energy production or power per wind speed and wind direction for each turbine in the wind farm.

FyndFarm and Fluxfarm calculate a different power curve for each turbine in the farm and these curves are loaded into EeFarm II at the start of the EeFarm II run. FyndFarm and Fluxfarm use coordinates for the position of the turbines and these coordinates can be used by EeFarm II to calculate the lengths of the cables connecting the turbines and the transformer platform(s).

For a description of FyndFarm is referred to the FyndFarm User Manual [5]. FluxFarm is the successor of FyndFarm and includes a multi-wake calculation as well as a fast but simple wake estimation based on measurements.

2.2 GCL wind farm wake model

The GCL model, developed by G.C. Larsen of Risoe National Laboratory in Denmark, is described in the EWTS-II project [7]. The GCL model determines the wake deficit, the wake turbulence intensity, the wake turbulence length scale and the wake coherence decay factor of a single wind turbine. Only the wake deficit is used in EeFarm-II.

The GCL model is included in EeFarm II. In principle, it requires turbine locations and wind rose to determine the average wind speed deficit for each turbine and each wind speed and wind direction. The model is simplified by defining turbine categories: at the farm border and inside the farm and by using an average distances to wake generating turbines. This eliminates the wind rose dependency but yield only a rough approximation.

The model is based on simple engineering formulas. The wake radii at location x , at the turbine (location x_0) and at the location $9.5D$ behind the turbine are:

$$R_{wx} = \left(\frac{105}{2\pi}\right)^{0.2} c_l^{0.4} (c_{d,ax} Ax)^{0.333} \quad (1)$$

$$R_{wx_0} = \frac{D}{2} = \left(\frac{105}{2\pi}\right)^{0.2} c_l^{0.4} (c_{d,ax} Ax_0)^{0.333} \quad (2)$$

$$R_{w95} = \left(\frac{105}{2\pi}\right)^{0.2} c_l^{0.4} (c_{d,ax} A (x_0 + 9.5D))^{0.333} \quad (3)$$

R_{wx} is the wake radius at location x , with x the axial direction, D is the rotor diameter of the upstream turbine, c_l is the non-dimensional mixing length, depending on Prandtl's mixing length l , $c_{d,ax}$ is the thrust coefficient, also called axial force coefficient and A is the rotor area. The location of the turbine is x_0 .

From equation 2 and 3 x_0 and c_l can be determined:

$$x_0 = 9.5D / \left(\frac{2R_{w95}}{D}\right)^3 - 1$$

$$c_l = \sqrt{\left(\frac{D}{2}\right)^5 \frac{2\pi}{105} (c_{d,ax} A x_0)^{-1.667}}$$

The wind speed reduction due the wake equals:

$$\Delta V_x = -\frac{V_a}{9} (c_{d,ax} A x^{-2})^{0.333} [r^{1.5} (3c_l^2 c_{d,ax} A x)^{-0.5} - \left(\frac{35}{2\pi}\right)^{0.3} (3c_l^2)^{-0.2}]^2$$

V_a is the undisturbed (ambient) wind speed at hub height, r is the distance to the hub centre. To determine the wake radius R_{w95} at $9.5D$ can be used:

$$R_{wb} = \max[1.08D, 1.08D + 21.7D * (I_a - 0.05)]$$

$$R_{w95} = 0.5 * [R_{wb} + \min(H, R_{wb})]$$

R_{wb} is the boundary condition for the wake radius at location x , I_a is the ambient turbulence intensity at hub height (limited to 0.05-0.15) and H is the tower height of the upstream turbine. For a comparison of GCL model results and measurements is referred to [23].

The wind speed deficit in EeFarm-II is calculated for $r = 0$. The best estimate would require the position of all turbines with respect to each other, the wind rose and a calculation of the deficit for each turbine, wind direction and wind speed. To reduce the amount of input data required for each new wind farm layout, an average distance to the turbine that generates wake for the whole wind farm is used. The effect of the wind rose is taken into account by increasing or decreasing this average distance, depending on the orientation of the farm with respect to the main wind direction.

2.2.1 GCL model results

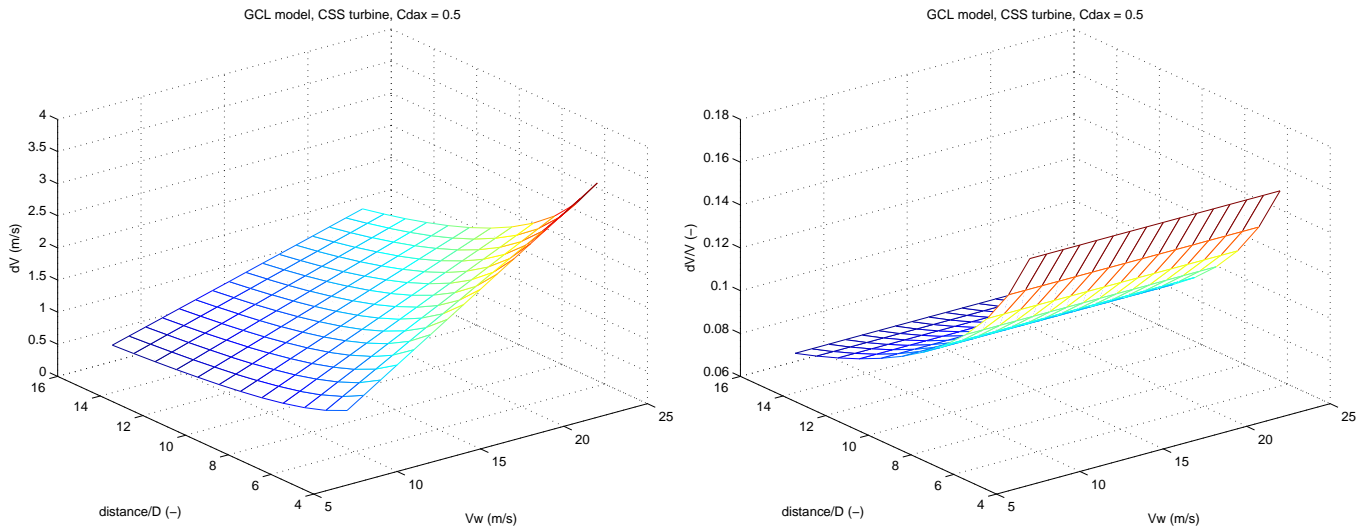


Figure 1: Absolute and relative wind speed deficit GCL model for variable wind speed and constant C_{dax} (0.5)

From the GCL model results in figure 1 can be seen that for constant thrust coefficient:

- the absolute wind speed deficit increases with decreasing distance;
- the relative wind speed deficit increases with decreasing distance;
- the absolute wind speed deficit increases with increasing wind speed;
- the relative wind speed deficit is independent of the wind speed.

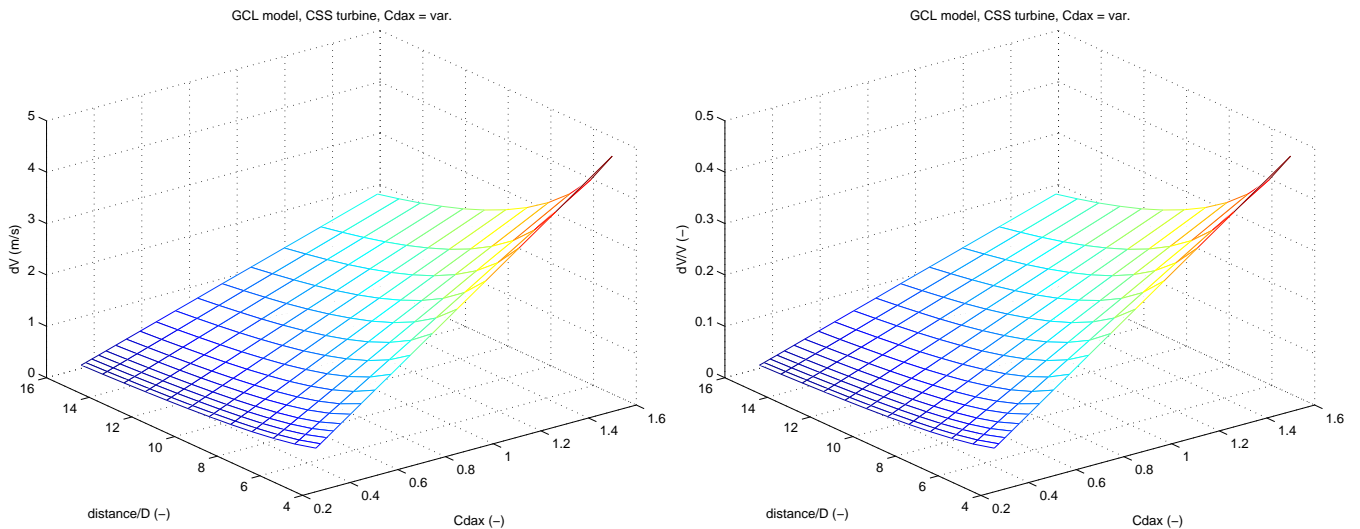


Figure 2: Relative wind speed deficit GCL model for constant wind speed (10 m/s) and variable C_{dax}

From the GCL model results in figure 2 can be seen that for constant wind speed:

- the absolute and relative wind speed deficit increases with decreasing distance;
- the absolute and relative wind speed deficit increases with increasing thrust coefficient.

2.2.2 GCL model implementation in EeFarm 2

The GCL model is implemented as a preprocessor which calculates the wind speed, distance and turbine type dependent wind speed deficit, power production and aerodynamic efficiency. The following steps are taken:

- determine the turbine type: CSP, CSS or VSP;
- calculate the wind speed deficit with the GCL model, dependent on type of turbine (R , H , C_{dax}), distance to wake generating turbine (D) and windspeed (V_w);
- calculate the aerodynamic power matrix $P_a(D, V_w)$ for undisturbed and full wake operation;
- determine the efficiency $Eff(D, V_w)$ of each type of location by averaging over wake and non wake operation;

The efficiency table is used in Simulink to determine the wind speed dependent power produced by each turbine. The $Eff(D, V_w)$ tables should be recalculated for each new turbine.

In EeFarm II the parameters per turbine are:

- the average distance to the neighbouring turbines;
- the location weight factor (based on the rings);
- $P(V)$ curve;
- wind speed and distance dependent efficiency table $Eff(D, V_w)$.

The EeFarm II implementation of the GCL model assumes:

- single wake operation;
- a symmetrical wind rose, i.e. no predominant wind directions;
- division the wind farm into concentric rings, see figure 3, in which the turbines experience the same wakes.

Figure 3 shows a FyndFarm result with rings of similar aerodynamic efficiency, a symmetrical wind rose was assumed.

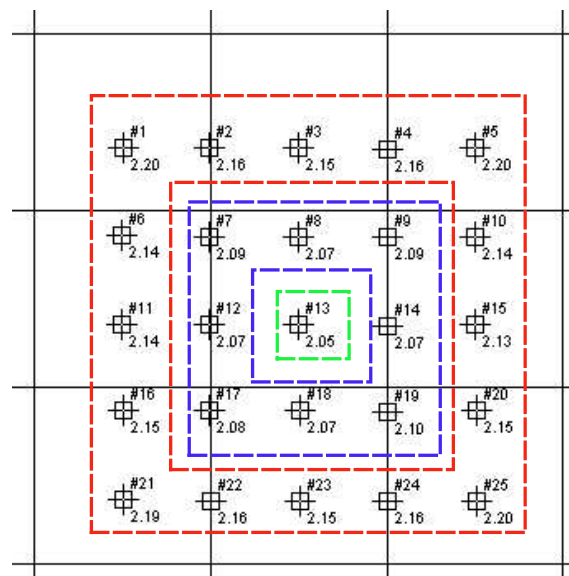


Figure 3: Fyndfarm result and rings of similar aerodynamic efficiency (symmetrical wind rose assumed)

Figure 4 shows the aerodynamic power and axial thrust coefficient of a constant speed pitch (CSP) turbine. The full wake aerodynamic efficiency for this turbine as function of the distance is plotted in figure 5. Figure 6 gives the overall aerodynamic efficiency for a 5x5 CSP wind farm, calculated by Fyndfarm and EeFarm-II. As can be expected, the overall wind farm efficiency calculated by Fyndfarm (also using the GCL model option with low accuracy option) and EeFarm-II are different.

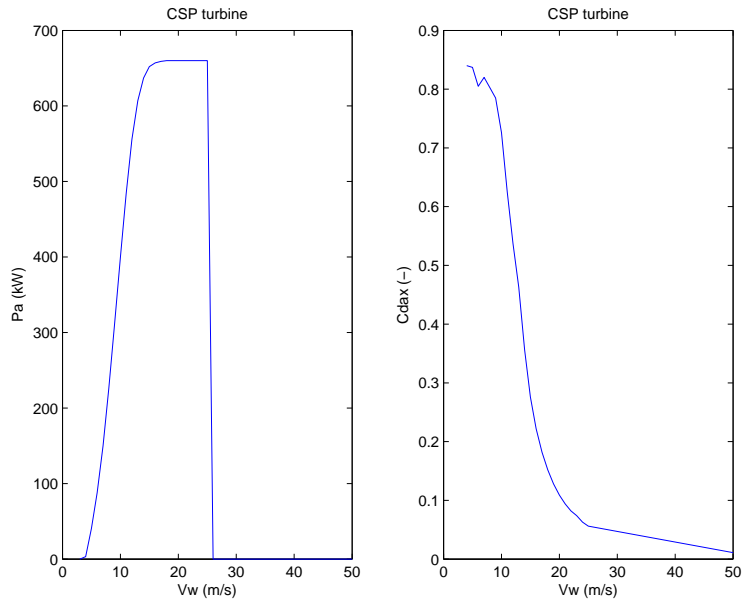


Figure 4: Aerodynamic power and axial thrust coefficient of a CSP turbine

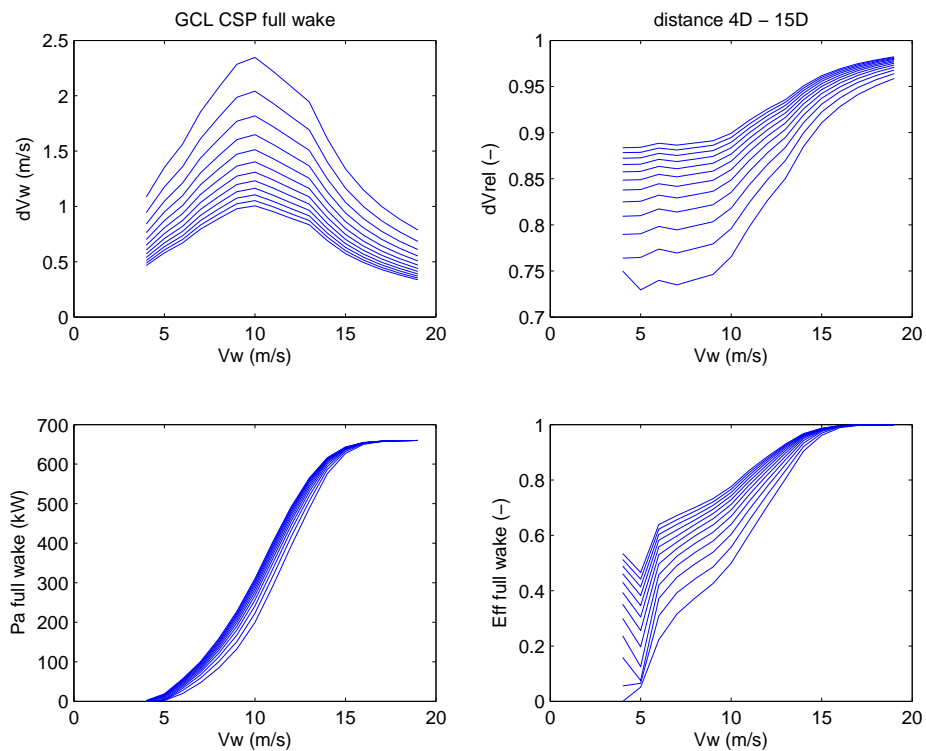


Figure 5: Turbine full wake efficiency calculated with GCL pre-processor for a CSP turbine

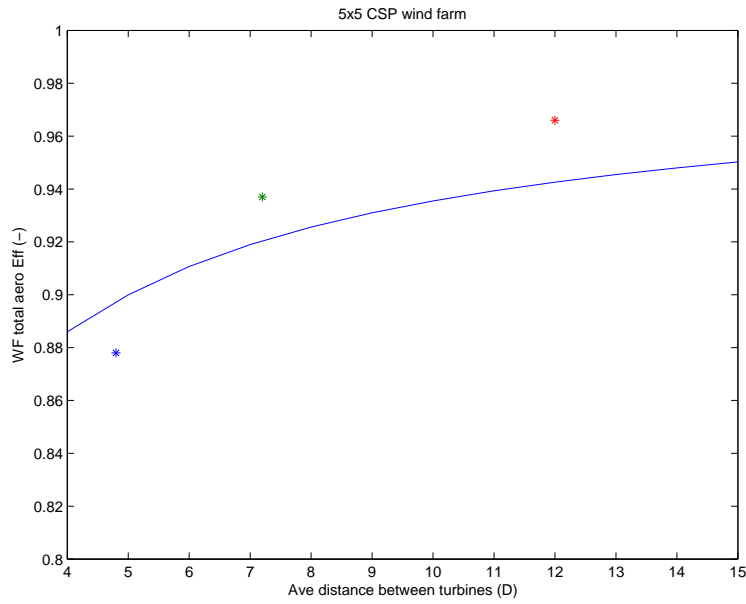


Figure 6: CSP 5x5 WF aerodynamic efficiency calculated with GCL pre-processor (-) and Fyndfarm (*)

Figure 7 shows the aerodynamic power and axial thrust coefficient of a variable speed pitch (VSP) turbine. The full wake aerodynamic efficiency for this turbine as function of the distance is plotted in figure 8. Figure 9 gives the overall aerodynamic efficiency for a 5x5 VSP wind farm.

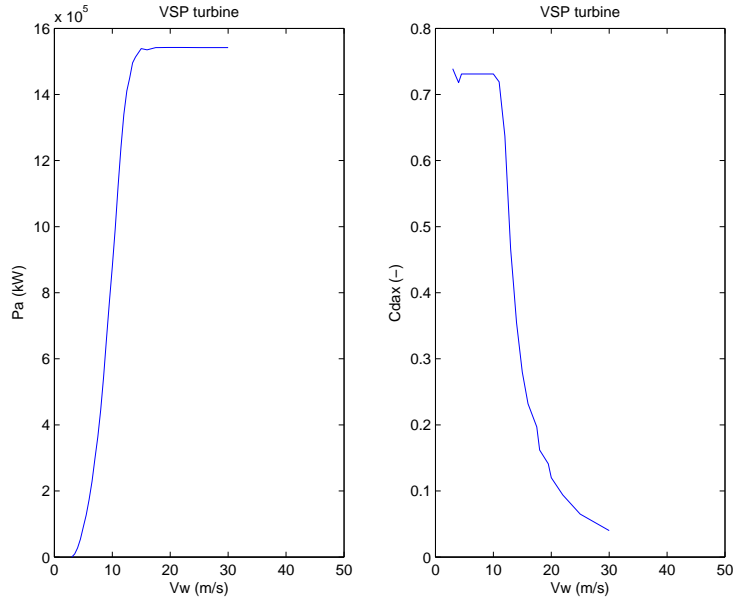


Figure 7: Aerodynamic power and axial thrust coefficient of a VSP turbine

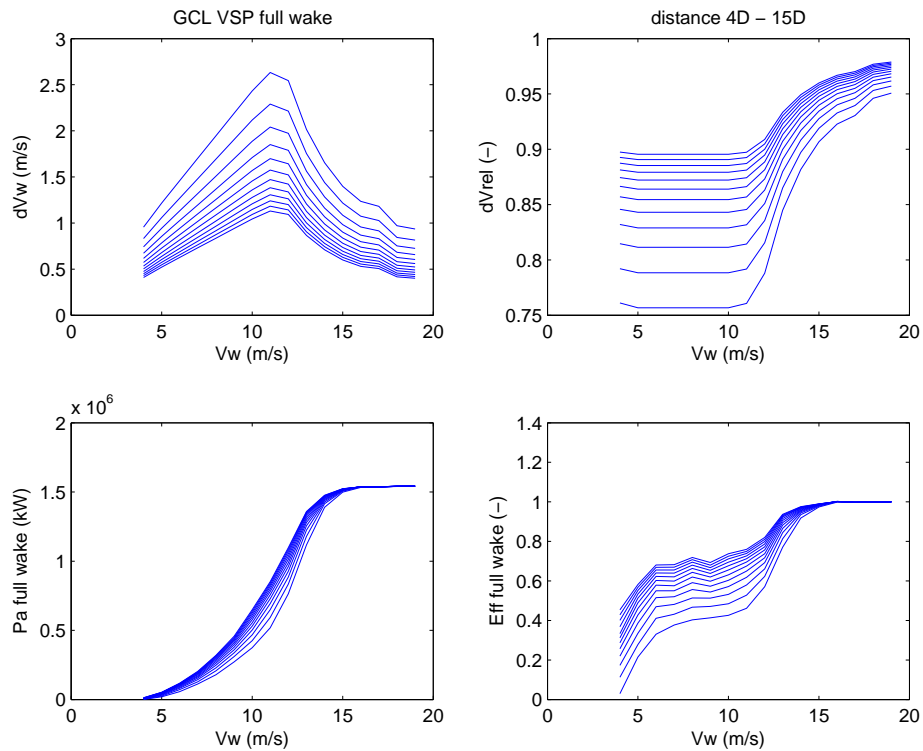


Figure 8: WF aerodynamic efficiency calculated with GCL pre-processor for a VSP turbine

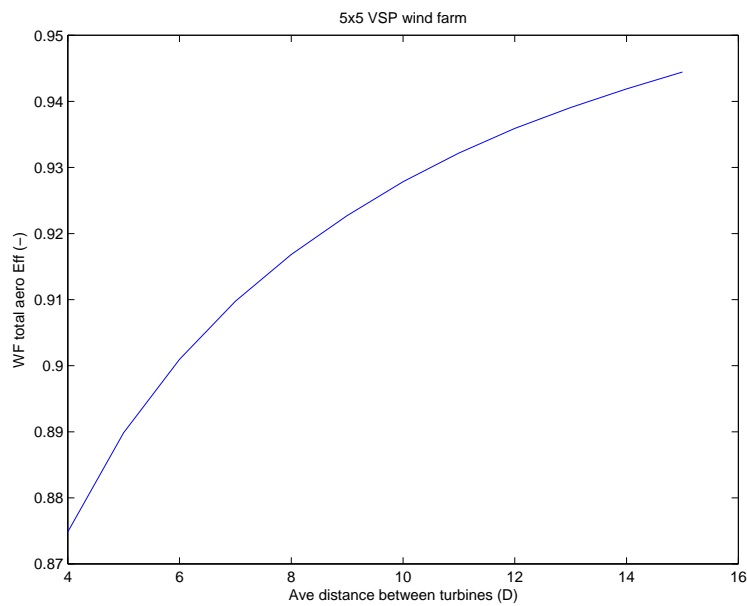


Figure 9: 5x5 VSP WF aerodynamic efficiency calculated with GCL pre-processor

Figure 10 shows the aerodynamic power and axial thrust coefficient of a constant speed stall (CSS) turbine. The full wake aerodynamic efficiency for this turbine as function of the distance is plotted in figure 11. Figure 12 gives the overall aerodynamic efficiency for a CSS 5x5 wind farm.

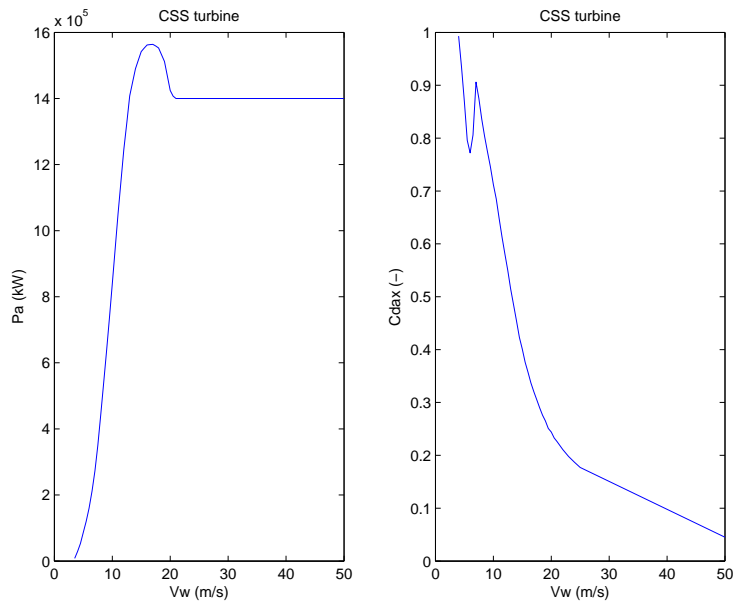


Figure 10: Aerodynamic power and axial thrust coefficient of a CSS turbine

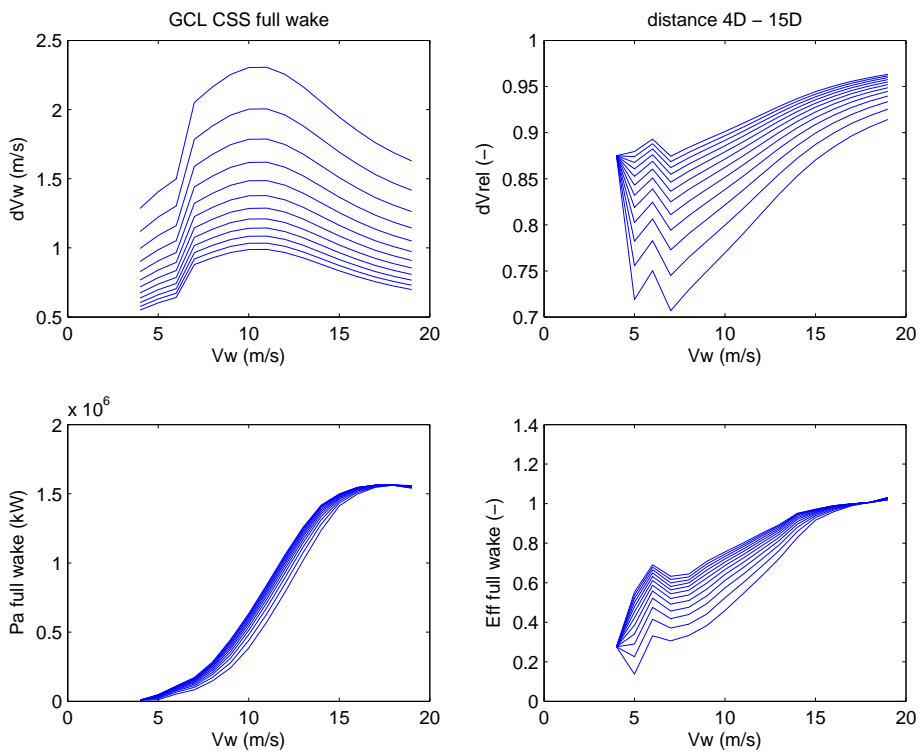


Figure 11: WF aerodynamic efficiency calculated with GCL pre-processor for a CSS turbine

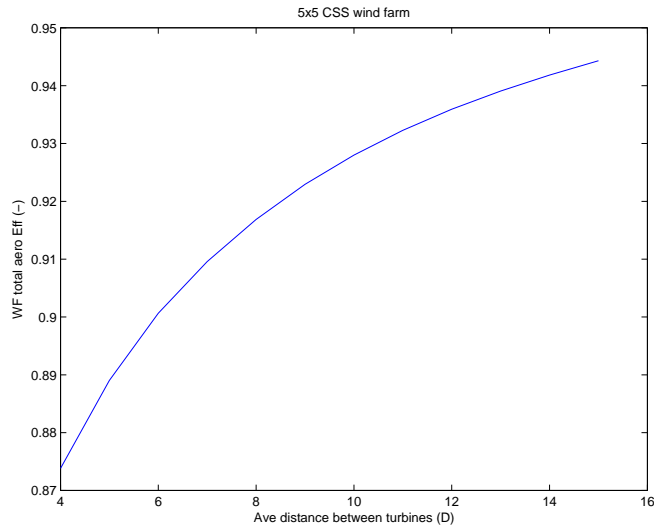


Figure 12: 5x5 CSS WF aerodynamic efficiency calculated with GCL pre-processor

2.3 Hagg model

The Hagg model uses a curve fit to determine the deficit for an individual turbine depending on two parameters: the average distance to the wake generating turbines and the number of turbines generating wakes [10]. This approach strongly reduces the amount of input and the calculation effort. The relative wind speed deficit caused by T turbines at average distance D equals:

$$\frac{dV}{V} = 1 + a_1 e^{b_1 \cdot D} \cdot \ln(T + 1) + a_2 e^{b_2 \cdot D}$$

The constants are:

$$\begin{aligned} a_1 &= -0.1870 \\ a_2 &= -0.0528 \\ b_1 &= -0.2100 \\ b_2 &= -0.1584 \end{aligned}$$

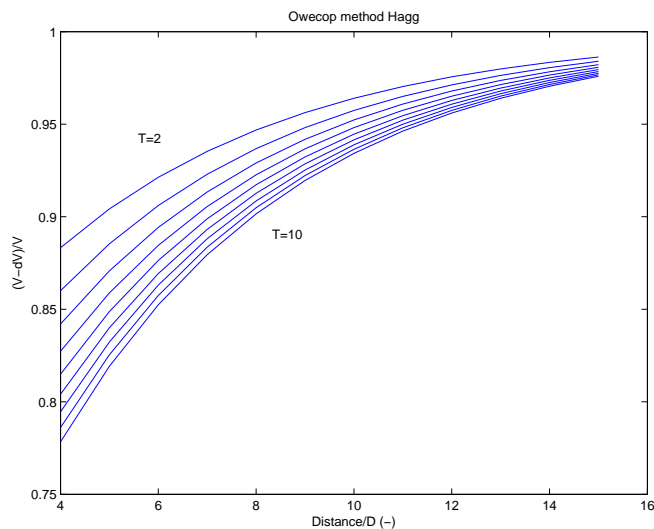


Figure 13: Relative wind speed deficit calculated by the Hagg model

The Hagg model has not been implemented in EeFarm-II.

3 EeFarm II description

The core of EeFarm II consists of steady state models of electrical components, AC as well as DC, and simple steady state models of different types of wind turbines. The EeFarm component models reside in a Simulink model library, see figure 14. A wind farm model is built by copying the model blocs to a Simulink model and connecting the models. The electrical blocs have one input and one output signal, which is a Simulink bus signal. See table 1 for the contents of this bus signal. The signal direction is from the individual wind turbine in the direction of the point of common coupling (PPC: the connection of the wind farm to the HV grid). So, for example, the cable side connected to the turbine generator is called *in* and the side connected to the turbine transformer is called *out*. The signal direction also shows the order in which the model blocks are evaluated, starting at the turbines and ending at the HV transformer at the PPC. The voltage at each wind turbine generator is set by the user and is assumed to be constant, all other voltages are calculated by the programme. If two outputs need to be joined, for instance two cables comming from two turbines, a node block is used. Table 2 gives an overview of the components in the library of EeFarm II.

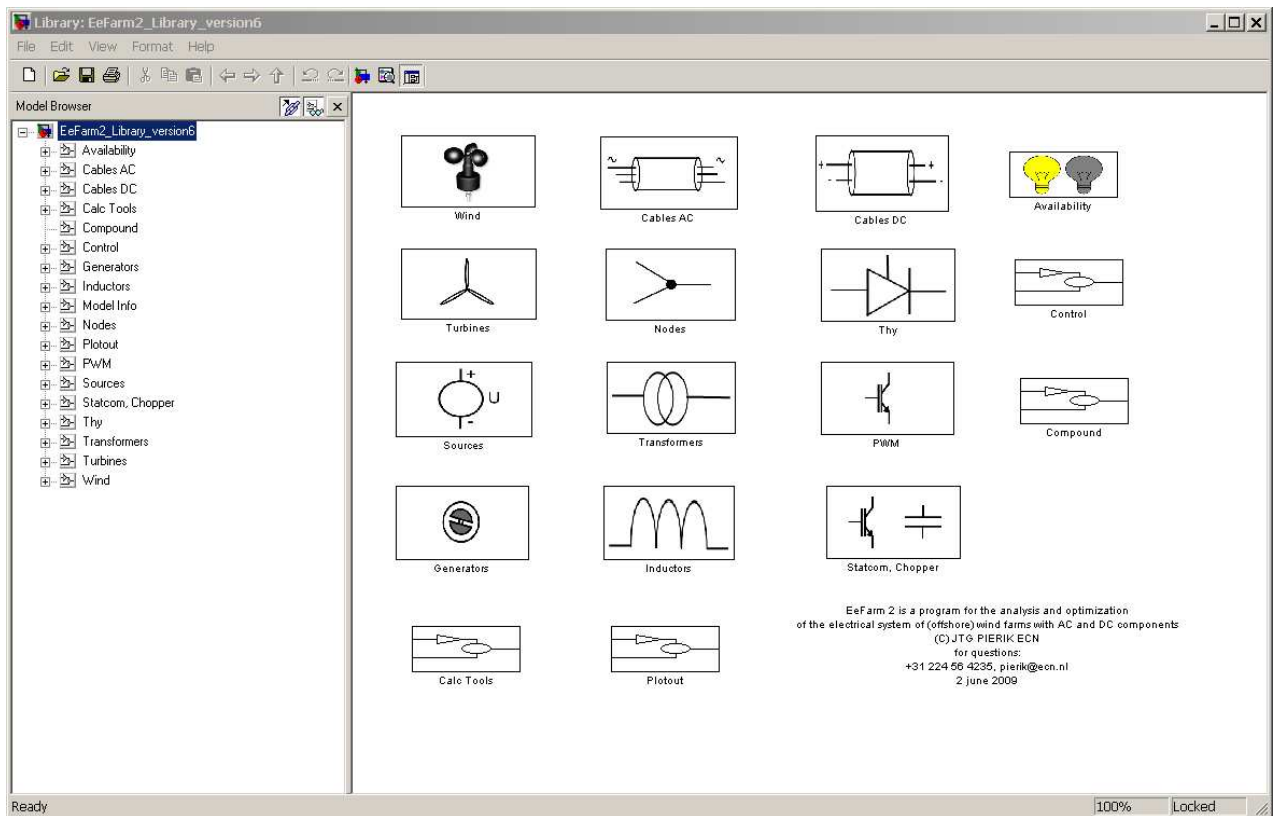


Figure 14: EeFarm model library

Table 1: Bus signals

$U_{line,out}$	line voltage phasor (RMS) at component output, complex number	(V)
$I_{phase,out}$	current phasor (RMS) at component output, complex number	(A)
P_{out}	power at component output	(W)
Q_{out}	reactive power at component output	(VA)
$P_{in} - P_{out}$	component losses	(W)
$Q_{in} - Q_{out}$	reactive power produced by component	(VA)
$\sum(P_{in} - P_{out})$	sum of component losses	(W)
f	frequency	(Hz)
$\sum Invcost$	sum of component investment costs	(kEuro)
P_{fail}	power not produced due to component failure	(W)
$\sum P_{fail}$	sum of power not produced due to component failure	(W)

Table 2: Overview of EeFarm II components

Model	Simulink block	Remarks
Wind	Wind	wind input block
	GCL	Simulink implementation of GCL model
Turbine	Turbine internal curve	single P(V) curve or FyndFarm or FluxFarm input
	Turbine WF eff.	VSP, CSP or CSS turbine, lookup table GCL preprocessor
	VSP turb	single P(V) curve or FyndFarm or FluxFarm input
Generator	Generator Generic	type independent simple generator model
	IM stat	directly connected induction machine
	DFIG	doubly fed induction machine
	FCIM	induction machine with full converter
	FCSM	synchronous machine with full converter
Transformer	TrafoQ	AC transformer with reactive power calculation
	Trafo Noloss Nofail	AC transformer, only the transformer ratio
Cable	CableAC	constant temperature π cable model
	CableDC	constant temperature, earth return DC cable
	CableDCbipolar	constant temperature, bipolar DC cable
Node	NodeAC	connects two AC bus signals
	NodeDC	connects two DC bus signals
	SplitterAC	splits an AC bus signal
	SplitterDC	splits a DC bus signal
Inductor	InductorQ	fixed size inductor for reactive power compensation
	Thy	
PWM	Thy rect	thyristor rectifier
	Thy inv	thyristor inverter
	PWM rect Kaz	IGBT rectifier Kazmierkowski model
	PWM inv Kaz	IGBT inverter Kazmierkowski model
	PWM rect TUD	IGBT rectifier TUD model
	PWM inv TUD	IGBT inverter TUD model
Chopper	PWM rect Inf	IGBT rectifier Infineon model
	PWM inv Inf	IGBT inverter Infineon model
Statcom	Step-up chopper	DC-DC transformer
Availability	Statcom TUD	IGBT inverter TUD model modified as Statcom
Control	Availability	power reduction due to component failure
	Qfeedback	sets the reactive power of individual turbines

The input for a EeFarm calculation is either the wind speed or the power of each individual wind turbine in the farm. In the first case, the EeFarm model includes turbine, turbine generator, turbine cable and turbine transformer models. In the second case it uses the wind turbine power curve specified by the turbine manufacturer and turbine generator, turbine cable and turbine transformer models are only required if the reactive power produced by the turbine has to be determined. Then the losses in these components are set to zero. In the second case, the power of each individual wind turbine in the farm, calculated by a wind farm wake program (for instance the ECN programs FyndFarm or FluxFarm) can be used. Figure 15 gives an overview of the different steps in the calculation of the Levelised Production Costs.

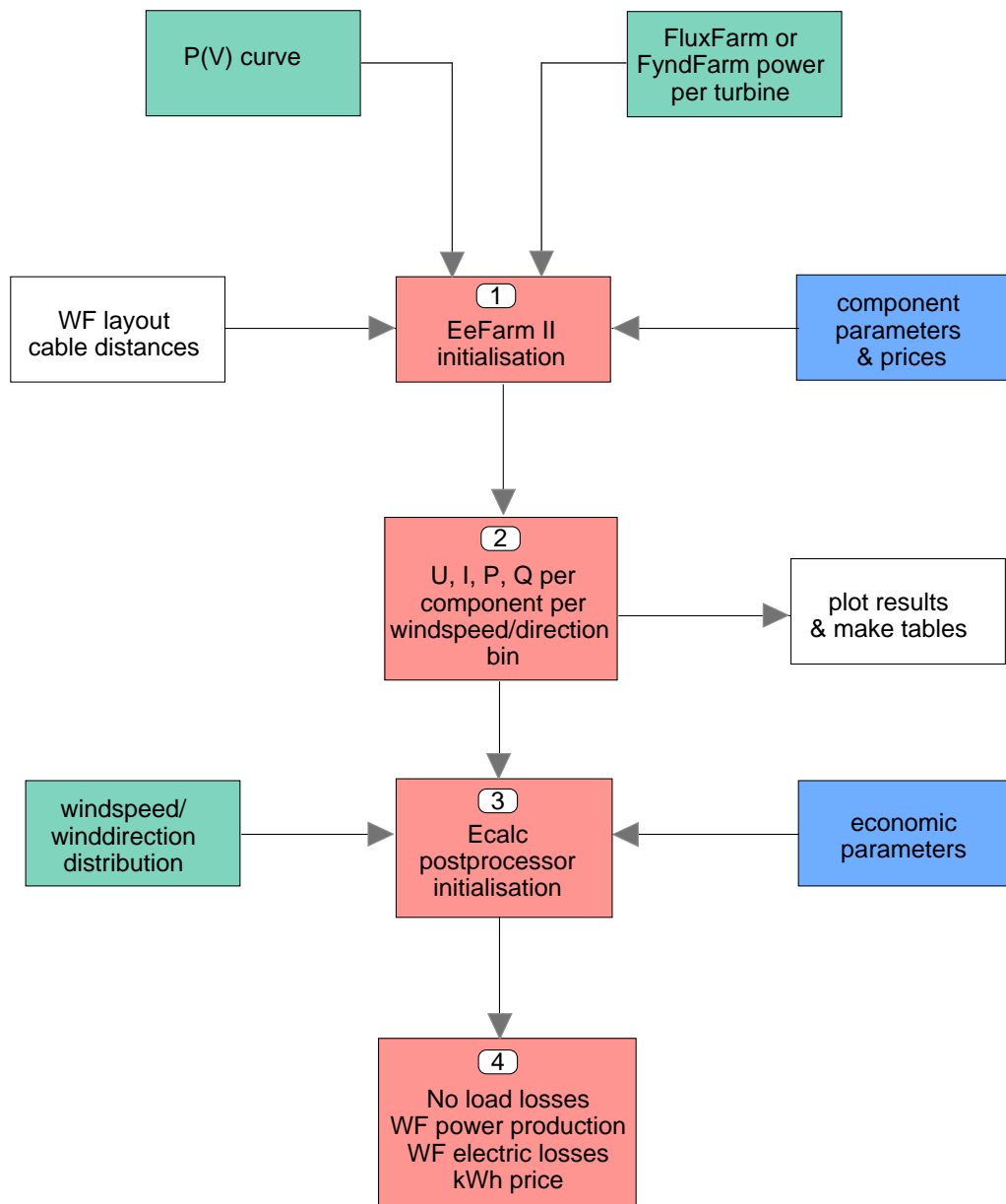


Figure 15: *EeFarm II* model overview

EeFarm-II includes a database with electrical parameters and costs of the components in wind farms. A wind farm specific m-file reads the required parameters from the database and fills the component specific parameters structures used in the EeFarm-II component model library. The EeFarm model parameters are passed to the simulation using a mask. This enables the use of different sets of parameters for one and the same library block [12].

The next sections describe the component models. For each model, the input, the output and the parameters are listed. This is followed by the model equations and a look inside the corresponding Simulink block.

3.1 Turbine models

3.1.1 P(V) curve, FluxFarm or FyndFarm input

Wind turbine manufacturers supply turbine performance information as a table of wind speed against electric power produced. This table can either be used directly as input in EeFarm-II or, if the wind farm layout and location is known, it can be used as input of a wind farm wake programme (for instance the ECN programmes FluxFarm or FyndFarm). The wind farm wake programme calculates the power of each individual turbine as function of wind speed and wind direction. The manufacturer supplied electric power curve already includes the electric losses in the turbine generator, turbine low voltage cable and turbine transformer, so the losses of these components need not to be included in the EeFarm-II calculation.

3.1.2 Compounded turbine model

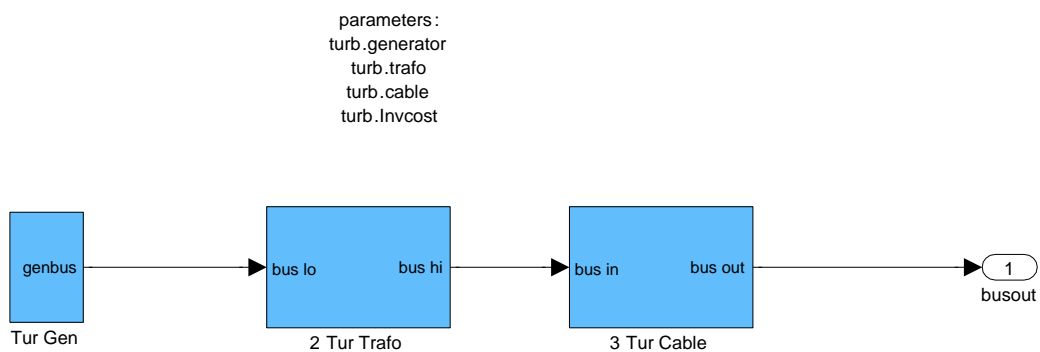


Figure 16: Simulink compound turbine model without input

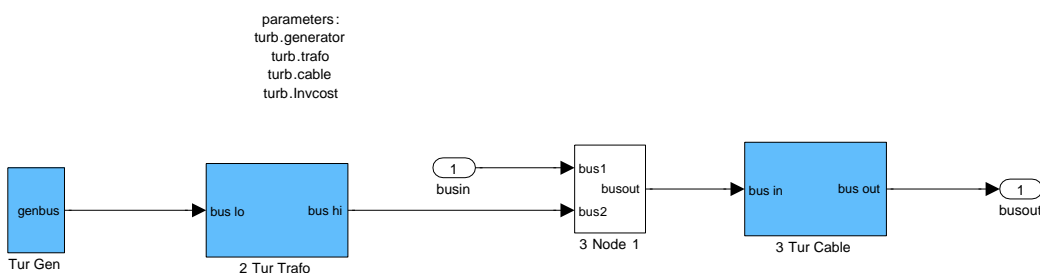


Figure 17: Simulink compound turbine model with input

Since the turbine model appears many times in the wind farm model, it is useful to combine the turbine components into a new model block, called compounded turbine model. Figure 16 shows a compounded turbine model, consisting of turbine generator, the turbine transformer and the cable connecting the turbine. The turbine low voltage cable inside the turbine, if present, is not included in the compound model. Figure 17 shows the Simulink compounded turbine model with input from a (string of) turbines (busin).

3.1.3 Turbine internal curve

The aerodynamic and mechanical part of the turbine internal curve is modelled by the power-wind speed and wind direction curves calculated by FyndFarm or FluxFarm. The curves are turbine specific, i.e. each turbine has its own set of curves. The electrical part is modelled by the generic generator model or the induction machine model. Figure 18 shows the Simulink implementation.

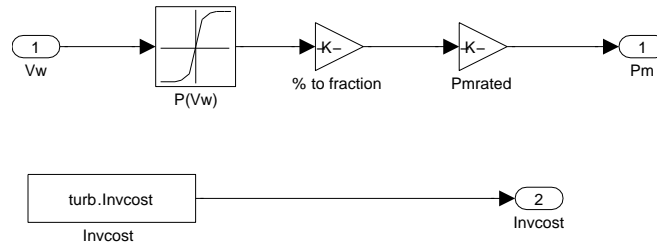


Figure 18: *EeFarm-II* model of a constant speed stall turbine with FyndFarm or FluxFarm input

3.1.4 Turbine WF eff

If the GCL approximation is used, a set of precalculated wind turbine aerodynamic efficiency curves are used. Based on the average distance of the turbine to neighbouring turbines $distD$ and a location factor $xLoc$ a correction on the power-wind speed curve is calculated, see figure 19.

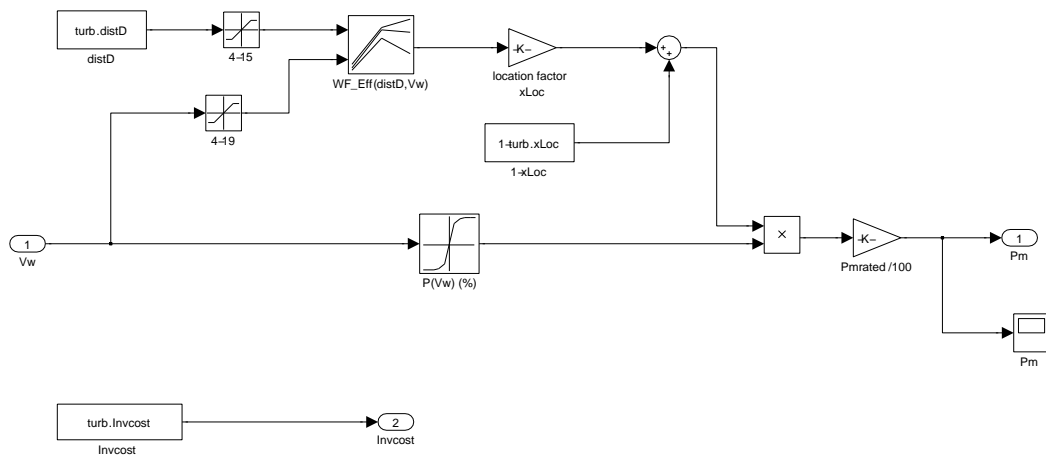


Figure 19: *EeFarm-II* model of a constant speed stall turbine based on GCL or Hagg approximation

3.1.5 VSP turbine

The variable speed pitch turbine is modelled by two curves: a power-wind speed curve and a speed-wind speed curve.

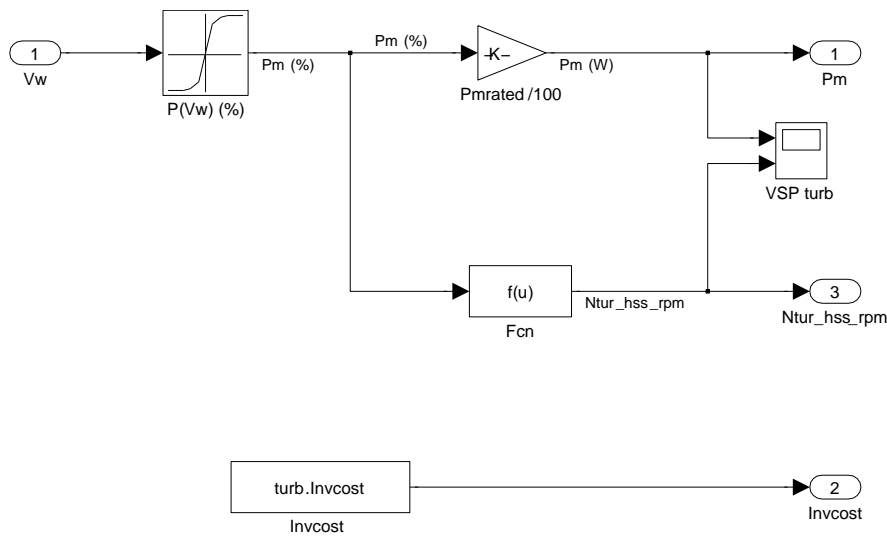


Figure 20: EeFarm-II model of a variable speed pitch turbine

3.2 Generator models

Sometimes, a generator model is needed to calculate the voltage and current phasor and the reactive power corresponding with the turbine power. A generator model can also calculate the generator electrical losses, which are not taken into account if the EeFarm-II calculation uses the electric power curve supplied by a turbine manufacturer.

3.2.1 Generic generator model

Model	Generator Generic
Input	P_m, \underline{U}, ϕ
Output	$P_e, \underline{I}, Q, P_{loss}, \sum P_{loss}, \sum Invcost, \sum P_{fail}$
Parameters	$\eta, Invcost, notavail$

The generic generator model is used if the type of turbine generator or the control of the turbine generator is not known. Input variables are the voltage phasor \underline{U} , the mechanical power P_m and the angle ϕ between current and voltage. The model determines the active power P_e , the current phasor \underline{I} , the reactive power Q , the generator losses P_{loss} , the cumulative losses $\sum P_{loss}$, the cumulative investment costs $\sum Invcost$ and the cumulative power not produced due to component failure $\sum P_{fail}$.

$$\begin{aligned}
 P_e &= \eta P_m \\
 P_{loss} &= P_m - P_e \\
 |\underline{I}| &= \frac{P_e}{\sqrt{3}|\underline{U}| \cos \phi} \\
 \alpha &= \angle \underline{U} \\
 \underline{I} &= |\underline{I}| e^{j(\alpha - \phi)} \\
 Q &= \text{sqrt}(3) (\text{Re}(\underline{I}) \text{Im}(\underline{U}) - \text{Im}(\underline{I}) \text{Re}(\underline{U})) \\
 \sum P_{loss} &= P_{loss} \\
 \sum Invcost &= Invcost \\
 \sum P_{fail} &= P_{fail}
 \end{aligned}$$

P_{fail} is determined by the Availability block.

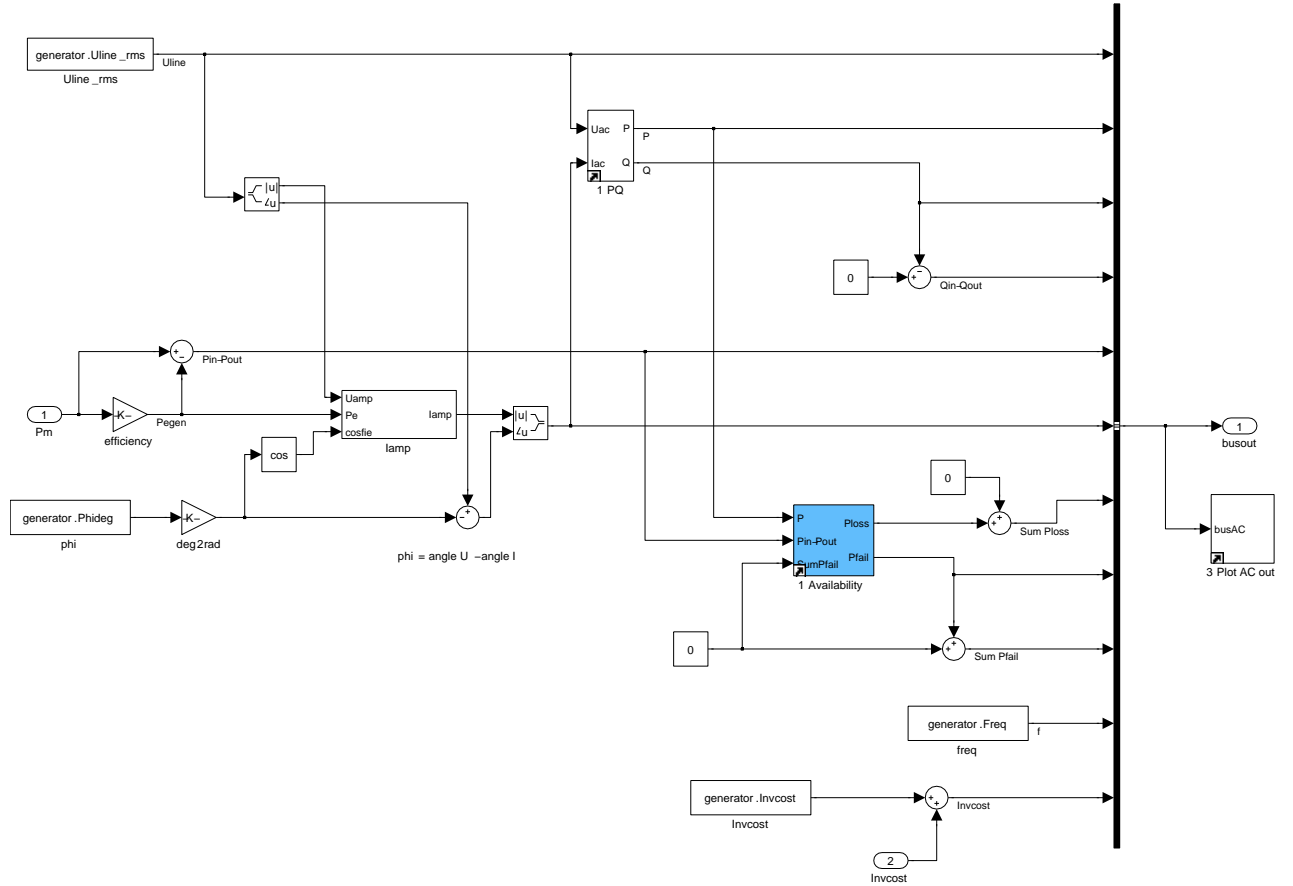


Figure 21: Simulink generator generic model

3.2.2 Constant speed induction machine

Model	IM stat
Input	P_m, \underline{U}_{gen}
Output	$\underline{I}_{gen}, P_e, Q, P_{loss}, \sum P_{loss}, \sum Invcost, \sum P_{fail}$
Parameters	$I_{sd}(P_m), I_{sq}(P_m), Invcost, notavail$

For the constant speed induction machine the input variables are the stator voltage \underline{U}_{gen} and the mechanical power P_m . The output variables are the stator current phasor \underline{I}_{gen} , the active and reactive power P_e, Q , the losses P_{loss} and the cumulative investment costs and power not produced due to failure $\sum Invcost, \sum P_{fail}$.

Based on the steady state voltage equations of the induction machine, an iteration would be require to determine the current from the inputs. This is caused by the fact that the slip is not known. The iteration can be prevented by a two step method:

1. the stator current phasor curves of the induction machine as a function of the mechanical power are calculated in a separate Matlab steady state model. The result is saved to file as per unit (PU) values of mechanical power and current phasor;
2. these values are used as a lookup table in EeFarm-II to determine the current phasor for a given mechanical power and voltage phasor.

The voltage phasor in EeFarm-II must be in the same direction as the voltage phasor in the separate steady state model (or an angle transformation has to be applied, which is not included

in the Simulink model block). Since per unit values are used, the choice of the transformation (i.e. power invariant versus amplitude invariant) may be different in the steady state model and EeFarm-II.

The induction machine voltage equations in the steady state model (generator convention) are:

$$\begin{pmatrix} u_d \\ u_q \\ 0 \\ 0 \end{pmatrix} = \begin{pmatrix} -r_s & -\omega_s l_s & 0 & -\omega_s l_m \\ \omega_s l_s & -r_s & \omega_s l_m & 0 \\ 0 & -(\omega_s - \omega_r) l_m & -r_r & -(\omega_s - \omega_r) l_r \\ (\omega_s - \omega_r) l_m & 0 & (\omega_s - \omega_r) l_r & -r_r \end{pmatrix} \begin{pmatrix} i_{sd} \\ i_{sq} \\ i_{rd} \\ i_{rq} \end{pmatrix}$$

To comply with the choice in section D.1, we choose:

$$\begin{aligned} \underline{u} &= u_q + j * u_d \\ u_q &= 0 \\ u_d &= |\underline{U}_{line}| \end{aligned}$$

Figure 22 shows the stator current curves for a 2.1 MW induction machine.

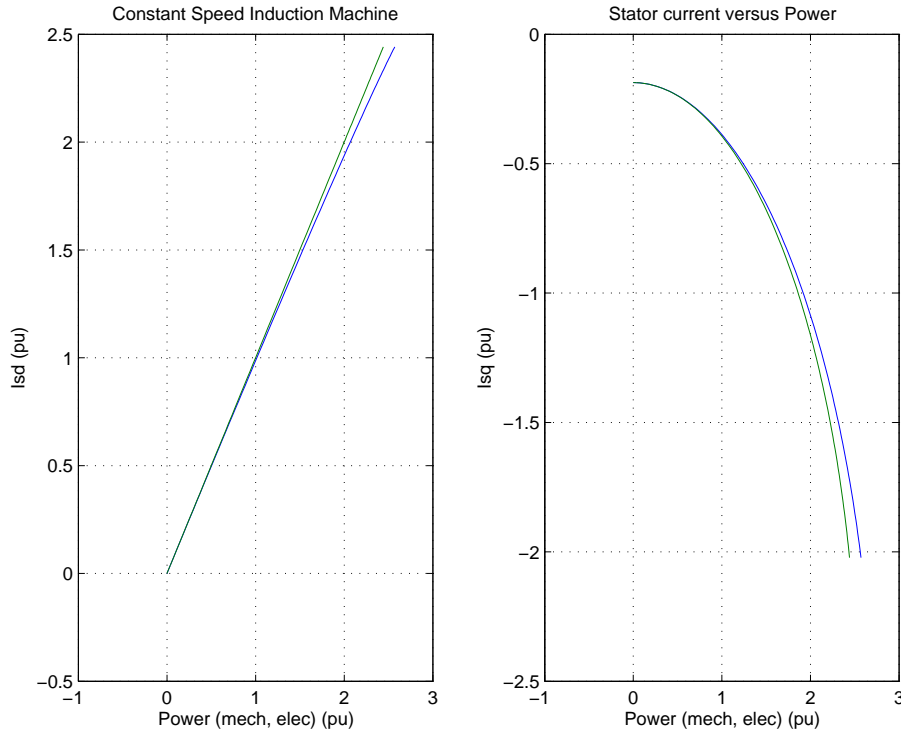


Figure 22: Induction Machine stator current in d and q direction as function of mechanical and electric power

If the stator current is known, the same equations are applied as in section 3.2.1 to determine the other output variables. The Simulink implementation of the constant speed induction machine is shown in figure 23 and 24.

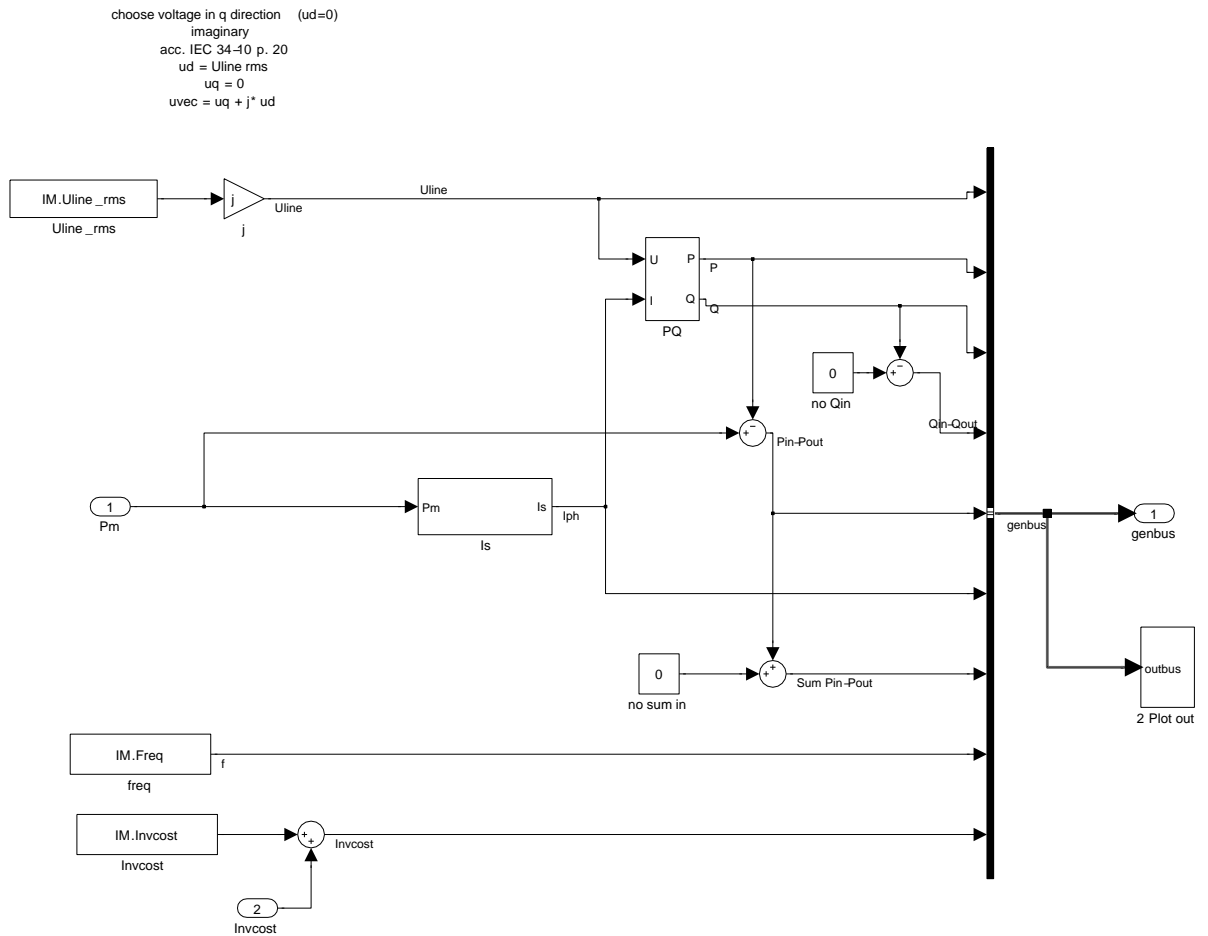


Figure 23: Simulink model Induction Machine

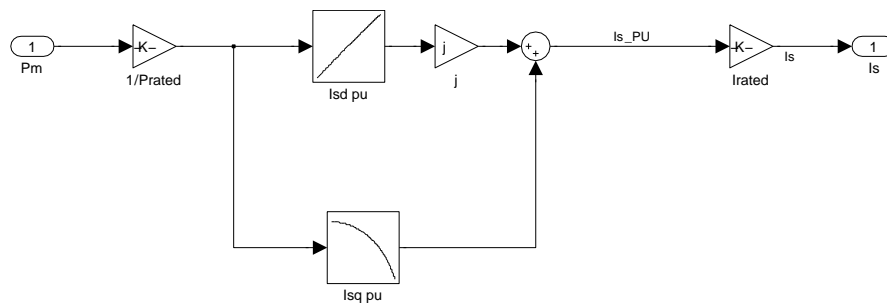


Figure 24: Simulink model Induction Machine, lookup table

3.2.3 DFIG

Model	DFIG
Input	$P_m, U_{sd}, U_{sq}, \omega_r$
Output	$I_{sd}, I_{sq}, I_{gcd}, I_{gcq}, P_e, Q, P_{loss}, \sum P_{loss}, \sum Invcost, \sum P_{fail}$
Parameters	$l_s, l_m, l_r, r_s, r_r, Invcost, notavail$

The input variables for the steady state Doubly Fed Induction Generator (DFIG) model are the voltage, the mechanical power and the speed. The output variable are the total current phasor

(current from stator plus current from grid side converter) and the losses.

Look-up table model

The steady state model of the DFIG can use the same two step approach used for the induction machine model. The voltage equation now includes the rotor voltage generated by the rotor converter (zero in the IMstat model). A controller determines the stator reactive power, for instance zero. The speed is determined by the power dependent rotor speed control of the turbine.

To comply with section D.1, we choose:

$$\begin{aligned}\underline{u} &= u_{qs} + j * u_{ds} \\ u_{qs} &= 0 \\ u_{ds} &= |\underline{U}_{line}|\end{aligned}$$

The steady state model of the DFIG is:

$$\begin{aligned}P_s &= (1 - s)P_m \\ Q_s &= 0 \\ i_{ds} &= \frac{2 P_s}{3 u_{ds}} \\ i_{qs} &= \frac{2 Q_s}{3 u_{ds}} \\ i_{qr} &= \frac{u_{ds} + r_s i_{ds} + \omega_s l_s i_{qs}}{-\omega_s l_m} \\ i_{dr} &= \frac{r_s i_{qs} - \omega_s l_s i_{ds}}{\omega_s l_m} \\ u_{dr} &= -(\omega_s - \omega_r) l_m i_{qs} - r_r i_{dr} - (\omega_s - \omega_r) l_r i_{qr} \\ u_{qr} &= +(\omega_s - \omega_r) l_m i_{ds} + (\omega_s - \omega_r) l_r i_{dr} - r_r i_{qr} \\ P_r &= \frac{3}{2}(u_{dr} i_{dr} + u_{qr} i_{qr}) \\ Q_r &= \frac{3}{2}(u_{dr} i_{qr} - u_{qr} i_{dr}) \\ P_c &= P_r - P_{loss,c} \\ P_{tot} &= P_s + P_c \\ Q_c &= 0 \\ i_{dc} &= \frac{2 P_c}{3 u_{ds}} \\ i_{qc} &= \frac{2 Q_c}{3 u_{ds}} \\ i_{d,tot} &= i_{ds} + i_{dc} \\ i_{q,tot} &= i_{qs} + i_{qc}\end{aligned}$$

For a given speed range, P_{tot} , P_m , N , $i_{d,tot}$, $i_{q,tot}$ and the losses are written to file. This file is loaded by the DFIG model block in EeFarm II and used as a lookup table to determine the current components to the grid for a given mechanical (or electrical) power and rotational speed. The reactive power of stator and converter are assumed to be zero. If the reactive power is not zero, the steady state model can be used to calculate the DFIG characteristics for these conditions but the lookup table has to be modified.

Figure 25 and 26 show the results of the DFIG steady state model. If the stator power is constant, the stator and rotor currents are constant and the stator and rotor losses are constant, independent of the speed.

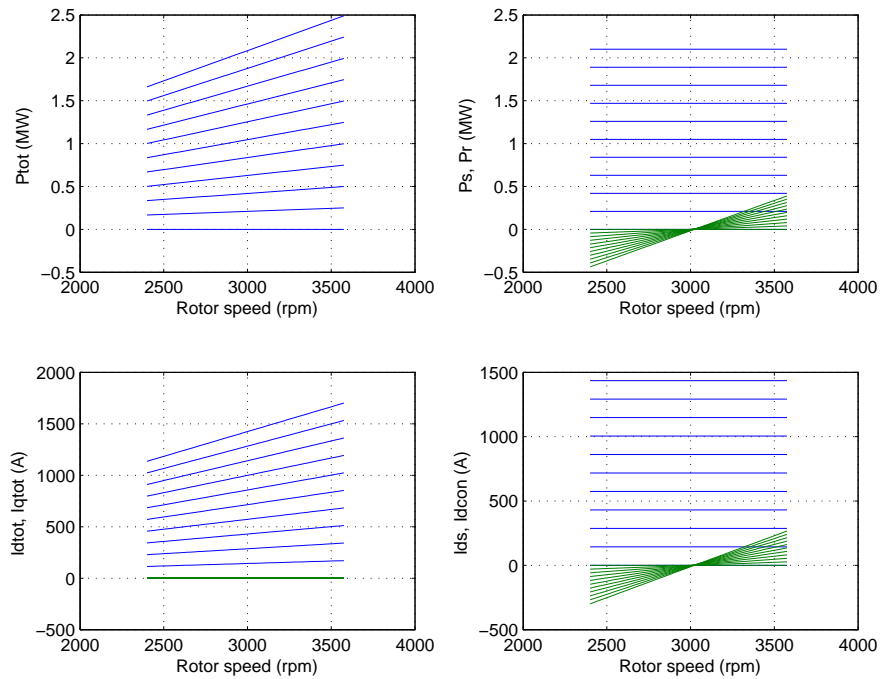


Figure 25: DFIG steady state model, variable speed and variable power

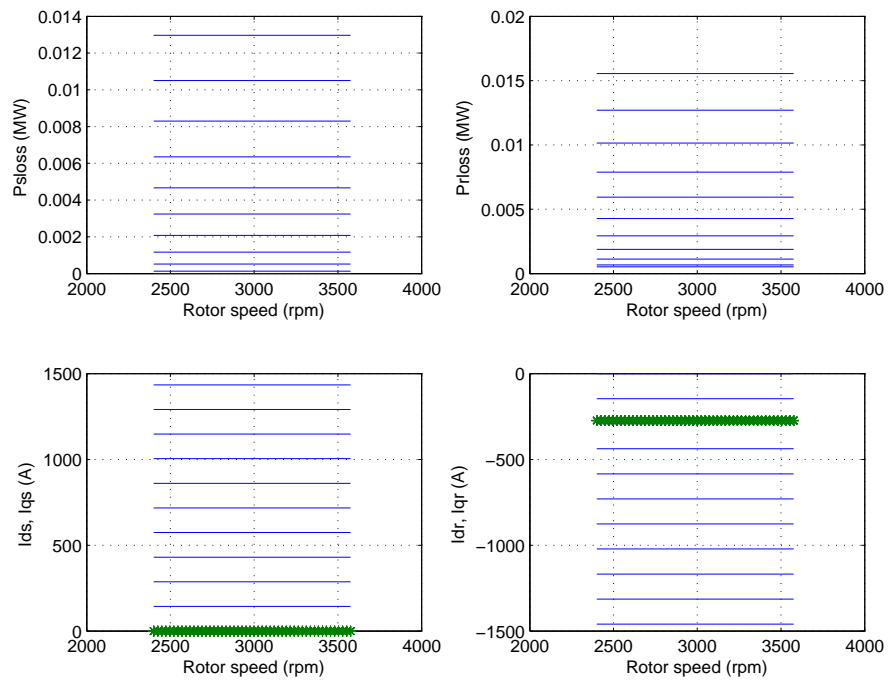


Figure 26: DFIG steady state model, variable speed and variable power

Simplified model without look-up table

The DFIG steady state model can be simplified if the stator and rotor power are estimated first from the mechanical power (the losses are, initially, neglected). The stator power can be calculated from the mechanical power:

$$P_s = \frac{P_m}{\left(1 - \frac{(\omega_s - \omega_r)}{\omega_s}\right)} \quad (4)$$

This can be seen as follows. If we choose $u_{qs} = 0$ and $i_{qs} = 0$ ($Q = 0$) and we (initially) neglect the stator and rotor resistance terms, the steady state DFIG equations are:

$$\begin{aligned} u_{ds} &= -\omega_s l_m i_{qr} \\ u_{dr} &= -(\omega_s - \omega_r) l_r i_{rq} \\ u_{qr} &= (\omega_s - \omega_r)(l_m i_{ds} + l_r i_{dr}) \\ P_r &= \frac{3}{2}(u_{dr} i_{dr} + u_{qr} i_{qr}) \\ &= \frac{3}{2}(-(\omega_s - \omega_r) l_r i_{qr} i_{dr} + (\omega_s - \omega_r)(l_m i_{ds} + l_r i_{dr}) i_{qr}) \\ &= \frac{3}{2}(\omega_s - \omega_r) l_m i_{ds} i_{qr} \\ &= \frac{3}{2}(\omega_s - \omega_r) l_m i_{ds} \frac{u_{ds}}{-\omega_s l_m} \\ &= -\frac{(\omega_s - \omega_r)}{\omega_s} P_s \\ P_m &= P_s + P_r \\ &= \left(1 - \frac{(\omega_s - \omega_r)}{\omega_s}\right) P_s \\ &= (1 + s) P_s \end{aligned}$$

If $\omega_r < \omega_s$, i.e. subsynchronous speed, P_r is negative if P_s is positive, so since we use generator convention, at subsynchronous speed the stator supplies power to the grid and the rotor absorbs power. At subsynchronous speed the stator power exceeds the mechanical power. At supersynchronous speed both stator and rotor supply power to the grid.

Neglecting the resistances in the voltage equations ($u_{qs} = 0$ is required, Q_s and Q_c are variable):

$$\begin{aligned} u_{ds} &= \hat{u}_{ph} \\ u_{qs} &= 0 \\ P_s &= \frac{P_m}{\left(1 - \frac{(\omega_s - \omega_r)}{\omega_s}\right)} \\ i_{qs} &= \frac{2}{3} \frac{Q_s}{u_{ds}} \\ i_{ds} &= \frac{2}{3} \frac{P_s}{u_{ds}} \\ i_{dr} &= -\frac{l_s i_{ds}}{l_m} \\ i_{qr} &= -\frac{u_{ds} + \omega_s l_s i_{qs}}{\omega_s l_m} \\ i_s &= \sqrt{i_{ds}^2 + i_{qs}^2} \\ i_r &= \sqrt{i_{dr}^2 + i_{qr}^2} \\ P_{rloss} &= \frac{3}{2} r_r i_r^2 \end{aligned}$$

$$P_{loss} = \frac{3}{2} r_s i_s^2$$

$$i_{d,tot} = \frac{2}{3} \frac{P_m - P_{sloss} - P_{rloss}}{u_{ds}}$$

$$i_{q,tot} = \frac{2}{3} \frac{Q_{tot}}{u_{ds}}$$

With this set of equations for the steady state DFIG model, there is no need for pre-calculated DFIG tables. A further advantage is that the reactive power can be externally set and variable. The rotor current is approximately equal to the stator current and both are independent of the speed. The relative losses (compared to mechanical or electrical input) are larger for subsynchronous speed since part of the machine power is absorbed from the grid by the rotor and fed back to the grid by the stator.

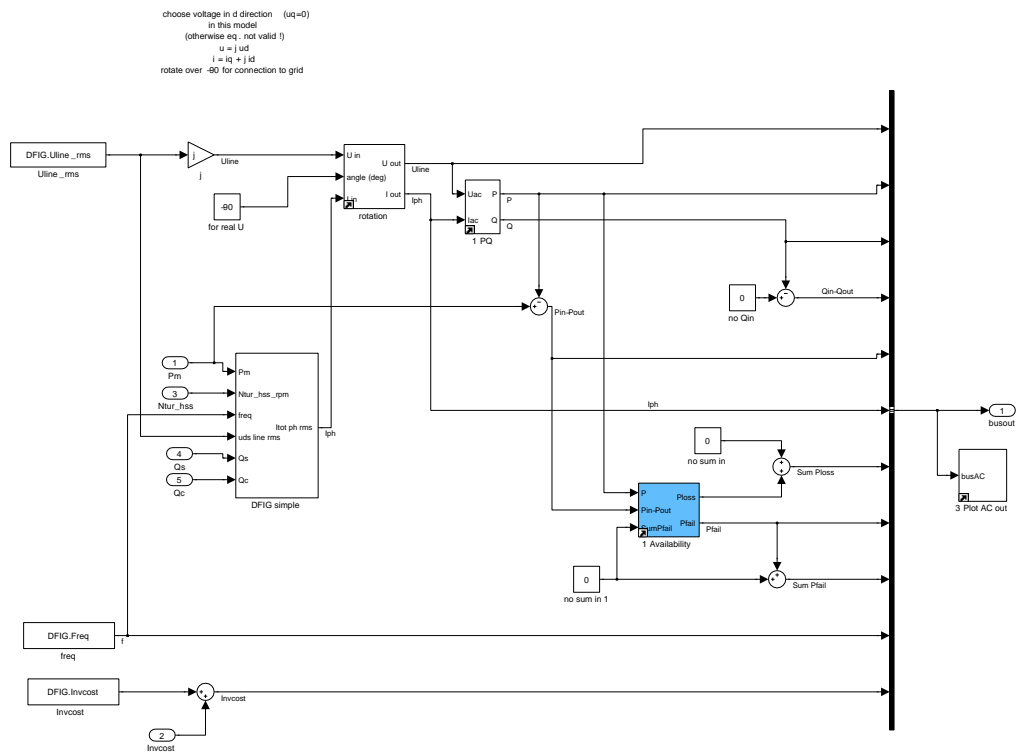


Figure 27: EeFarm-II model of the DFIG system

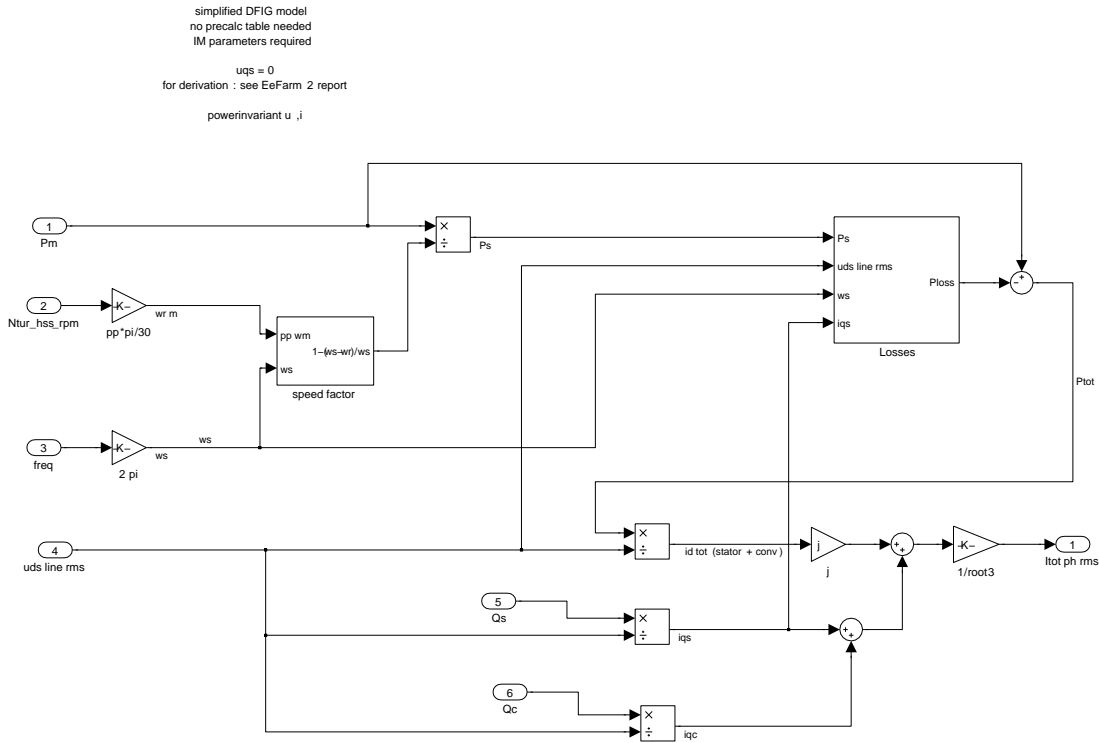


Figure 28: Calculation of the current in the DFIG model

3.2.4 FCIM

Model	Induction machine in FCIM
Input	P_m, ω_r
Output	$\underline{U}, \underline{I}, P, Q, P_{loss}, \sum P_{loss}, \sum Invcost, \sum P_{fail}$
Parameters	$I_{rated}, U_{rated}, l_s, l_m, l_r, r_s, r_r, Invcost, notavail$

The objective for the steady state model of the induction machine with full converter is to calculate the losses in the machine and the converter for variable rotational speed, constant stator voltage and variable active power. The losses in the machine are calculated from the rotor and stator current. To calculate the losses in the converter we need to know the AC current into the PWM rectifier. The equations are:

$$\begin{aligned}
 u_d &= -r_s i_{ds} - \omega_s (l_s i_{qs} + l_m i_{qr}) \\
 u_q &= -r_s i_{qs} + \omega_s (l_s i_{ds} + l_m i_{dr}) \\
 0 &= -r_r i_{dr} - s \omega_s (l_m i_{qs} + l_r i_{qr}) \\
 0 &= -r_r i_{qr} + s \omega_s (l_m i_{ds} + l_r i_{dr}) \\
 P &= \sqrt{3} (u_d i_d + u_q i_q) = C_1 \\
 u_d &= C_2 \\
 u_q &= 0 \\
 u &= \sqrt{u_d^2 + u_q^2} = C_2 \\
 i_s &= \sqrt{i_{ds}^2 + i_{qs}^2} \\
 i_r &= \sqrt{i_{dr}^2 + i_{qr}^2} \\
 P_{loss} &= 3 \cdot (r_s i_s^2 + r_r i_r^2)
 \end{aligned}$$

Although the steady state model of the induction machine is relatively simple, the stator and rotor current can not be calculated easily with rotational speed, stator voltage and active power as input. Therefore, a two step solution with a lookup table is used again. First, the equations are solved with stator frequency ω , slip s and voltage amplitude as input, see figure 29. The result is a set of matrices for the mechanical power P_m , the stator currents i_{ds}, i_{qs} , the stator voltages u_{ds}, u_{qs} and the total losses P_{loss} for variable speed and slip. The slip corresponds strongly with the electric power and the losses.

The matrices plus the speed vector are used in the EeFarm-II FCIM model as a lookup table to find AC current into the rectifier and the induction machine losses.

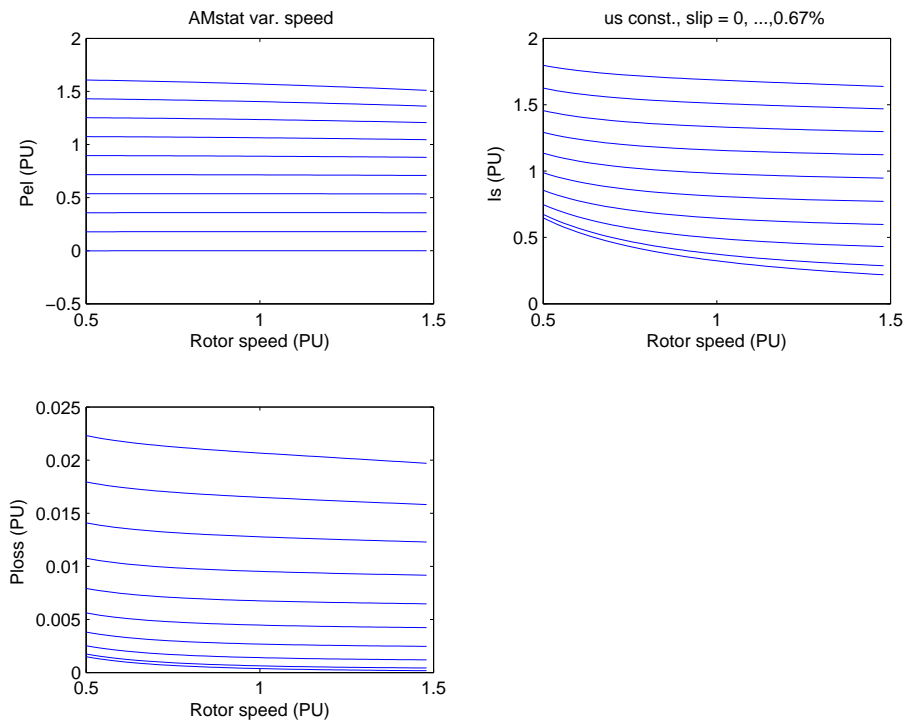


Figure 29: Steady state model of the induction machine: variable speed, constant stator voltage and variable slip 0 - 0.67%

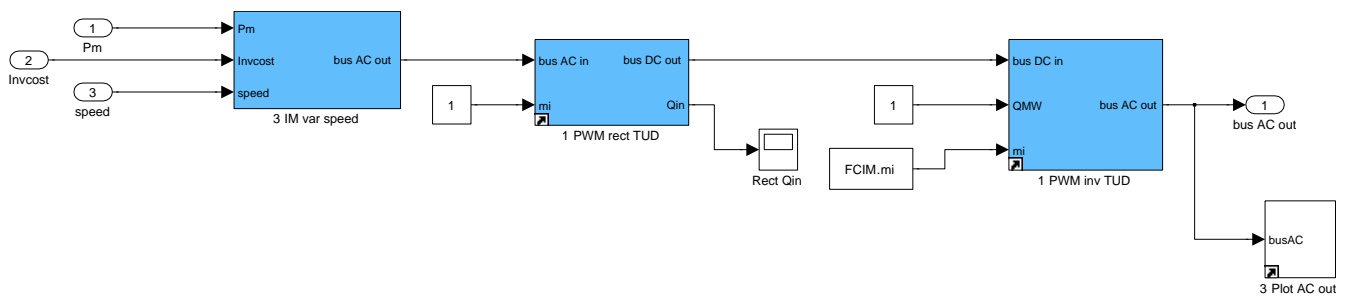


Figure 30: EeFarm-II model of the FCIM system

Figure 30 shows the model of the FCIM system consisting of the induction machine model described above, a rectifier and an inverter. The rectifier and inverter models are described in section 3.9.

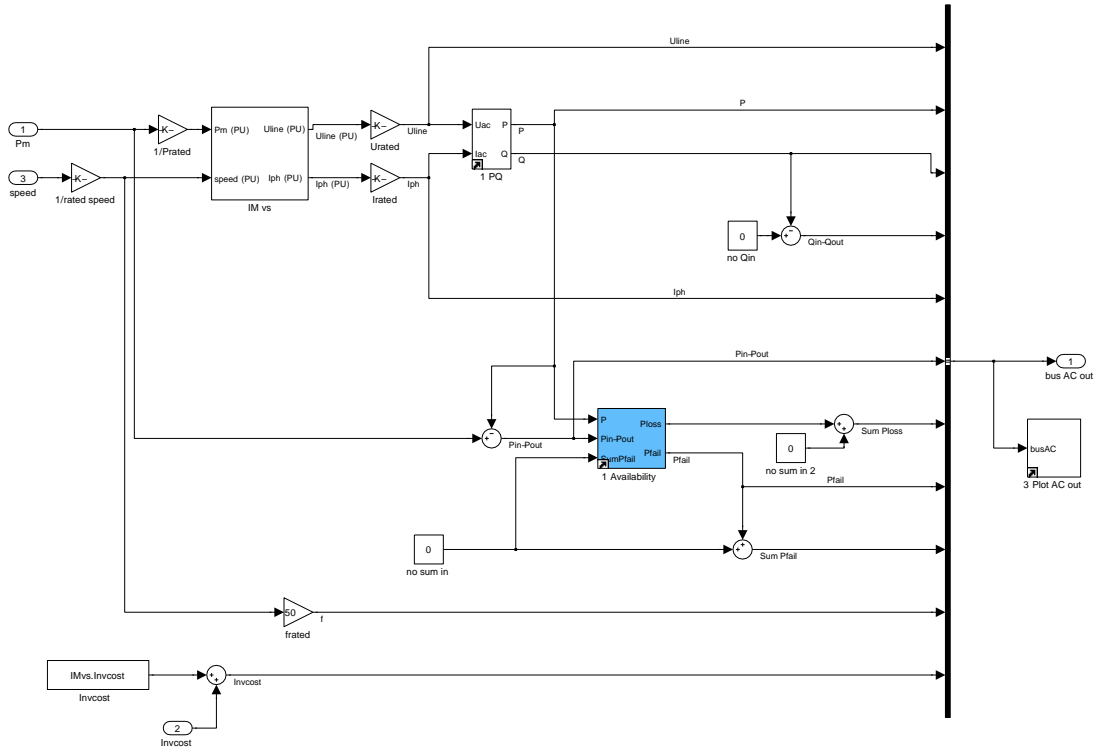


Figure 31: EeFarm-II model of the variable speed induction machine in the FCIM system

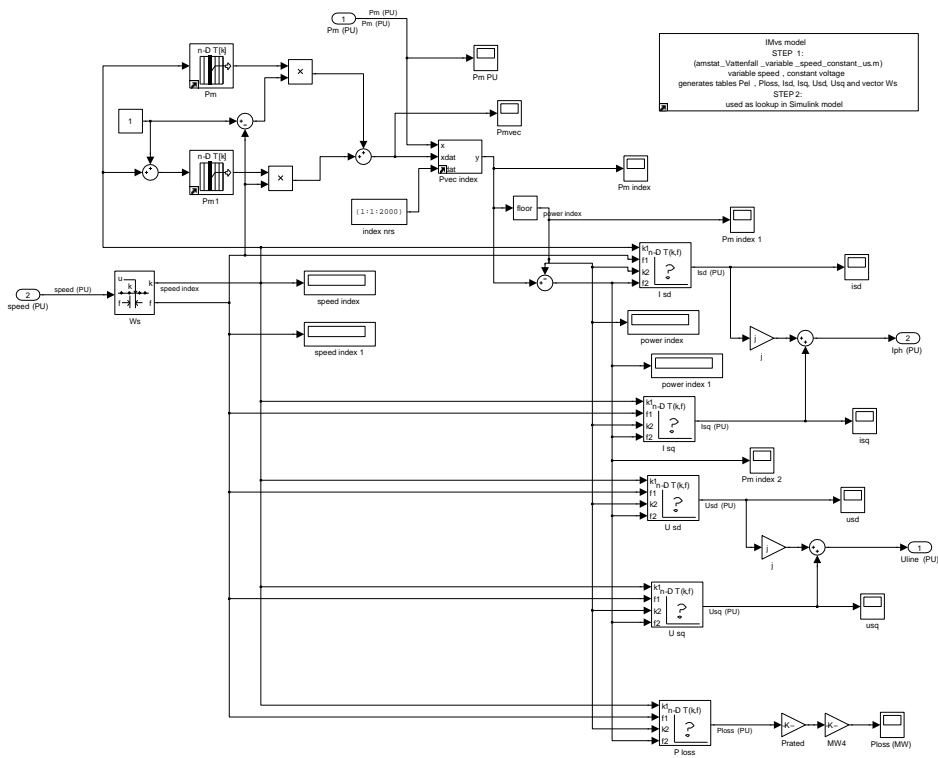


Figure 32: Lookup table evaluation in the FCIM model

3.2.5 FCSM

Model	Synchronous machine in FCSM
Input	P_m, ω_r, Q
Output	$\underline{U}, \underline{I}, P, P_{loss}, \sum P_{loss}, \sum Invcost, \sum P_{fail}$
Parameters	$I_{rated}, U_{rated}, l_s, l_m, l_r, r_s, r_r, Invcost, notavail$

The objective for the EeFarm-II steady state model of the synchronous machine with full converter is to calculate the losses in the machine and the converter. To calculate the losses in the rectifier, the input current phasor is required. This section describes the model of the synchronous machine, which calculates the current phasor and the losses in the machine. The input values of the synchronous machine model are the rotational speed ω_r and the mechanical and the reactive power P_m, Q . The reactive power is assumed to be zero, since this is the condition with the lowest losses. The steady state model of the synchronous machine is relatively simple, but the stator and field current can not be calculated easily for the chosen variables ω_r, P_m and Q , due to the nonlinearity of the set of equations. The equations are (conventions according to IEC 34-10):

$$\begin{aligned}
P &= \sqrt{3}(u_d i_d + u_q i_q) = C_1 \\
Q &= \sqrt{3}(u_d i_q - u_q i_d) = 0 \\
u_d &= -r_s i_d - \omega l_s i_q \\
u_q &= -r_s i_q + \omega(l_s i_d + l_{afd} i_f) \\
u &= \sqrt{u_d^2 + u_q^2} = C_2 \\
u_d &= -u \sin \delta \\
u_q &= u \cos \delta \\
i &= \sqrt{i_d^2 + i_q^2} \\
P_{loss} &= 3 \cdot r_s i^2 + r_f i_f^2
\end{aligned}$$

To prevent iteration, the equations will first be solved for a different set of input variables: speed ω_r , stator voltage u , load angle δ and field current i_f :

$$\begin{aligned}
u_d &= -u \sin \delta \\
u_q &= u \cos \delta \\
i_q &= \frac{\omega l_s u_d + r_s u_q - r_s \omega l_{afd} i_f}{-r_s^2 - (\omega l_s)^2} \\
i_d &= \frac{u_d + \omega l_s i_q}{-r_s} \\
P &= \sqrt{3}(u_d i_d + u_q i_q) \\
Q &= \sqrt{3}(u_d i_q - u_q i_d) \\
P_{loss} &= 3 \cdot r_s i^2 + r_f i_f^2 \\
i &= \sqrt{i_d^2 + i_q^2}
\end{aligned}$$

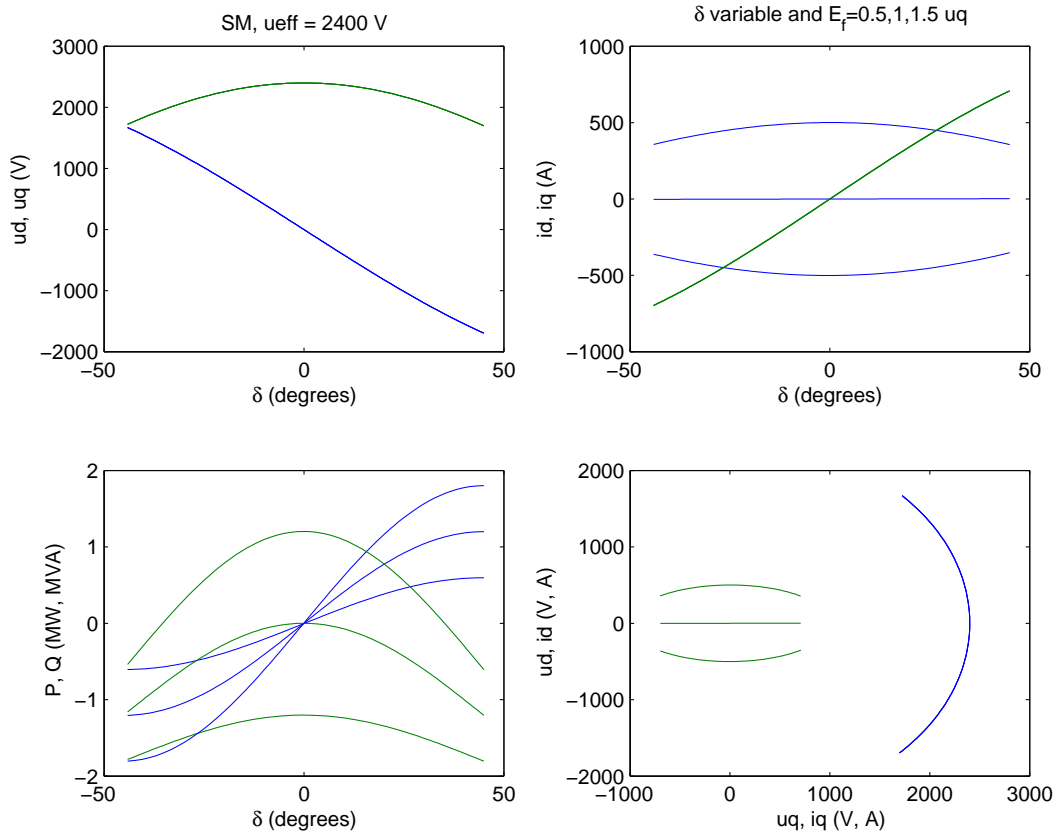


Figure 33: Steady state model of the synchronous machine: load angle $\delta = -45, \dots, +45^\circ$ and EMF $E_f = 0.5, 1, 1.5 \times u_q$

Figure 33 shows the effect of the load angle δ and the EMF E_f on the power, the reactive power, the d- and q-voltage and the d- and q-current at constant speed and constant voltage amplitude. To be able to have reactive power zero, the EMF needs to be higher than u_q and increasingly so at higher power. For each value of speed and field current, there will be only one positive load angle value with zero reactive power Q .

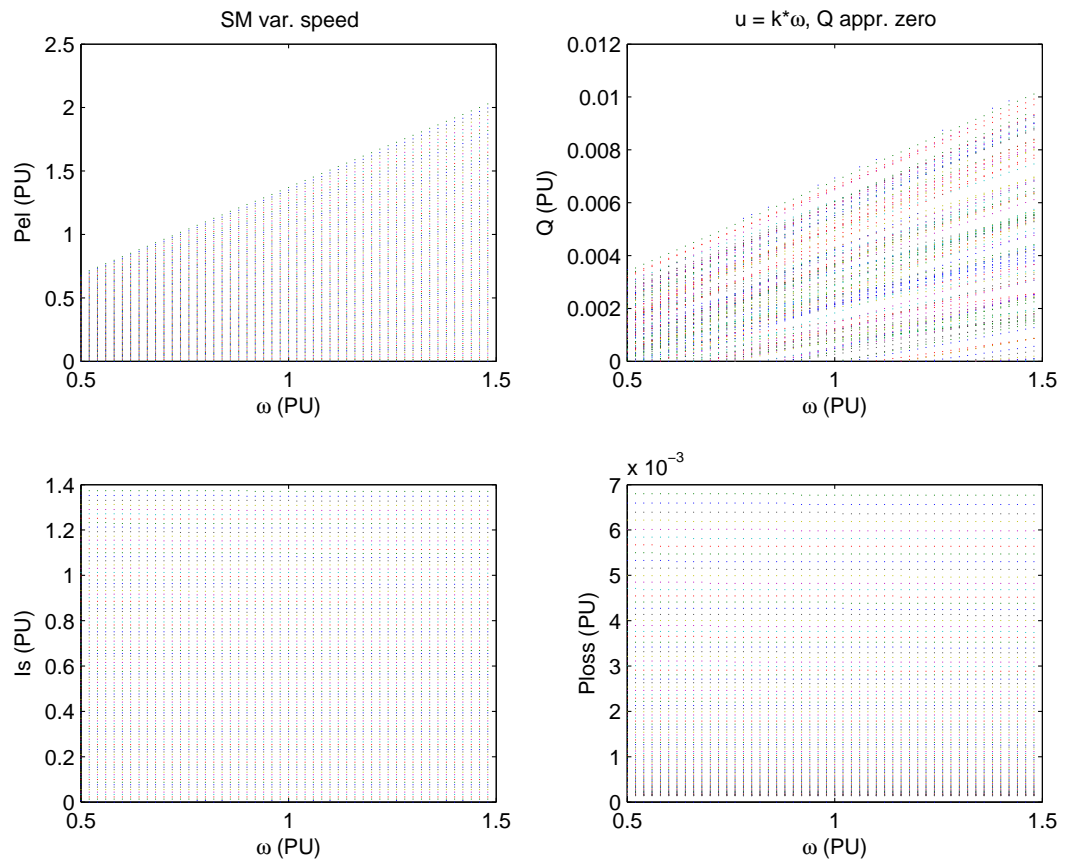


Figure 34: Steady state model of the synchronous machine: lookup table values for reactive power $Q = 0$

Next, the effective stator voltage is chosen proportional to the rotational speed: $u = \frac{\omega_r}{\omega_{rated}} u_{rated}$. The speed ω_r , electric power P , losses P_{loss} and AC current and voltage i, i at zero reactive power are saved to corresponding matrices. Figure 34 shows the results, with speed at the x-axis and power, reactive power, current and losses at the y-axis. The matrices $u(\omega, P)$, $i(\omega, P)$ and $P_{loss}(\omega, P)$ are used in the Simulink model as a lookup table, see figure 37.

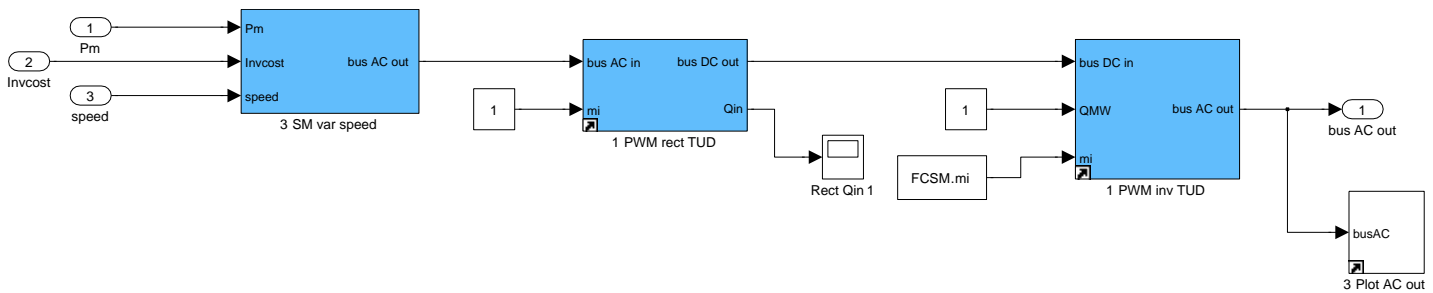


Figure 35: EeFarm-II model of the FCSM system

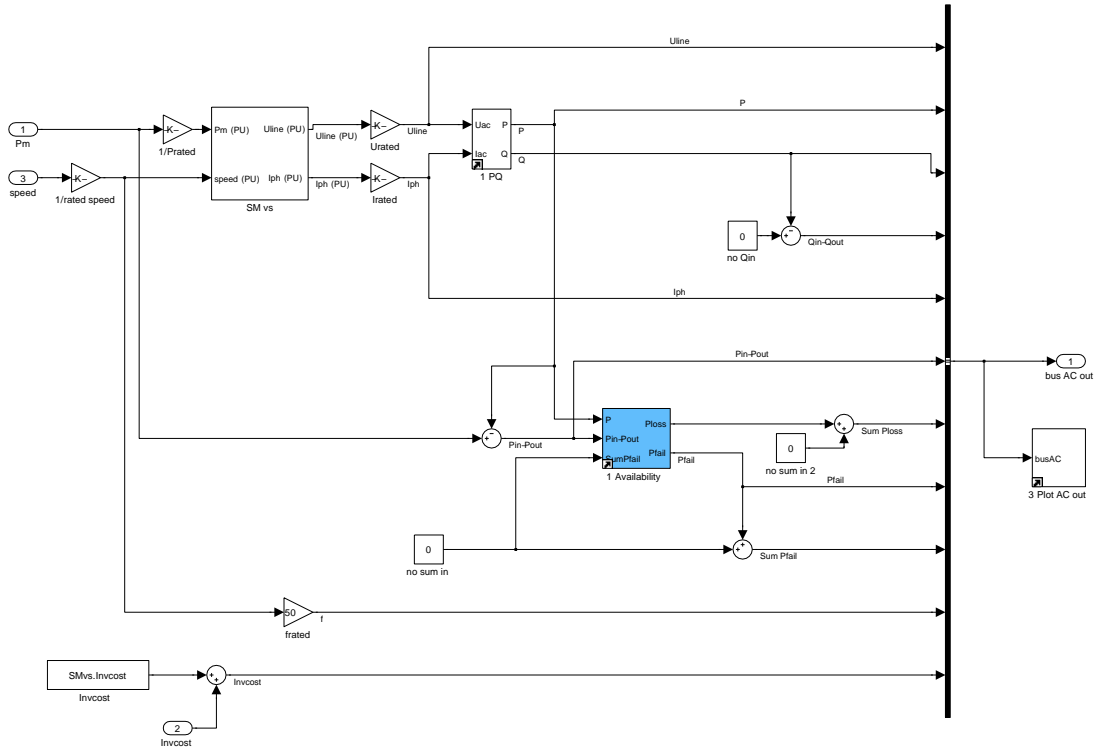


Figure 36: EeFarm-II model of the variable speed induction machine in the FCSM system

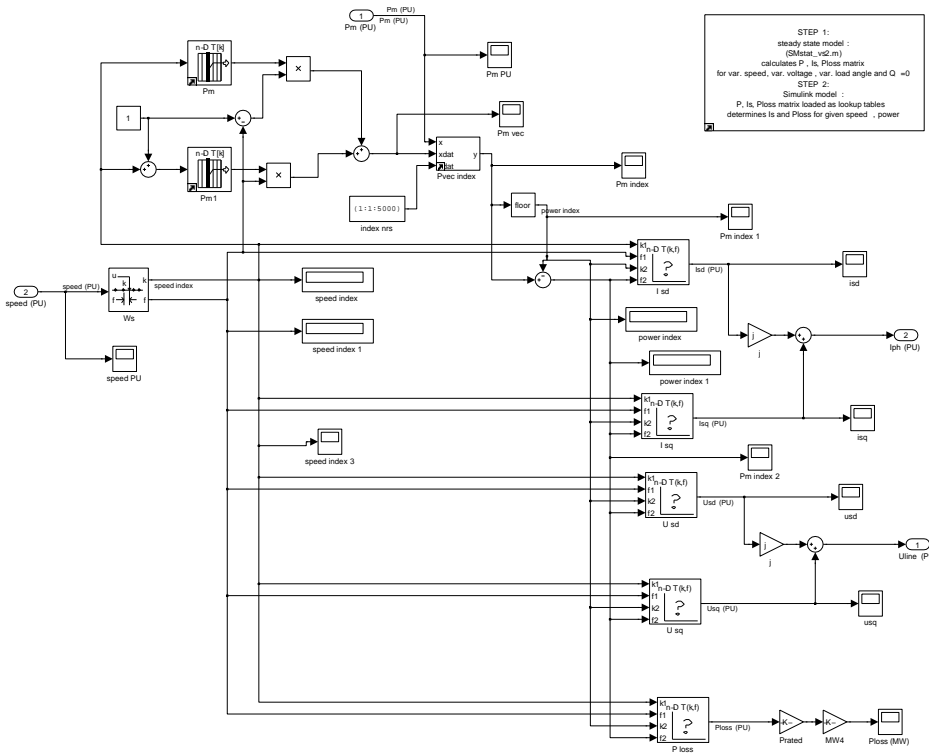


Figure 37: Lookup table evaluation in the FCSM model

3.3 AC cable models

3.3.1 Constant temperature AC cable model

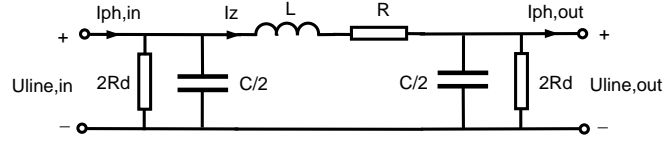


Figure 38: AC cable single line diagram

Model	AC cable, constant temperature
Input	$\underline{U}_{line,in}, \underline{I}_{line,in}$
Output	$\underline{U}_{line,out}, \underline{I}_{line,out}, P, P_{loss}, \sum P_{loss}, \sum Inv_{cost}, \sum P_{fail}$
Parameters	$f, C_{km}, R_{ac20,km}, R_{ac90,km}, R_{dc20,km}, R_{dc90,km}, L_{km}, \tan(\delta), Length$

with δ the dielectric loss factor.

$$\begin{aligned}
 C &= Length \cdot C_{km} \\
 L &= Length \cdot L_{km} \\
 R &= Length \cdot R_{km} \\
 R_d &= \frac{1}{\omega C \tan \delta} \\
 \underline{I}_{C,in} &= \frac{j\omega C \underline{U}_{line,in}}{2} \\
 \underline{I}_{d,in} &= \frac{\underline{U}_{line,in}}{2R_d} \\
 \underline{I}_Z &= \underline{I}_{ph,in} - \underline{I}_{C,in} - \underline{I}_{d,in} \\
 \underline{U}_{line,out} &= \underline{U}_{line,in} - (R + j\omega L) \underline{I}_Z \\
 \underline{I}_{C,out} &= \frac{j\omega C \underline{U}_{line,out}}{2} \\
 \underline{I}_{d,out} &= \frac{\underline{U}_{line,out}}{2R_d} \\
 \underline{I}_{ph,out} &= \underline{I}_Z - \underline{I}_{C,out} - \underline{I}_{d,out}
 \end{aligned}$$

with R_d the equivalent dielectric loss resistance [25].

The resistance R_{km} is calculated during initialisation for a fixed temperature and a fixed frequency using:

$$\begin{aligned}
 R_{20,km} &= R_{dc20,km} + (R_{ac20,km} - R_{dc20,km}) \cdot \frac{f}{50} \\
 R_{90,km} &= R_{dc90,km} + (R_{ac90,km} - R_{dc90,km}) \cdot \frac{f}{50}
 \end{aligned}$$

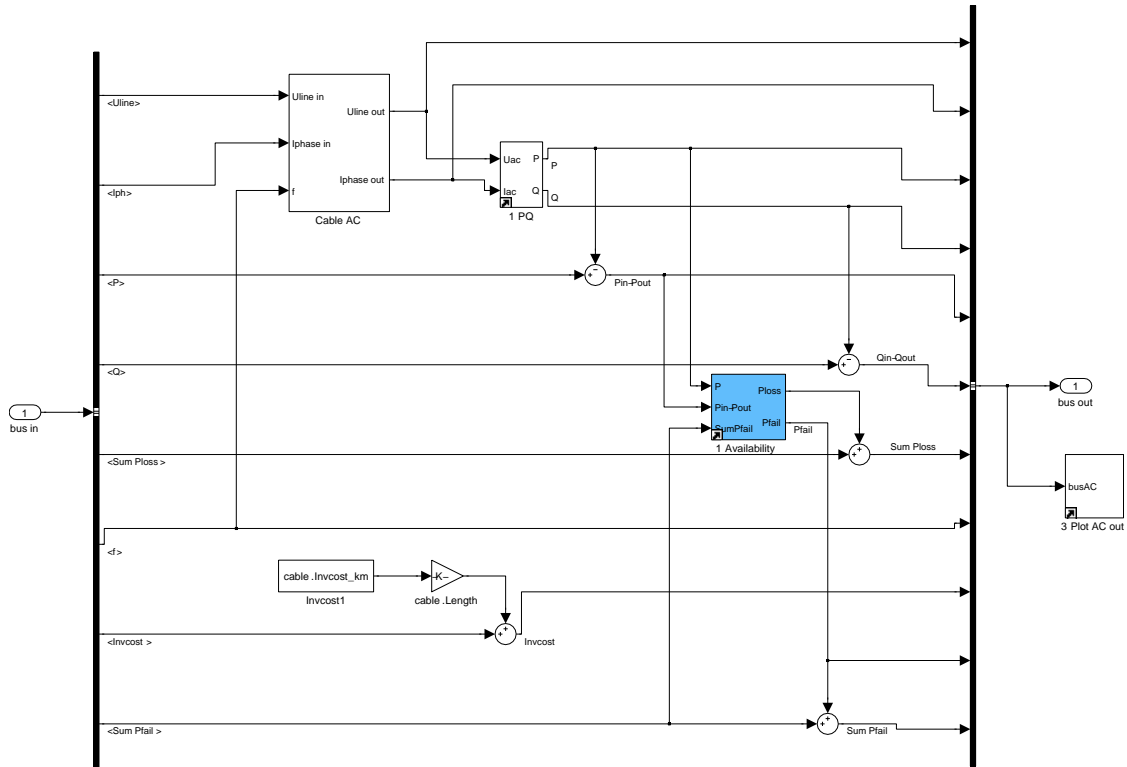


Figure 39: EeFarm-II model of an AC cable

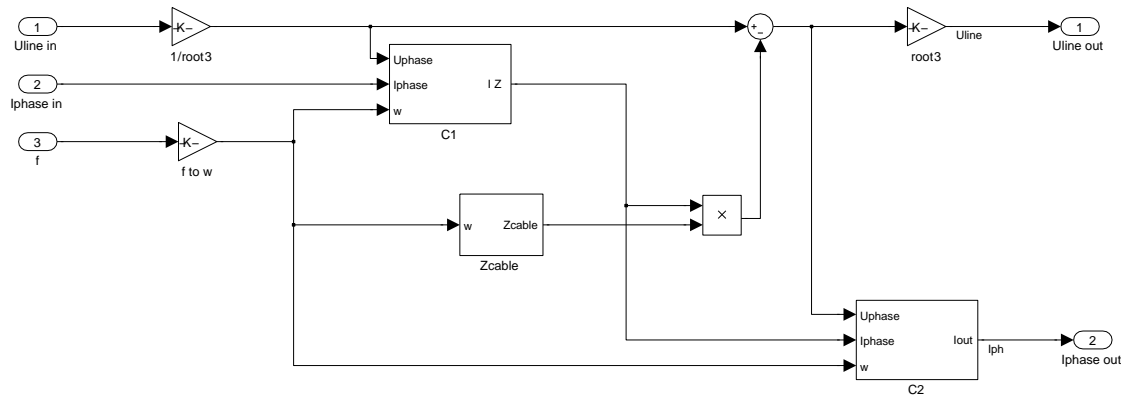


Figure 40: EeFarm-II model of an AC cable

3.3.2 AC cable model with temperature dependent resistance

Model	AC cable, variable temperature
Input	$\underline{U}_{line,in}, \underline{I}_{line,in}$
Output	$\underline{U}_{line,out}, \underline{I}_{line,out}, P, P_{loss}, \sum P_{loss}, \sum Invcost, \sum P_{fail}$
Parameters	$f, C_{km}, R_{ac20,km}, R_{ac90,km}, R_{dc20,km}, R_{dc90,km}, L_{km}, \tan(\delta), Length, R_{th}, T_{sur}$

This model is electrically the same as the constant turbine model, extended with an iterative calculation of the cable temperature and a temperature dependent cable resistance.

$$T_{cable} = T_{sur} + \frac{R_{th}}{1000} \cdot \frac{P_{loss}}{3Length}$$

$$R_{km} = R_{20,km} + (T_{cable} - T_{sur}) \cdot \frac{R_{90,km} - R_{20,km}}{70}$$

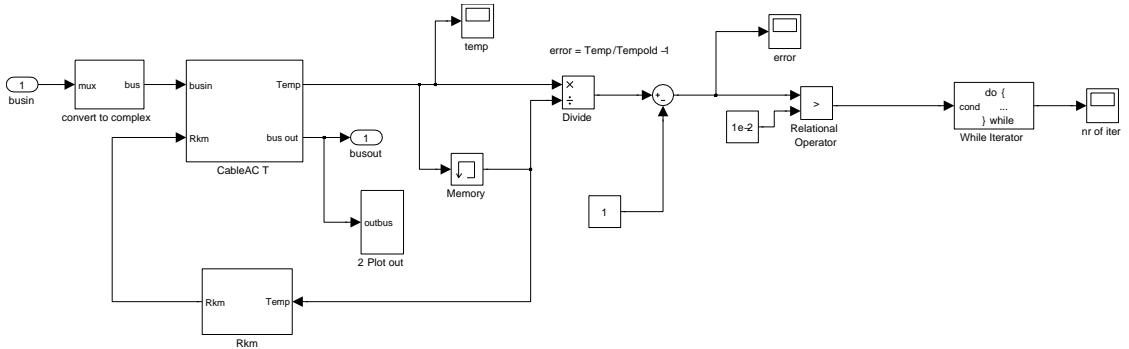


Figure 41: EeFarm-II model of an AC cable with variable temperature

Since the iteration increases the simulation time considerably, a AC cable model with temperature dependent resistance without iteration should be developed. A possible option is to use a pre-calculated relation between T and I , see Appendix D.3. The relation between the cable current and the cable temperature is determined, based on the assumption that the cable temperature is 20° at zero current and 90° at maximum cable current. In EeFarm II this can be implemented as a precalculated lookup table with the cable AC current as input and the cable temperature as output.

3.4 Transformer model

3.4.1 Transformer without reactive power consumption

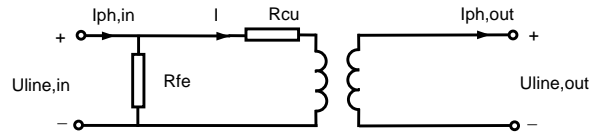


Figure 42: Transformer single line diagram

Model	Transformer without reactive power consumption
Input	$\underline{U}_{in}, \underline{I}_{in}$
Output	$\underline{U}_{out}, \underline{I}_{out}, P, P_{loss}, \sum P_{loss}, \sum Invcost, \sum P_{fail}$
Parameters	$R_{cu,lo}, R_{fe,lo}$

The parameters needed for the transformer model are the voltage ratio U_{hi}/U_{lo} , the iron losses $R_{fe,lo}$ and the copper losses $R_{cu,lo}$ (referring to the low voltage side of the transformer). The transformer voltage equations are:

$$I = I_{ph,in} - \frac{U_{line,in}}{\sqrt{3}R_{fe,lo}}$$

$$I_{ph,out} = \frac{U_{lo}}{U_{hi}} I$$

$$U_{line,out} = \frac{U_{hi}}{U_{lo}} (U_{line,in} - \sqrt{3}R_{cu,lo}I)$$

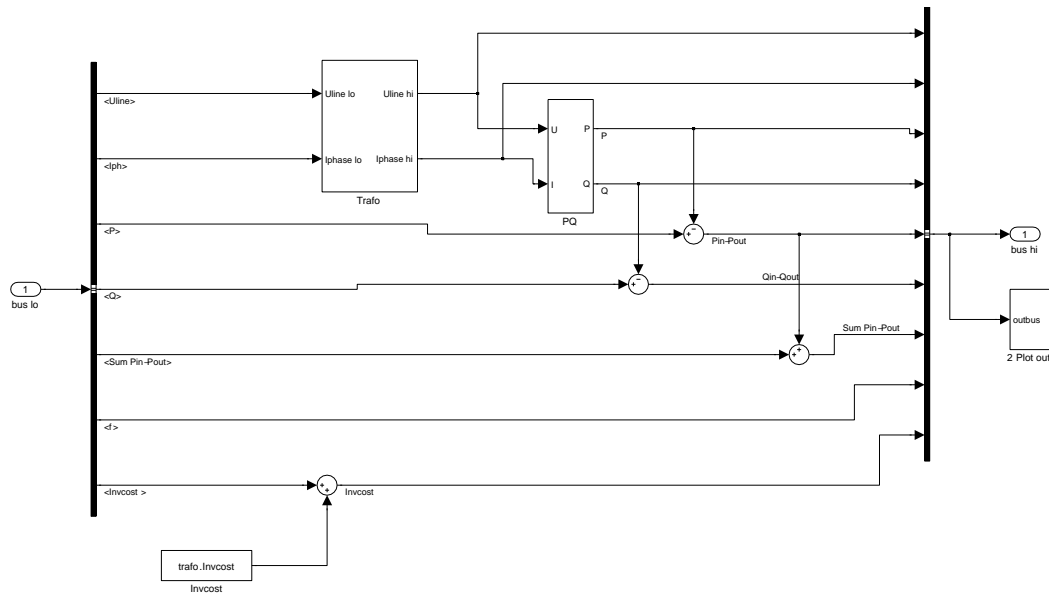


Figure 43: EeFarm-II model of a transformer

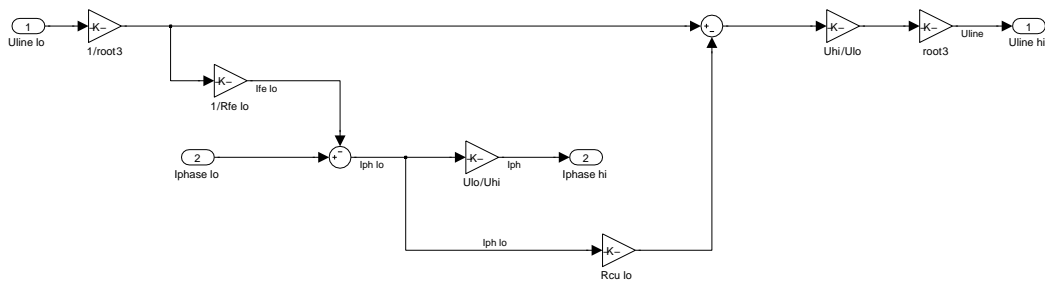


Figure 44: EeFarm-II model of a transformer, part 2

3.4.2 Transformer with reactive power consumption

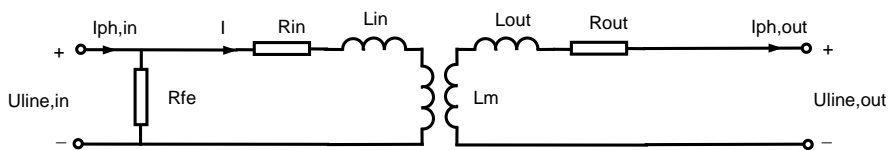


Figure 45: Transformer single line diagram

Model	Transformer with reactive power consumption
Input	$\underline{U}_{in}, \underline{I}_{in}$
Output	$\underline{U}_{out}, \underline{I}_{out}, P, P_{loss}, \sum P_{loss}, \sum Invcost, \sum P_{fail}$
Parameters	$R_{fe}, R_{in}, L_{in}, L_m, L_{out}, R_{out}$

with R_{fe} the equivalent magnetising loss resistance
 R_{in}, R_{out} the resistance of primary and secondary side
 L_{in}, L_{out} the leakage inductance of primary and secondary side
 L_m the mutual inductance

The equations for the transformer model with magnetising and ohmic losses and reactive power consumption are:

$$\begin{aligned}
 i_{d,fe} &= \frac{u_{d,in}}{R_{fe}} \\
 i_{q,fe} &= \frac{u_{q,in}}{R_{fe}} \\
 i_{d,1} &= i_{d,in} - i_{d,fe} \\
 i_{q,1} &= i_{q,in} - i_{q,fe} \\
 i_{q,out} &= \frac{u_{d,in} - r_{in}i_{d,in} - \omega(l_{in} + l_m)i_{q,in}}{\omega l_m} \\
 i_{d,out} &= \frac{u_{q,in} - r_{in}i_{q,in} + \omega(l_{in} + l_m)i_{d,in}}{-\omega l_m} \\
 u_{d,out} &= \omega l_m i_{q,in} + r_{out}i_{d,out} + \omega(l_{out} + l_m)i_{q,out} \\
 u_{q,out} &= -\omega l_m i_{d,in} + r_{out}i_{q,out} - \omega(l_{out} + l_m)i_{d,out}
 \end{aligned}$$

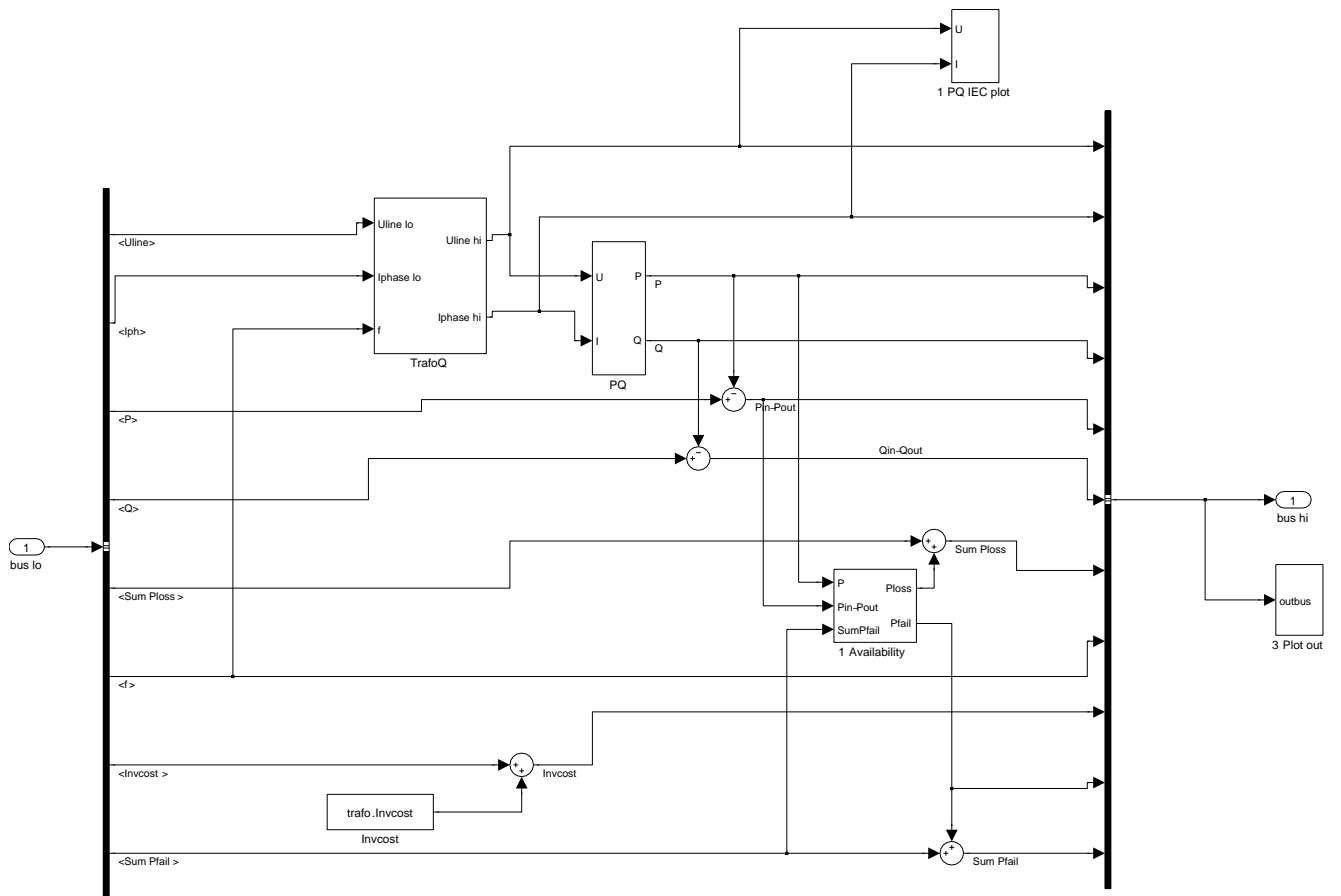


Figure 46: EeFarm-II of a transformer reactive power consumption

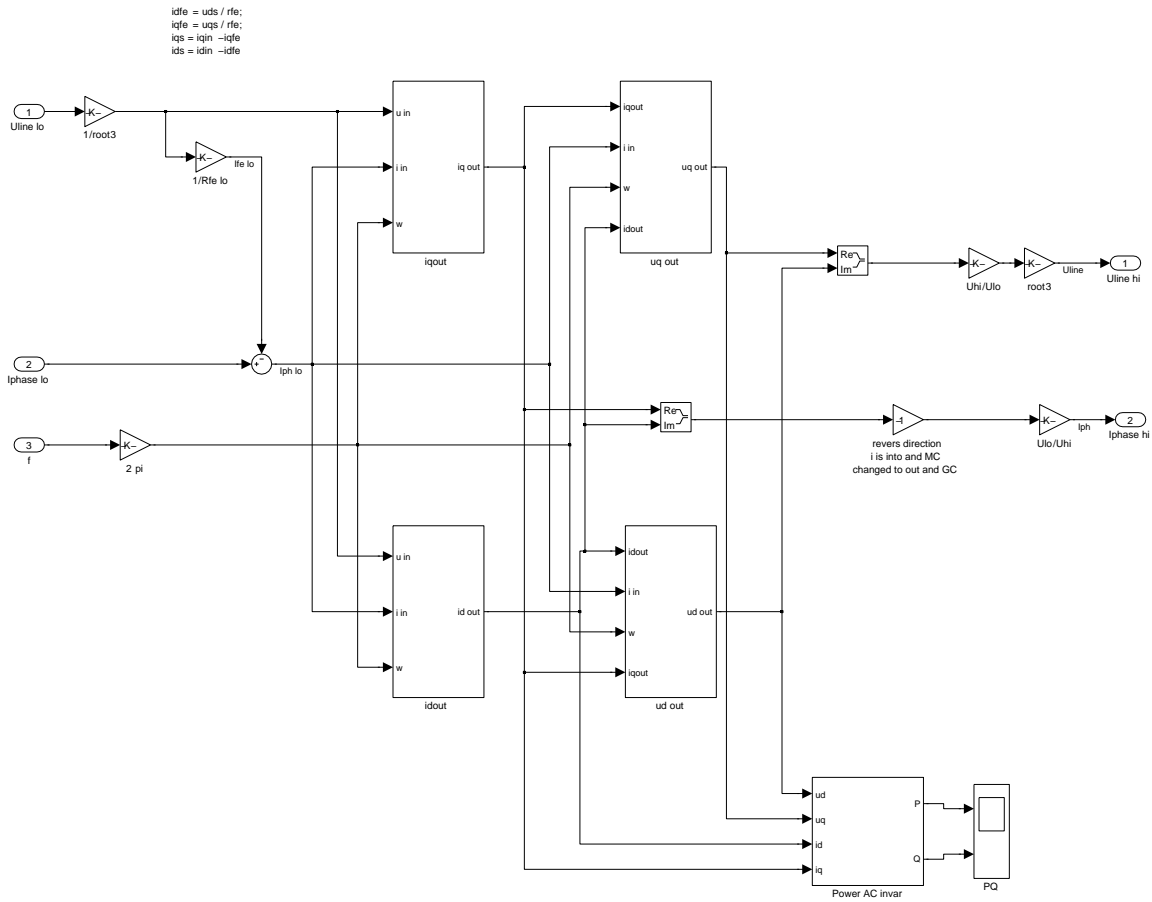


Figure 47: EeFarm-II model of a transformer reactive power consumption

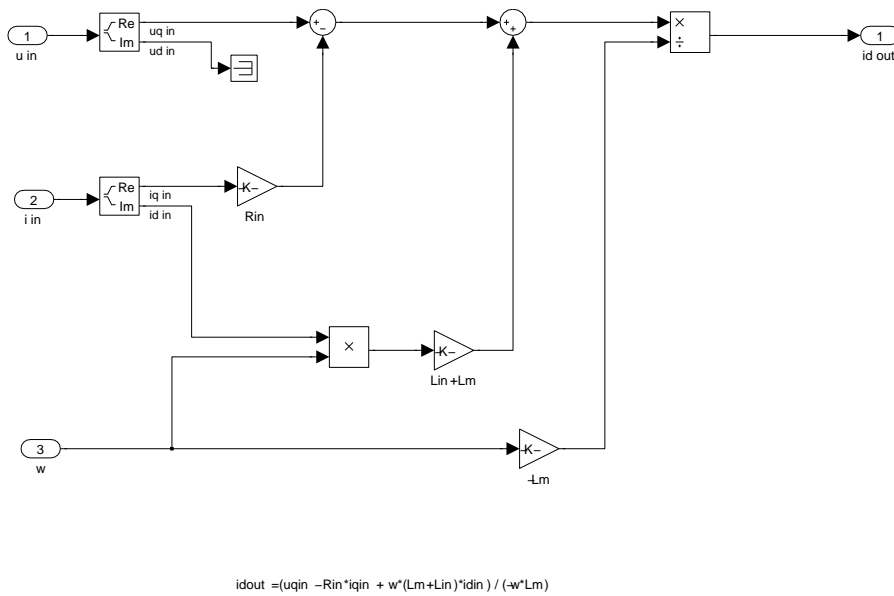


Figure 48: EeFarm-II model of a transformer reactive power consumption

3.5 Inductor model

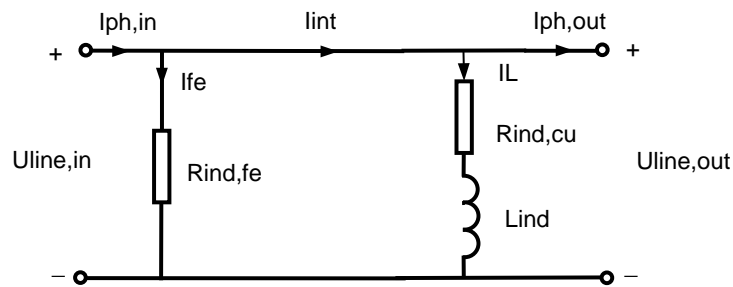


Figure 49: Inductor single line diagram

Model	Inductor
Input	$\underline{U}_{line,in}, \underline{I}_{in}$
Output	$\underline{U}_{line,out}, \underline{I}_{out}, P, P_{loss}, \sum P_{loss}, \sum Invcost, \sum P_{fail}$
Parameters	L, R_{cu}, R_{fe}

The inductor is delta connected and the model is similar to the transformer model:

$$\begin{aligned}
 \underline{U}_{line,out} &= \underline{U}_{line,in} \\
 \underline{I}_{fe} &= \frac{\underline{U}_{line,in}}{\sqrt{3}R_{fe}} \\
 \underline{I}_L &= \frac{\underline{U}_{line,in}}{\sqrt{3}(R_{cu} + j\omega L)} \\
 \underline{I}_{induc} &= \underline{I}_L + \underline{I}_{fe} \\
 \underline{I}_{out} &= \underline{I}_{in} - \underline{I}_{induc} \\
 P_{loss} &= 3 \cdot (R_{fe}I_{fe}^2 + R_{cu}I_L^2) \\
 Q &= 3 \cdot \omega L \cdot I_L^2
 \end{aligned}$$

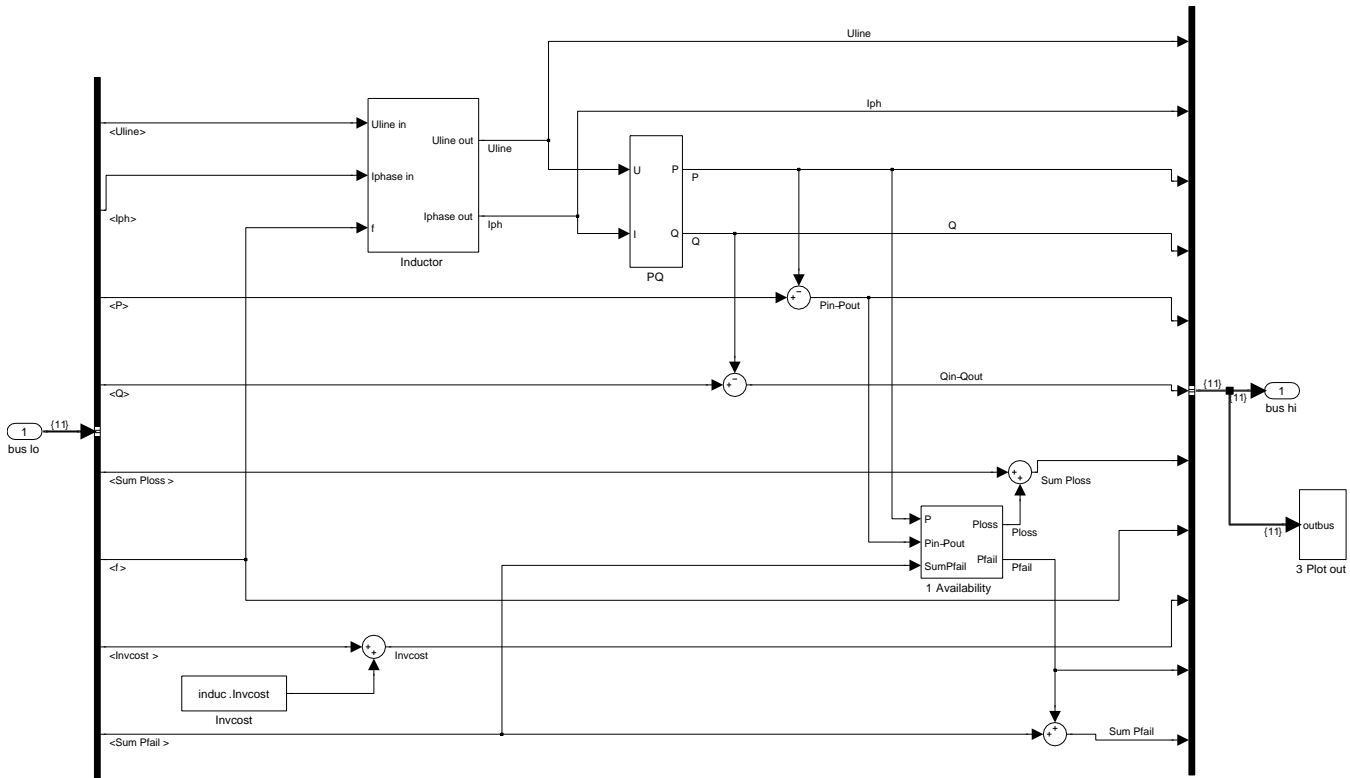


Figure 50: EeFarm-II model of an inductor

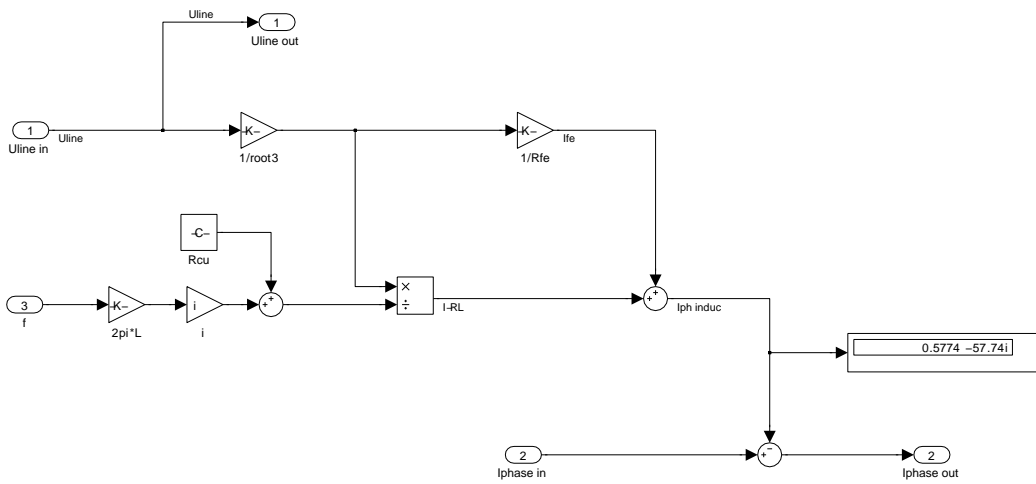


Figure 51: EeFarm-II model of an inductor

3.6 AC and DC node model

Model	AC node
Input	$\underline{U}_{in,1}, \underline{I}_{in,1}, \underline{U}_{in,2}, \underline{I}_{in,2}$
Output	$\underline{U}_{out}, \underline{I}_{out}, P, P_{loss}, \sum P_{loss}, \sum Invcost, \sum P_{fail}$
Parameters	none

An AC node is used to connect the output of two AC components. The EeFarm program does not include an iteration to match voltages at locations in the farm where two or more AC

components, for instance AC cables, with possibly slightly different voltages meet. Since the difference in angle and magnitude between two voltage phasors at any connection point inside a wind farm is expected to be very small if the component have the same voltage rating (a difference of less than a percent is expected), the output voltage of the AC node is calculated as the average of the two connecting voltages. The output current of the AC the node (magnitude and angle) is calculated from the active and reactive power balance. Since in this way no iteration is required, this simplifies the EeFarm-II calculation and makes it very fast.

$$\begin{aligned}
 \underline{U}_{out} &= \frac{U_{line,in,1} + U_{line,in,2}}{2} \\
 A &= \frac{P}{\sqrt{3}|\underline{U}_{out}|} = I_{out} \cos \phi_{out} \\
 B &= \frac{Q}{\sqrt{3}|\underline{U}_{out}|} = I_{out} \sin \phi_{out} \\
 I_{out} &= \sqrt{A^2 + B^2} \\
 \phi_{out} &= \arctan \frac{B}{A} \\
 \alpha &= \angle \underline{U}_{out} \\
 \underline{I}_{out} &= I_{out} e^{j(\alpha - \phi_{out})}
 \end{aligned}$$

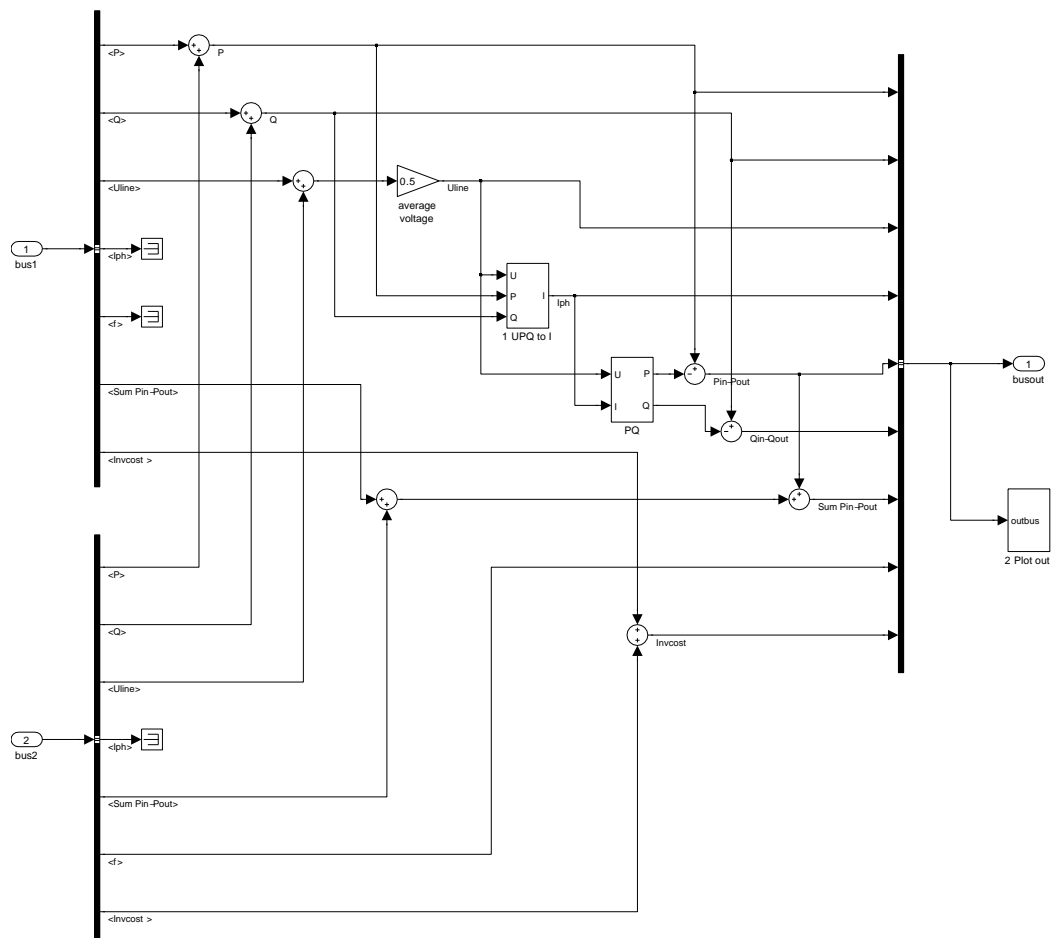


Figure 52: EeFarm-II model of a node

A DC node is used to connect the output of two DC components. It operates in exactly the same way as the AC node except that voltage and current are scalars.

3.7 DC cable model

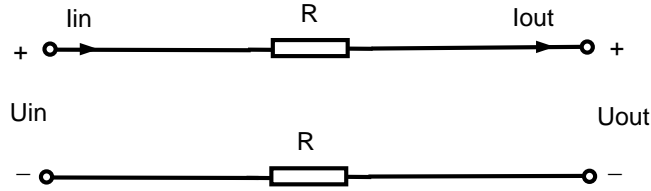


Figure 53: DC cable diagram

Model	DC cable
Input	$U_{dc,in}, I_{dc,in}$
Output	$U_{dc,out}, I_{dc,out}, P_{dc,out}, P_{dc,loss}, \sum P_{loss}, \sum Invcost, \sum P_{fail}$
Parameters	$R_{dc,20}, R_{dc,90}, T_{cable}$

The cable model assumes a bipolar configuration using two identical cables. The cable resistance is calculated assuming a constant, load independent cable temperature:

$$R_{dc} = R_{dc,20} + (T_{cable} - 20) \frac{R_{dc,90} - R_{dc,20}}{70}$$

Since the DC current and the input voltage are known, the output voltage can be determined:

$$U_{dc,out} = U_{dc,in} - 2R_{dc}I_{dc,in}$$

The voltage U_{dc} is measured between the plus and the minus pole. This is consistent with the definition of the voltage in the converter models. The equations for the power and the power loss complete the model:

$$\begin{aligned} P_{dc,in} &= U_{dc,in}I_{dc,in} \\ P_{dc,out} &= U_{dc,out}I_{dc,out} \\ P_{dc,loss} &= P_{dc,in} - P_{dc,out} \end{aligned}$$

Appendix D.3 describes the effect of the temperature on the cable resistance. The relation between the cable current and the cable temperature is determined, based on the assumption that the cable temperature is 20° at zero current and 90° at maximum cable current. In EeFarm II this can be implemented as a precalculated lookup table with the cable DC current as input and the cable temperature as output.

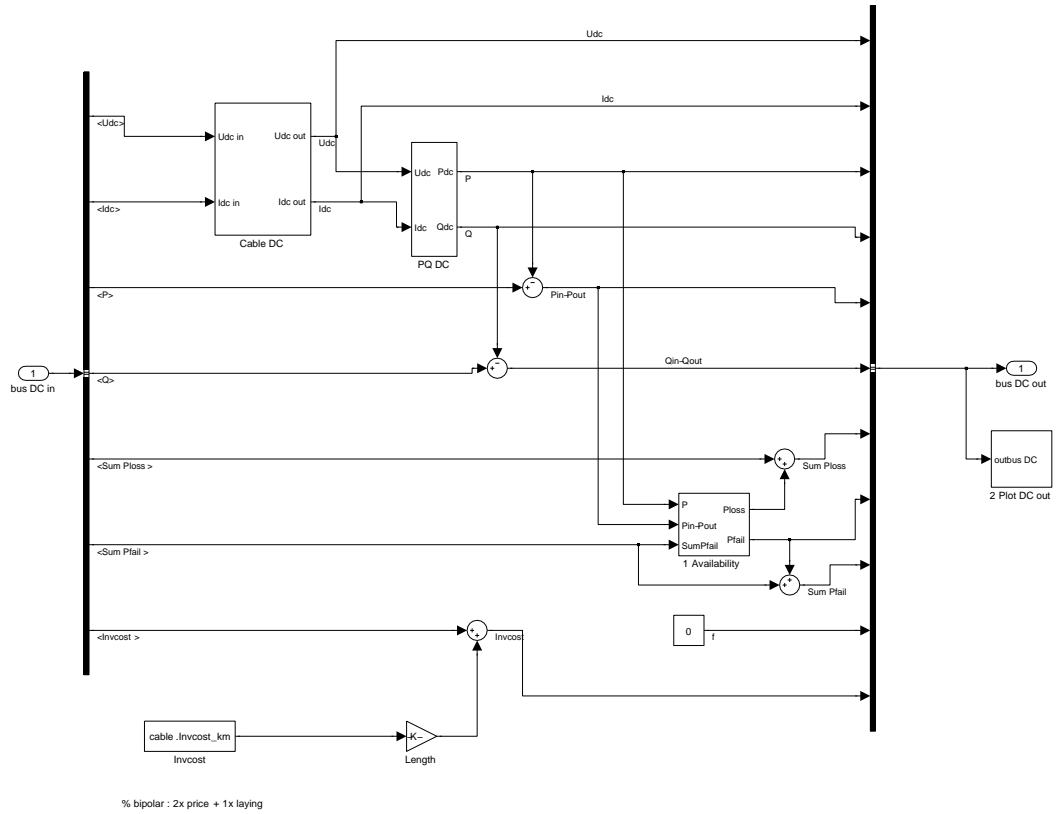


Figure 54: EeFarm-II model of the DC cable

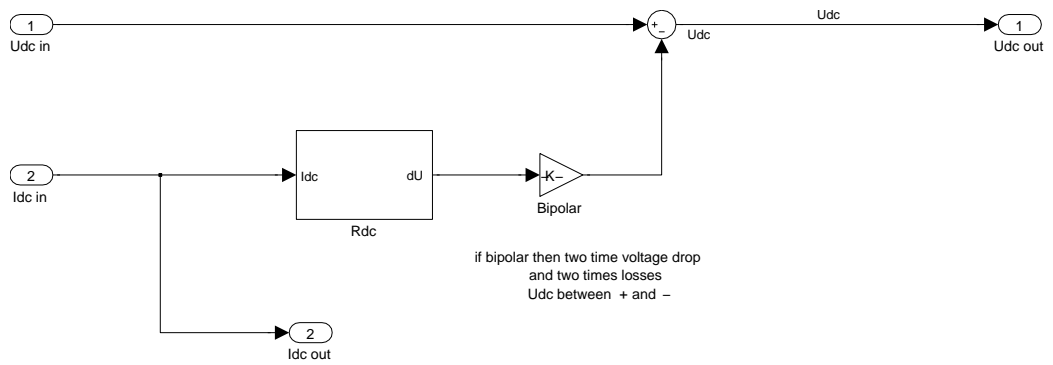


Figure 55: EeFarm-II model of the losses in the DC cable

3.8 Diode and thyristor rectifier, inverter and back-to-back converter models

3.8.1 Diode rectifier and thyristor rectifier

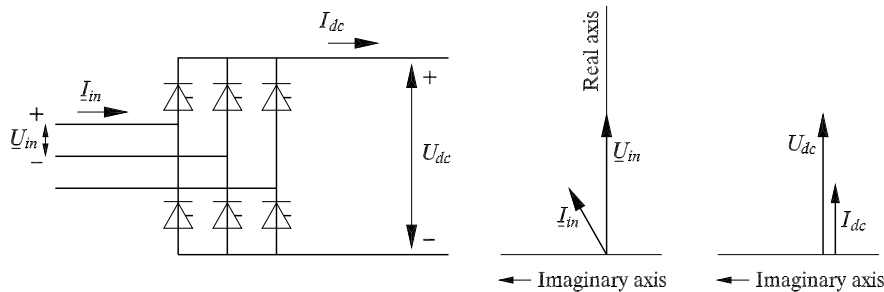


Figure 56: Thyristor rectifier diagram

Model	Thyristor rectifier
Input	$\underline{U}_{ac}, P_{ac}, \alpha$
Output	$U_{dc}, I_{dc}, \underline{I}_{ac}, Q_{ac}, P, P_{loss}, \sum P_{loss}, \sum Inv_{cost}, \sum P_{fail}$
Parameters	E_0, R_{on}

with E_0 the thyristor voltage drop,
 R_{on} the thyristor internal resistance

For the diode and thyristor rectifier model is assumed that the input AC power, the input AC voltage and the firing angle are known. The losses of the diode and thyristor rectifier are the result of a threshold voltage E_0 and an internal resistance R_{on} (see figure 57). The effect of commutation is neglected, so the displacement power factor $\cos \phi_1$ is equal to $\cos \alpha$ and the power factor $\frac{P}{S}$ is equal to $\frac{3 \cos \alpha}{\pi}$ [13].

The thyristor rectifier consumes reactive power, it can not supply reactive power. The reactive power required by the rectifier and by the AC components connected to the rectifier terminals are assumed to be supplied by a reactive power source, e.g. the AC grid or a switched condenser battery or statcom connected at or near the rectifier terminals.

The rectifier model calculates the average DC voltage, the average DC current and the losses. Since commutation is neglected, the average DC voltage of the thyristor rectifier equals:

$$U_{dc} = \frac{3\sqrt{2}}{\pi} |\underline{U}_{ac, line, rms}| \cos \alpha$$

In case of a diode rectifier, the firing angle α is zero.

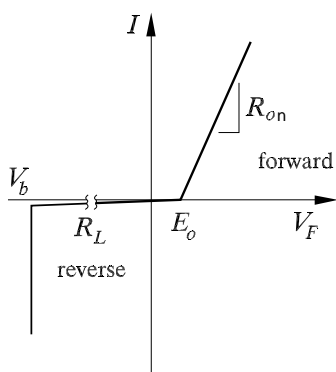


Figure 57: Idealized VA curve of diode and thyristor

The AC current amplitude is equal to:

$$|\underline{I}_{ac, rms}| = \frac{P_{ac}}{\sqrt{3}|\underline{U}_{ac, line, rms}| \cos \alpha}$$

The apparent power and the reactive power consumed by the rectifier are:

$$\begin{aligned} S_{in} &= \sqrt{3}|\underline{U}_{ac, line, rms}||\underline{I}_{ac, rms}| = \frac{P_{ac}}{\cos \alpha} \\ Q_{in} &= S_{in} \sin \alpha \end{aligned}$$

If the angle of the AC voltage is equal to β , the AC current is equal to

$$\underline{I}_{ac, rms} = |\underline{I}_{ac, rms}|(\cos(\alpha + \beta) + j \sin(\alpha + \beta))$$

Since commutation is neglected, two switches are conducting and the losses are:

$$P_{loss} = 2E_0 I_{dc} + 2R_{on} I_{dc}^2$$

The input power equals:

$$P_{ac} = (U_{dc} + 2E_0)I_{dc} + 2R_{on} I_{dc}^2$$

Since the DC current is positive, it is equal to:

$$I_{dc} = -\frac{U_{dc} + 2E_0}{4R_{on}} + \sqrt{\left(\frac{U_{dc} + 2E_0}{4R_{on}}\right)^2 + \frac{P_{ac}}{2R_{on}}}$$

If the resistance $R_{on} = 0$, this reduces to:

$$I_{dc} = \frac{P_{ac}}{U_{dc} + 2E_0}$$

The output power of the rectifier equals:

$$P_{dc} = U_{dc} I_{dc}$$

For a firing angle between 0 and 90 degrees, the amount of reactive power increases, at 90 degrees the active power is zero. To carry the same amount of input power, the DC current has to increase if the firing angle is increased and the DC voltage decreases. This corresponds to an increasing amount of reactive power requested by the rectifier and increasing losses.

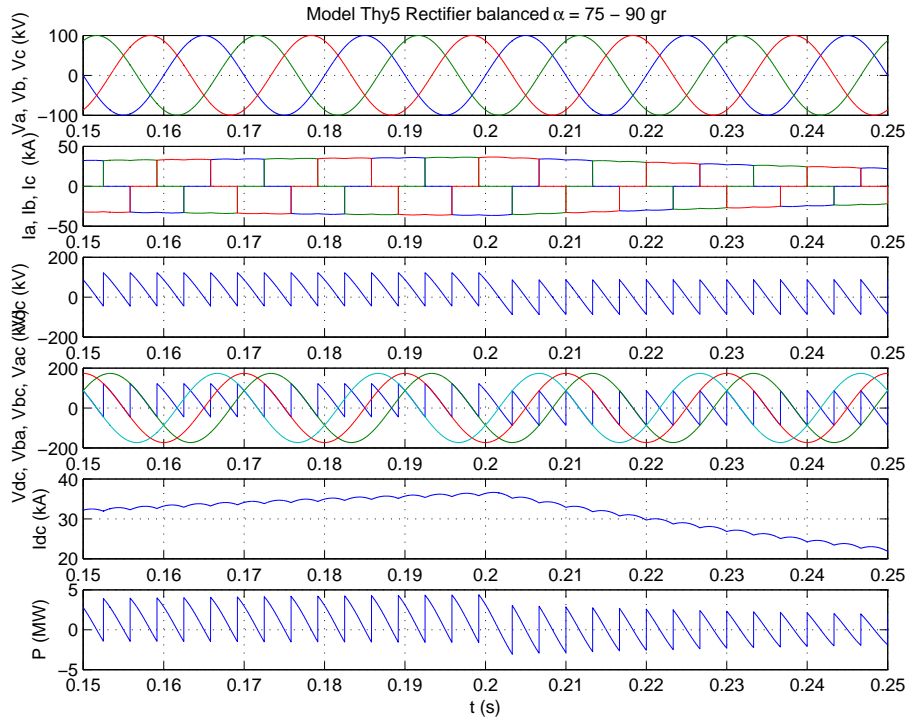


Figure 58: Thyristor rectifier operating at 75 and 90 degree firing angle (DynFarm)

Voltage and current wave forms as well as the instantaneous power of a thyristor rectifier using a instantaneous dynamic model (DynFarm) are plotted in figure 58 for a firing angle of 75 and 90 degrees.

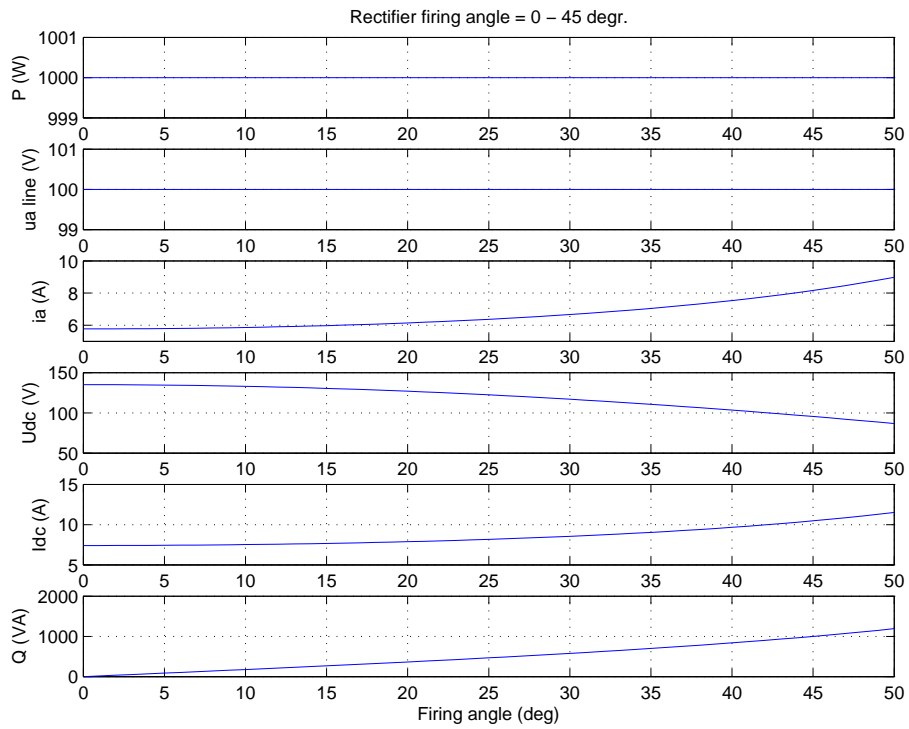


Figure 59: Thyristor rectifier curves for a firing angle between 0 and 50 degrees (EeFarm)

Figure 59 shows that an increasing firing angle results in an increasing AC as well as an increasing DC current and thus increasing losses in the rectifier (constant power assumed). The thyristor rectifier can be controlled by the firing angle.

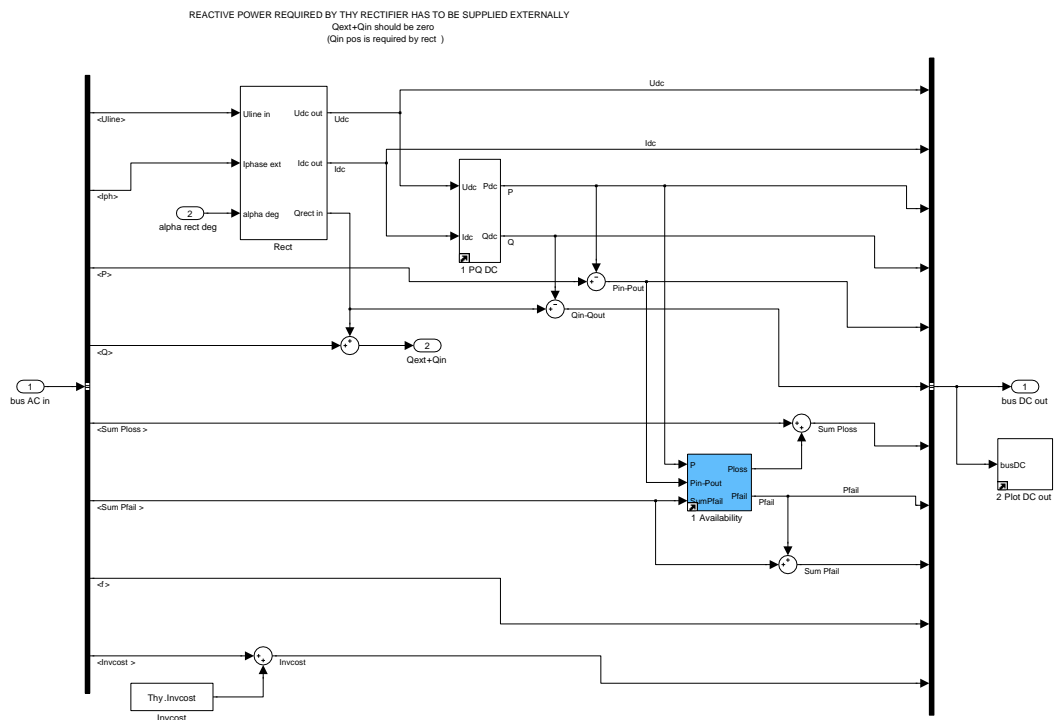


Figure 60: EeFarm-II model of a thyristor rectifier

$0 < \text{firing angle } \alpha < 90 \text{ gr}$
 firing angle is w. r.t. U_{a-Uc} (coupled voltage)
 i_{f} is practically equal to α
 MOTORCONVENTION :
 $P > 0$,
 $Q > 0$,
 underexcited
 $0 < i_{f} < 90 \text{ gr}$

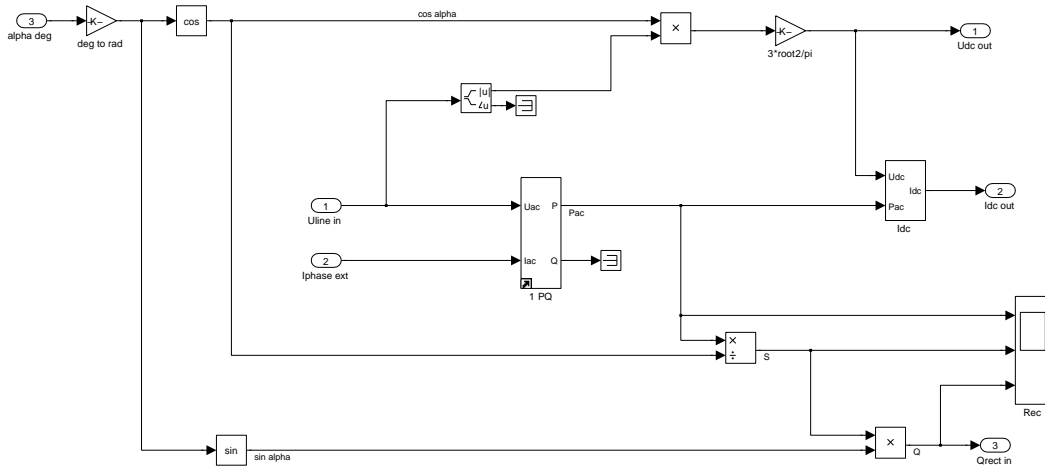


Figure 61: EeFarm-II thyristor rectifier power and voltage calculation

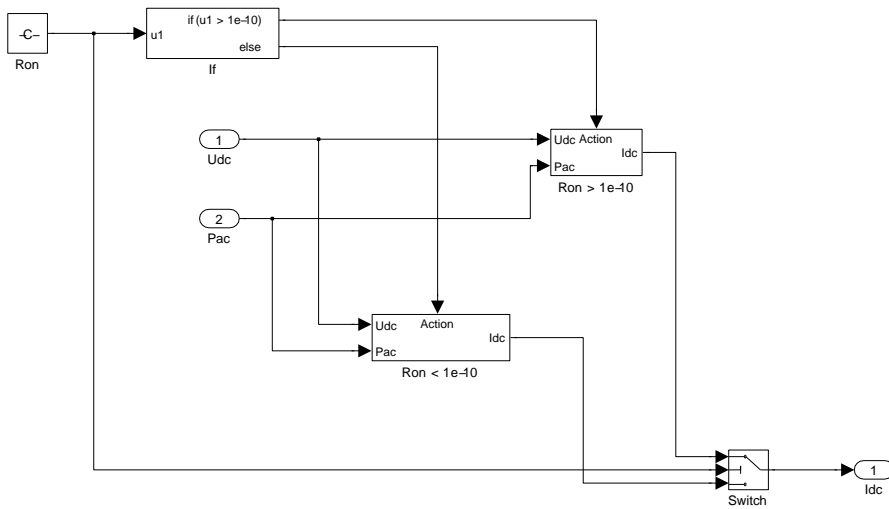
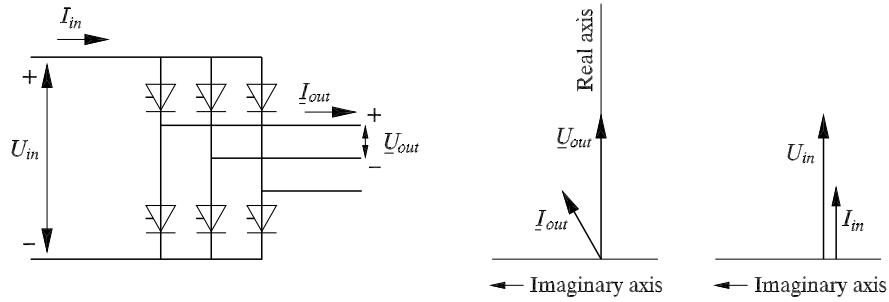


Figure 62: EeFarm-II thyristor rectifier current calculation

3.8.2 Thyristor inverter

Figure 63: *Thyristor inverter diagram*

Model	Thyristor inverter
Input	U_{dc}, I_{dc}, α_i
Output	$\underline{U}_{ac}, \underline{I}_{ac}, P, P_{loss}, \sum P_{loss}, \sum Inv_{cost}, \sum P_{fail}$
Parameters	E_0, R_{on}

with E_0 the thyristor voltage drop,
 R_{on} the thyristor internal resistance

The model of the thyristor inverter is similar to that of the thyristor rectifier, but now the point of departure is the DC voltage and current. E_0 is the threshold voltage and R_{on} is the resistance in on state. Commutation is neglected. The losses are:

$$P_{loss} = 2E_0I_{dc} + 2R_{on}I_{dc}^2$$

The AC power equals:

$$P_{ac} = U_{dc}I_{dc} - P_{loss}$$

The output AC voltage equals:

$$U_{ac, line, rms} = \frac{\pi}{3\sqrt{2}} \frac{U_{dc}}{\cos \alpha_i}$$

The AC current amplitude is equal to:

$$|\underline{I}_{ac, rms}| = \frac{P_{ac}}{\sqrt{3}|\underline{U}_{ac, line, rms}| \cos \alpha_i}$$

The apparent power and the reactive power are:

$$\begin{aligned} S_{in} &= \sqrt{3}|\underline{U}_{ac, line, rms}||\underline{I}_{ac, rms}| \\ Q_{in} &= S_{in} \sin \alpha_i \end{aligned}$$

The angle of the AC voltage is assumed to be zero. The AC voltage and current are:

$$\begin{aligned} \underline{U}_{ac, rms} &= |\underline{U}_{ac, rms}|(1 + 0j) \\ \underline{I}_{ac, rms} &= |\underline{I}_{ac, rms}|(\cos \alpha_i + j \sin \alpha_i) \end{aligned}$$

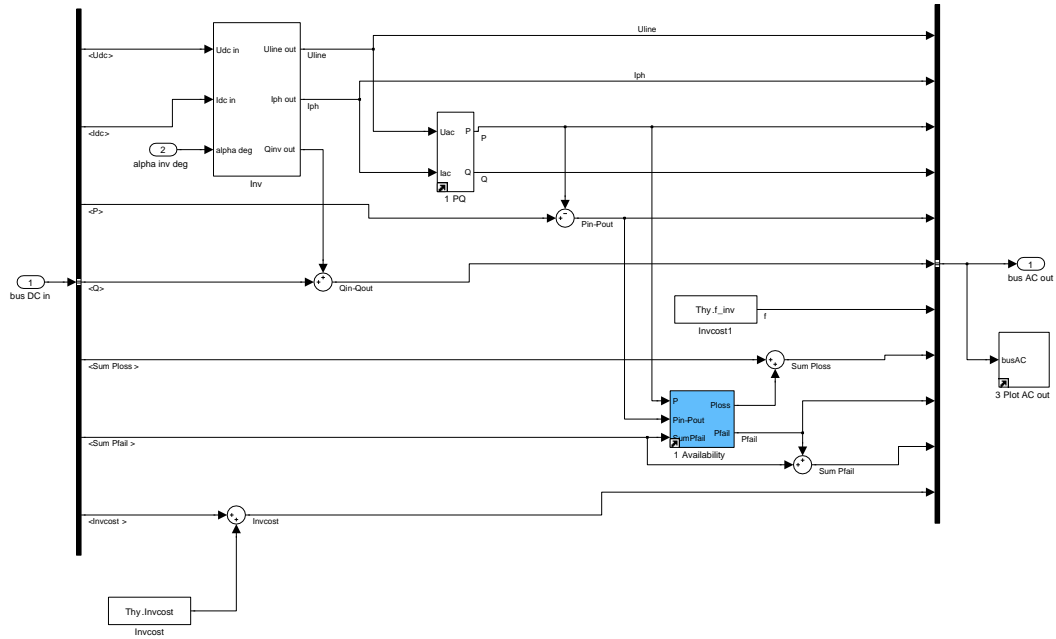


Figure 64: EeFarm-II model of a thyristor inverter

$90 < \text{firing angle } \alpha < 180 \text{ gr}$
 firing angle α is w.r.t. U_a-U_c (coupled voltage)
 f is practically equal to α
 MOTORCONVENTION :
 $P < 0$,
 $Q > 0$,
 $90 < f \leq 180 \text{ gr}$
 GENERATOR CONVENTION :
 $P > 0$
 $Q < 0$
 $-90 < f \leq 0$

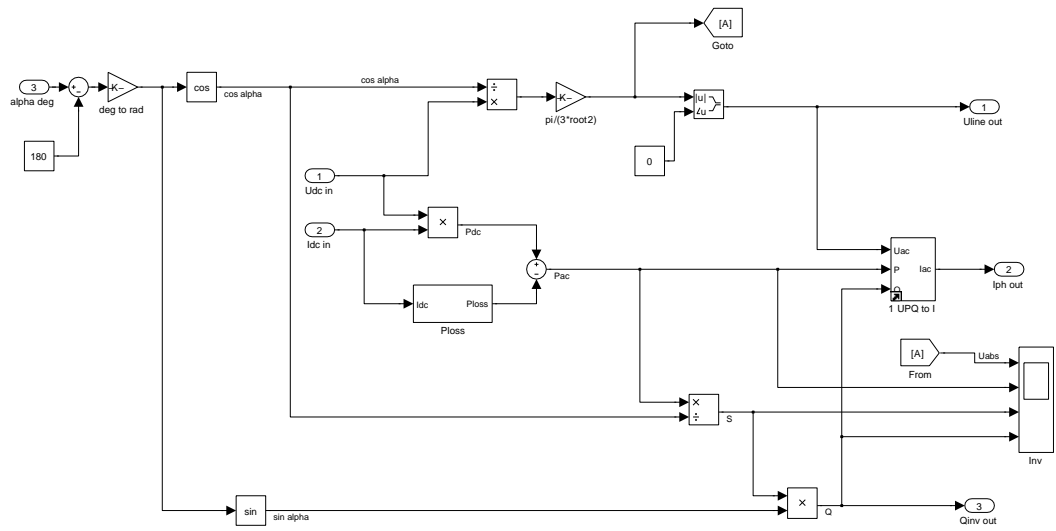


Figure 65: EeFarm-II thyristor inverter voltage and current calculation

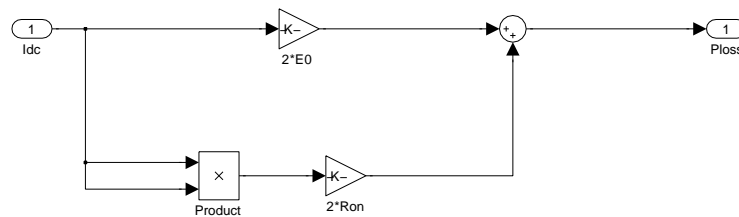


Figure 66: EeFarm-II thyristor inverter losses calculation

3.8.3 Thyristor back-to-back converter

The model of a back-to-back converter consists of a thyristor rectifier model with the output (DC) connected to the input (DC) of the thyristor inverter model.

3.9 PWM rectifier, inverter and back-to-back converter models

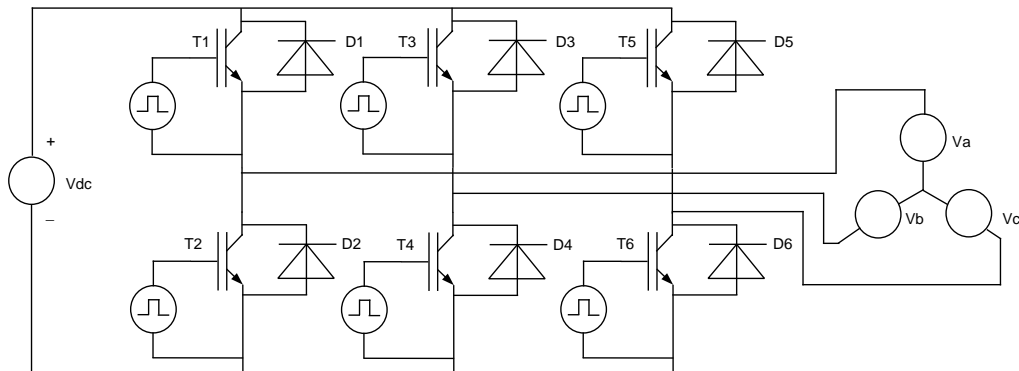


Figure 67: PWM inverter

Three different models for the losses of the PWM rectifier and inverter have been investigated. These models have been developed by TU Delft [17], Kazmierkowski [1] and Infineon [9]. The reason for three models of the same component was that the first two can not handle a small or zero power factor. The TUD model could handle a small or zero power factor after a small modification: the current used to calculate the losses is based on the apparent power instead of the active power. The Infineon model has no limitations with respect to the power factor.

3.9.1 PWM rectifier (Infineon)

Component	Input	Output	Parameters
PWM rectifier	$\underline{U}_{ac}, \underline{I}_{ac}, m, f$	$U_{dc}, I_{dc}, P_{loss},$ $\sum P_{loss}, \sum Inv_{cost}, \sum P_{fail}$	$V_{T0}, r_T, f_{sw}, E_{Ton}, E_{Toff}$ $I_{nom}, V_{nom}, V_{D0}, r_D, E_{Drec}$

with V_{T0}, V_{D0} the current independent part of transistor and diode voltage drops,

r_T, r_D the transistor and diode resistances,

m the modulation index,

I_{nom} rated AC current,

U_{nom} rated DC voltage,

E_{Ton} the turn-on energy dissipation per switching pulse at nominal current and voltage I_{nom}, V_{nom} ,

E_{Toff} the turn-off energy dissipation per switching pulse at nominal current and voltage I_{nom}, V_{nom} ,

f_{sw} the switching frequency

The following model of the switching and conduction losses is based on the description of the Infineon dimensioning program IPOSIM, which estimates the losses and the temperature of Infineon IGBT modules [9]. A more detailed description of this IGBT loss model is given by Radun [24]. This section gives the Infineon equations used in the EeFarm II recifier model. The losses consist of four parts: the conduction and switching losses of the IGBTs and the conduction and switching losses of the diodes. The conduction losses of the IGBTs (subscript T) are:

$$P_{cond,T} = \frac{1}{2}(V_{T0}\frac{\hat{i}}{\pi} + r_T\frac{\hat{i}^2}{4}) + m \cos \phi (V_{T0}\frac{\hat{i}}{8} + r_T\frac{\hat{i}^2}{3\pi})$$

with

$$\begin{aligned} i(t) &= \hat{i} \sin \omega t && \text{the sinusoidal input current} \\ v_T(t) &= V_{T0} + r_T i(t) && \text{the IGBT on-state voltage according to } i = f(v_T) \end{aligned}$$

m is the modulation factor. For $0 < m \leq 1$ (linear mode of the PWM), the AC voltages are:

$$\begin{aligned} v_a(t) &= V_{DC}(\frac{1}{2} + \frac{m}{2} \sin \omega t) \\ v_b(t) &= V_{DC}(\frac{1}{2} + \frac{m}{2} \sin(\omega t - \frac{2\pi}{3})) \\ v_{ab}(t) &= V_{DC}\frac{m}{2}(\sin \omega t - \sin(\omega t - \frac{2\pi}{3})) \end{aligned}$$

This corresponds to $\hat{V}_{ab} = \sqrt{3}\frac{m}{2}V_{DC}$, so $\hat{V}_a = \frac{m}{2}V_{DC}$.

For $1 \leq m \leq \frac{4}{\pi}$ the operational mode is nonlinear (overmodulation) and for $m = \frac{4}{\pi}$ the AC voltage is square. The switching losses of the IGBTs are:

$$P_{sw,T} = \frac{1}{\pi} f_{sw}(E_{Ton}(I_{nom}, V_{nom}) + E_{Toff}(I_{nom}, V_{nom})) \frac{\hat{i}}{I_{nom}} \frac{V_{dc}}{V_{nom}}$$

The diode conduction losses are:

$$P_{cond,D} = \frac{1}{2}(V_{D0}\frac{\hat{i}}{\pi} + r_D\frac{\hat{i}^2}{4}) - m \cos \phi (V_{D0}\frac{\hat{i}}{8} + r_D\frac{\hat{i}^2}{3\pi})$$

with:

$$v_D(t) = V_{D0} + r_D i(t) \text{ the diode on-state voltage according to } i = f(v_D)$$

The diode turn-on losses can be neglected. The diode turn-off losses are:

$$P_{sw,D} = \frac{1}{\pi} f_{sw} E_{Drec}(I_{nom}, V_{nom}) (0.45 \frac{\hat{i}}{I_{nom}} + 0.55) \frac{V_{dc}}{V_{nom}}$$

with $E_{Drec}(I_{nom}, V_{nom})$ the diode recovery energy at nominal current and voltage I_{nom}, V_{nom} .

The losses have been calculated per set of one diode and one IGBT, based on the fact that when a particular IGBT is on, either this IGBT is conducting or its anti-parallel diode is conducting, depending on the potential difference and thus the current direction. If upper and lower leg IGBTs are conducting (but not in the same leg), the external current is from positive to negative potential, see figure 67 and the power direction is DC to AC (DC source generator operation). If upper and lower leg diodes are conducting (not possible in the same leg, an external voltage is required), the external current is minus to plus and the power direction is AC to DC. If, for some reason, an IGBT and a diode in another leg are conducting, there is no energy transport between the AC and DC side, since the IGBT and the diode are connected to the same DC

potential, so the AC voltage source is shortcircuited. It is also clear that if only reactive power is produced, on average, sets IGBTs are conducting half the time and sets of diodes the other half. If an IGBT is switched off, the current is initially taken over by the diode in the other part of the same leg because the current can not go to zero instantaneously.

Since the losses in the previous equations have been determined per set of one IGBT and one diode, the total losses of a three phase converter are:

$$P_{PWM} = 6(P_{cond,T} + P_{sw,T} + P_{cond,D} + P_{sw,D})$$

The parameters r_T , V_{T0} , r_D and V_{D0} are temperature dependent [27]. The switching losses are junction temperature dependent:

$$P_{sw,T}(T_J) = P_{sw,T}(T_{nom}) \left(\frac{T_J}{T_{nom}} \right)^\alpha$$

$$P_{sw,D}(T_J) = P_{sw,D}(T_{nom}) \left(\frac{T_J}{T_{nom}} \right)^\alpha$$

This temperature dependency is not implemented in EeFarm-II.

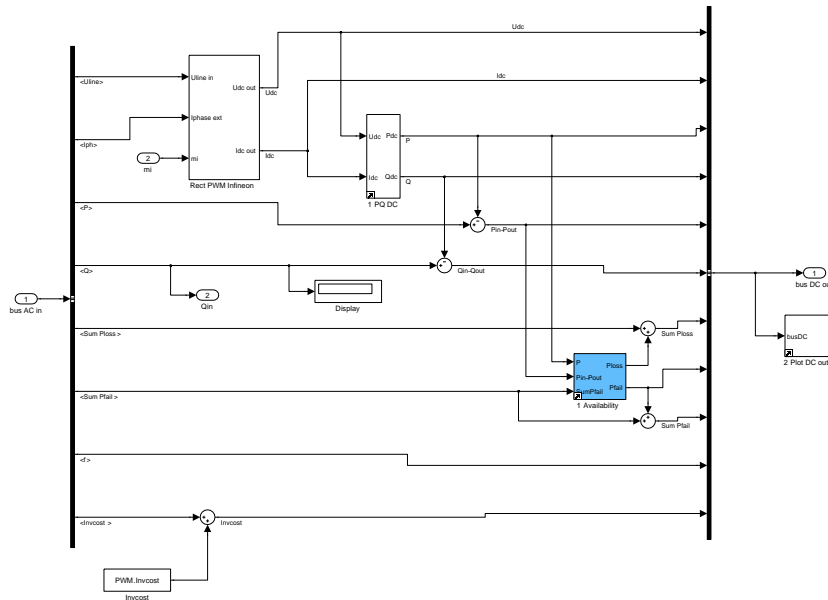


Figure 68: EeFarm-II Infineon model of the PWM rectifier

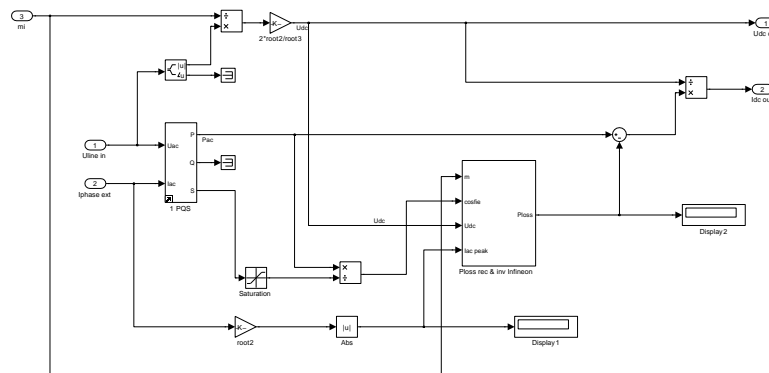


Figure 69: EeFarm-II Infineon PWM rectifier voltage and current calculation

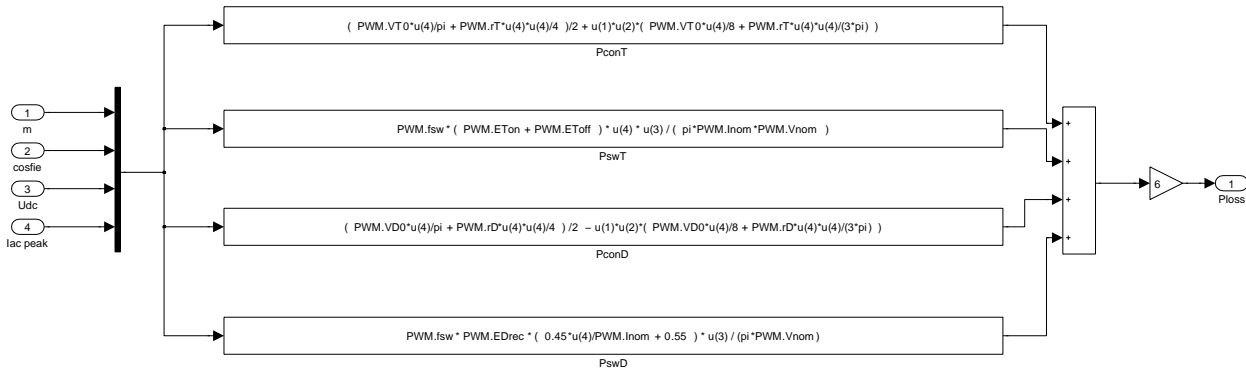


Figure 70: EeFarm-II Infineon PWM rectifier losses calculation

3.9.2 PWM inverter (Infineon)

Component	Input	Output	Parameters
PWM inverter	U_{dc}, I_{dc}, m, Q	$\underline{U}_{ac}, \underline{I}_{ac}, f, P_{loss}, \sum P_{loss}, \sum Invcost, \sum P_{fail}$	$V_{T0}, r_T, f_{sw}, E_{Ton}, E_{Toff}, I_{nom}, V_{nom}, V_{D0}, r_D, E_{Drec}$

The PWM inverter model is the same as the rectifier model, but now the DC values are input and the AC values are output. Since the AC current determines the losses and vice versa, a quadratic equation has to be solved. Alternatively, the losses can be determined based on the AC current without taking the losses into account. In the EeFarm 2 model, the AC current without losses is used to check the solution of the quadratic equation. For a very small power factor, the solution is not correct and the losses are based on the AC current without losses. These losses are then used to calculate the approximate AC current. The quadratic equation is:

$$U_{dc} I_{dc} = \sqrt{\frac{3}{2}} U_{ac} \hat{i} \cos \phi - 6(A \hat{i}^2 + B \hat{i} + C)$$

The coefficients are:

$$\begin{aligned}
 A &= A_{cond,T} + A_{cond,D} \\
 B &= B_{cond,T} + B_{sw,T} + B_{cond,D} + B_{sw,D} \\
 C &= C_{sw,D} \\
 A_{cond,T} &= \frac{1}{2} \frac{r_T}{4} + m \cos \phi \frac{r_T}{3\pi} \\
 A_{cond,D} &= \frac{1}{2} \frac{r_D}{4} - m \cos \phi \frac{r_D}{3\pi} \\
 B_{cond,T} &= \frac{1}{2} \frac{V_{T0}}{\pi} + m \cos \phi \frac{V_{T0}}{8} \\
 B_{cond,D} &= \frac{1}{2} \frac{V_{D0}}{\pi} - m \cos \phi \frac{V_{D0}}{8} \\
 B_{sw,T} &= \frac{f_{sw}}{\pi} (E_{Ton} + E_{Toff}) \frac{V_{DC}}{I_{nom} U_{nom}} \\
 B_{sw,D} &= \frac{f_{sw}}{\pi} E_{Drec} \frac{0.45 V_{DC}}{I_{nom} U_{nom}} \\
 C_{sw,D} &= \frac{f_{sw}}{\pi} E_{Drec} \frac{0.55 V_{DC}}{U_{nom}}
 \end{aligned}$$

When the AC current has been calculated, the equations in section 3.9.1 are used to determine the losses. The next figures show the implementation of the model in EeFarm 2.

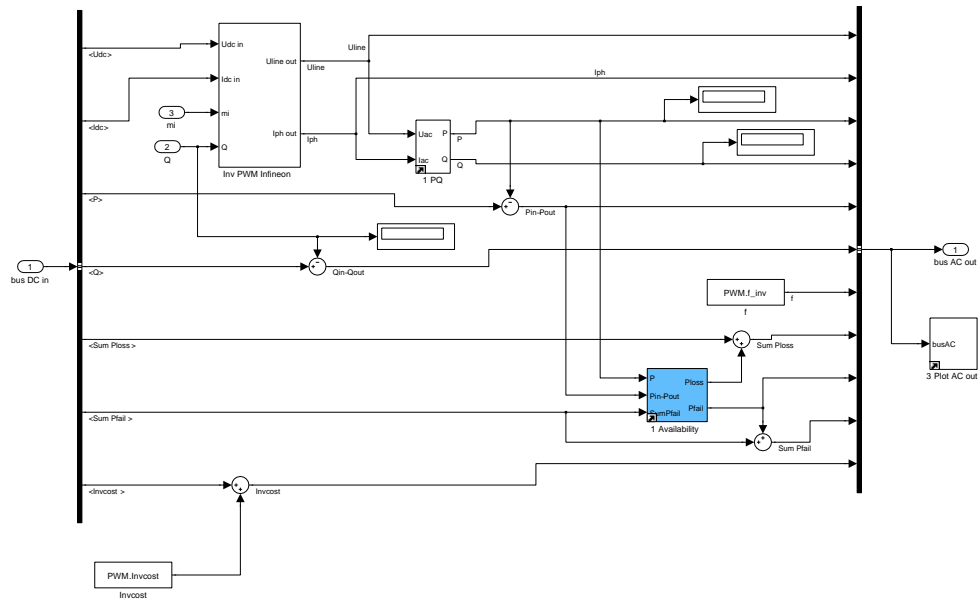


Figure 71: EeFarm-II model of the Infineon model of the PWM inverter

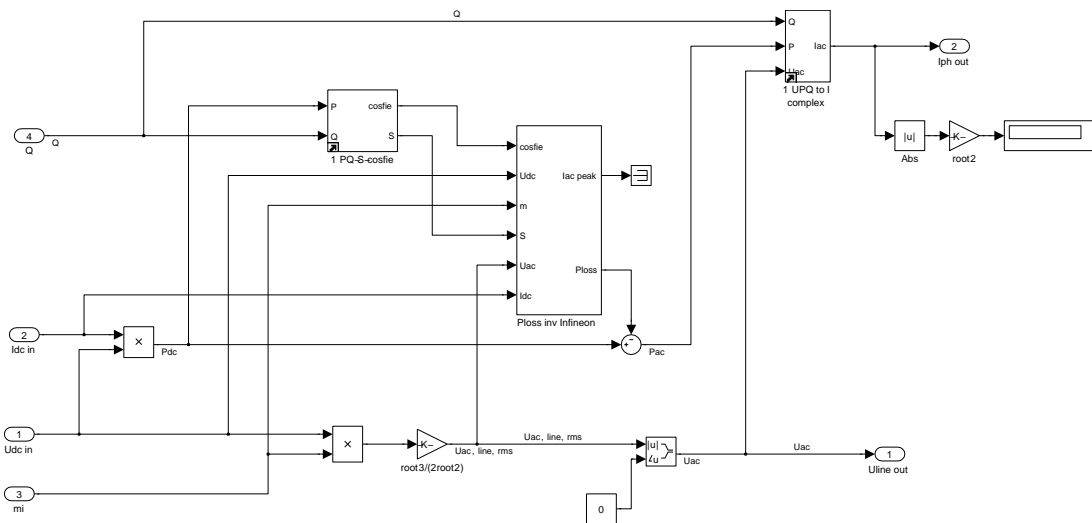


Figure 72: EeFarm-II Infineon inverter model current and voltage calculation

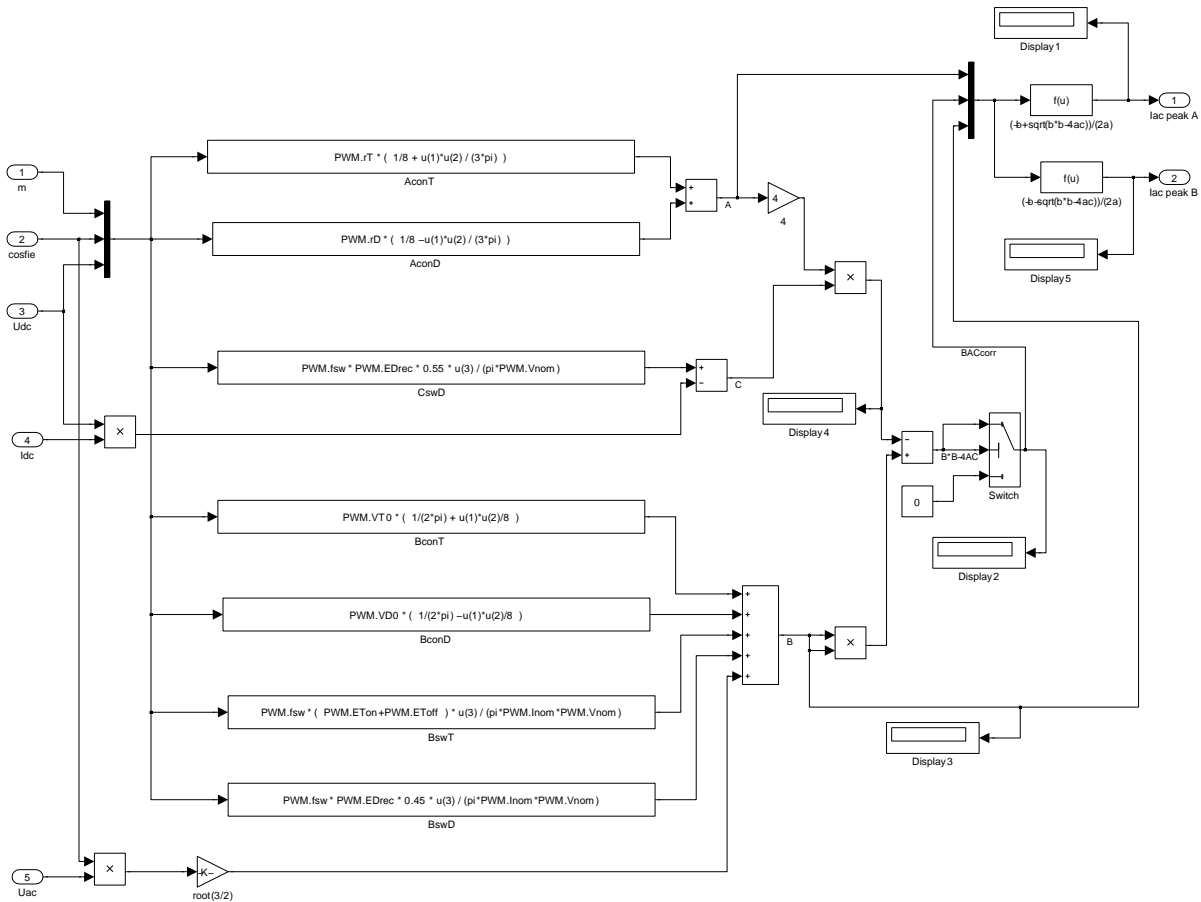


Figure 73: EeFarm-II Infineon inverter model losses calculation

3.9.3 PWM rectifier (Kazmierkowski)

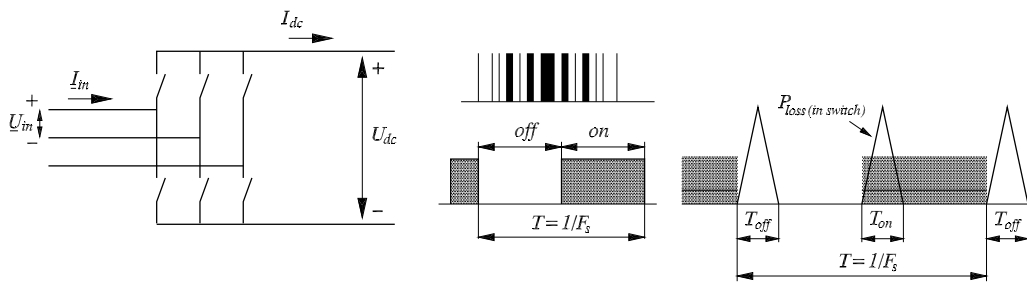


Figure 74: PWM rectifier diagram and operation

Component	Input	Output	Parameters
PWM rectifier	$\underline{U}_{ac}, \underline{I}_{ac}, f$	U_{dc}, I_{dc}, P_{loss} $\sum P_{loss}, \sum Invcost, \sum P_{fail}$	$m_i, V_{0,T}, V_{0,D}, R_{0,T},$ $R_{0,D}, C_{sw}, f_{sw}$

with $V_{0,T}, V_{0,D}$ the current independent part of transistor and diode voltage drops,
 $R_{0,T}, R_{0,D}$ the transistor and diode resistances,
 m_i the modulation index

C_{sw} the switching loss constant (empirically determined) and f_{sw} the switching frequency.

As switching device an IGBT, GTO or IGCT is assumed. The next considerations are made

on the basis of an IGBT switch, but they are applicable to other switches as well.

The PWM rectifier model assumes that AC active and reactive power and the AC voltage are given. When connected to a wind turbine or a wind farm, the PWM rectifier is often controlled to keep the input voltage constant. This is realised by controlling the current, i.e. the active and reactive power of the rectifier.

The reactive power at the PWM rectifier terminal is supplied by the rectifier. The PWM converter can control the ratio between the input AC voltage and the DC voltage. The rectifier is connected to an inverter, either directly or by means of a cable and the DC voltage is controlled by the inverter.

If the switching frequency of the converter is high and a filter with negligible energy storage is inserted on the AC side of the converter, the AC voltage and current are sinusoidal without a ripple. If the losses are neglected, the instantaneous DC current of a three phase PWM inverter can be calculated from the instantaneous phase voltages and currents [14]:

$$\begin{aligned}
 U_{dc}(t)I_{dc}(t) &= u_a(t)i_a(t) + u_b(t)i_b(t) + u_c(t)i_c(t) = \\
 &= \hat{u}\hat{i}[\cos \omega t \cdot \cos(\omega t - \phi) + \cos(\omega t - 120^\circ) \cdot \cos(\omega t - \phi - 120^\circ) + \\
 &\quad + \cos(\omega t + 120^\circ) \cdot \cos(\omega t - \phi + 120^\circ)] = \\
 &= \frac{3}{2}\hat{U}_{ac}\hat{I}_{ac}\cos \phi
 \end{aligned}$$

For constant power and constant DC voltage, the instantaneous DC current is constant:

$$I_{dc}(t) = \frac{P_{ac}(t)}{U_{dc}(t)}$$

So, only the active power contributes to the DC current if the instantaneous DC voltage is assumed constant. In reality, the instantaneous DC voltage will be variable and the instantaneous DC current will change due to the reactive power.

The PWM rectifier and inverter loss model is based on the converter loss model description in chapter 6 of *Control in Power Electronics - Selected Problems - M. Kazmierkowski et. al.* [1]. The rectifier and inverter loss consists of two parts: the conduction and the switching losses. The on-state transistor and diode voltage drop are approximated by:

$$\begin{aligned}
 v_{con,T} &= V_{0,T} + R_{0,T}i_T \\
 v_{con,D} &= V_{0,D} + R_{0,D}i_D
 \end{aligned}$$

with $v_{con,T}, v_{con,D}$ the transistor and diode voltage drops and i_T, i_D the transistor and diode currents. The conduction loss is calculated for sinusoidal modulation with an injected third harmonic and the result is nearly identical to the loss generated by the commonly used space-vector modulation:

$$\begin{aligned}
 P_{con,T} &= \frac{V_{0,T}I_{ac,rms}\sqrt{2}}{\pi} + \frac{V_{0,T}I_{ac,rms}m_i \cos \phi}{\sqrt{6}} + \frac{R_{0,T}I_{ac,rms}^2}{2} + \\
 &\quad + \frac{R_{0,T}I_{ac,rms}^2 m_i}{6\pi\sqrt{3}\cos \phi} - \frac{4R_{0,T}I_{ac,rms}^2 m_i \cos(3\phi)}{45\pi\sqrt{3}}
 \end{aligned} \tag{5}$$

$$\begin{aligned}
 P_{con,D} &= \frac{V_{0,D}I_{ac,rms}\sqrt{2}}{\pi} - \frac{V_{0,D}I_{ac,rms}m_i \cos \phi}{\sqrt{6}} + \frac{R_{0,D}I_{ac,rms}^2}{2} - \\
 &\quad - \frac{R_{0,D}I_{ac,rms}^2 m_i}{6\pi\sqrt{3}\cos \phi} + \frac{4R_{0,D}I_{ac,rms}^2 m_i \cos(3\phi)}{45\pi\sqrt{3}}
 \end{aligned} \tag{6}$$

with $I_{ac,rms}$ the RMS current, m_i the modulation index, which varies from 0 to 1 and ϕ the phase shift between the stator voltage and the stator current.

$$\begin{aligned}m_i &= \frac{\hat{V}_{control}}{\hat{V}_{sawtooth}} \\ \hat{U}_{ac} &= \frac{m_i U_{dc}}{2} \\ U_{dc} &= \frac{2\sqrt{2}U_{ac,line,rms}}{\sqrt{3}m_i}\end{aligned}$$

The total switching losses can be approximated by a linear function of the stator current [1]:

$$P_{sw} = C_{sw} I_{ac,rms} f_{sw}$$

The total losses and the DC current follow from:

$$\begin{aligned}P_{total\ loss} &= 3(P_{con,T} + P_{con,D}) + P_{sw} \\ P_{in} &= U_{dc} I_{dc} + P_{total\ loss} \\ I_{dc} &= \frac{P_{in} - P_{total\ loss}}{U_{dc}}\end{aligned}$$

Figure 75 shows that, for the chosen parameters:

$$V_{0D} = \frac{U_{rated}}{300}, V_{0T} = \frac{U_{rated}}{400}, P_{loss,R_{0D}} = \frac{P_{rated}}{300}, P_{loss,R_{0T}} = \frac{P_{rated}}{400}, P_{loss,SW} = \frac{P_{rated}}{200}$$

the losses mainly depend on the current and not on the current angle or the modulation index.

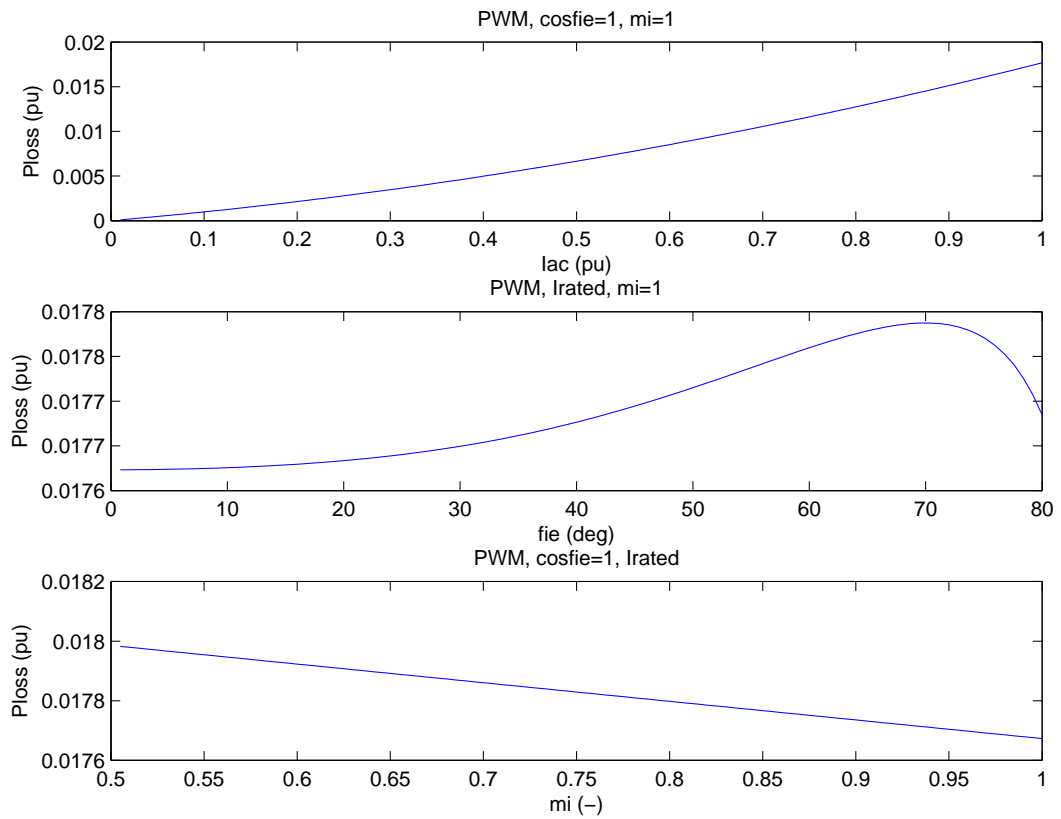


Figure 75: PWM rectifier losses as function of the AC current, the angle ϕ and the modulation index

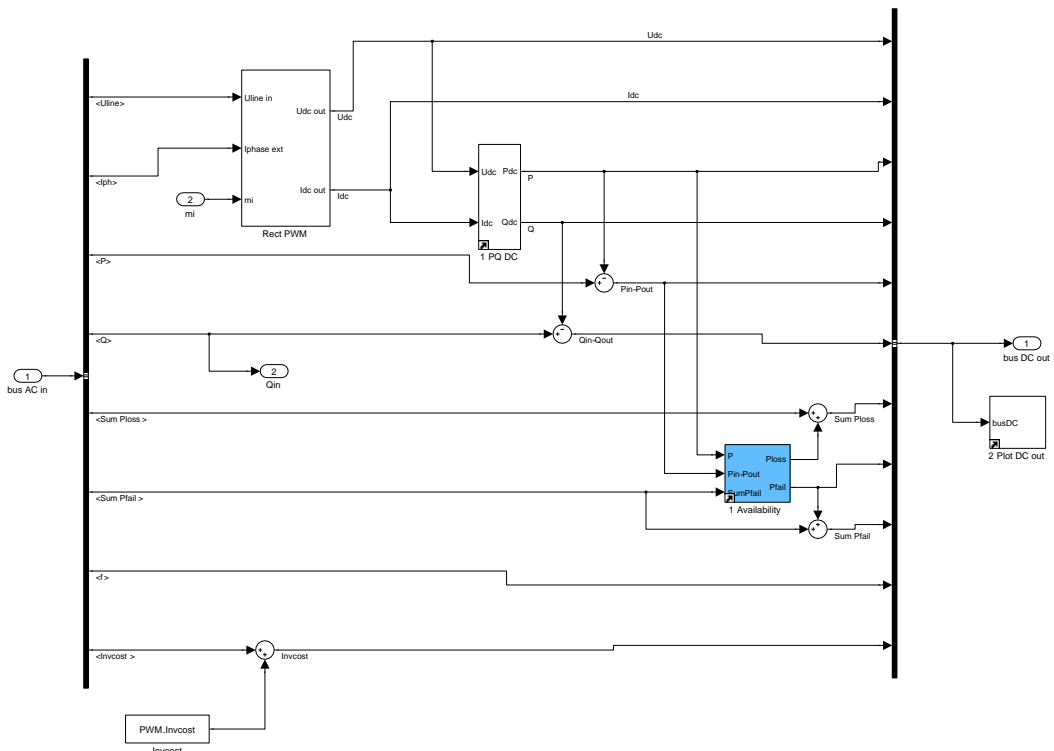


Figure 76: EeFarm-II Kazmierkowski model of the PWM rectifier

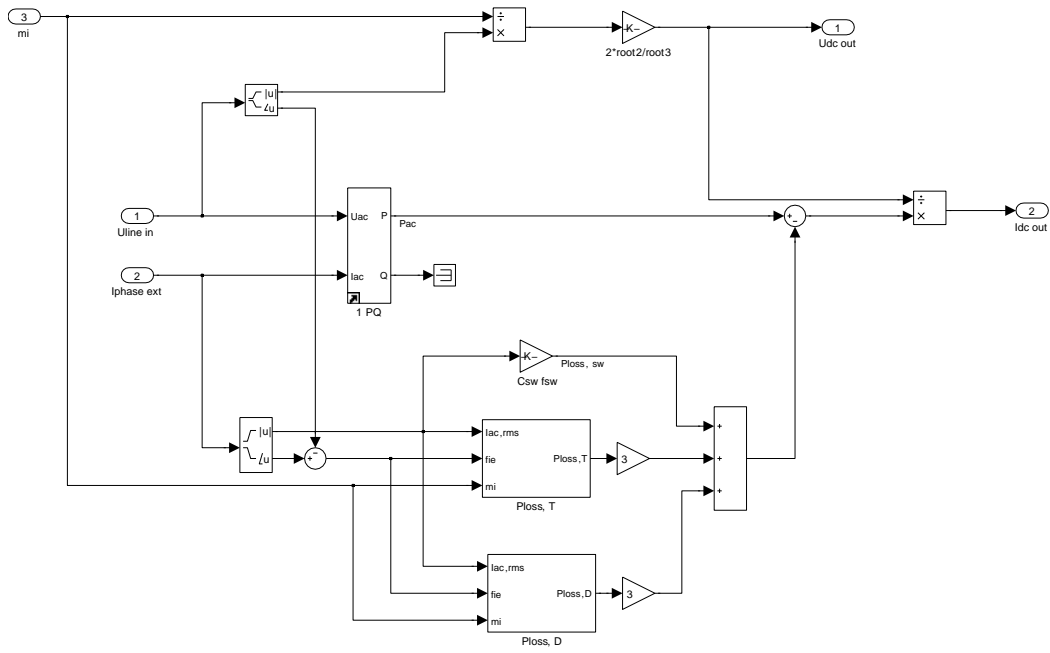


Figure 77: EeFarm-II Kazmierkowski rectifier model voltage and current calculation

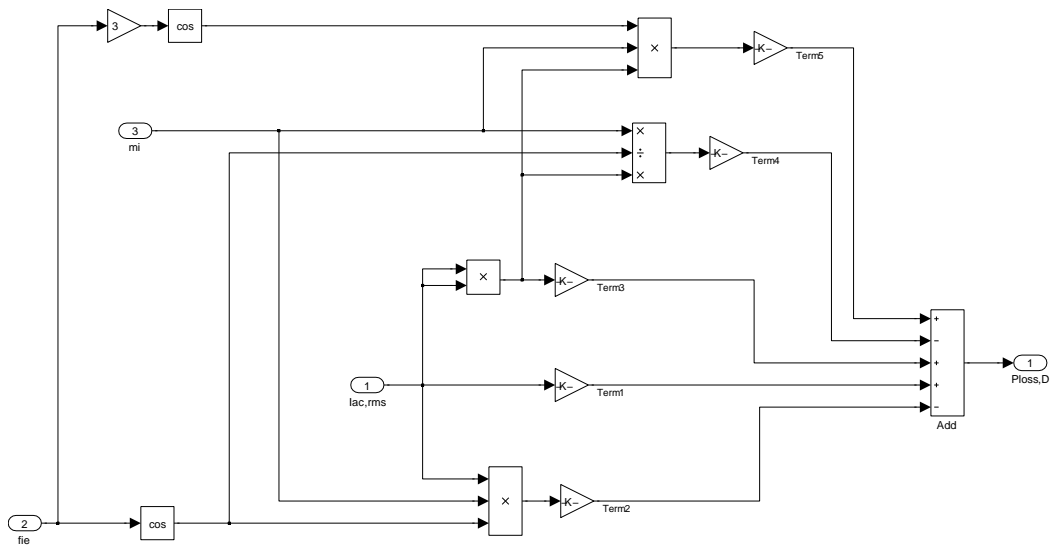


Figure 78: EeFarm-II Kazmierkowski rectifier model losses calculation

3.9.4 PWM inverter model (Kazmierkowski)

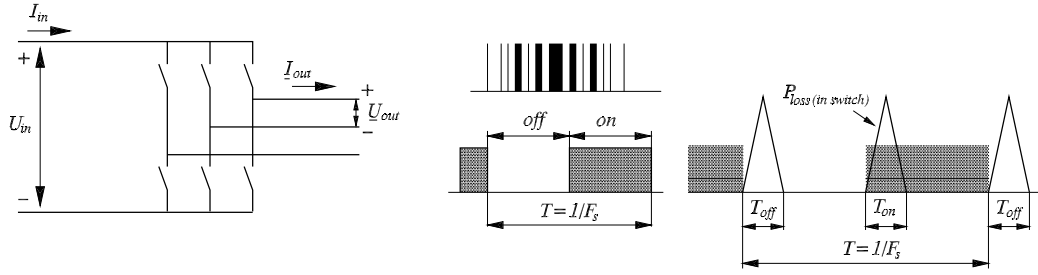


Figure 79: PWM inverter diagram and operation

Component	Input	Output	Parameters
PWM inverter	$U_{dc}, I_{dc}, f, \cos \phi$	$\underline{U}_{ac}, \underline{I}_{ac}, P_{loss}$ $\sum P_{loss}, \sum Inv_{cost}, \sum P_{fail}$	$m_i, V_{0,T}, V_{0,D}, R_{0,T},$ $R_{0,D}, C_{sw}, f_{sw}$

with $V_{0,T}, V_{0,D}$ the transistor and diode constant voltage drops,

$R_{0,T}, R_{0,D}$ the transistor and diode voltage dynamic resistances,

m_i the modulation index

C_{sw} the switching loss constant (empirically determined) and f_{sw} the switching frequency.

The PWM inverter Kazmierkowski loss model is the same as the rectifier model. Now the DC voltage and current are known, which effects the way the equations are evaluated. The total losses can be written as:

$$P_{total\ loss} = 3(P_{con,T} + P_{con,D}) + P_{sw} = d_{inv} I_{ac,rms} + a_{inv} I_{ac,rms}^2$$

with:

$$d_{inv} = 3V_{0,T} \left(\frac{\sqrt{2}}{\pi} + \frac{m_i \cos \phi}{\sqrt{6}} \right) + 3V_{0,D} \left(\frac{\sqrt{2}}{\pi} - \frac{m_i \cos \phi}{\sqrt{6}} \right) + C_{sw} f_{sw}$$

$$a_{inv} = 3R_{0,T} \left(\frac{1}{2} + \frac{m_i}{6\pi\sqrt{3}\cos\phi} - \frac{4m_i \cos(3\phi)}{45\pi\sqrt{3}} \right) + 3R_{0,D} \left(\frac{1}{2} - \frac{m_i}{6\pi\sqrt{3}\cos\phi} + \frac{4m_i \cos(3\phi)}{45\pi\sqrt{3}} \right)$$

The AC voltage is:

$$U_{ac,line,rms} = \frac{\sqrt{3}m_i U_{dc}}{2\sqrt{2}}$$

From the power balance, the active part of the current is determined:

$$a_{inv} I_{act,rms}^2 + (\sqrt{3}U_{ac,line,rms} \cos \phi + d_{inv}) I_{act,rms} - P_{dc} = 0$$

$$I_{act,rms} = \frac{-(\sqrt{3}U_{ac,line,rms} \cos \phi + d_{inv}) + \sqrt{(\sqrt{3}U_{ac,line,rms} \cos \phi + d_{inv})^2 + 4a_{inv} P_{dc}}}{2a_{inv}}$$

since the RMS value is positive.

The AC current is:

$$I_{ac,rms} = \frac{I_{act,rms}}{\cos \phi}$$

Figure 75 shows that, for the following parameter choice:

$$V_{0D} = \frac{U_{rated}}{300}, V_{0T} = \frac{U_{rated}}{400}, P_{loss,R_{0D}} = \frac{P_{rated}}{300}, P_{loss,R_{0T}} = \frac{P_{rated}}{400}, P_{loss,SW} = \frac{P_{rated}}{200}$$

the losses mainly depend on the current and also on the current angle ϕ and the modulation index ($P_{dc} = P_{rated}$ so for changing angle and modulation index the AC current also changes).

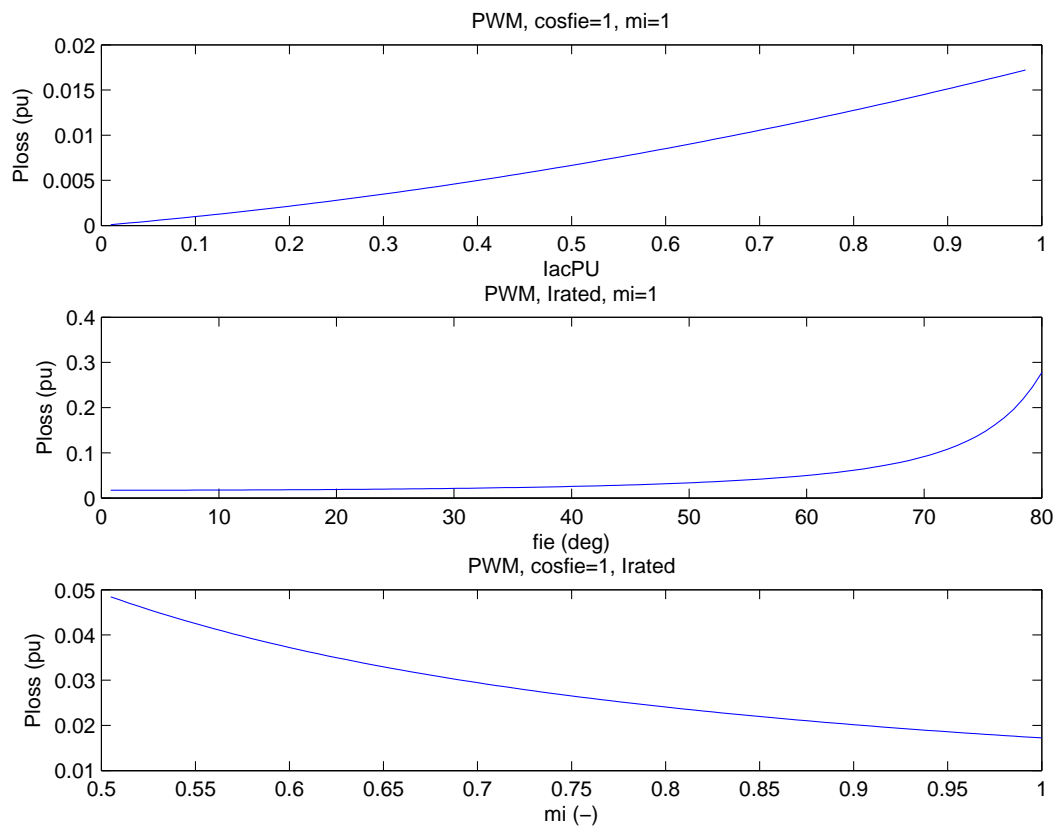


Figure 80: PWM inverter losses as function of the AC current, the (I,U) angle ϕ and the modulation index

The reactive power of the IGBT inverter can be controlled. There is a problem with this model, however. If the power factor is small, a_{inv} will be very large, depending on the difference between $R_{0,T}$ and $R_{0,D}$. This model is not suitable for small power factor and for application as a Statcom.

-60 < fie PWM inv < 60
equations not valid for very large fie
and at 90 degrees division by zero

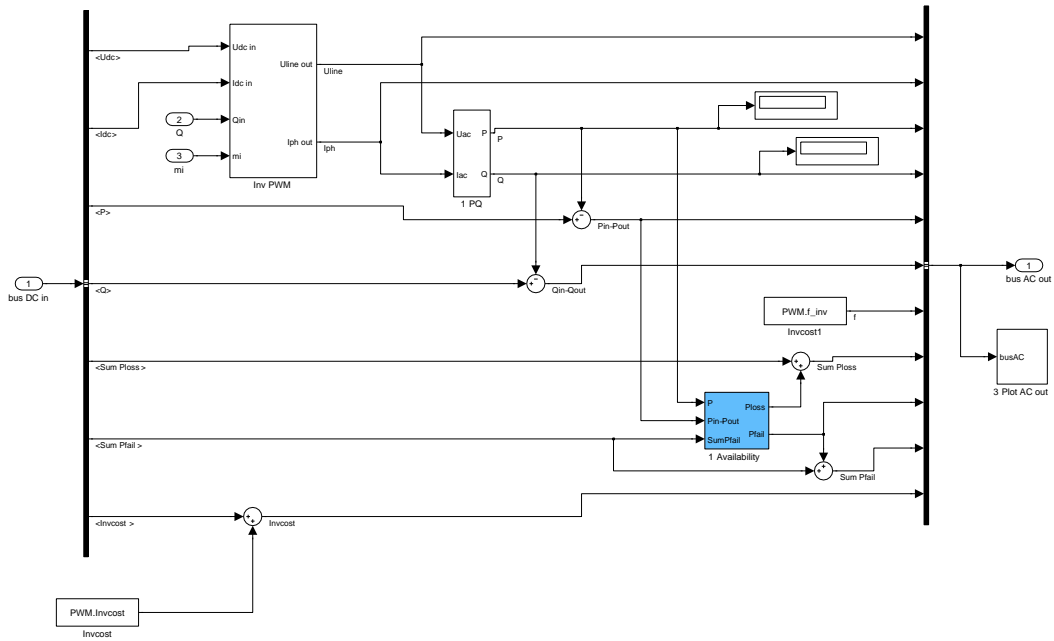


Figure 81: EeFarm-II Kazmierkowski model of the PWM inverter

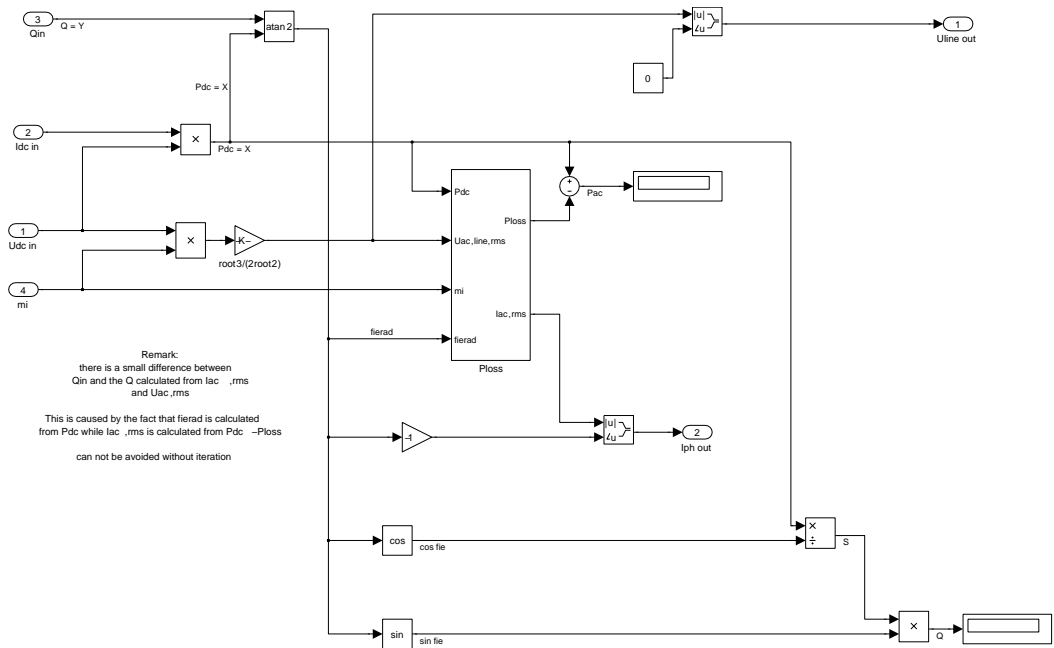


Figure 82: EeFarm-II Kazmierkowski inverter model voltage and current calculation

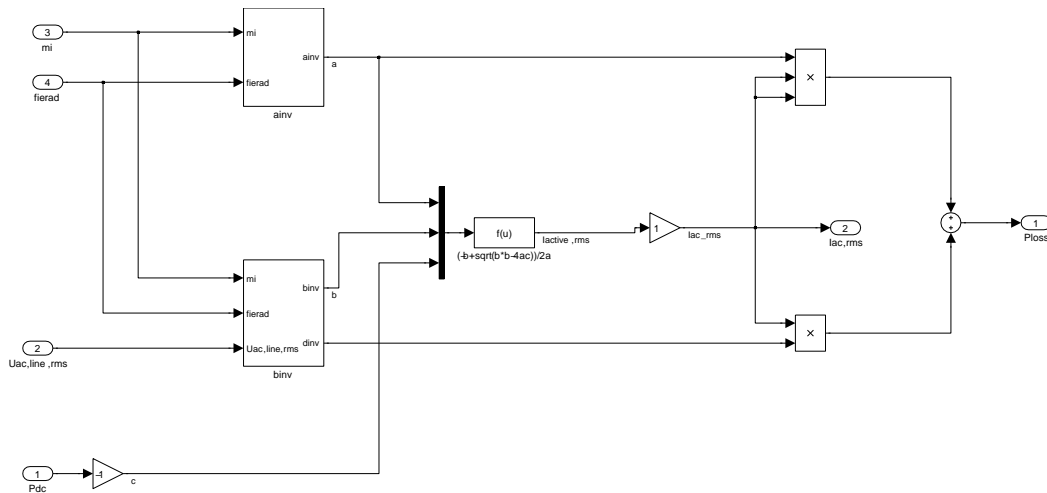


Figure 83: EeFarm-II Kazmierkowski inverter model losses calculation

3.9.5 PWM back-to-back converter (Kazmierkowski)

The PWM back-to-back converter is built by connecting the DC side of a PWM rectifier model to the DC side of a PWM inverter model.

3.9.6 PWM rectifier (TUD)

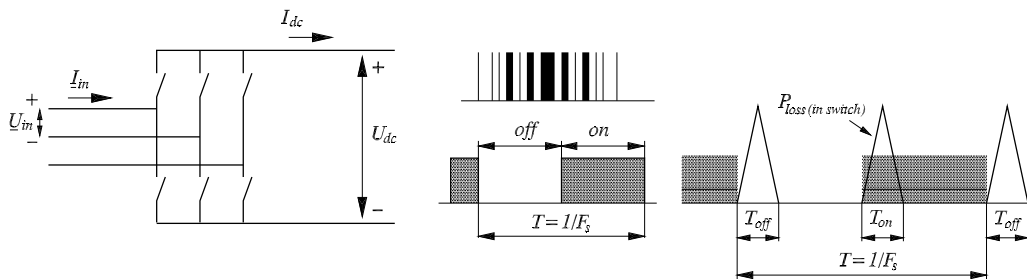


Figure 84: PWM rectifier model

Component	Input	Output	Parameters
PWM rectifier	$\underline{U}_{ac}, \underline{I}_{ac}, f, m_i$	U_{dc}, I_{dc}, P_{loss} $\sum P_{loss}, \sum Invcost, \sum P_{fail}$	f_s, T_{on}, T_{off} E_0, R_{on}

with E_0 the threshold voltage
 R_{on} the resistance in on state
 T_{on}, T_{off} the switch on and off time
 f_s the switching frequency
 m_i the modulation index

The PWM rectifier model assumes that the AC active and reactive power and the AC voltage are given. When connected to a wind turbine or a wind farm, the PWM rectifier is often controlled to keep the AC voltage constant. This is realised by controlling the current, i.e. the active and reactive power of the rectifier.

The reactive power at the PWM rectifier terminal is supplied by the rectifier. The PWM converter can control the ratio between the input AC voltage and the DC voltage. The rectifier is connected to an inverter, either directly or by means of a cable and the DC voltage is controlled by the inverter.

To estimate the conduction losses of the switch a $V - A$ curve is assumed similar to a diode (figure 57). To be able to estimate the conduction losses the parameters U_{ce} (equivalent to E_0) and R_{on} are used. With these parameters it is possible to estimate the voltage drop over the IGBT in the conducting state.

The on-state losses are:

$$P_{on-state, loss} = 2 \cdot (U_{ce} \cdot I_{dc} + I_{dc}^2 \cdot R_{on}) \left(\frac{T_s - T_{on} - T_{off}}{T_s} \right)$$

with T_s the inverse of the switching frequency:

$$T_s = \frac{1}{F_s}$$

The switching losses, their calculation and background are shown in figure 85. The switching characteristics of an IGBT for a non-inductive load are taken, figure 85.

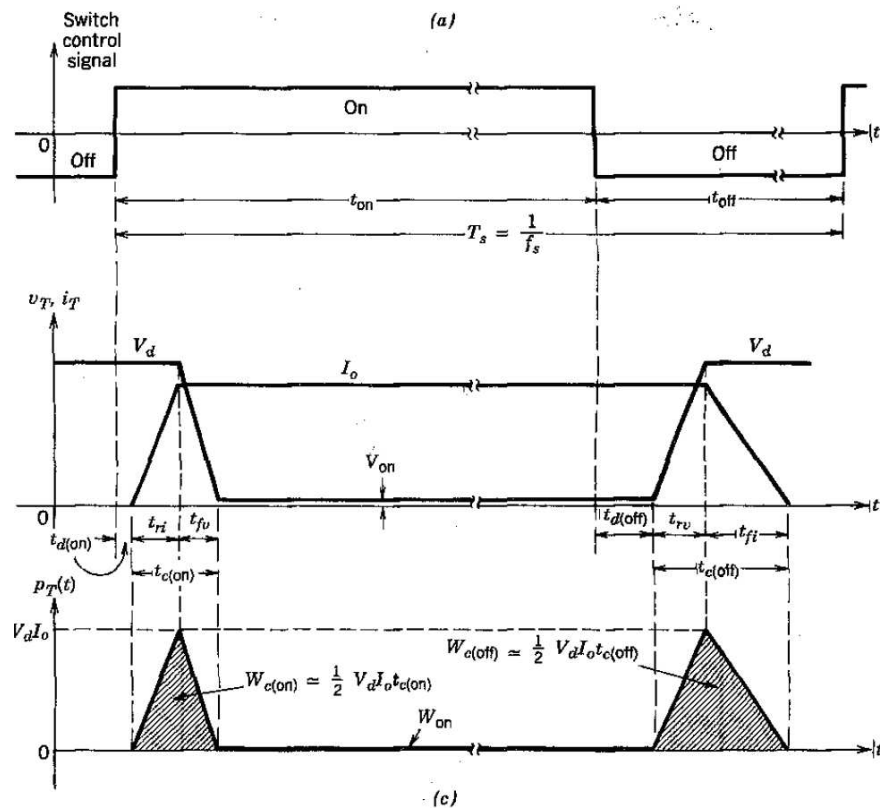


Figure 85: Generic-switch switching characteristics (linearized) [14]

The switching losses are calculated by:

$$P_{switch-on, loss} = 3 \frac{U_{dc} \cdot I_{dc}}{2} \cdot \frac{T_{on}}{T_s}$$

$$P_{switch-off, loss} = 3 \frac{U_{dc} \cdot I_{dc}}{2} \cdot \frac{T_{off}}{T_s}$$

The total losses are calculated as a sum of the switching and conduction losses:

$$P_{total\ loss} = P_{on-state, loss} + P_{switch-on, loss} + P_{switch-off, loss}$$

With:

$$x_{on-state} = \frac{T_s - T_{on} - T_{off}}{T_s}$$
$$x_{switch} = \frac{T_{on} + T_{off}}{T_s}$$

This can be rewritten as:

$$P_{total\ loss} = 2 \left(U_{ce} I_{dc} + I_{dc}^2 R_{on} \right) (x_{on-state}) + \frac{3}{2} U_{dc} I_{dc} (x_{switch})$$

The power losses in the switch will be estimated from the average current in the switch $I_{dc,switch}$, calculated from the active and reactive power into the rectifier. The average DC current in the DC link $I_{dc,link}$ is calculated from the input AC power. In case of a reactive power component, the switching and on state losses would be underestimated if based on the average current from the active power. Therefore, the average DC current in the switch (IGBT) is based on the apparent power S instead of from the active power.

$$S_{in} = \sqrt{3} |U_{in}| |I_{in}|$$
$$= U_{dc} I_{dc,switch}$$

The input power equals:

$$P_{in} = \sqrt{3} \operatorname{Re} (U_{in} I_{in}^*)$$
$$= P_{out} + P_{total\ loss}$$
$$= U_{dc} I_{dc,link} + P_{total\ loss}$$

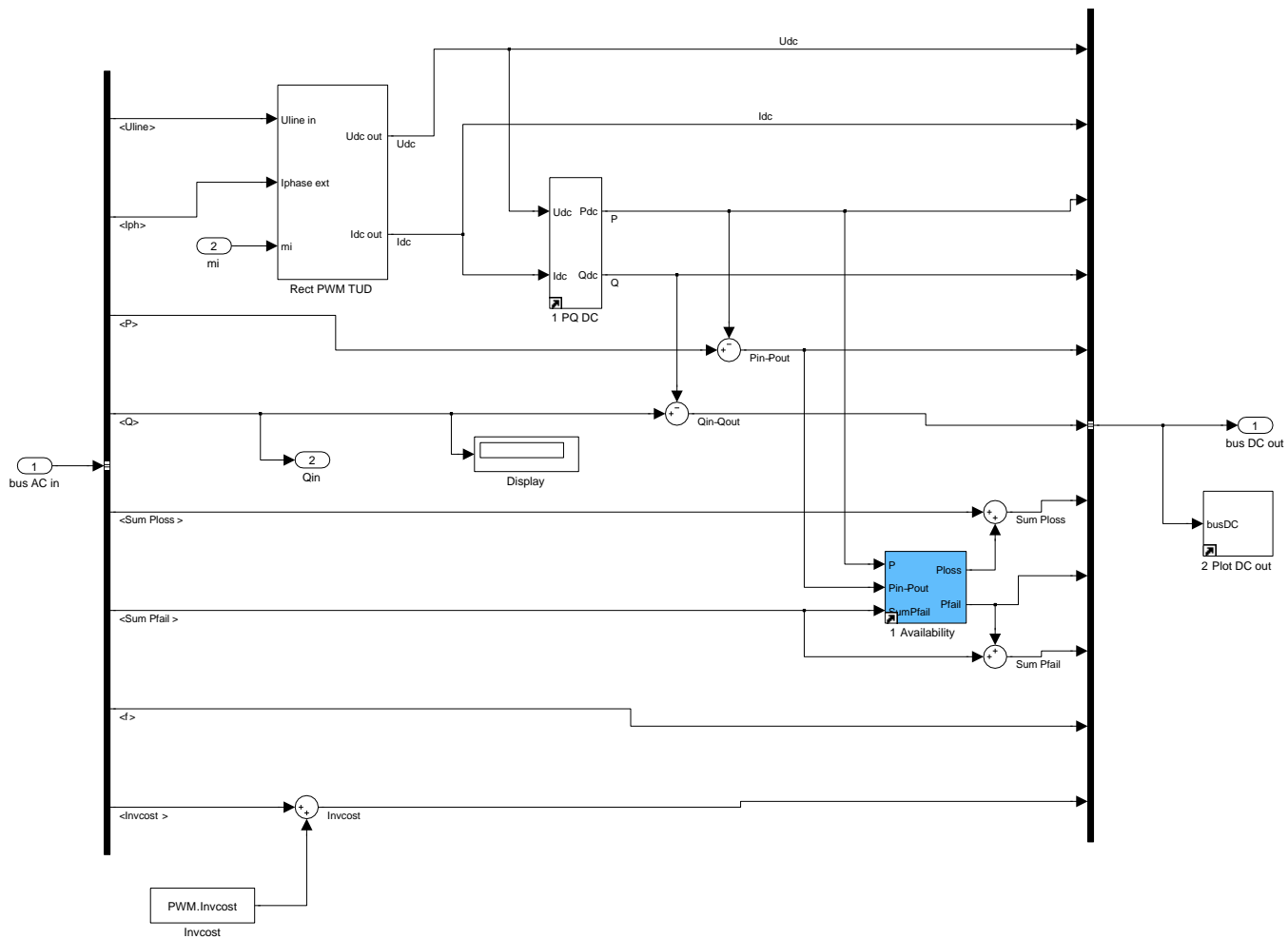


Figure 86: EeFarm-II TUD model of the PWM rectifier

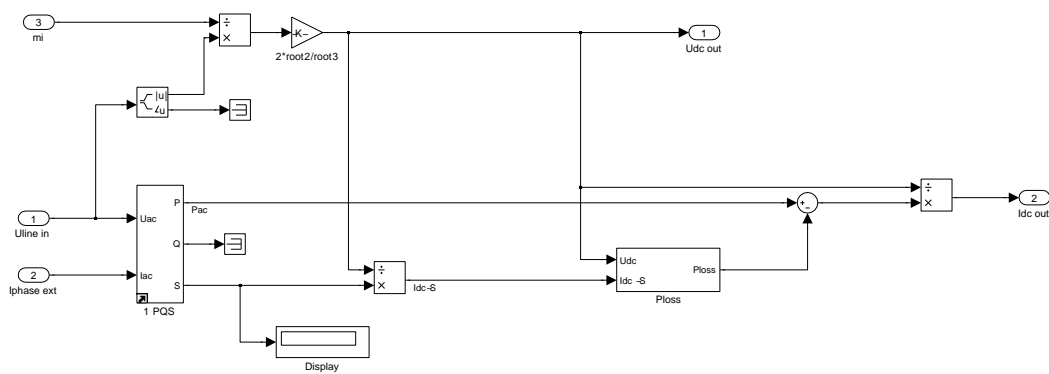


Figure 87: EeFarm-II TUD rectifier model voltage and current calculation

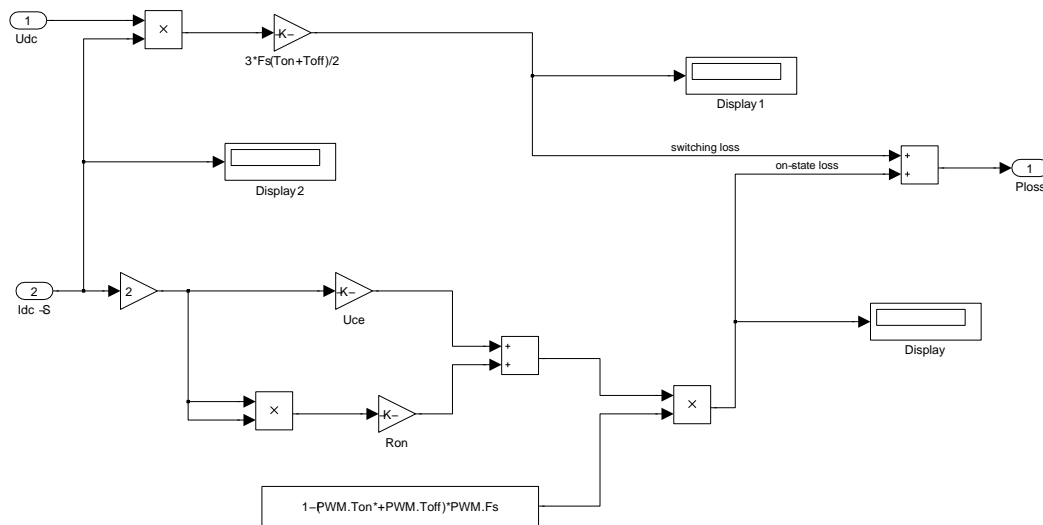


Figure 88: EeFarm-II TUD rectifier model losses calculation

3.9.7 PWM inverter (TUD)

Component	Input	Output	Parameters
PWM inverter	$U_{dc}, I_{dc}, f, m_i, Q$	U_{ac}, I_{ac}, P_{loss} $\sum P_{loss}, \sum Invcost, \sum P_{fail}$	$f_s, T_{on}, T_{off}, E_0, R_{on}$

with E_0 the threshold voltage
 R_{on} the resistance in on state
 T_{on}, T_{off} the switch on and off time
 f_s the switching frequency
 m_i the modulation index

The TUD version of the PWM inverter uses the same loss calculation as the TUD rectifier model. The Simulink implementation is slightly different due to the different input and output variables, see figures 89, 90 and 91.

-60 < fie PWM inv < 60
 equations not valid for very large fie
 and at 90 degrees division by zero

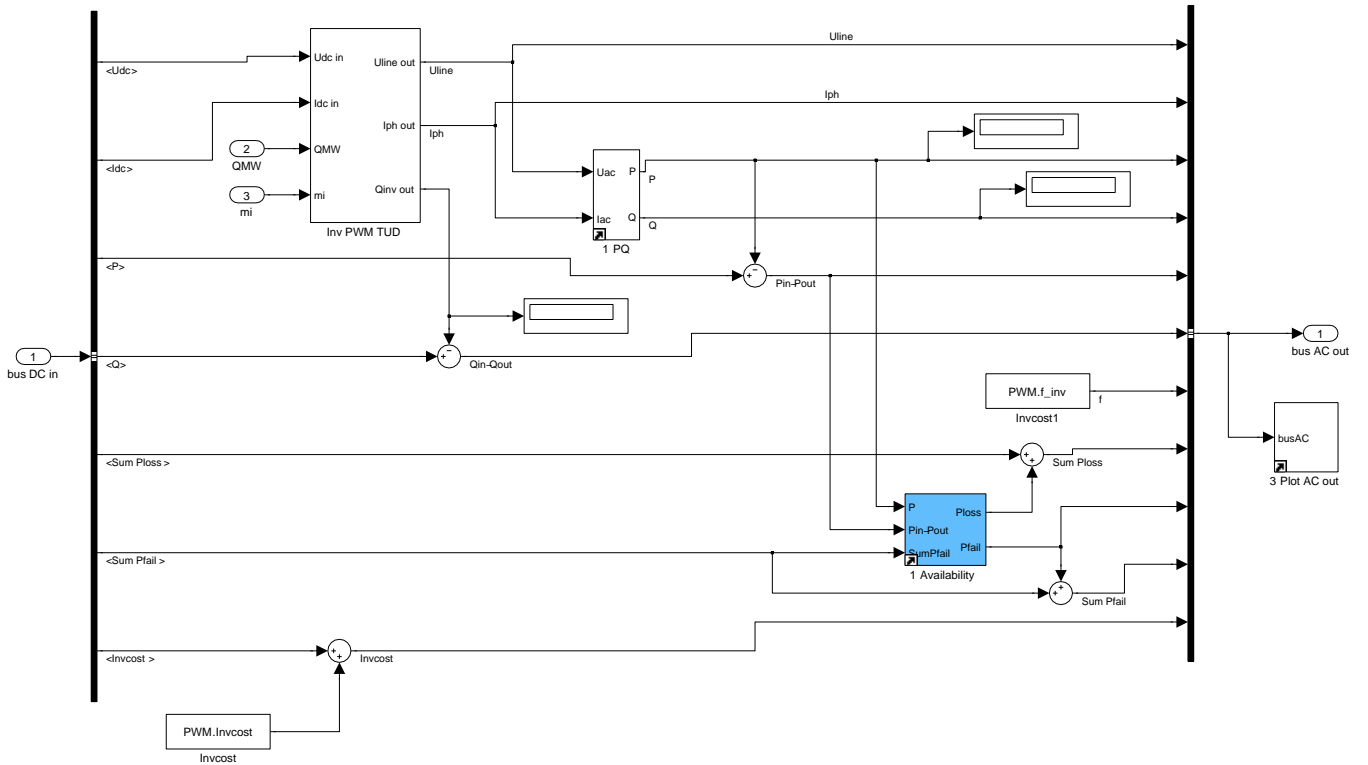


Figure 89: EeFarm-II TUD model of the PWM inverter

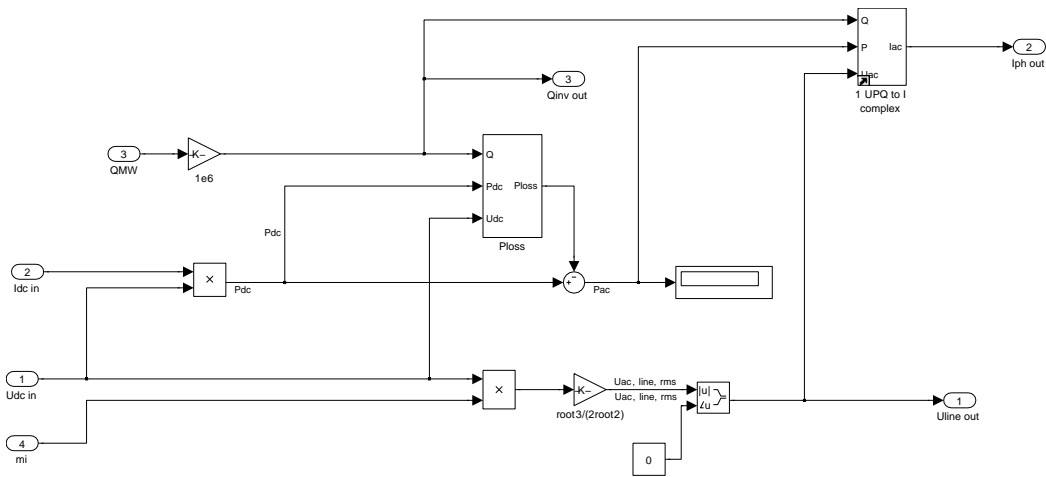


Figure 90: EeFarm-II TUD inverter model voltage and current calculation

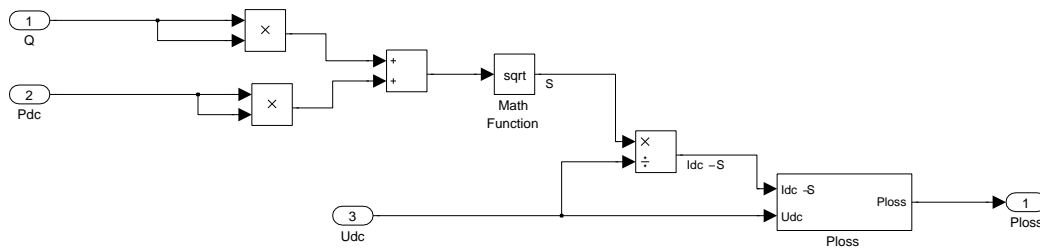


Figure 91: EeFarm-II TUD inverter model losses calculation

3.10 Statcom

Component	Input	Output	Parameters
Statcom	$\underline{U}_{ac}, \underline{I}_{ac,excl.Q}, f_s, Q_{set}, m_i$	$\underline{I}_{ac,incl.Q}, P_{loss}, \sum P_{loss}, \sum Invcost, \sum P_{fail}$	$f_s, T_{on}, T_{off}, E_0, R_{on}$

with E_0 the threshold voltage
 R_{on} the resistance in on state
 T_{on}, T_{off} the switch on and off time
 f_s the switching frequency
 m_i the modulation index

The Statcom is modelled as reactive power controlled PWM inverter with zero AC power. The DC voltage depends on the modulation index. The average DC current is zero, but the RMS value is not. The DC current is calculated from the reactive power. The statcom model uses the same loss calculation as the TUD rectifier model in section 3.9.6 (modified to handle zero active power).

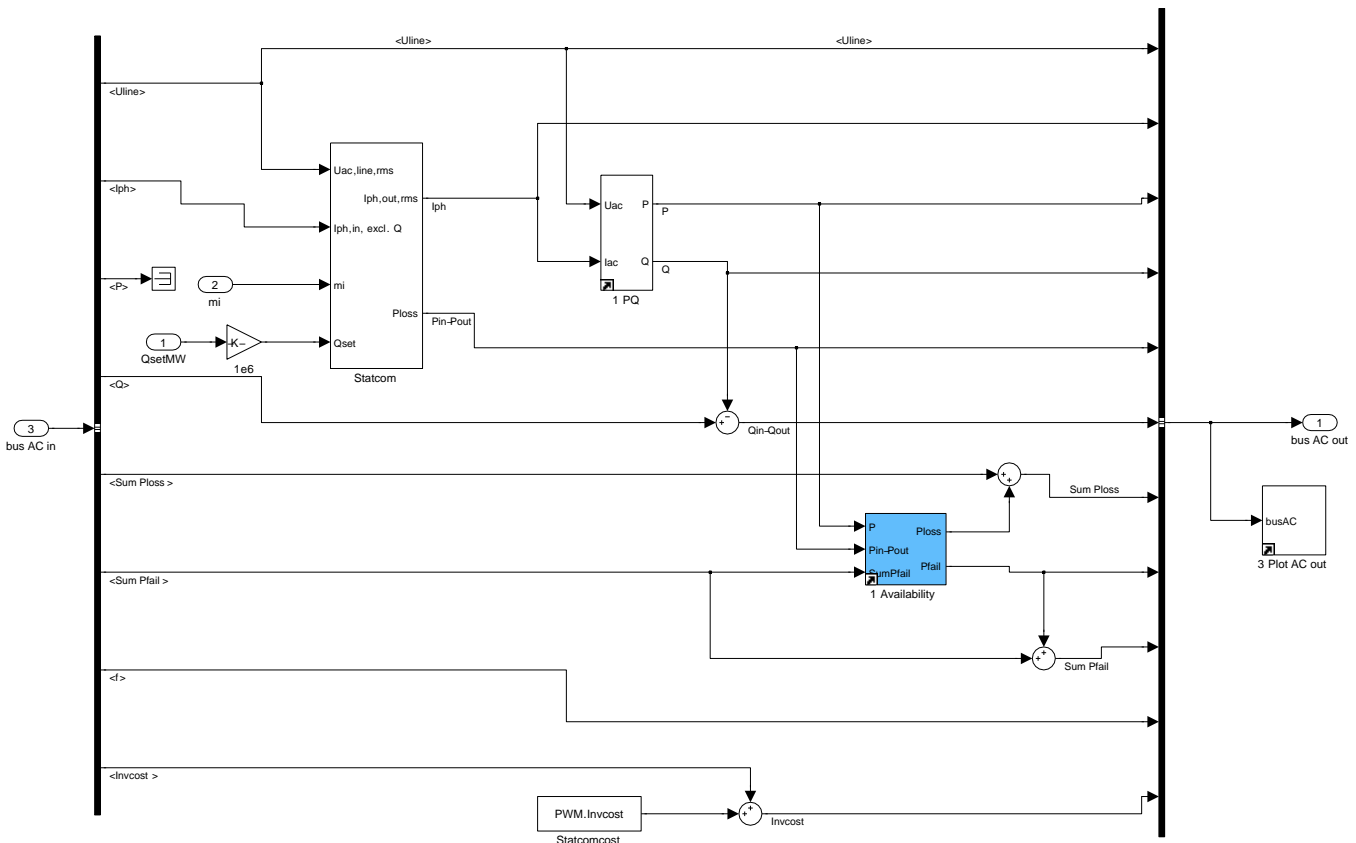


Figure 92: EeFarm-II model of the Statcom

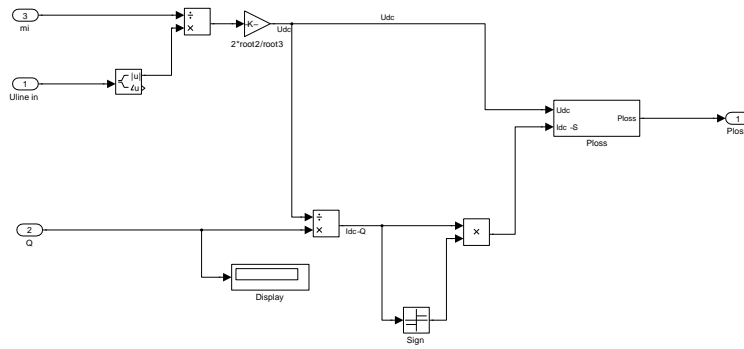


Figure 93: Voltage and current calculation the Statcom

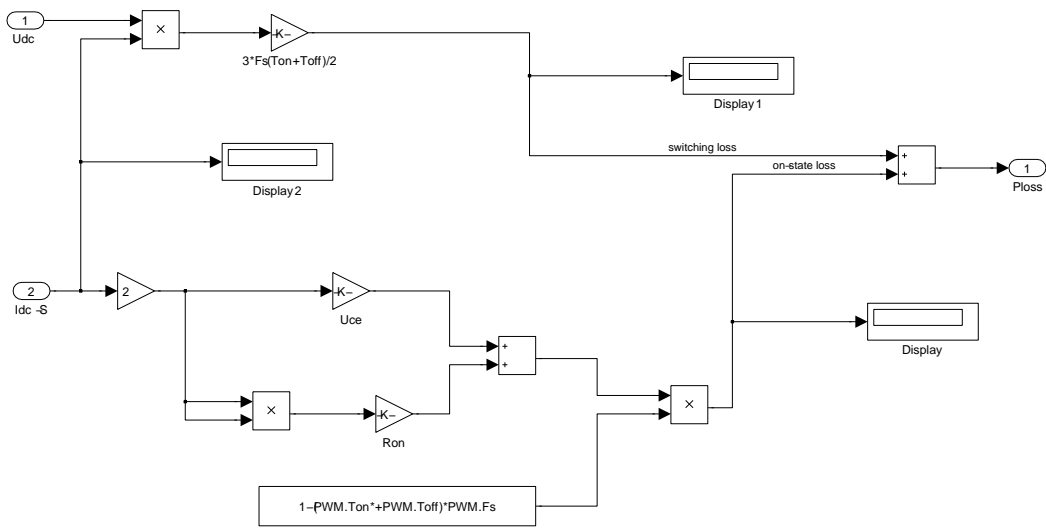


Figure 94: Losses in the Statcom model

3.11 Step-up chopper

Component	Input	Output	Parameters
Step-up chopper	U_{in}, I_{in}, k	$U_{out}, I_{out}, P_{loss}$ $\sum P_{loss}, \sum Inv_{cost}, \sum P_{fail}$	$F_{sw}, T_{switch-on}, T_{switch-off},$ $V_{diode}, R_{diode}, V_{switch}, R_{switch}$

with k the transformation ratio $\frac{U_{out}}{U_{in}}$

F_{sw} the switching frequency

T_{on}, T_{off} the switch-on and switch-off time of the switch

V_{diode}, V_{switch} the diode and switch threshold voltage

R_{diode}, R_{switch} the diode and switch resistance in on state

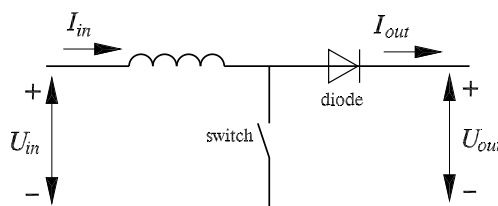


Figure 95: Step-up chopper

The step-up chopper is a DC/DC converter (figure 95). The input power of the converter is calculated from the input voltage and current:

$$P_{in} = U_{in} \cdot I_{in}$$

The duty cycle ratio of the converter is defined as ratio between the on-time of the switch and switching period of the converter.

$$D = \frac{T_{on}}{T}$$

The duty cycle ratio determines the transformation ratio of the converter k , which is defined as:

$$k = \frac{U_{out}}{U_{in}} = \frac{1}{1 - D}$$

hence

$$D = 1 - \frac{1}{k}$$

The model of the converter losses is derived from the converter circuit and is based on a simple model of the diode and the switch (see the section on the diode rectifier and figure 57). The converter losses are the on-state losses and the switching losses of the switch and the on-state losses of the diode. The diode on-state conduction losses are:

$$P_{diode,cond} = I_{in} (I_{in} \cdot R_{diod} + V_{tdio}) \cdot (1 - D)$$

The IGBT on-state conduction losses are:

$$P_{switch,cond} = I_{in} (I_{in} \cdot R_{sch} + V_{tsch}) \cdot D$$

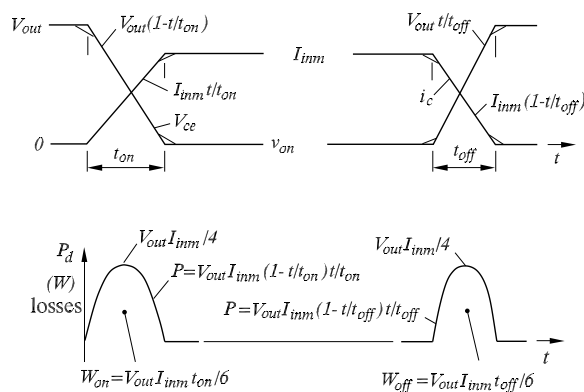


Figure 96: Wave forms of switching process of the step-up chopper

For the calculation of the IGBT switching losses the waveforms of figure 96 are used. The switching losses are:

$$P_{switch-on} = \frac{1}{6} I_{in} U_{out} T_{switch-on} F_{sw}$$

$$P_{switch-off} = \frac{1}{6} I_{in} U_{out} T_{switch-off} F_{sw}$$

$T_{switch-on}$ and $T_{switch-off}$ represent the time it takes to switch the IGBT on or off. The total losses of the DC-DC converter are:

$$P_{loss} = P_{diode,cond} + P_{switch,cond} + P_{switch-on} + P_{switch-off}$$

The output power and current of the converter are:

$$P_{out} = P_{in} - P_{loss}$$

$$I_{out} = \frac{P_{out}}{U_{out}}$$

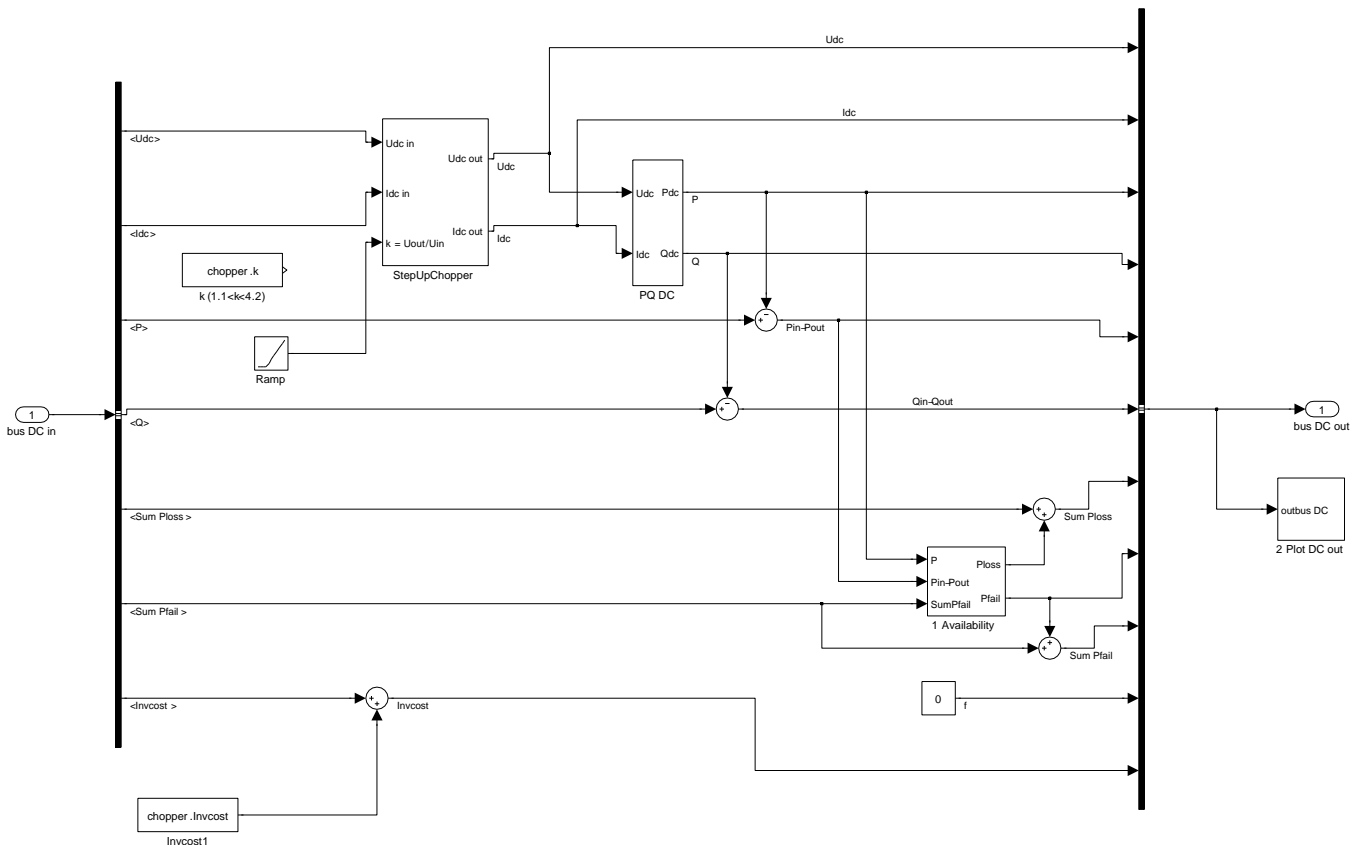


Figure 97: EeFarm-II model of the Chopper

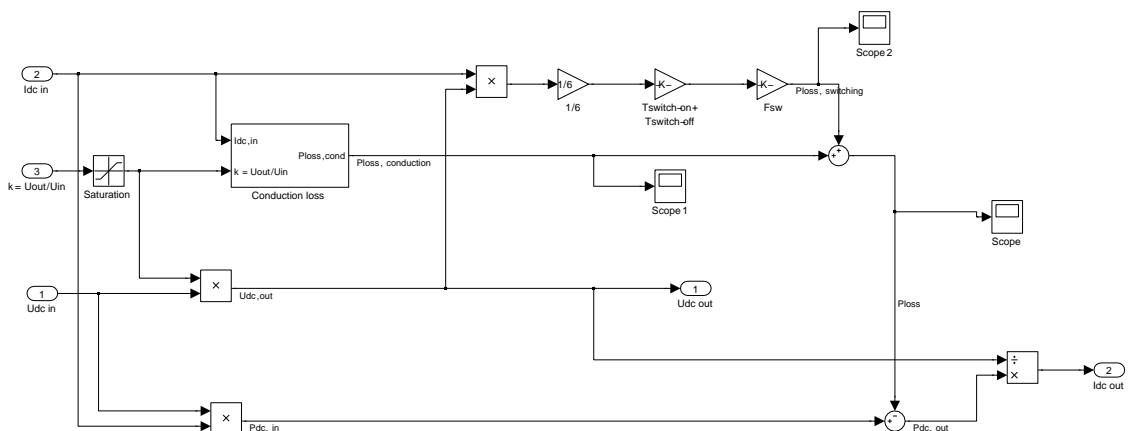


Figure 98: Calculation of the chopper output current

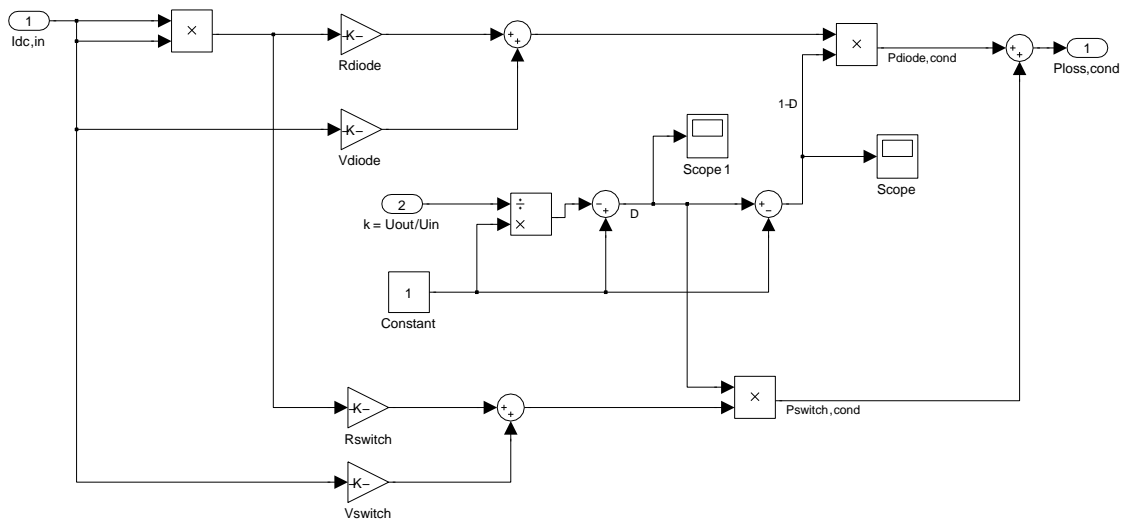


Figure 99: Calculation of the chopper conduction losses

4 Availability

Load flow programs such as Vision can calculate the overall electrical system reliability from the system layout and the reliability of the individual components [15]. Since component failure can have a significant effect on the production of offshore wind farms, due to the low accessibility of the wind farm and the time it takes to repair components such as offshore cables, the effect of component reliability and repair times should be included in wind farm electrical and economic evaluations. EeFarm II takes the effect of component failure on the power production of the wind farm into account, but in a different way than for instance Vision. In Vision, the effect of failure of an individual components and redirection of the power flow is evaluated, including possible overloading of the grid. This redirection of power flows is essential in medium voltage meshed grids, the main application of Vision. The medium voltage grid is designed with this redirection in mind. In the case of offshore wind farms however, there is no meshed grid. Generally there is only one route for the power from any turbine location in the farm to the HV grid connection point at shore. In rare cases, more than one route is possible, for instance if the total farm power is divided over two high voltage cables to shore. Only in these rare cases a limited amount of redundancy (at below rated power) exists. Due to the simplicity of offshore wind farm grids, the effect of component failure on the total production can be determined in a relatively simple way: by applying a component non-availability factor to the power produced by or passing through each component. This method is implemented in EeFarm-II, under the following considerations:

- The non-availability factor is calculated from the MTBF (Mean Time Between Failure, failure rate) and the MTTR (Mean Time To Repair). The MTTR has to include the effect of the weather on the possibility to repair offshore wind farm components.
- EeFarm-II determines the power produced by or passing through a component at a given location in the farm for a given wind speed bin. The average power lost due to failure is determined by multiplying the power minus the power lost due to failure of upstream components by the non-availability factor of the component.
- EeFarm-II component output power, voltage, current and reactive power are not corrected for the power loss due to non-availability. The component is either failed (off state) or in operation (on-state). The output power, voltage, current and reactive power are values in the on-state.
- EeFarm-II corrects the ohmic losses for component non-availability.
- EeFarm-II assumes that only one component fails at a time (no multiple failure). Then there are no upstream components of a failed component which failed at the same time, which would reduce the total power lost by failure of the downstream component.
- Wind farm maintenance can be included in the non-availability if it is assumed that the maintenance is random, i.e. it is not executed during low wind periods. In that case the maintenance frequency and the maintenance duration have to be known.

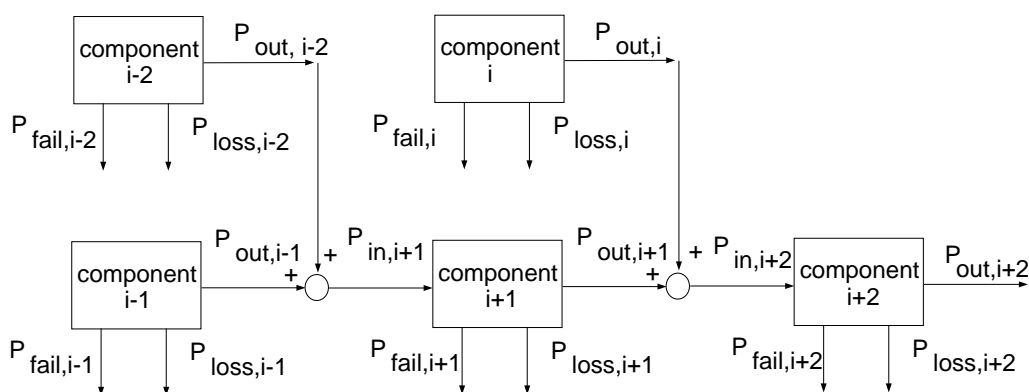


Figure 100: *Component string availability calculation*

Figure 100 shows the availability calculation. The ohmic losses $P_{loss,i}$ and the energy not produced due to failure $P_{fail,i}$ are added for all components and are determined by:

$$\begin{aligned} P_{fail,i} &= f_{na,i}(P_{in,i} - \Sigma P_{fail,i}) \\ P_{out,i} &= P_{in,i} - P_{ohmic,i} \\ P_{loss,i} &= (1 - f_{na,i})P_{ohmic,i} \end{aligned}$$

with:

$P_{in,i}$:	input power of component i
$P_{out,i}$:	output power of component i
$\Sigma P_{fail,i}$:	sum of average power reduction of components upstream of component i due to failure of components upstream of component i
$f_{na,i}$:	the non-availability factor of component i: i.e. the fraction of time that component i is not in operation due to failure (and possibly also maintenance)
$P_{fail,i}$:	average output power reduction of component i due to failure of component i
$P_{ohmic,i}$:	ohmic and switching losses in component i (not corrected for the failure of component i)
$P_{loss,i}$:	average ohmic and switching losses in component i, i.e. corrected for the failure of component i
$\Sigma P_{loss,i}$:	total ohmic losses of component i and components upstream of component i (corrected for the failure of component i and components upstream of component i)

The calculation can be represented by Sankey diagram, with three flows for each component: the generated power, the power lost due to internal resistance and the power not produced due to failure and repair.

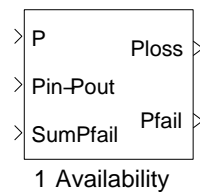


Figure 101: *EeFarm II Availability block*

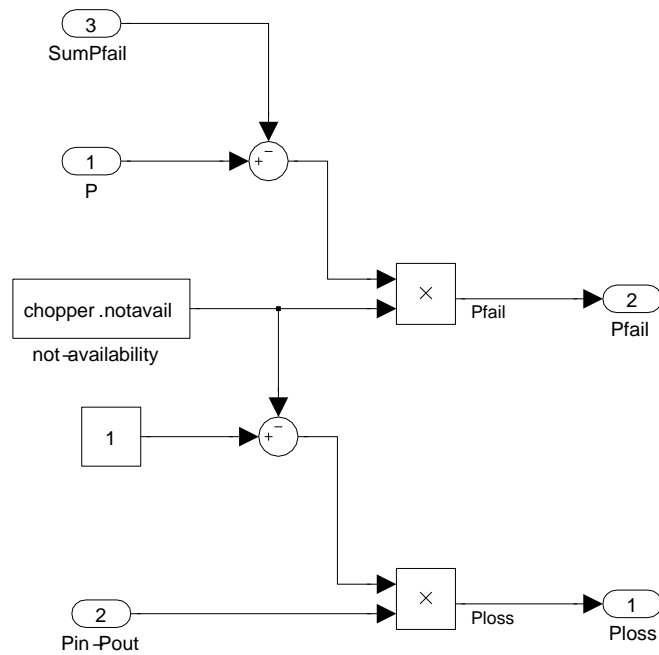


Figure 102: *EeFarm II* Availability block

In case of redundancy, for example more than 1 cable to shore, not produced power due non-availability will only occur if the current exceeds the rating of the remaining cable. A redundancy power value P_{redun} could be used to calculate not produced power due non-availability only if $P > P_{redun}$. This has not been implemented in EeFarm-II yet.

5 Power performance and Economic calculation

5.1 Annual energy production

After the voltage, current, power, reactive power, losses and not produced power due to component failure per wind speed bin have been determined, the Ecalc postprocessor combines these results with the probability of each wind speed bin to obtain the annual energy production (see figure 15 in chapter 3).

For the wind speed distribution the Weibull distribution is used. The cumulative probability distribution $H(V)$ of the wind speed is:

$$H(V_i) = Prob(V \leq V_i)$$

The probability density function is given by:

$$\begin{aligned} h(V) &= Prob(V_{i-1} \leq V \leq V_i) \\ h(V) &= \frac{H(V) - H(V - \Delta V)}{\Delta V} = \frac{dH}{dV} \end{aligned}$$

The average wind speed is:

$$V_{av} = \lim_{T \rightarrow \infty} \frac{1}{T} \int_0^T V(t) dt = \int_0^{\infty} V h(V) dV$$

and the annual energy in the wind flowing thru an area A_{rotor} :

$$E_{annual} = \frac{1}{2} \rho A_{rotor} \int_{dV=0}^{\infty} V^3 h(V) dV$$

The 10 minutes averaged wind speed is often described by a Weibull distribution:

$$H(V_i) = Prob(V \leq V_i) = 1 - \exp\left(-\left[\frac{V_i}{A}\right]^k\right)$$

with k the shape factor and A the scale factor.

The probability density function of the Weibull distribution is:

$$h(V) = \frac{dH}{dV} = \frac{k}{A} \left(\frac{V}{A}\right)^{k-1} \exp\left(-\left[\frac{V}{A}\right]^k\right)$$

Using the gamma function, a simple expression for the average wind speed depending on the shape and scale factor results:

$$\begin{aligned} \Gamma(x) &= \int_0^{\infty} \zeta^{x-1} \exp(-\zeta) d\zeta \\ \zeta &= \left(\frac{V}{A}\right)^k \\ d\zeta &= k \left(\frac{V}{A}\right)^{k-1} \frac{1}{A} dV \\ \overline{V_{annual}} &= \int_0^{\infty} V h(V) dV = \end{aligned}$$

$$\begin{aligned}
& \int_0^\infty V \frac{k}{A} \left(\frac{V}{A}\right)^{k-1} \exp\left(-\left[\frac{V}{A}\right]^k\right) dV = \\
& = A\Gamma\left(1 + \frac{1}{k}\right) \\
\Gamma\left(1 + \frac{1}{k}\right) & \approx \left(0.568 + \frac{1.434}{k}\right)^{1/k} \pm 0.5\% \\
E_{av} & = \frac{1}{2}\rho A_{rotor} (V^3)_{av} = \frac{1}{2}\rho A_{rotor} A^3 \Gamma\left(1 + \frac{3}{k}\right)
\end{aligned}$$

5.2 Economic calculation

To calculate the production costs of a wind farm, the method described by the Expert Group on Recommended Practices for Wind Turbine Testing and Evaluation [26] is applied. The levelised production cost LPC is defined as the production cost of one unit of energy delivered at the point of coupling to the HV grid. The production cost is determined by averaging the costs and revenues over the life time of the wind farm.

All costs are expressed in Euro of year 1 ($t = 0$). The costs of subsequent years are discounted or depreciated to $t = 0$. The levelised production cost is defined by the ratio of the total discounted costs and the total discounted energy output. Discounting of the produced energy is required to account for the moment a revenue is received (an early revenue increases in value with the real interest rate compared to a later revenue).

The Levelised Production Cost LPC equals:

$$LPC = \frac{TC}{\sum_{t=1}^n AUE_t (1+r)^{-t}}$$

with:

$$TC = I + \sum_{t=1}^n OMR_t (1+r)^{-t} - SV (1+r)^{-n} \quad (7)$$

- TC = present value of all costs, i.e. total cost discounted to year $t = 0$
- AUE_t = annual utilized energy output in kWh in year t , all losses included
- I = investment, including possible interest during construction
- OMR_t = operation and maintenance costs during year t
including eventual retrofit costs
- SV = salvage value at the end for the economic life $t = n$
- n = economic life time in years
- r = discount or depreciation rate, i.e. the real interest rate:

$$1 + r = \frac{1 + i}{1 + v}$$

with:

- i = nominal interest rate
- v = inflation rate

In many cases it is appropriate to assume the annual utilized energy to be constant from year to year, i.e. $AUE_t = AUE$ for $t = 1$ to n . In such cases, the LPC equals:

$$LPC = \frac{I}{a \cdot AUE} + \frac{TOM}{AUE}$$

The factor a is the annuity factor:

$$a = \sum_{t=1}^n (1+r)^{-t} = \frac{1 - (1+r)^{-n}}{r}$$

and TOM is the total levelised annual downline costs:

$$TOM = \frac{\sum_{t=1}^n OMR_t (1+r)^{-t} - SV(1+r)^{-n}}{a}$$

6 EeFarm-II parameter database

The database is a crucial part of the EeFarm-II program. For each component, the database contains a number of options, especially for different component sizes. Then a user can choose the component from the database which is best suitable for his application. The entries in the database are based on data obtained from component manufacturers. Some of the parameters are copied one on one from the information supplied by manufacturers, in other cases the manufacturer data did not fit the EeFarm-II requirements directly and had to be recalculated and sometimes approximations had to be applied. All parameters, including the investment costs, are based on data supplied by manufacturers, with the exception of failure data and repair time, which was not supplied by manufacturers.

6.1 Component parameter list

Turbine	Manufacturer	
	Type	for example: NM1500
	S_{nom}	rated apparent power (MVA)
	D	diameter (m)
	Control	for instance: constant speed stall
	P(V)	power-wind speed table
	P(n)	power-rotor speed table ¹
	Cdax(V)	thrust coefficient-wind speed table ²
	$Invcost$	turbine investment cost (kEuro)
	$Instcost$	installation cost (kEuro)
Generic generator	η	efficiency (-)
	$Invcost$	investment cost (kEuro)
Induction generator	Manufacturer	
	Type	for example:
	U_{nom}	rated rms line voltage (kV)
	S_{nom}	rated apparent power (MVA)
	l_s, l_m, l_r	stator leakage, mutual, rotor leakage inductance (H)
	r_s, r_r	stator, rotor resistance (Ω)
	$Invcost$	investment cost (kEuro)
DFIG	Manufacturer	
	Type	for example:
	U_{nom}	rated rms line voltage (kV)
	S_{nom}	rated apparent power (MVA)
	l_s, l_m, l_r	stator leakage, mutual, rotor leakage inductance (H)
	r_s, r_r	stator, rotor resistance (Ω)
	pp	number of pole pairs (-)
	$Invcost$	investment cost (kEuro)
AC cable	Manufacturer	
	Type	for example: XLPE, Cu-1x3x240
	U_{nom}	rated rms line voltage (kV)
	S_{nom}	rated apparent power (MVA)
	A	area of cross section of conductor (mm ²)
	f	frequency (Hz)
	C	capacitance (F/km)
	$R_{ac,20}, R_{ac,90}$	frequency dependent part of resistance (Ω /km)
	$R_{dc,20}, R_{dc,90}$	frequency independent part of resistance (Ω /km)
	L	inductance (H/km)
	$\tan \delta$	dielectric loss factor (-)
		$Invcost$
	$Instcost$	cable laying cost (kEuro/km)

¹ for variable speed turbine; ² for GCL model;

Transformer	Manufacturer		
	Type	for example: three way transformer	
	U_{lo}	rated rms line voltage LV side	(kV)
	U_{hi}	rated rms line voltage HV side	(kV)
	S_{nom}	rated apparent power	(MVA)
	$P_{loss_{fl}}$	full load losses	(kW/MVA)
	$P_{loss_{nl}}$	no load losses	(kW/MVA)
	R_{lo}	resistance LV side	(Ω)
	R_{hi}	resistance HV side	(Ω)
	L_{lo}	leakage inductance LV side	(H)
	L_{hi}	leakage inductance HV side	(H)
	L_m	mutual inductance side	(H)
	Inv_{cost}	investment cost	(kEuro)
$Inst_{cost}$	installation cost ¹	(kEuro)	
Inductor	Manufacturer		
	U	rated rms line voltage side	(kV)
	S_{nom}	rated apparent power	(MVA)
	L	inductance	(H)
	R_{cu}	ohmic resistance	(Ω)
	R_{fe}	equivalent magnetizing resistance	(Ω)
	Inv_{cost}	investment cost	(kEuro)
$Inst_{cost}$	installation cost ¹	(kEuro)	
DC cable	Manufacturer		
	Type	for example: XLPE, Cu-1x3x240	
	U_{nom}	rated rms line voltage	(kV)
	P_{nom}	rated apparent power	(MW)
	A	area of cross section of conductor	(mm ²)
	$R_{dc,20}, R_{dc,90}$	resistance	(Ω /km)
Inv_{cost}	cable investment cost	(kEuro/km)	
$Inst_{cost}$	cable laying cost	(kEuro/km)	
Thyristor rectifier	Manufacturer		
	Type		
	$U_{ac,nom}$	rated rms line voltage	(kV)
	$U_{dc,nom}$	rated DC voltage at zero firing angle	(kV)
	S_{nom}	rated apparent power	(MVA)
	E_0	thyristor threshold voltage	(V)
	R_{on}	thyristor resistance in on state	(Ω)
Inv_{cost}	investment cost	(kEuro)	
$Inst_{cost}$	installation cost ¹	(kEuro)	
Thyristor inverter	same as thyristor rectifier		

¹ this may include platform investment and installation cost

PWM rectifier	Manufacturer		
	Type		
	U_{ac}	rated rms line voltage	(kV)
	U_{dc}	DC voltage	(kV)
	S_{nom}	rated apparent power	(MVA)
	E_0	threshold voltage	(V)
	R_{on}	internal resistance	(Ω)
	F_s	IGBT switching frequency	(Hz)
	T_{on}	time needed to switch on an IGBT	(s)
	T_{off}	time needed to switch off an IGBT	(s)
	$Invcost$	investment cost	(kEuro)
	$Instcost$	installation cost ¹	(kEuro)
PWM inverter		same as PWM rectifier	
Step up chopper	Manufacturer		
	Type		
	U_{lo}	DC voltage LV side	(kV)
	U_{hi}	DC voltage HV side	(kV)
	S_{nom}	rated apparent power	(MVA)
	E_0	threshold voltage	(V)
	R_{on}	internal resistance	(Ω)
	F_s	IGBT switching frequency	(Hz)
	T_{on}	time needed to switch on an IGBT	(s)
	T_{off}	time needed to switch off an IGBT	(s)
	$Invcost$	investment cost	(kEuro)
	$Instcost$	installation cost ¹	(kEuro)
Wind Farm	TOM	wind farm operation and maintenance cost	(Euro/kWh)

¹ this may include platform investment and installation cost

6.2 Database implementation

For the EeFarm II database the Matlab structure format has been used [11]. Each component type is represented by a numbered structure, i.e. DB.turb(n).xxx or DB.rectPWM(n).xxx, with xxx the parameter name, i.e. R_{on} or $Invcost$, corresponding to the parameters of the component in the list in section 6.1. At the start of each simulation, EeFarm-II runs a Matlab initialisation file, which specifies which component parameters will be used in the simulation.

Sets of component parameters, for instance the parameters of all components in a turbine, are loaded into a new structure, named *turb*. in order to reduce the number of changes that have to be made for each occurrence of the block in the Simulink model. In case of a turbine, the length of the cable connecting the turbine to the next turbine and sometimes the cable type will be different. Since the turbine block is masked, by changing the name under the mask in the simulation model, the location specific parameters are transmitted.

7 Component model testing

This chapter documents the component test results. For each component model a test program is made to check the model results over the range of operation. Since the models have frequently been modified during the course of the project, the test programs served an important purpose, viz. to demonstrate the proper operation of the component models during the development phase. Before examining the test results, table 3 lists the sign conventions in the component models.

Table 3: Overview of corresponding signs of angles and powers

	Input					Output					
	\hat{i}	$\angle i$	ϕ	P	Q	\hat{i}	$\angle i$	ϕ	P	Q	op.-conv.-exc. (output) ¹
Cable AC	0	0	0	0	0	+	≈ -90	$\approx +90$	-	+	NL-GC-cap
	+	0	0	+	0	+	-	+	+	+	GO-GC-cap
Trafo	0	0	0	0	0	+	180	-180	-	0	NL-GC-neu
	+	0	0	+	0	+	0	0	+	0	GO-GC-neu
Trafo with Q	0	0	0	0	0	+	90	-90	-	-	NL-GC-ind
	+	0	0	+	0	+	3	-3	+	-	GO-GC-ind
Inductor Source	0	0	0	0	0	+	90	-90	-	-	NL-GC-ind
						+	0	0	+	0	GO-GC-neu
Generic Gen						+	-90	+90	0	+	NL-GC-cap
				0		0	0	0	0	0	NL-GC-neu
IM				+		0	-	+	+	+	GO-GC-cap
				0		+	+90	-90	0	-	NL-GC-ind
DFIG				+		+	+	-	+	-	GO-GC-ind
				+		0	0	0	+	0	GO-GC-neu
FCIM				+		0	0	0	+	0	GO-GC-neu
FCSM				+		0	0	0	+	0	GO-GC-neu
Cable DC	0	0	0	0	0	0	0	0	0	0	NL-GC-neu
	+	0	0	+	0	+	0	0	+	0	GO-GC-neu
Thy. rectifier	+	0	0	+	+	+			+	0	GO-GC-neu
Thy. inverter	+			+		+	+	-	+	-	GO-GC-ind
PWM rectifier (TUD)	+	0	0	+	+	+			+		GO-GC-neu
PWM inverter (TUD)	+			+		+	+	-	+	-	GO-GC-ind
PWM rectifier (Kaz)	+	0	0	+	+	+			+		GO-GC-neu
PWM inverter (Kaz)	+			+		+	+	-	+	-	GO-GC-ind

¹ operating condition (No Load, Generator Operation, Motor Operation) - sign convention (Generator Convention, Motor Convention) - excitation (capacitive, neutral, inductive)

The next sections show the test results for all model blocks for an increasing wind speed and steps in some of the input or control signals, for instance a step in the reactive power or the firing angle of a converter.

7.1 Turbine models

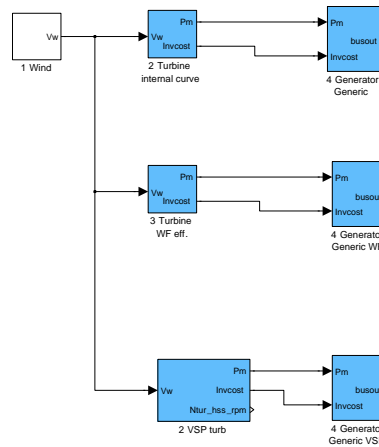


Figure 103: Testmodel for the Turbine

Three turbine models are tested: the turbine model with internal curve, the turbine with wind farm correction and the variable speed turbine model. All three are connected to the same Generator Generic model to produce the standard bus signal output. Figures 104 to 106 show the results. The voltage, voltage angle and output reactive power are constant. The power and the current amplitude follow the mechanical power. The generic generator losses were set to zero. The not produced power due to component failure is proportional to the produced power.

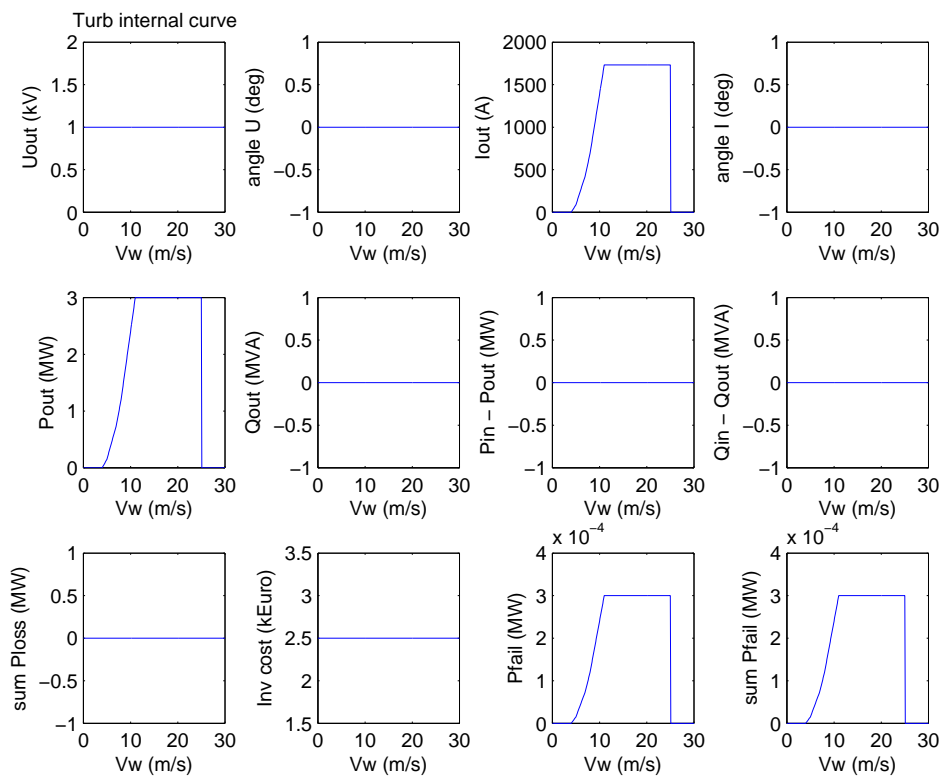


Figure 104: Bus signals of the generic generator connected to the turbine with internal curve

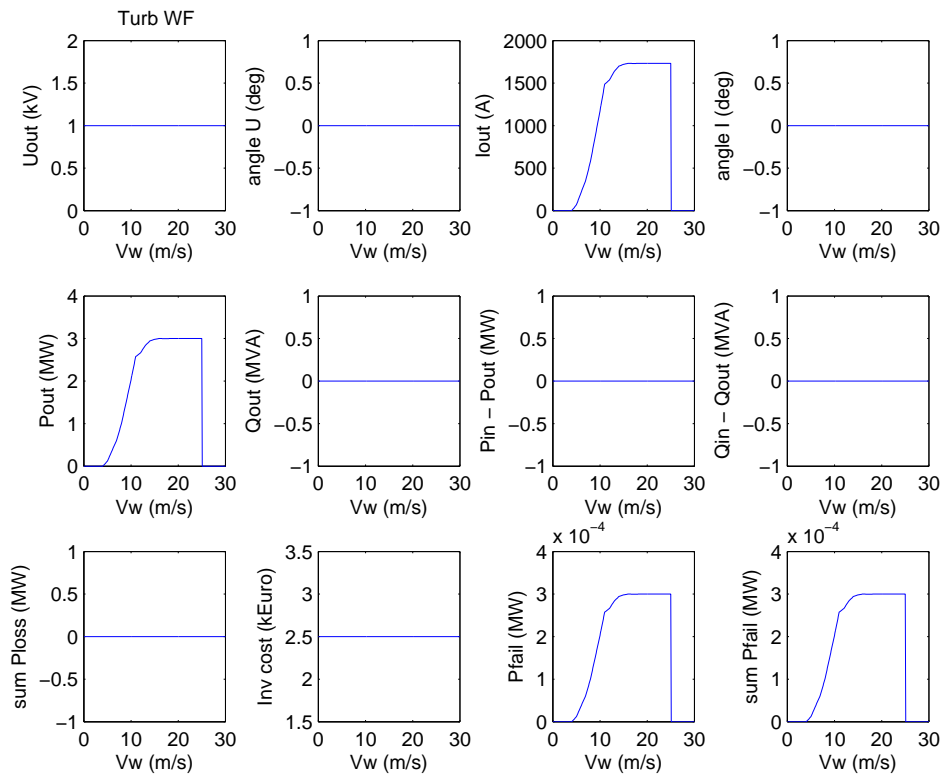


Figure 105: *Bus signals of the generic generator connected to the turbine with wind farm correction*

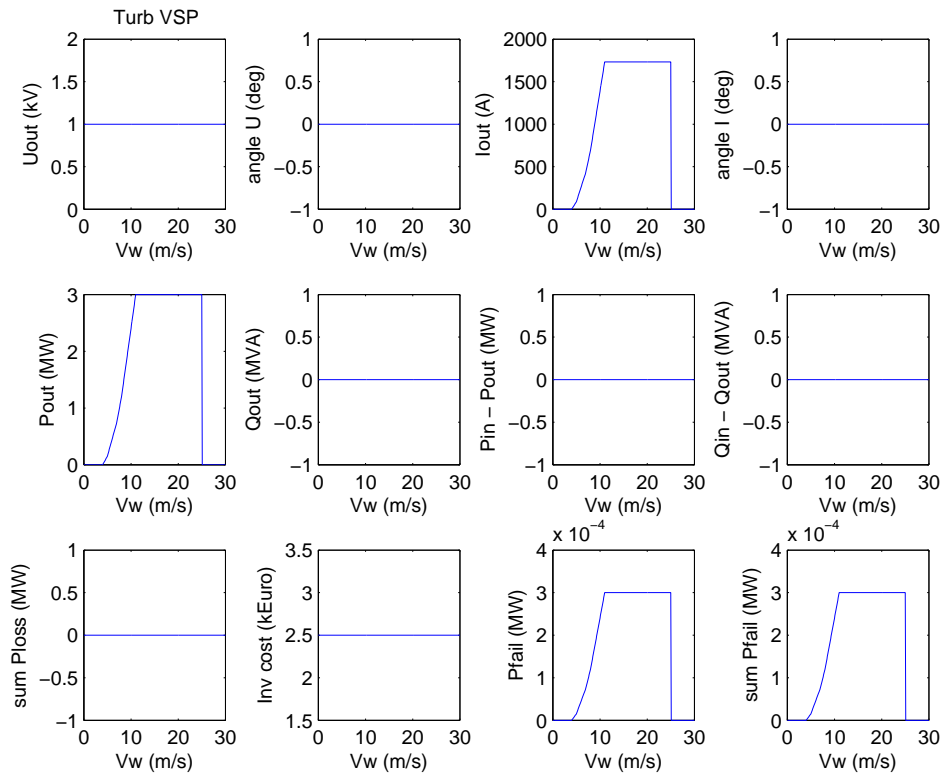


Figure 106: *Bus signals of the generic generator connected to the variable speed turbine*

7.2 Generator models

The five generator models in EeFarm-II are:

- the generic model (a controllable P, Q, U, I source without specific generator type characteristics);
- the constant speed induction machine model;
- the doubly fed induction generator model;
- the full converter induction machine model;
- the full converter synchronous machine model.

7.2.1 Generic Generator

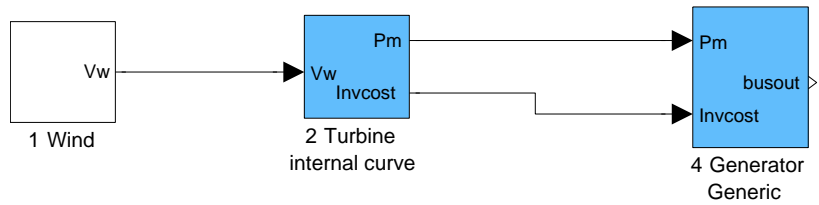


Figure 107: Testmodel for the Generic Generator

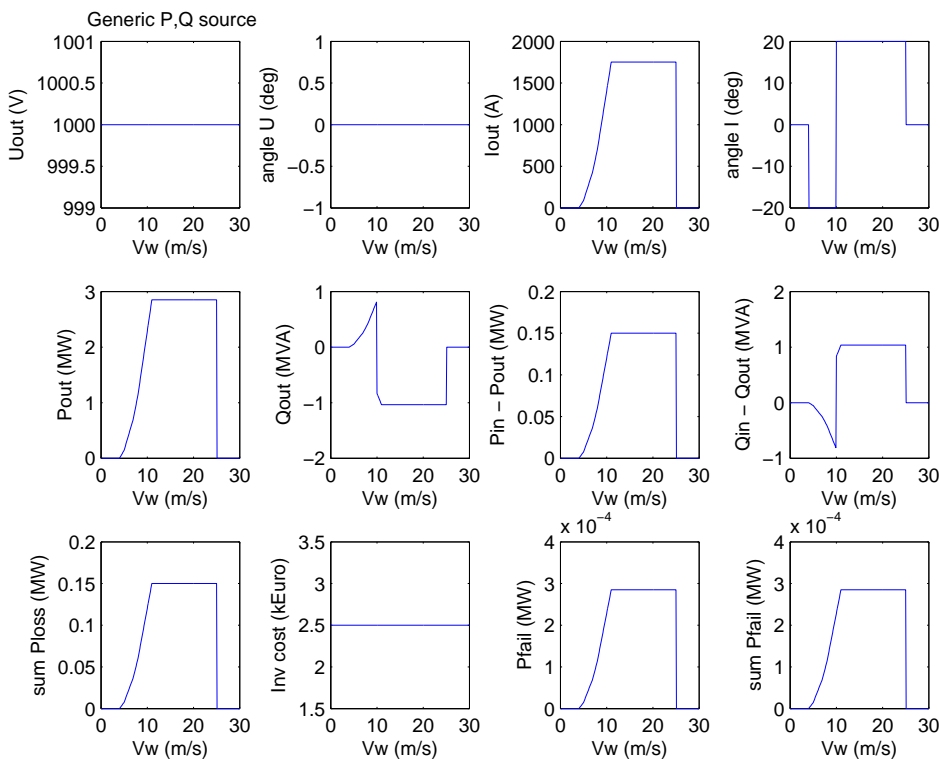


Figure 108: Bus signals for the Generic Generator model

Figure 108 shows the bus signals for the Generic Generator model for increasing wind speed. The current angle changes from -20 to 20 degrees at $V_w = 10$ m/s. The reactive power follows

the active power, with a sign change at $V_w = 10$ m/s. The losses and the not produced power due to component failure are proportional to the produced power (a constant efficiency is assumed, the generic generator model does not use resistances and inductances).

7.2.2 Constant speed induction machine

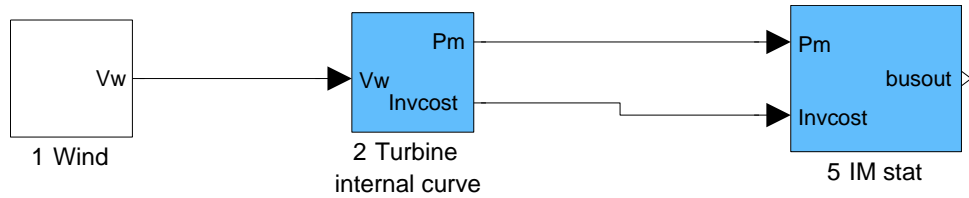


Figure 109: Testmodel for the Constant speed Induction Machine

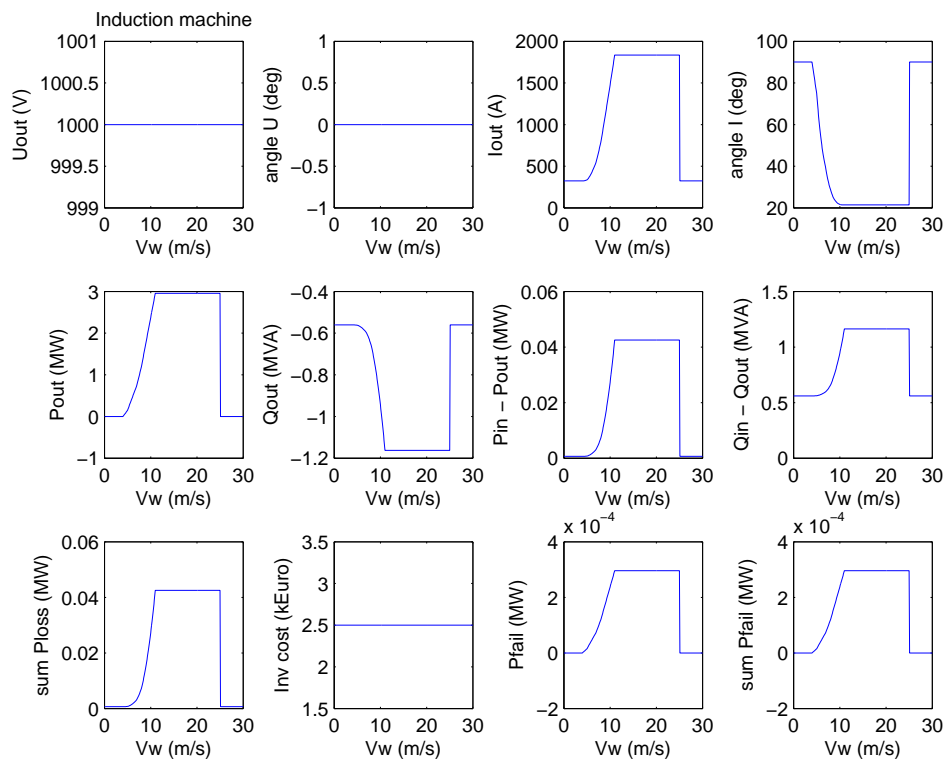


Figure 110: Bus signals for the Constant speed Induction Machine model

Figure 110 shows the bus signals for the Constant speed Induction Machine model for increasing wind speed. The current and the current angle depend on the slip. The reactive power changes from about -0.6 MVA at no load to -1.2 MVA at full load. The losses are not proportional to the produced power.

7.2.3 DFIG

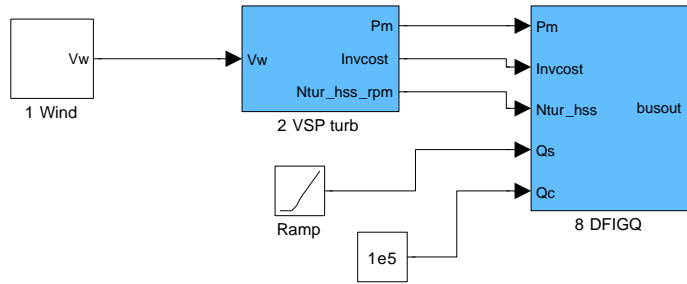


Figure 111: Testmodel for the Doubly Fed Induction Machine

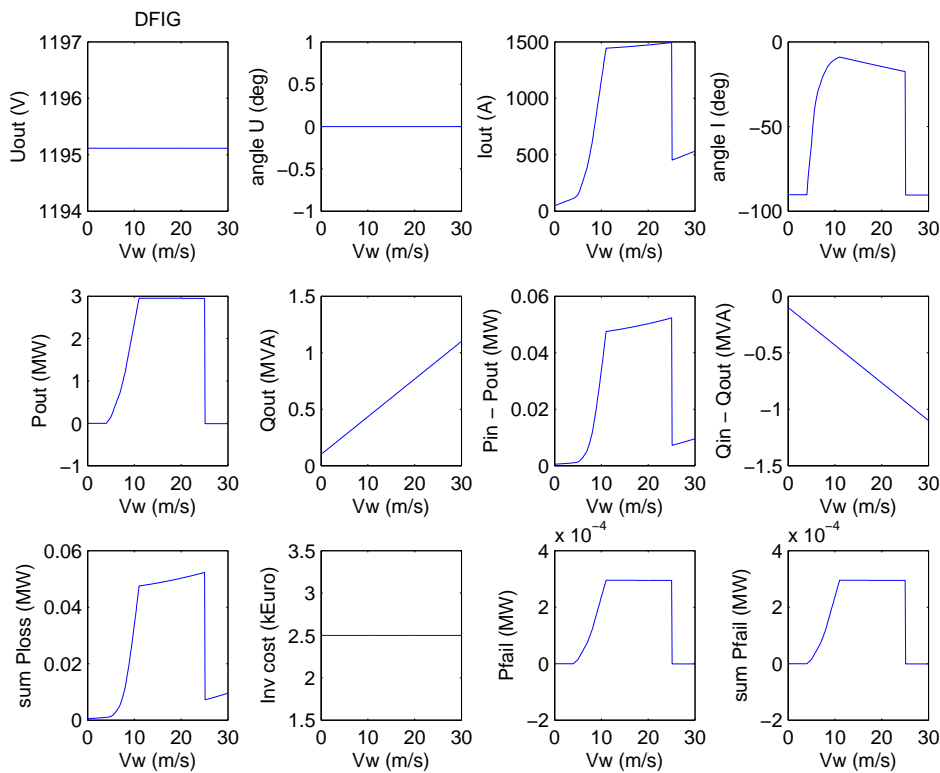


Figure 112: Bus signals for the Doubly Fed Induction Machine model

Figure 110 shows the bus signals for the Doubly Fed Induction Machine model with increasing wind speed. The input mechanical power, rotational speed, stator reactive power setpoint and grid converter reactive power setpoint determine the point of operation of the DFIG. The stator reactive power is increased in the test and the grid converter reactive power is kept constant. The DFIG model calculates the magnitude and the angle of the total current (stator plus grid side converter).

7.2.4 FCIM

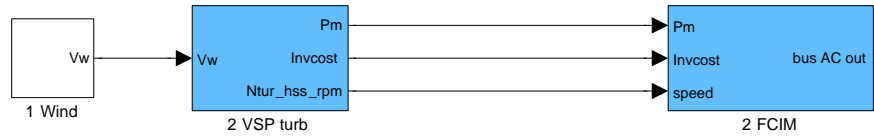


Figure 113: Testmodel for the Full Converter Induction Machine

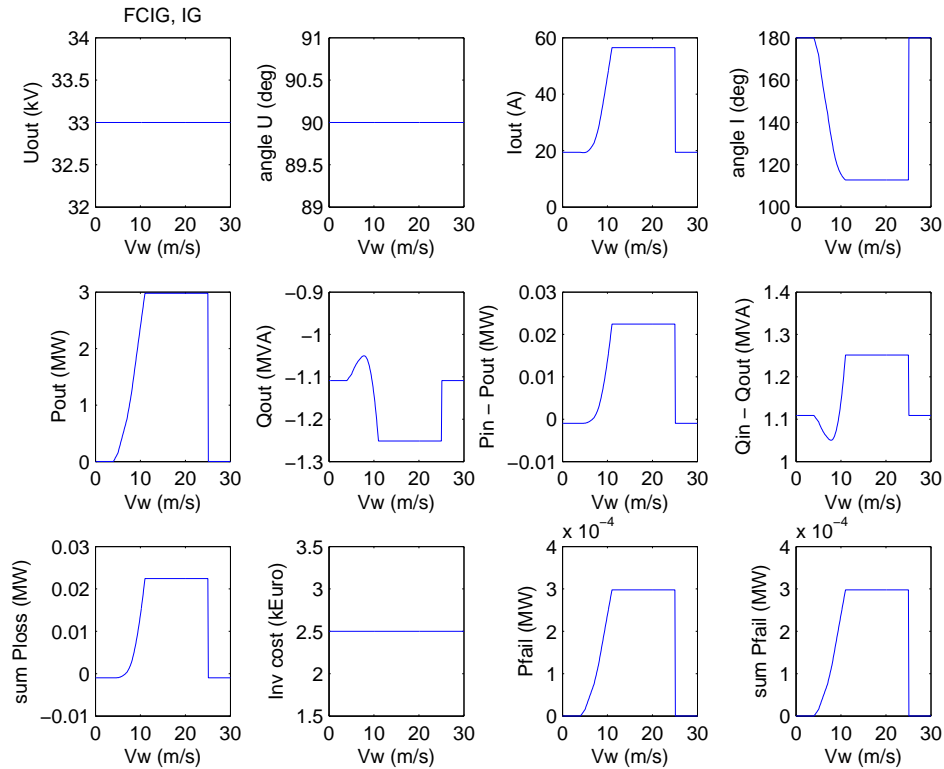


Figure 114: Bus signals of the Induction Machine in the FCIM model

The Full Converter Induction Machine model is more complicated than the DFIG model because the rectifier and inverter are modelled separately. Figure 114 shows the bus signals for the variable speed, constant voltage induction machine. Due to the use of the dq-model for the induction machine, the reference angle for the voltage is 90 degrees instead of 0 degrees used elsewhere. This explains an angle of 180 degrees at the start of the simulation (the machine consumes only reactive power). The model uses precalculated tables for P_{el} , P_{loss} , I_{sd} , I_{sq} and ω_s .

Figures 115 and 116 give the output signals of the rectifier and the inverter. The rectifier output voltage and current are DC, so there is no angle and no output reactive power. On the AC side (input) the rectifier supplies the reactive power requested by the induction machine, which adds to the losses in the rectifier. The losses are relatively large, as a result of the chosen rectifier parameters.

The voltage angle of the inverter is zero, in line with the chosen voltage phasor reference for the non dq-models in EeFarm-II. The output reactive power was set to 1 MVA. Then the inverter bus variables change with the wind speed and the produced power.

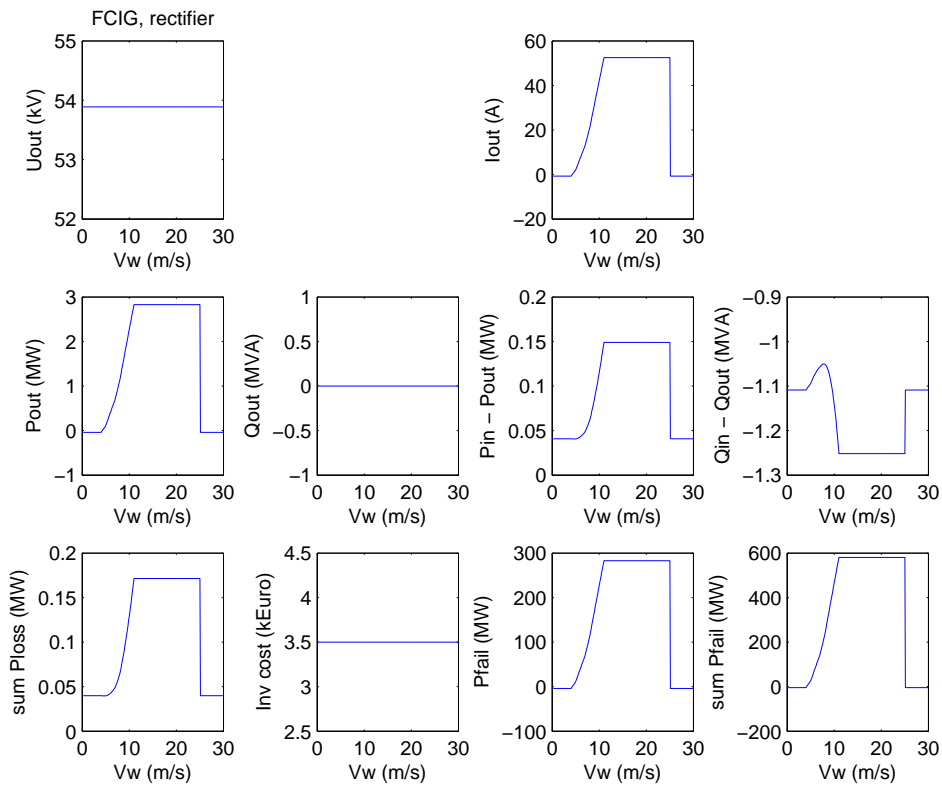


Figure 115: *Bus signals of the Rectifier in the FCIM model*

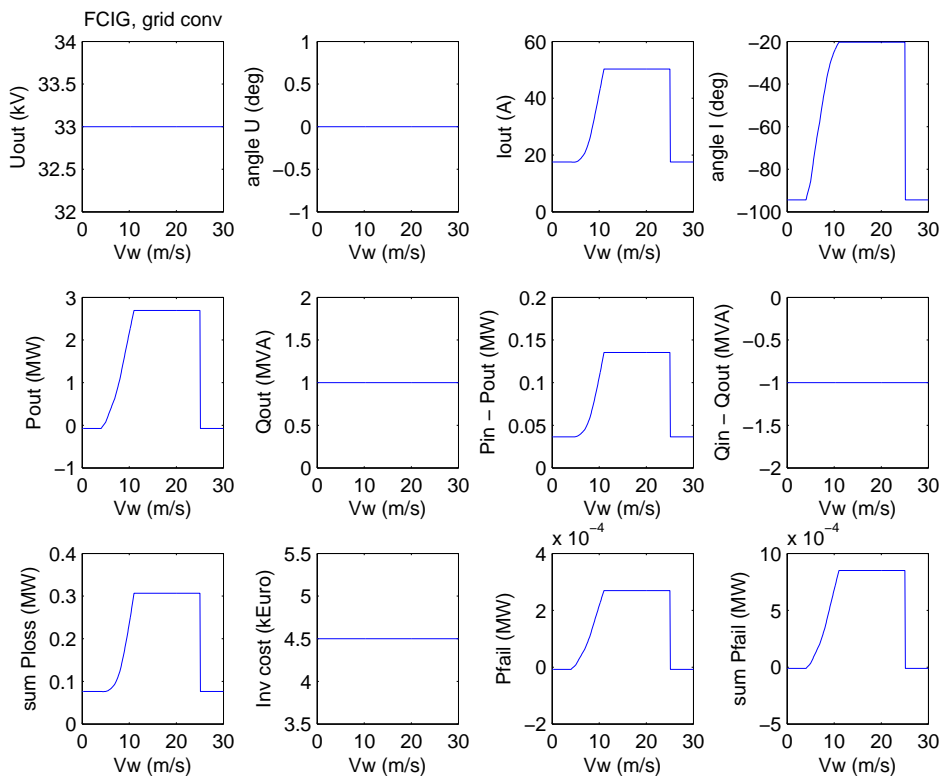


Figure 116: *Bus signals of the Inverter in the FCIM model*

7.2.5 FCSM

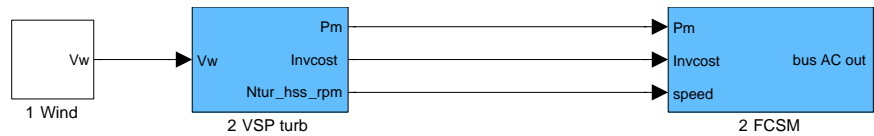


Figure 117: Testmodel for the Full Converter Synchronous Machine

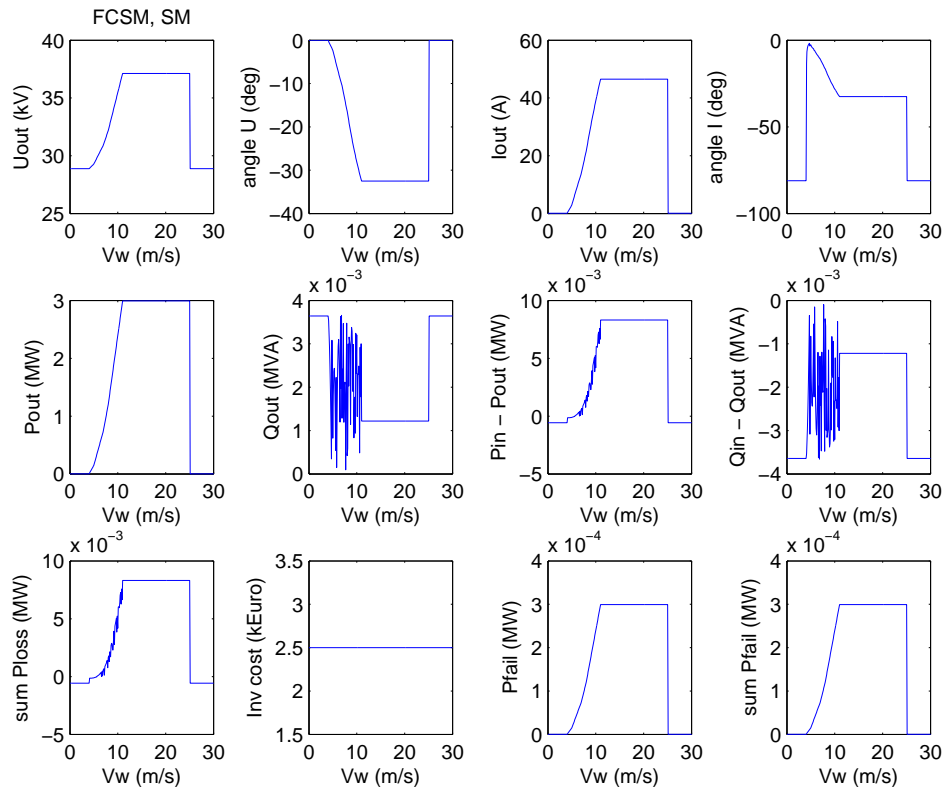


Figure 118: Bus signals of the Synchronous Machine in the FCSM model

Figure 118 to 120 show the bus signals for the FCSM model for increasing wind speed. Figure 118 shows the variable speed, variable voltage synchronous machine. The reactive current is controlled to practically zero by adjusting the field current. Due to the step size in the field current, the reactive power oscillates a little. The scale in the reactive power plots is 10^{-3} MVA, so the variations in reactive power are irrelevant. The change in angle of the current is not determined by the small change in reactive power but by the rotation of the voltage phasor. The losses (stator and field ohmic losses) are relatively small (almost 1 %). The synchronous machine model is implemented as precalculated tables for P_{el} , P_{loss} , I_{sd} , I_{sq} for variable speed, variable voltage and variable synchronous machine load angle and for zero reactive power (minimal current and losses).

Figures 119 and 120 give the output signals of the rectifier and the inverter of the FCSM model. The rectifier output voltage and current are DC, so there is no angle and no output reactive power. On the AC side (input) the rectifier supplies no the reactive power (not requested by synchronous machine), which reduces the losses of the rectifier. The losses are relatively large, as a result of the chosen rectifier parameters.

The voltage angle of the inverter is zero, in line with the chosen voltage phasor reference for the non dq-models in EeFarm-II. The output reactive power was set to 1 MVA. Then the inverter bus variables change with the wind speed and the produced power.

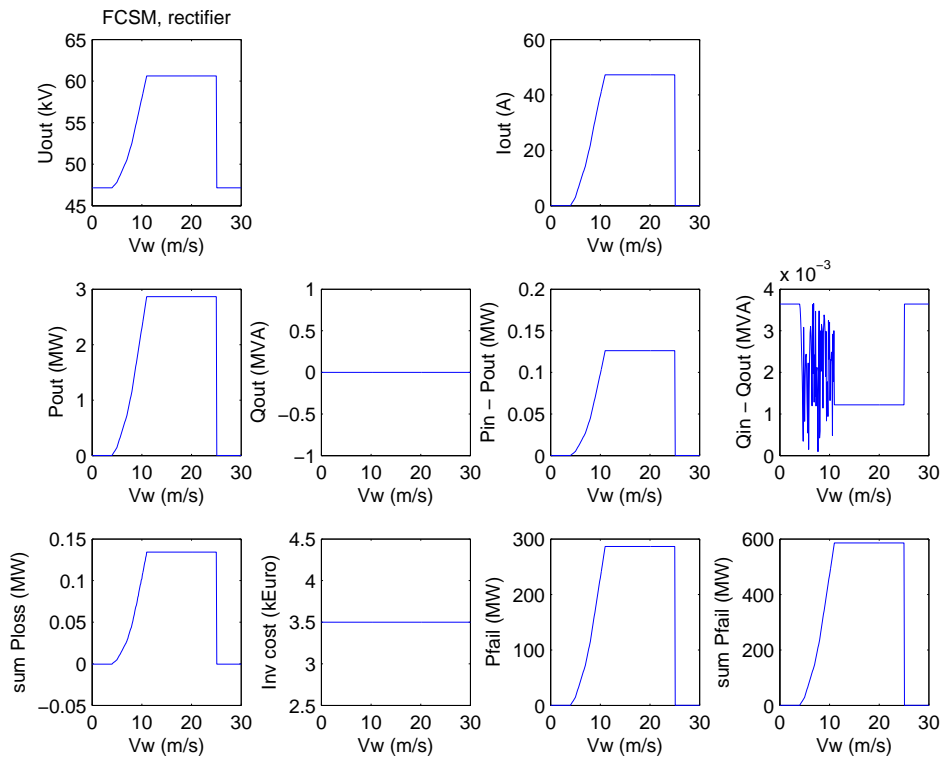


Figure 119: Bus signals of the Rectifier in the FCSM model

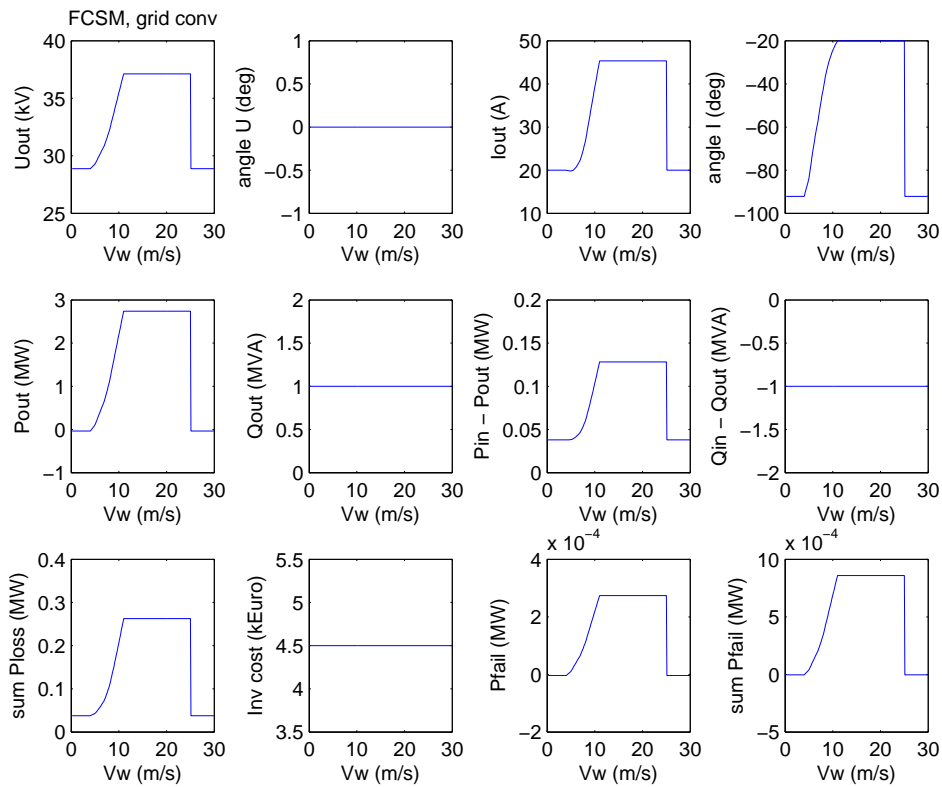


Figure 120: Bus signals of the Inverter in the FCSM model

7.3 AC cable models

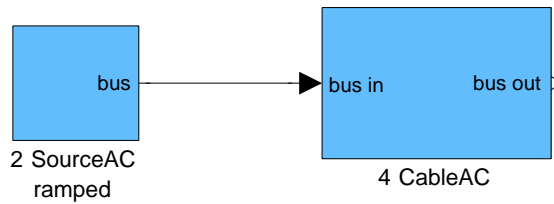


Figure 121: Testmodel for AC cable

The AC cable is connected to a ramped current source, figure 121. First, the input current amplitude is increased at constant current phase angle and subsequently the phase angle is increase at constant current amplitude, see figure 122. The cable output power increases from about 16 MW to about 50 MW and then decreases to just below zero. The reactive power supplied by the cable is relatively low compared to the power and the change in input reactive power: about -0.7 MVA compared to about -50 MVA. For increasing power, the output voltage amplitude decreases. For decreasing power and decreasing output reactive power (at constant current amplitude), the output voltage amplitude increases. The change in output voltage angle is relatively small.

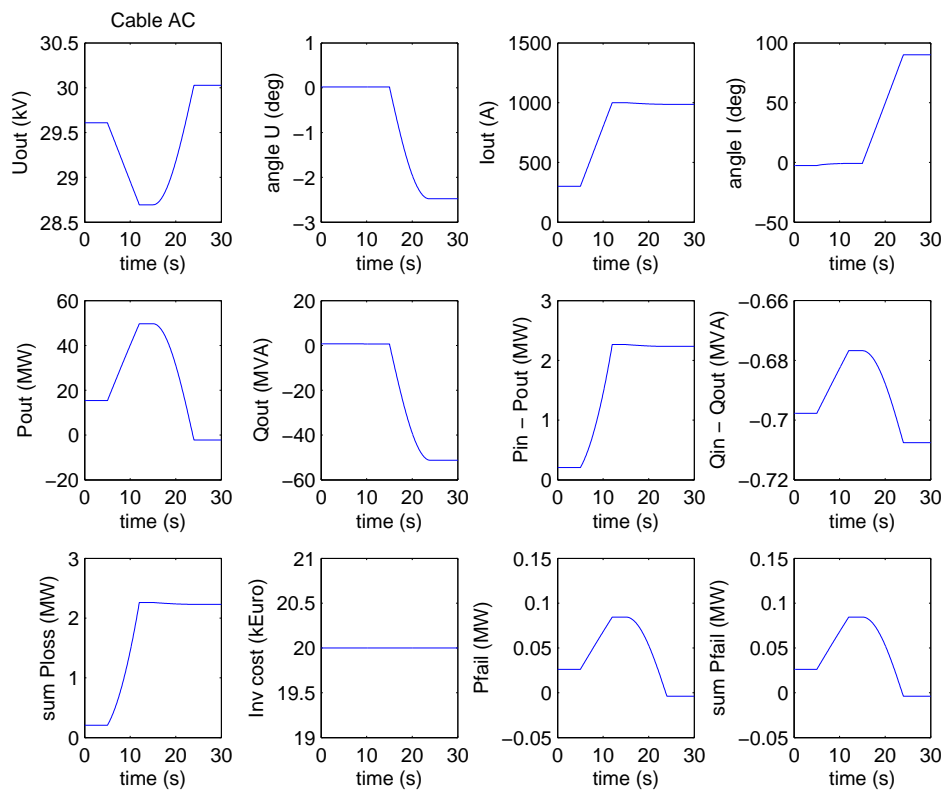


Figure 122: Bus signals of the AC cable

7.4 Transformer model

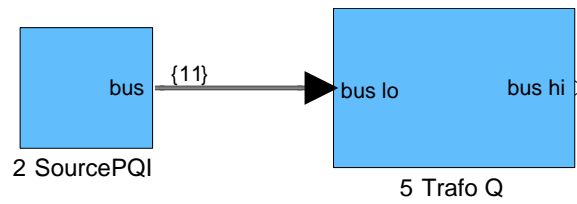


Figure 123: Testmodel for Trafo

The transformer model is connected to an active and reactive power source, figure 123. Parameters of a relatively small transformer of 10 kVA have been used in this test. Initially the input active and reactive power are zero and the output current is purely inductive (negative reactive power), see figure 124. At $t=5$ s the input power is increased until it reaches its maximum at $t=10$ s. This decreases the reactive power (more inductive reactive power needed) but decreases the power angle. At $t=20$ s a step occurs in the input reactive power in the capacitive direction. This increases the current amplitude additionally and therefore the losses increase as well.

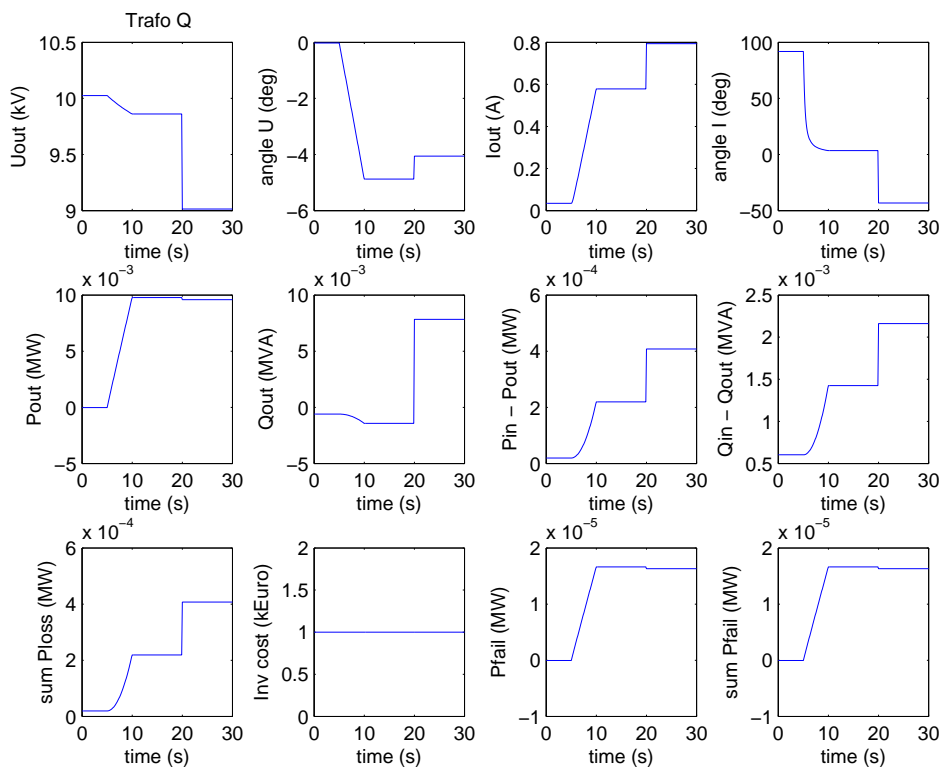


Figure 124: Bus signals of the trafo model

7.5 Inductor model

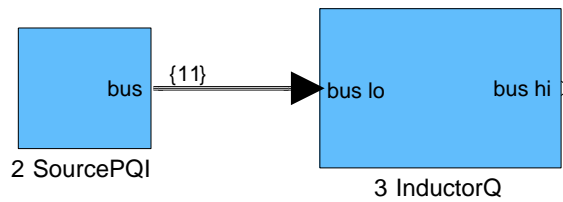


Figure 125: Testmodel for Inductor

The inductor model is connected to a power and reactive power source, figure 125. The inductor consumes 1 MVA at 10 kV (Q_{out} -1 MVA). Initially the input power and reactive power are zero and the output current is purely inductive. At $t=5$ s the input power is increased until it reaches 1 MW at $t=10$ s, see figure 126. Current amplitude increases and current angle decreases. At $t=20$ s the input reactive power is increased to +1 MVA (capacitive), which results in zero reactive power output, i.e. the reactive power of the inductor is now produced at the input instead of the output.

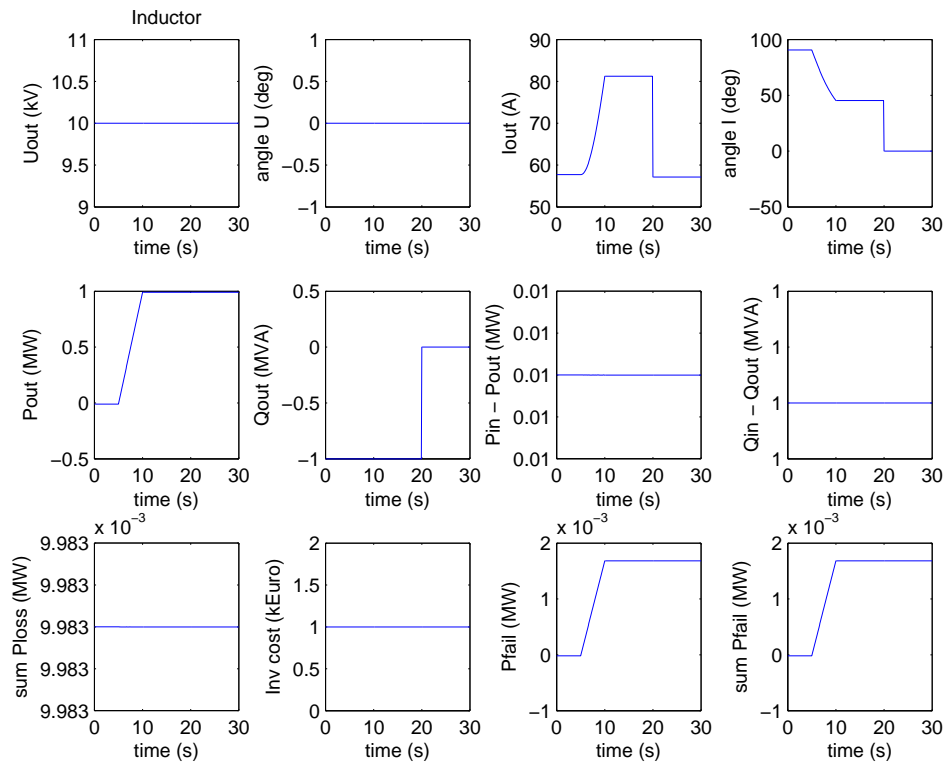


Figure 126: Bus signals of the Inductor model

7.6 TUD-PWM rectifier, inverter and DC cable model

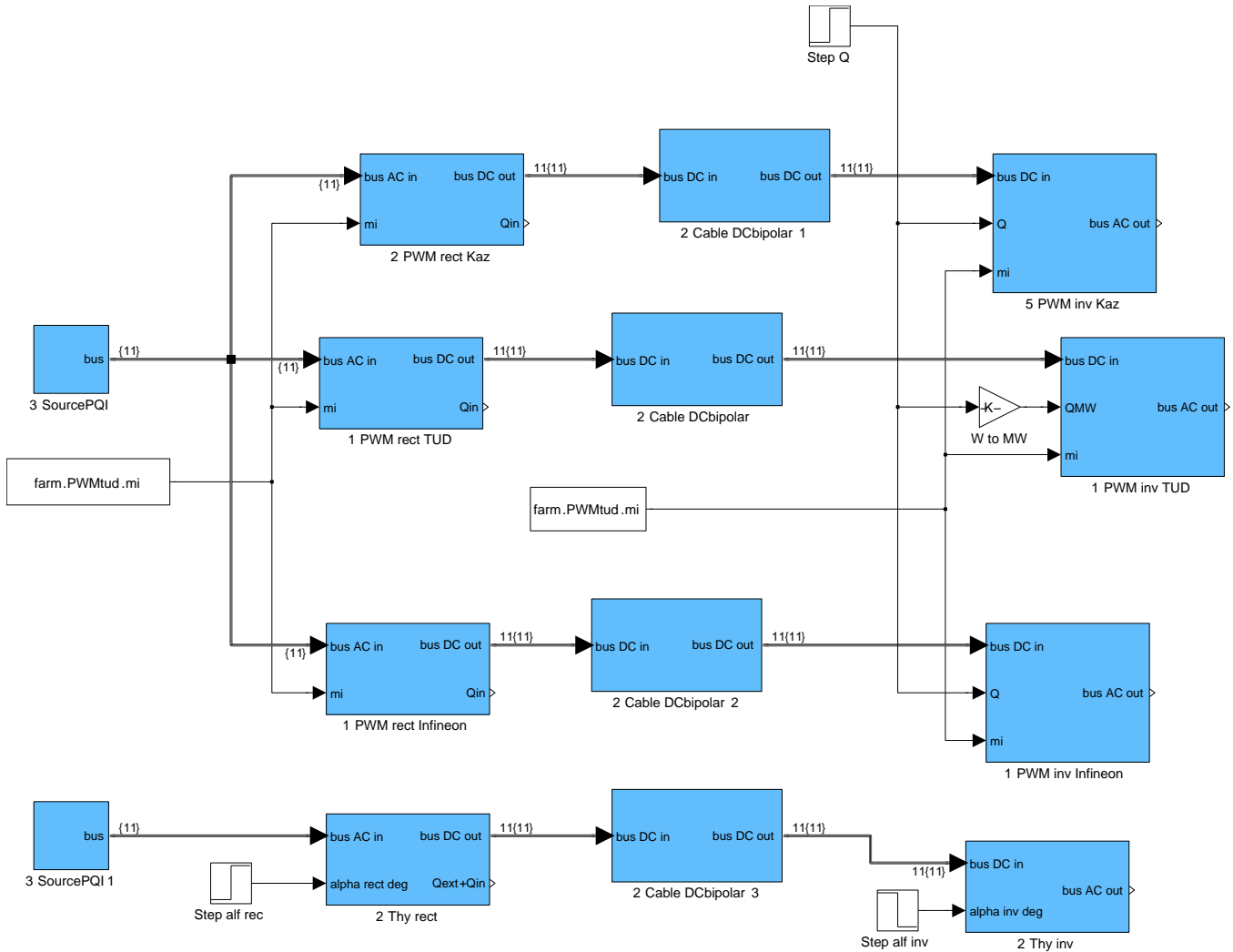


Figure 127: Testmodel for most of the DC component

To test the TUD-PWM, Kaz-PWM, Inf-PWM and the thyristor converter models as well as the DC cable model, the layout of figure 127 is used. The same AC input is fed into the three PWM rectifiers. The AC input of the thyristor rectifier is different, due to the smaller rating of this converter. The power is increased to the rated power of the converters in 5 seconds. At 8s the rectifier reactive power is increased to 100 MVA for the PWM rectifiers and inverters and the firing angles of the thyristor rectifier and inverter are changed from 20 to 30 degrees and from 160 to 150 degrees.

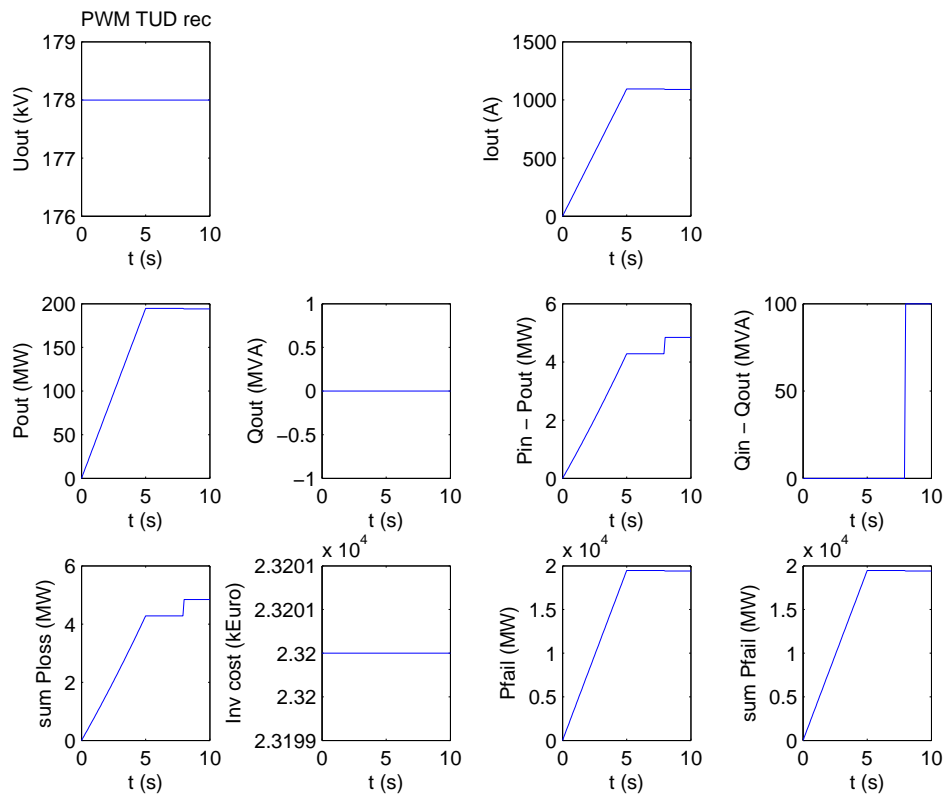


Figure 128: Bus signals of the TUD-PWM rectifier model

Figure 128 shows the output of the TUD PWM rectifier model. The DC voltage is not affected by the changes. The DC current increases with the input power and decreases slightly with an increase in reactive power (increasing losses).

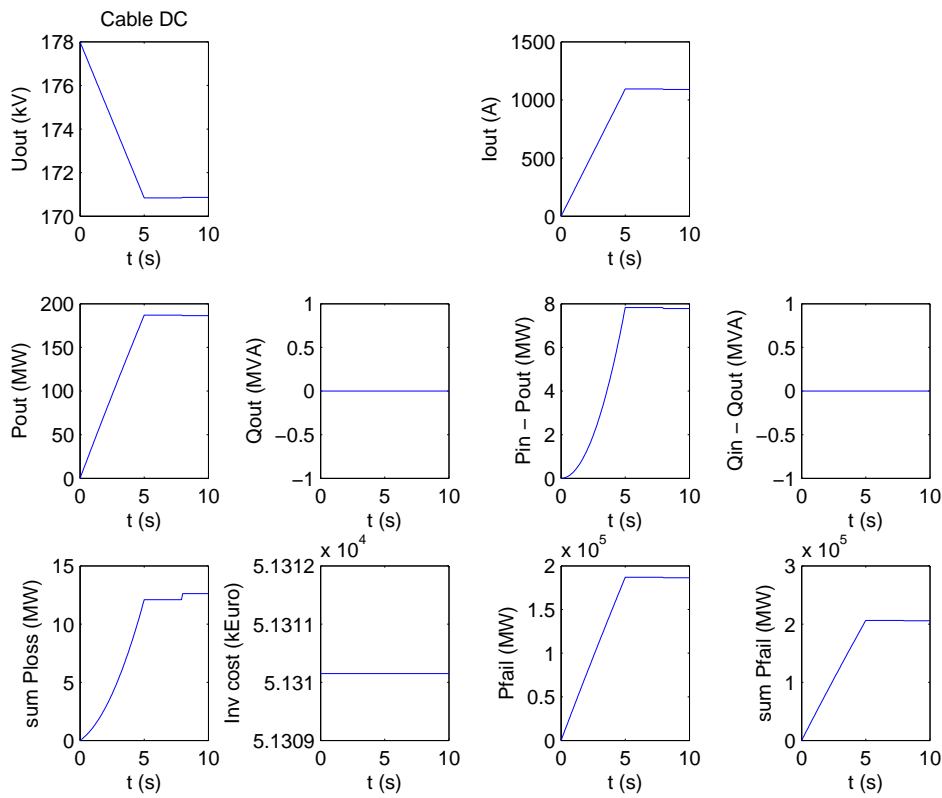


Figure 129: Bus signals of the DC cable model

Figure 129 shows the output of the DC cable connecting the TUD-PWM rectifier and inverter. The DC voltage decreases with increasing power and current. The step in reactive power decreases the losses slightly (the input power is reduced).

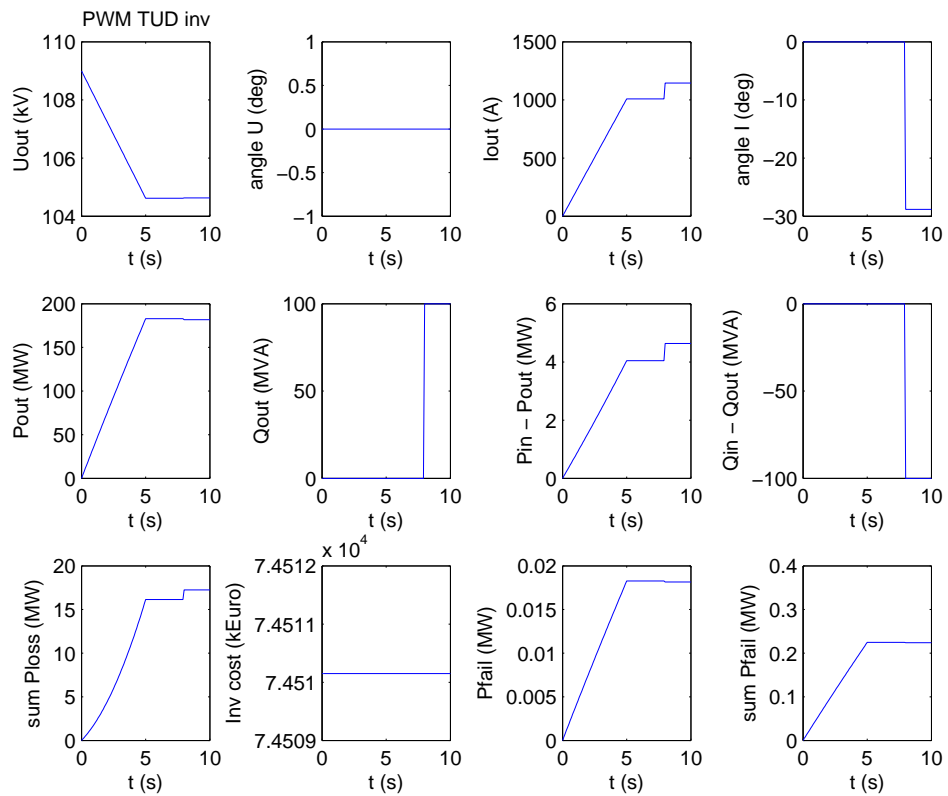


Figure 130: Bus signals of the TUD-PWM inverter model

The inverter current follows the increase in power and the step in reactive power. The losses increase with the current. The output voltage is reduced due to the reduced input voltage, determined by the cable losses.

7.7 Kaz-PWM rectifier and inverter model

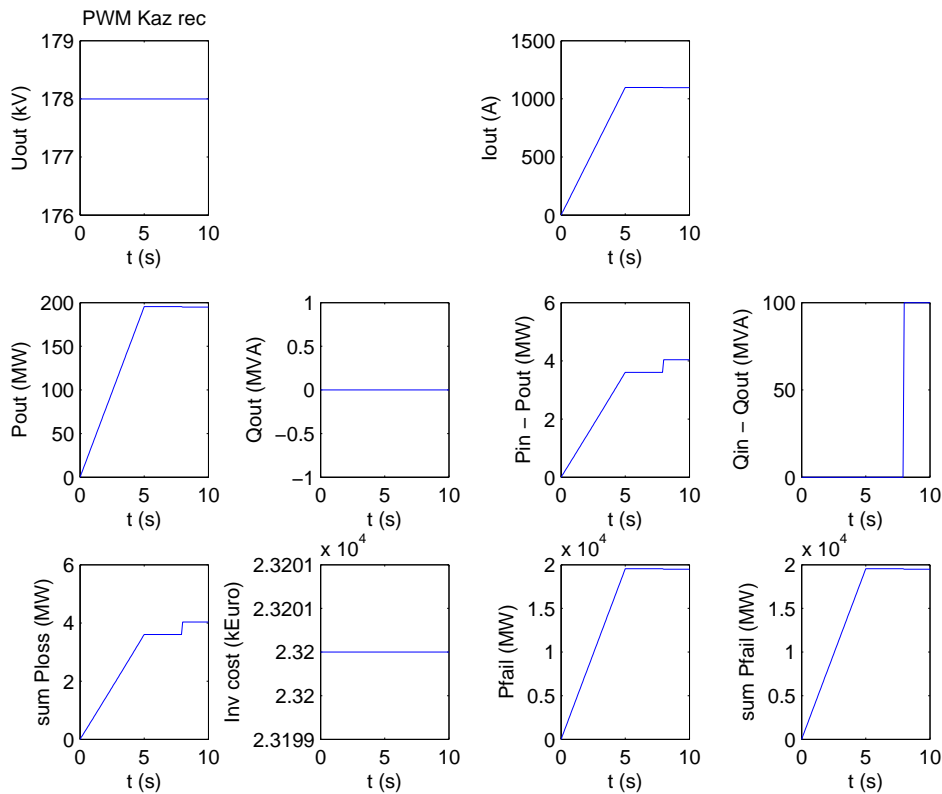


Figure 131: Bus signals of the Kaz-PWM rectifier model

Figure 131 shows the output of the Kazmierkowski PWM rectifier model. The input power is increased to rated power in 5 seconds. At 8s the input reactive power is increased to 100 MVA. The DC voltage is not affected by the changes. The DC current increases with the input power and decreases slightly with an increase in reactive power (increasing losses).

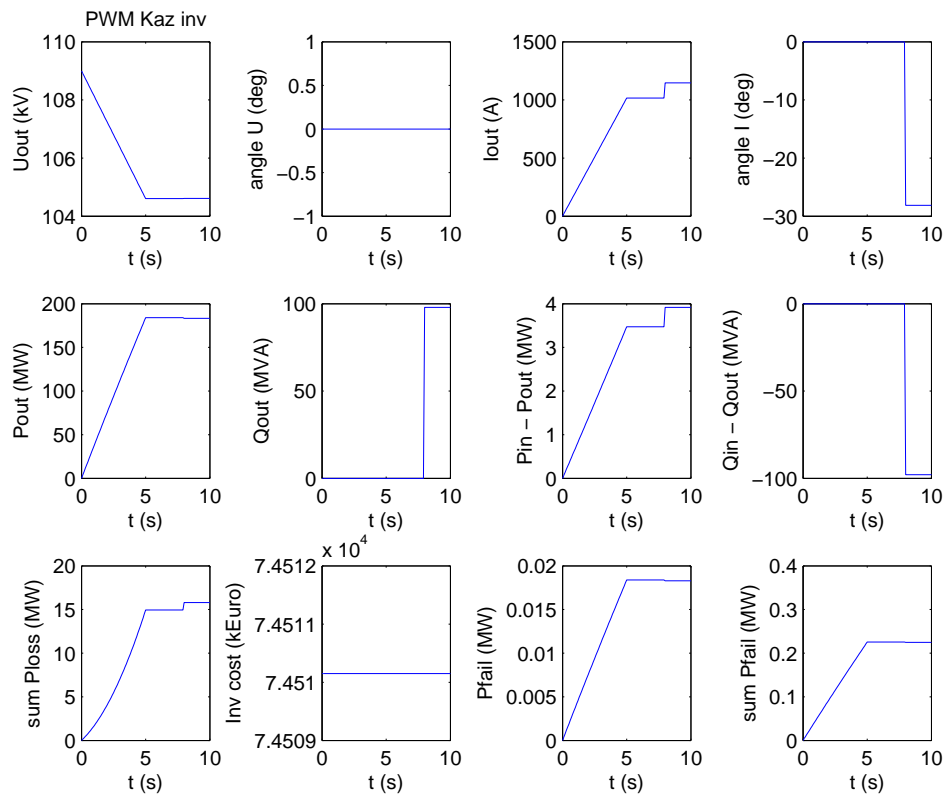


Figure 132: Bus signals of the Kaz-PWM inverter model

The AC voltage of the Kaz-PWM inverter model follows the input voltage (figure 132). The current follows the active and reactive power changes.

7.8 Inf-PWM rectifier and inverter model

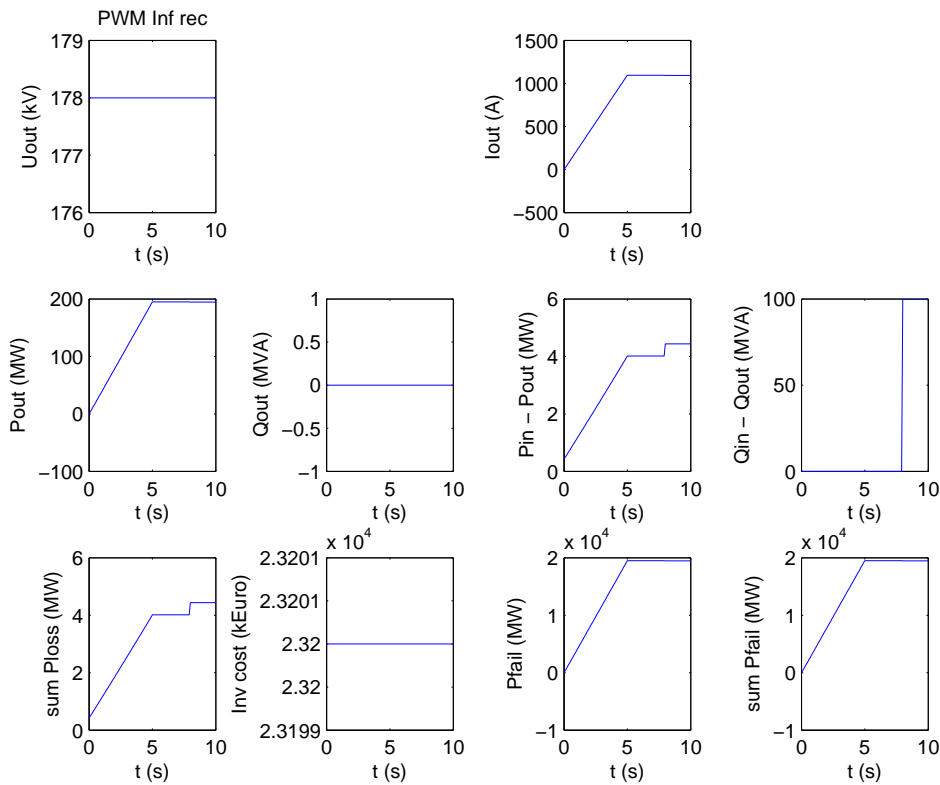


Figure 133: Bus signals of the Inf-PWM rectifier model

Figure 133 shows the output of the Infineon PWM rectifier model. The input power is increased to rated power in 5 seconds. At 8s the input reactive power is increased to 100 MVA. The DC voltage is not affected by the changes. The DC current increases with the input power and decreases slightly with an increase in reactive power (increasing losses).

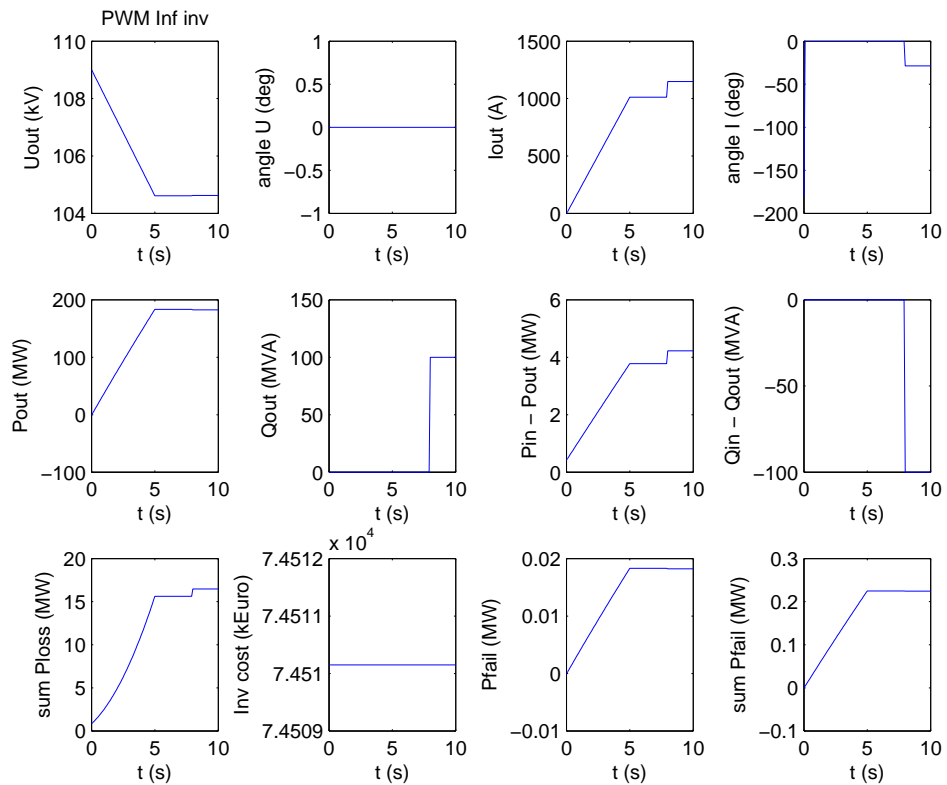


Figure 134: Bus signals of the Inf-PWM inverter model

The AC voltage of the Inf-PWM inverter model follows the input voltage (figure 134). The current follows the active and reactive power changes.

7.9 Thyristor rectifier and inverter model

Figure 135 shows the output of the thyristor rectifier. The output power follows the input power increase. At $t=8$ s the rectifier firing angle is increased from 20 degrees to 30 degrees. This decreases the DC voltage and increases the DC current (power almost constant requires a higher current). $Q_{in} - Q_{out}$ is the reactive power required by the rectifier, which has to be supplied externally (this reactive power supply is not included in the test model).

Figure 136 shows the output of the thyristor inverter. The AC voltage decrease between 0 and 5 s is caused by the decreasing output voltage of the DC cable (cable losses increase). The decrease of the DC voltage at 8 s is caused by the decrease of the rectifier voltage and the step in the firing angle of the inverter.

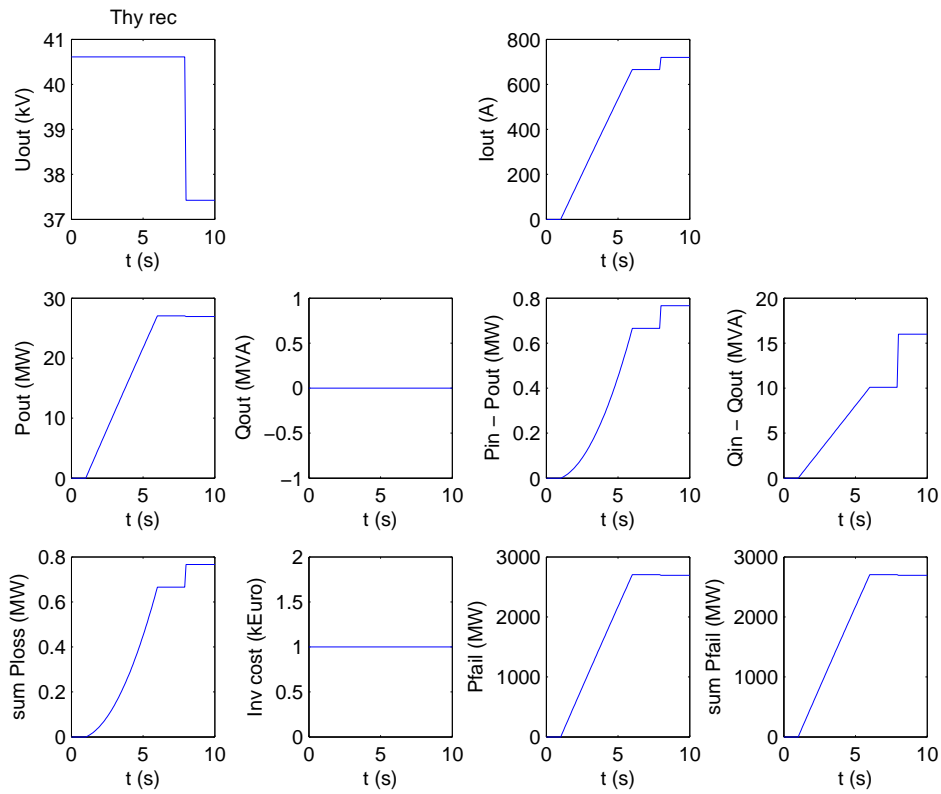


Figure 135: Bus signals of the thyristor rectifier model

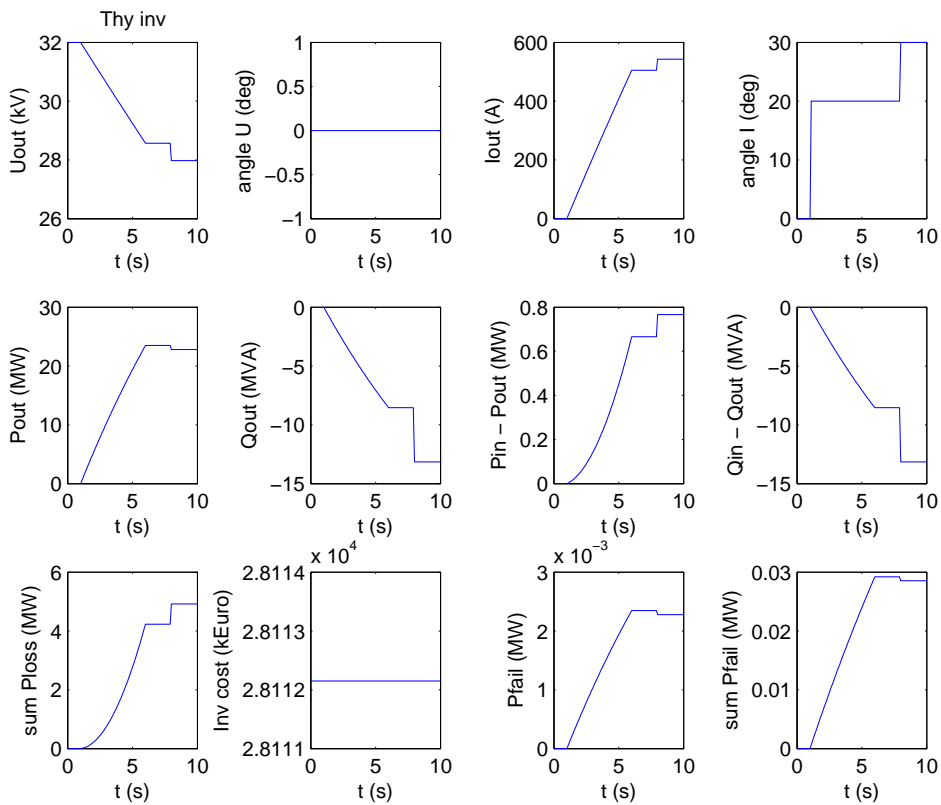


Figure 136: Bus signals of the thyristor inverter model

7.10 Statcom

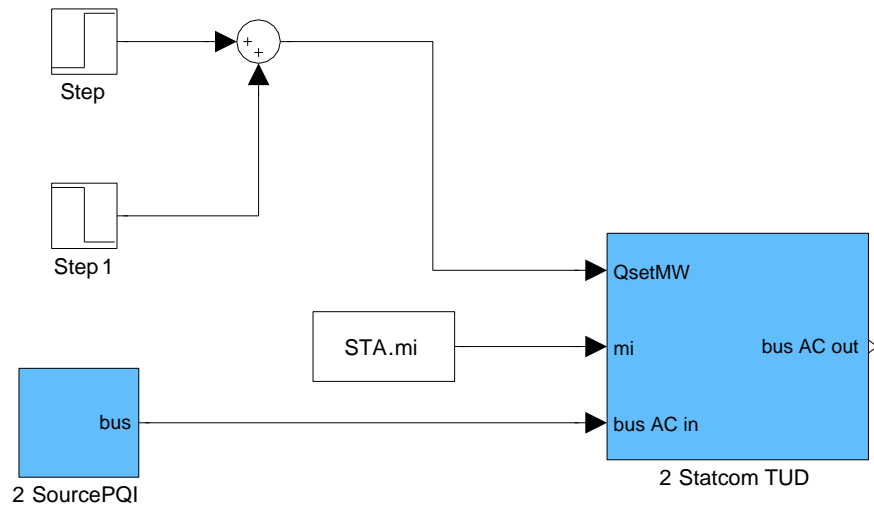


Figure 137: Testmodel for the Statcom

Figure 138 shows the output of the Statcom model, i.e. the sum of input and production by the statcom. The initial input power and reactive power is zero. At $t=5s$ the input power is increased to 10 MW in 5 seconds. The Statcom initially produces 0 MVA, which is changed to 5 MVA at $t=10s$ and to -10 MVA at $t=15s$. At $t=20s$ the input reactive power is increased to 10 MVA. The change in produced reactive power affects the losses, the change in input active or reactive power does not.

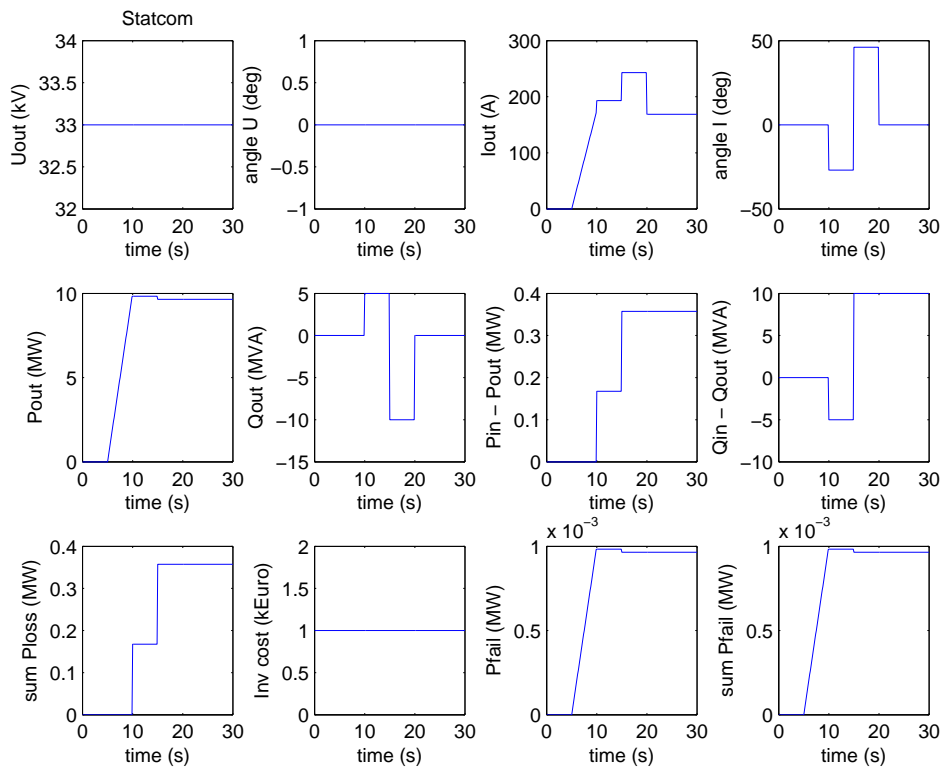


Figure 138: Bus signals of the Statcom

7.11 Step-up chopper

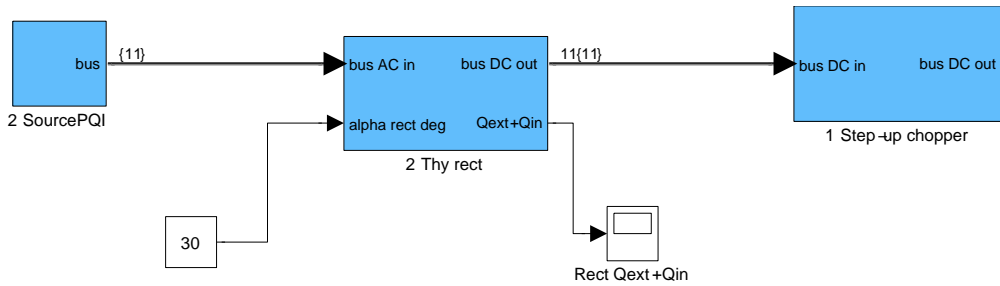


Figure 139: Testmodel for the Chopper

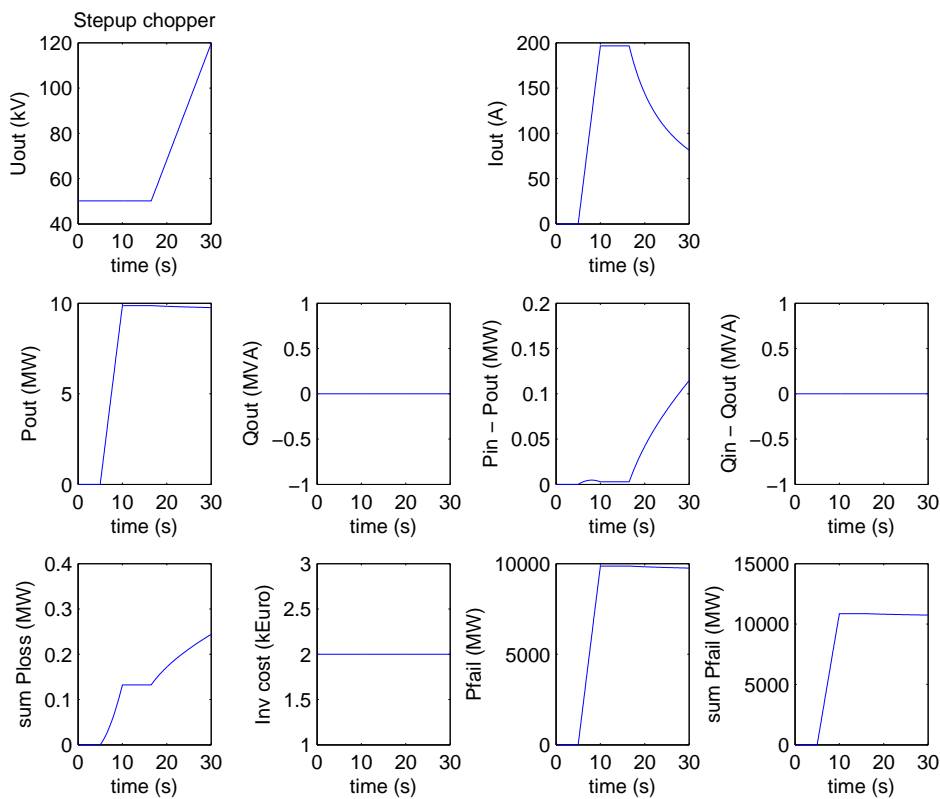


Figure 140: Bus signals of the Chopper

Figure 140 shows the output of the Chopper model. The initial input power is zero. At $t=5s$ the input power is increased to 10 MW in 5 seconds. At $t=15s$ the k-factor (U_{in}/U_{out}) is increased from 1.1 to about 3 at $t=30s$. The losses depend on the current and strongly on the k-factor. The parameters are arbitrary.

8 EeFarm-II application to Erao-1 system evaluation

8.1 System description

The Erao-1 study [17] compared thirteen electrical systems for the connection of a wind farm to the grid. Since 2001 prices and performance of some of the components have changed considerably. Therefore, the Erao-1 systems have been re-evaluated, using the EeFarm2 program with updated database. Figures 141-refPV1 give the layout of the Erao-1 systems.

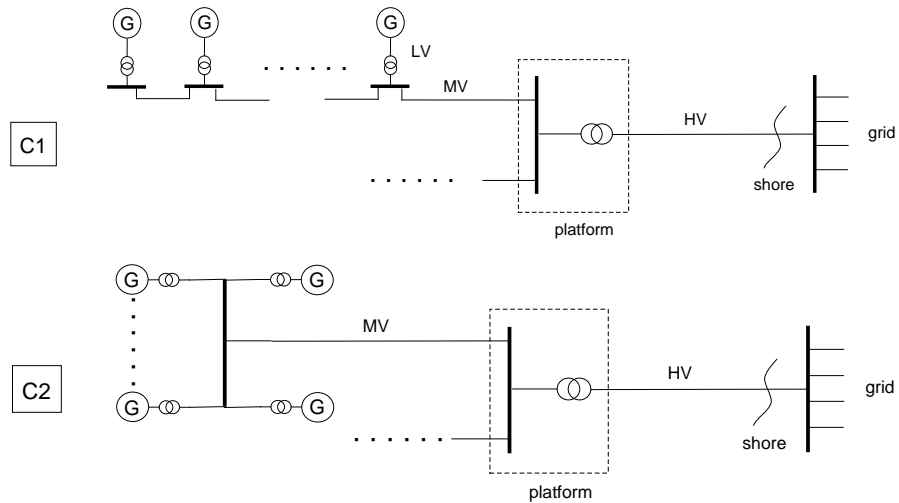


Figure 141: *Constant speed systems*

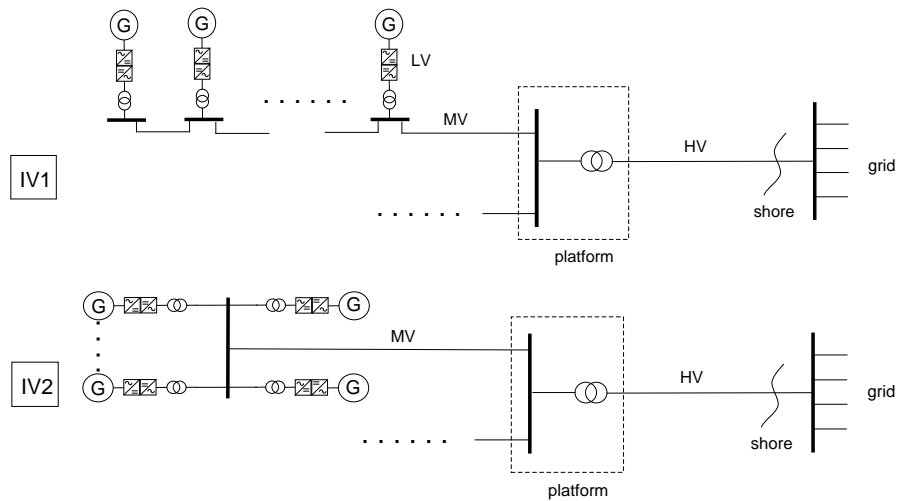


Figure 142: *Individual variable speed with back-to-back converters*

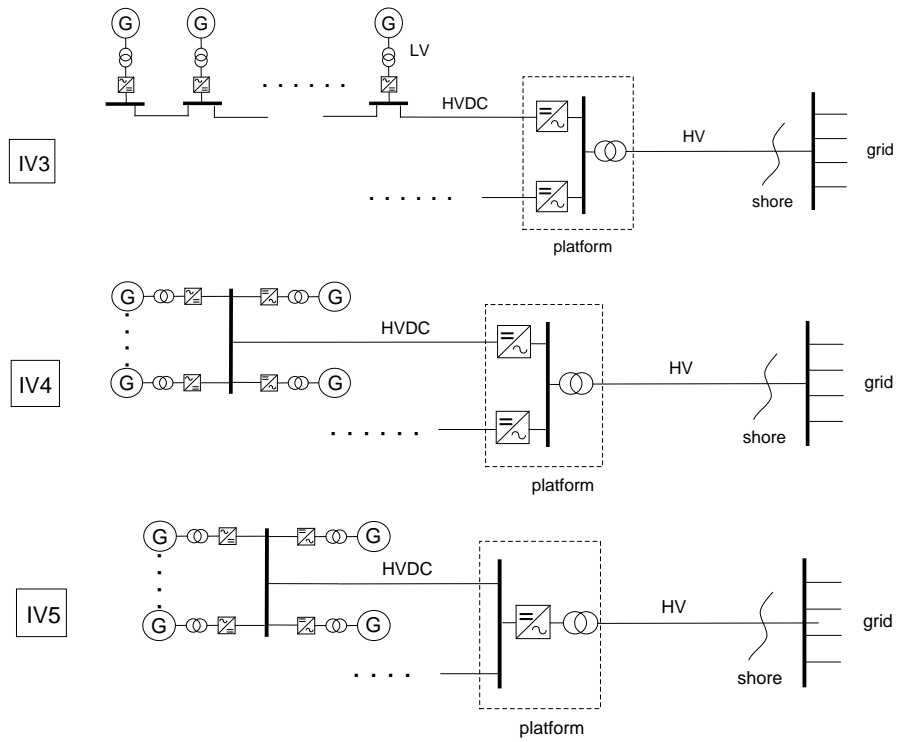


Figure 143: Individual variable speed with multi-terminal HVDC system

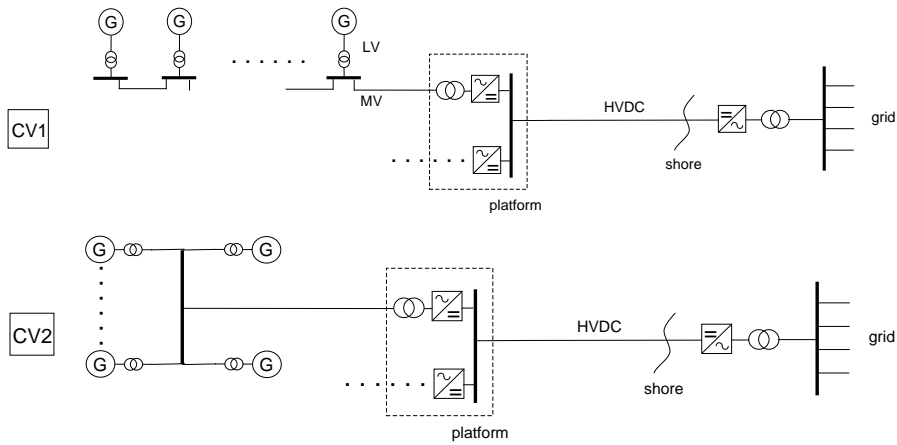


Figure 144: Cluster-coupled variable-speed with multi-terminal HVDC system

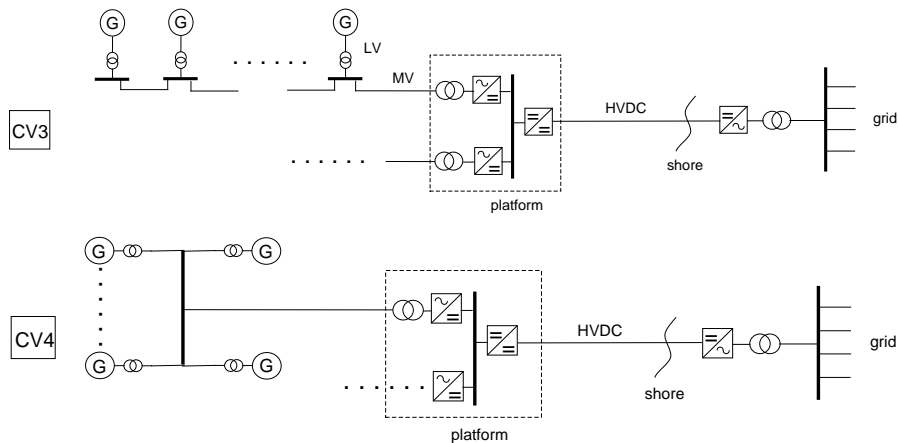


Figure 145: Cluster-coupled variable-speed HVDC system and step-up chopper

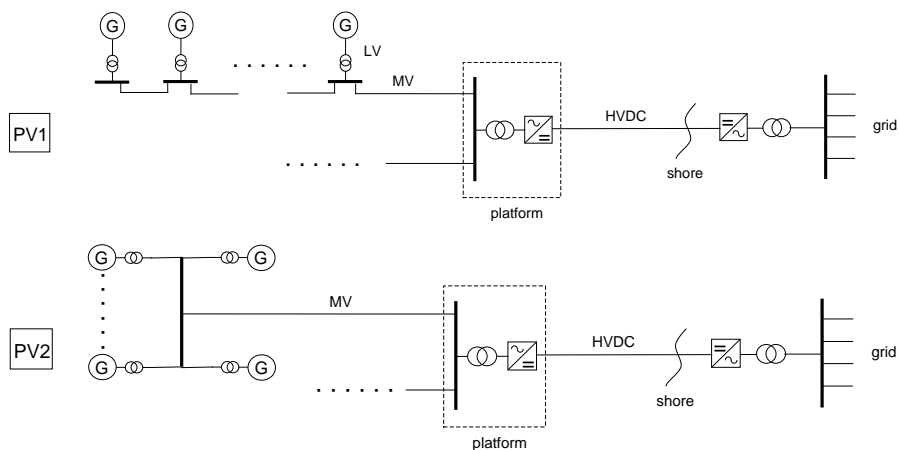


Figure 146: Park-coupled variable-speed system with HVDC system

The main characteristics of the thirteen systems are:

- a wind farm size of 200 MW;
- a wind turbine size of 5 MW;
- the length of the cable to shore is 100 km;
- two wind farm layouts: strings of 5 turbines (daisy chain) or stars of 9 turbines connected to turbine number 10 at the center;
- four types of system operation:
 - constant speed, all AC system (C1 and C2);
 - individual variable speed with AC or DC connection to shore (IV1-IV5);
 - cluster variable speed with a number of turbines AC connected to a single rectifier (CV1-CV4);
 - park variable speed: all turbines in the farm are connected to a single AC-DC converter with a DC connection to shore (PV1 and PV2);
- in configuration CV3 and CV4 a chopper is used to increase the DC voltage of the DC connection to shore.

The wind farm size has been based on commercially available AC and DC cables and commercially available PWM converters (the smallest available 150kV converters in the database are 100 and 200 MW). The electrical parameters and budget prices of all components have been supplied by component manufacturers in 2009, with two exceptions: the electrical parameters and budget prices of the choppers (configurations CV3 and CV4) and of the converters with a relatively high voltage and low power rating (configurations IV3, IV4 and IV5) are based on data supplied by component manufacturers in 2001.

The economic parameters for the calculation of the levelised production cost (LPC) are:

- a wind farm life time of 12 years;
- a nominal interest rate of 7% and an inflation of 1.5%;
- the LPC in the presented results in this chapter does not include the turbine costs, it only includes the costs of the electrical components connecting the turbines in the farm to the HV grid on land;
- the LPC does not include operation and maintenance costs.

The wind speed distribution parameters to calculation of the levelised production cost are:

- an average wind speed of 9.7 m/s;
- a Weibul factor $k = 2.08$.

The effect of component failure on the power production of the systems is not included in the results because reliable failure data for some of the components was missing.

8.2 Results

Table 4: *Electrical parameters at connection to the HV grid at rated power of 13 electrical systems for 200 MW wind farm with 100 km connection to shore*

	Voltage (kV)	Current (A)	Power (MW)	Reactive Power (MVA)	Losses (MW)	Relative losses (-)
C1	133	902	189.2	87.3	10.8	0.0538
C2	133	903	188.6	86.6	11.4	0.0570
IV1	128	914	188.7	74.0	11.3	0.0566
IV2	127	915	187.9	73.3	12.1	0.0604
IV3	138	912	186.8	112.6	13.2	0.0659
IV4	132	993	185.1	132.2	14.9	0.0743
IV5	133	980	184.9	129.9	15.1	0.0755
CV1	142	725	177.9	-12.2	22.1	0.1106
CV2	140	733	177.5	-12.4	22.5	0.1125
CV3	128	813	179.9	-12.0	20.1	0.1007
CV4	125	829	179.4	-12.5	20.6	0.1031
PV1	143	718	177.9	-11.9	22.1	0.1104
PV2	141	732	177.9	-12.4	22.1	0.1105

Table 4 lists the electrical parameters at connection to the HV grid at maximum power of the thirteen electrical systems. The systems with AC connecting produce reactive power at the point of connection to the HV grid. To include the effect of the decreasing capacitive current of the 100 km long AC cable, the AC cable was divided into 5 sections. For the all-AC systems, about half of the reactive power supplied by the 100 km long AC cable was consumed by a fixed size inductor located at the connection of the cable to the farm. The other half is supplied by the HV grid on land. The higher Q values of IV3, IV4 and IV5 are caused by a lower reactive power consumption at the farm side of the cable. These systems do not have an inductor but use partial compensation by the PWM inverter at the wind farm platform. The

systems with DC connection to shore have a negative reactive power caused by the on-shore transformer. The losses for the systems with AC connection to shore are considerably less than for the DC connected systems.

In figure 147 the rated power losses are plot per system component. The cable to shore causes the largest portion of the losses. This is true for the AC as well as for the DC connected cases. The AC connected systems use two 138 kV three phase cables with rated apparent power of 149 MVA. The DC connected systems use a single ± 80 kV, 200 MW cable. Comparing the AC and DC cable losses:

$$R_{dc} = 0.0283 \text{ Ohm/km (100 km, } P_r = P_{max} = 200 \text{ MW)}$$

$$P_{dc,loss} = 2 \cdot 0.0283 \cdot 1170 \cdot 1170 \cdot 100 \cdot 10^{-6} = 7.7\text{MW} \approx 4\%$$

$$R_{ac} = 0.0619 \text{ Ohm/km (100 km, } P_r = 149 \text{ MVA, } P_{max} = 100 \text{ MW), } I_{max} = 451 \text{ A)}$$

$$P_{ac,loss} = 2 \cdot 3 \cdot 0.0619 \cdot 451 \cdot 451 \cdot 100 \cdot 10^{-6} = 7.5\text{MW} \approx 4\%$$

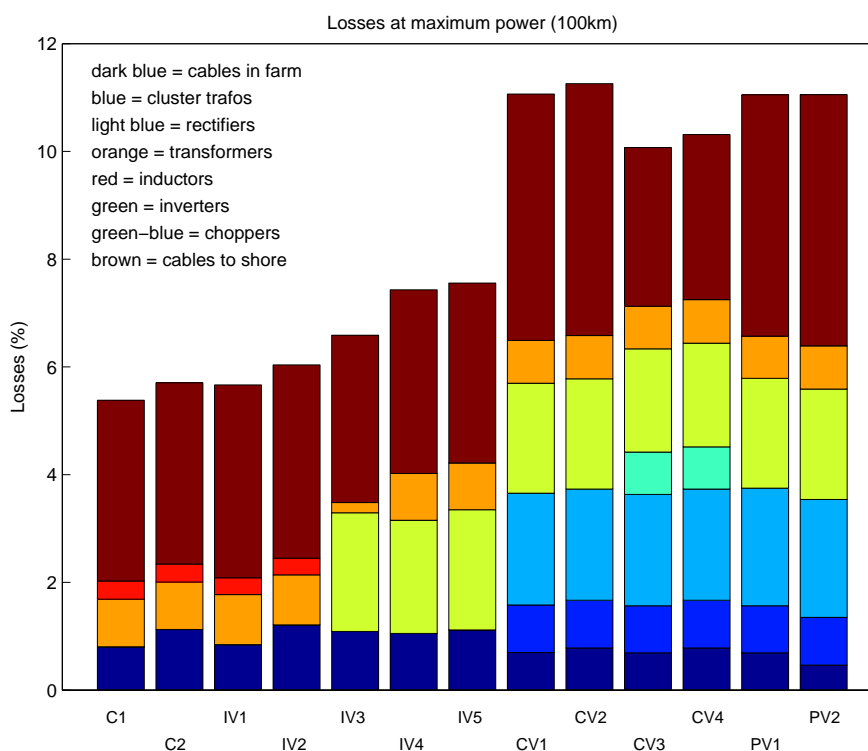


Figure 147: Losses at rated power divided over the system components

Figure 147 also shows that the farm cable losses in the CV and PV systems are lower than in systems C1 and C2. C1 and PV1 use the same farm cable (30kV, nr. 9) but PV1 has a slightly higher voltage (33 versus 30 kV) and thus a lower current (86 versus 95 A).

The losses calculated for the PV systems are relatively high compared to the loss evaluation by Negra et.al. [4]. This evaluation states the transmission losses over the total operating range: 4-5% for VSC systems. This is low compared to 11% for PV1,2 at full load. For a better comparison the relative losses over the total operating range were calculated. However, the relative overall losses are not much lower than the full load losses, see figure 148. This is counterintuitive, one might expect that the relative losses at low power decrease due to the quadratic relation with the current. But in the AC systems, the cable current does not decrease linearly with the power due to the cable capacitive current. Therefore there is a substantial no-load loss which affects the relative losses at low power. For the DC systems a similar effect is present. The converter losses increase almost linearly with the power. Secondly, the presented results in [4] use a much lower DC cable resistance: 0.01-0.014 Ω versus 0.0283 Ω

(20 C). Figure 149 compares the PWM converter losses in models to typical manufacture data. The models give a linear relation between the relative losses (as function of the rated power). The typical manufacture data [2] is nonlinear, with a tendency to be higher at low power and lower at high power.

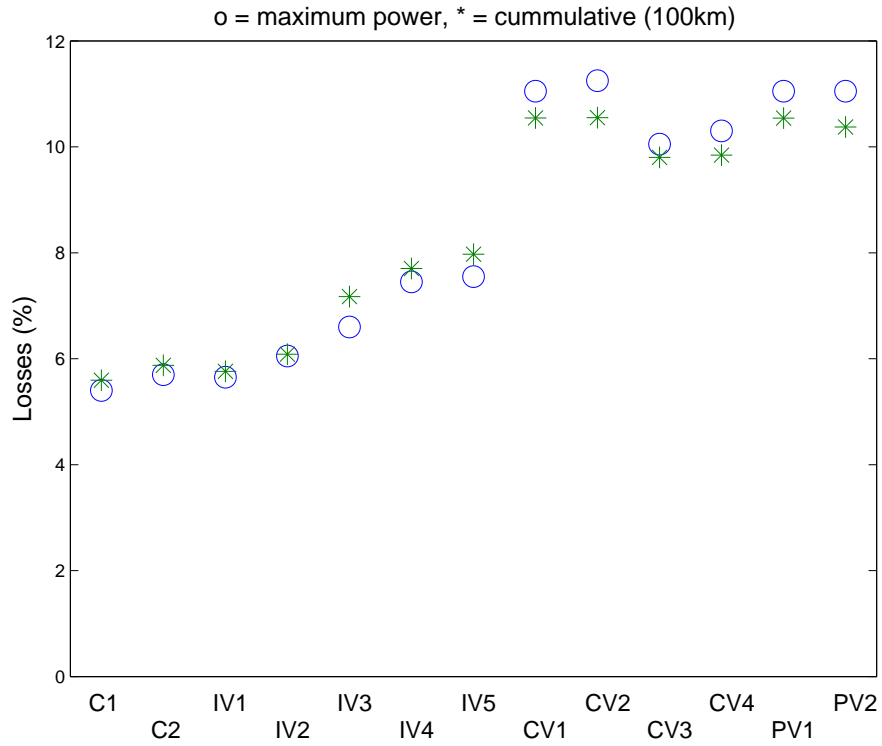


Figure 148: Losses at maximum power and cummulative over the whole range of operation

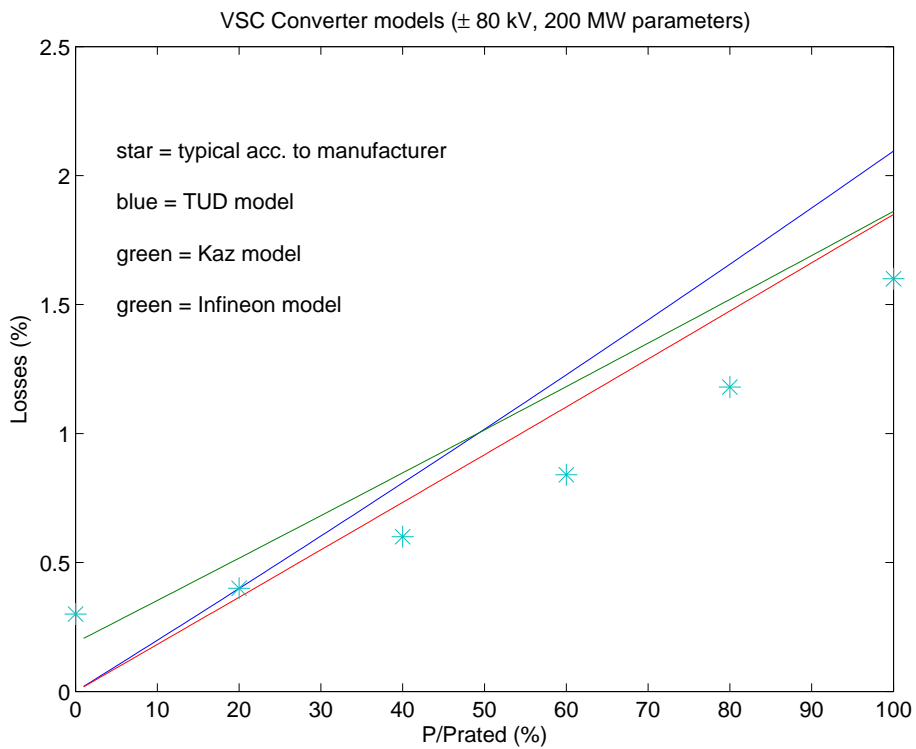


Figure 149: PWM converter losses (divided by the rated power): models compared to typical manufacture data

Table 5: Energy produced and energy losses

	Energy produced (MWh/y)	Energy losses (MWh/y)	Relative losses (-)
C1	938940	55638	0.0593
C2	936141	58437	0.0624
IV1	937275	57303	0.0611
IV2	934051	60527	0.0648
IV3	923253	71341	0.0773
IV4	917979	76611	0.0835
IV5	915285	79299	0.0866
CV1	889662	104875	0.1179
CV2	889597	104944	0.1180
CV3	897070	97480	0.1087
CV4	896641	97913	0.1092
PV1	889702	104835	0.1178
PV2	891353	103189	0.1158

Table 6: Investment and LPC (investment costs of turbines are not included)

	Investment (MEuro)	Energy produced (MWh/y)	Specific investment (MEuro/MW)	LPC (Euro/kWh)
C1	110.6	935227.7	0.5530	0.0137
C2	116.4	932445.8	0.5820	0.0144
IV1	110.6	933371.3	0.5530	0.0137
IV2	117.6	930167.4	0.5881	0.0146
IV3	195.0	921950.9	0.9751	0.0244
IV4	197.6	917680.2	0.9881	0.0249
IV5	193.1	913794.9	0.9655	0.0244
CV1	114.8	884801.7	0.5742	0.0150
CV2	120.6	886043.7	0.6031	0.0157
CV3	185.1	892104.8	0.9256	0.0240
CV4	190.9	892962.7	0.9546	0.0247
PV1	110.9	884866.5	0.5544	0.0145
PV2	113.6	887782.1	0.5680	0.0148

Finally, table 6 list the investment costs of the thirteen electrical systems, the produced energy and the Levelised Production Costs (turbine investment excluded). The investment costs per component are plotted in figure 150. For the AC connected systems the most expensive component is the cable to shore, for the DC connected systems it is the rectifier, the inverter and especially the chopper, if present. The rectifiers appear to be more expensive than the inverters. This is caused by the platform costs, which are included in the rectifier costs.

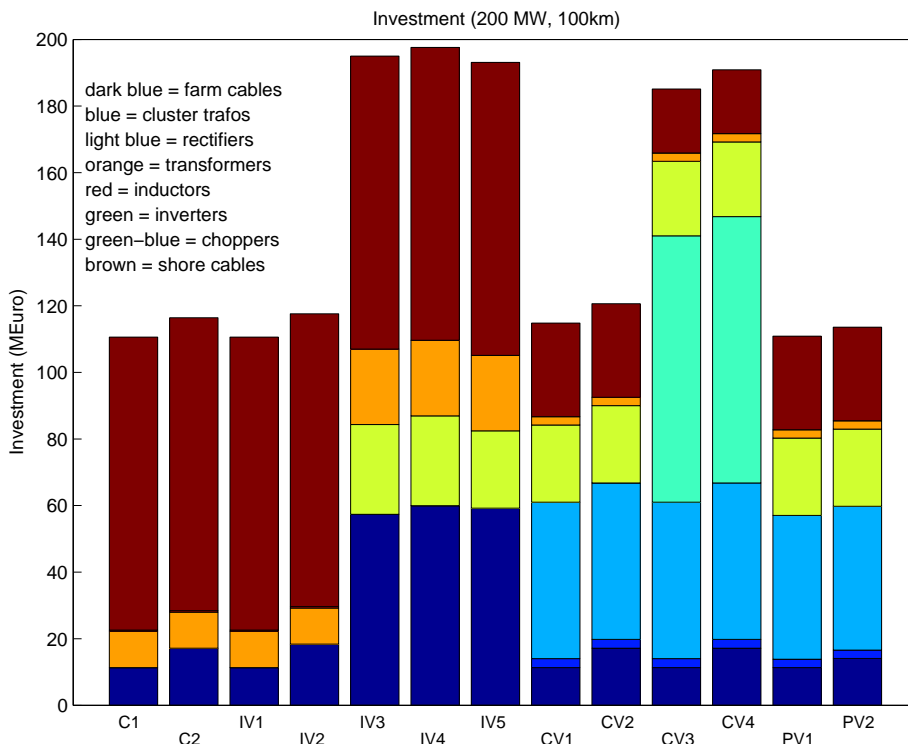


Figure 150: Investment costs

9 Conclusions

A user friendly computer program, EeFarm-II, for wind farm electrical and economic evaluation has been developed. EeFarm-II has been built as a Simulink Library in the graphical interface of Matlab-Simulink. The EeFarm-II Simulink Library consists of wind farm component models, such as models of wind turbines, generators, transformers, AC cables, inductors, nodes, splitters, PWM converters, thyristor converters, DC cables, choppers and Statcoms. A system model is built by copying the component models from the library and connecting the models. EeFarm-II includes a database with component parameters and prices, supplied by manufacturers. This database is confidential, however.

Each EeFarm-II component model calculates the output voltage and current phasor (AC) or voltage and current value (DC) based on the input voltage and current and the component parameters. The component models are steady state, with emphasis on the electrical losses and the not produced energy due to component failure. This is repeated for the complete operation range of the wind farm, i.e. the range of input wind speed. Secondly, the total price of the electrical system (if wind turbine prices are not included) or of the wind farm (if wind turbine prices are included) is determined. Based on the output power for each wind speed bin and the wind speed distribution, the annual produced energy is determined. The final step is the calculation of the Levelised Production Costs (LPC).

For each component model a test environment was prepared, consisting of a Simulink program with the model to be tested, the correct input to the model, a consistent set of parameters and the handling of the output. The results of the component test have been described in chapter 7. The test environments can be used each time a substantial change has been made to a model.

After EeFarm-II testing at ECN, the EeFarm-II program has been made available to Vattenfall for testing and application. Appendix A reports the Vattenfall EeFarm-II validation and the application to a specific wind farm case (Lillgrund). Vattenfall concluded that "Working with MatLab/Simulink is very convenient since it is possible to build advanced systems utilizing both a GUI and text files for programming. The available models in EeFarm II for components within the turbine and in the electric grid cover the range of studies from simple and generic overviews to detailed and specific investigations. This makes it very easy to start building simple systems with a low level of required data in order to get a rough estimate. These systems can easily be improved and more details can be added along the way to improve the accuracy of the calculations. In order to obtain relevant results it is necessary to go through the database and update and check it with the latest values from manufacturers before each new project."

EeFarm-II has also been used to re-evaluate the thirteen electrical systems of the Erao-1 study of 2001. Since 2001 prices and performance of some of the components have changed. A wind farm size of 200 MW has been chosen and a distance to shore of 100 km. Chapter 8 gives the results. In the Erao-1 study (with two system sizes, 100 and 500 MW and two distances to shore, 20 and 60 km), the AC connected systems are the most cost effective (lowest LPC). In the present study, the difference in LPC between the AC connected systems and the Park Variable (PV) DC connected systems is too small to be significant. This can partly be explained by the longer distance to shore. The investment costs of the AC and PV-DC systems are about the same, due to the high AC cable costs. The losses in the PV systems are a bit higher than in the AC case.

References

- [1] et. al., M.K. (2002): *Control in Power Electronics - Selected Problems*. Academic Press, Series in Engineering.
- [2] Ann. (21 nov 2008): *Losses for a typical VSC converter*. Personal communication U. Axelsson.
- [3] Anon. (2001): *Afleiding kabelparameters normaal bedrijf*. Report 01-153 PMO, Phase to Phase.
- [4] Barberis Negra, N., J. Todorovic and T. Ackermann (2006): *Loss evaluation of HVAC and HVDC transmission solutions for large offshore wind farms*. Electric Power Systems Research 76(2006) 916-927.
- [5] Bulder, B. (2001): *FyndFarm, User's Manual*. Report ECN-IÚ01-0?? Ú rev. 0.2, ECN.
- [6] Committee, I.T. (1995): *Electric cables - Part 3 Sections on operating conditions - Section 2: Economic optimization of power cable size*. Report IEC 60287-3-2, IEC.
- [7] Dekker, J. and J.T.G. Pierik (ed.) (1999): *European Wind Turbine Standards II*. Report ECN-C-99-073, ECN.
- [8] IEC (1975): *Rotating electrical machines, Part 10: Conventions for description of synchronous machines*. Report IEC 34-10, IEC.
- [9] Infineon (2009): *Dimensioning program IPOSIM for the loss and thermal calculation of Infineon IGBT modules*. Report, Infineon. www.infineon.com.
- [10] Machielse, L. (2007): *OWECOP2 R17-5MW-DeWith.xls*.
- [11] MathWorks (2000): *Matlab: Using Matlab*. Report Version 6, MathWorks. Chapter 20.
- [12] MathWorks (2000): *Simulink: Dynamic system simulation for Matlab. Using Simulink*. Report Version 4, MathWorks. Chapter 7.
- [13] Mohan, N., T. Undeland and W. Robbins (1995): *Power Electronics – Converters, Applications and Design*. John Wiley & Sons, New York. Page 56.
- [14] Mohan, N., T. Undeland and W. Robbins (1995): *Power Electronics – Converters, Applications and Design*. John Wiley & Sons, New York.
- [15] PhasetoPhase (2001): *Betrouwbaarheid @ Vision*. Report 01-119 pmo, PhasetoPhase.
- [16] Pierik, J. (2008): *We@sea proposal - Appendix to Software and Development agreement between Vattenfall and ECN*. Unpublished.
- [17] Pierik, J., M. Damen, P. Bauer and S. de Haan (2001): *Electrical and control aspects of Offshore wind farms, Phase 1: Steady state electrical design and economic modeling, Vol. 1: Project results*. Report ECN-CX-01-083, ECN Wind Energy.
- [18] Pierik, J. and J. Morren (2007): *Constant Speed Wind Farm Dynamic Model Validation; Alsvik measurements and simulations*. Report ECN-E-07-007, ECN.
- [19] Pierik, J. and J. Morren (2007): *Validation of dynamic models of wind farms (Erao-3): Executive summary, benchmark results and model improvements*. Report ECN-E-07-006, ECN.
- [20] Pierik, J. and J. Morren (2007): *Variable Speed Wind Turbine Dynamic Model Validation; JWT measurements and simulations*. Report ECN-E-07-008, ECN.
- [21] Pierik, J., J. Morren, E. Wiggelinkhuizen, S. de Haan, T. van Engelen and J. Bozelie (2004): *Electrical and Control Aspects of Offshore Wind Turbines II (Erao-2). Volume 1: Dynamic models of wind farms*. Report ECN-C- -04-050, ECN. Available at the web site of ECN (www.ecn.nl, use search option).

- [22] Pierik, J., J. Morren, E. Wiggelinkhuizen, S. de Haan, T. van Engelen and J. Bozelie (2004): *Electrical and Control Aspects of Offshore Wind Turbines II (Erao-2). Volume 2: Offshore wind farm case studies* . Report ECN-C- -04-051, ECN. Available at the web site of ECN (www.ecn.nl, use search option).
- [23] Pierik, J., Y. Zhou and P. Bauer (2008): *Wind Farm as Power Plant: Dynamic modelling studies* . Report ECN-E-08-017, ECN .
- [24] Radun, A.V. (2009): *PWMinverterLosses*. Report EE603 LectureNotes, *University of Kentucky* . [Www.engr.uky.edu/radun/EE603/LectureNotes/PWMinverterLosses.doc](http://www.engr.uky.edu/radun/EE603/LectureNotes/PWMinverterLosses.doc).
- [25] Siemens (1971): *Handbuch der Elektrotechnik*. Girardet Verlag, Essen.
- [26] Tande, J. and R. Hunter (1994): *Estimation of Cost of Energy from Wind Energy Conversion Systems*. Report 2e edition, IEA. Recommended practices for wind turbine testing.
- [27] Thoben, M., K. Mainka, R. Bayerer, I. Graf and M. Muezer (2009): *From vehicle drive cycle to reliability testing of Power Modules for hybrid vehicle inverter*. Report, *Infineon* . [Www.infineon.com](http://www.infineon.com).

A Vattenfall EeFarm-II validation and application to Lillgrund case

EEFARM II

Emil Eriksson
Daniel Salomonsson

EeFarmII

From Vattenfall Research and Development AB, U-NE	Date 2009-07-02	Serial No.
Author/s Emil Eriksson Daniel Salomonsson	Access Full Access	Project No. PR.138.1.4.54
Customer	Reviewed by Urban Axelsson	
	Issuing authorized by Viktoria Neimane	
Key Word	No. of pages	Appending pages

Summary

Distributionlist

Company	Department	Name	Number of

Table of Contents

Page

1	INTRODUCTION	1
2	COMPONENT VALIDATION AND USABILITY	1
2.1	Wind Turbine Components	1
2.1.1	Wind Models	1
2.1.2	Turbine Models	1
2.1.3	Generator Models	2
2.2	Electric Grid Components	2
2.2.1	Transformer and Inductor Models	2
2.2.2	Cable Models	2
2.2.3	Power Electronic Models	3
2.2.4	Miscellaneous	3
2.3	Usability	3
3	CASE STUDY LILLGRUND	4
3.1	Validating EeFarm II by modelling Lillgrund	5
3.2	Lillgrund characteristics	7
3.3	Results	8
3.3.1	Reactive power	8
3.3.2	Energy yield, power outputs and energy losses	9
3.3.3	Investment costs for the AC solution	11
3.3.4	Reliability	12
3.3.5	AC compared to a DC solution	12
4	CONCLUSIONS	14
5	REFERENCES	15

Appendices

Number of Pages

APPENDIX

pp

1 Introduction

Vattenfall and Energy Research Centre of the Netherlands (ECN) have work together in a project with a goal to make an updated and more user-friendlier version of the simulation tool EeFarm, earlier developed by ECN and Delft University of Technology (TUD) [1]. This tool can be used to make a first analysis of technical and economical performance of new wind farms.

Energy Research Centre of the Netherlands was responsible for updating EeFarm to version II, which has several new component models and a whole new set of component data. The task for Vattenfall was to deliver data to the new component database, and to validate the tool through setting up a test case. Vattenfalls offshore wind farm Lillgrund was selected to be used in the case study [2].

2 Component Validation and Usability

In this section the component validation and usability will be summarised. EeFarm II is a model library implemented in MatLab/Simulink [3]. Each of the implemented models have been studied and compared to standard models. The full description of each model is given in [4]. Any deviations and abnormalities have been reported to ECN during the project in order to correct errors in the models.

2.1 Wind Turbine Components

2.1.1 Wind Models

Wind data is used as input to EeFarm II, and is usually given in W/m² for each wind speed and wind direction together with a distribution of wind speed and wind direction during one year. Here it is important to consider the wake effect caused by surrounding turbines in order to obtain a realistic simulation result. Hence wind data will be given specific for each turbine.

Wind data used in EeFarm II can be measurement data, calculated data from external software or from the included GCL model [4]. The GCL only requires turbine locations and a site-specific wind rose. This built-in model can be an option to use when no pre-calculated wind data exists. However, Vattenfall will use the external software WindPRO to calculate wind data [5].

2.1.2 Turbine Models

The included turbine models calculate mechanical power from the given wind data. In EeFarm II three different turbine models are implemented. The simplest model calculates the mechanical power using an internal power curve. Some power curves for existing turbines are included in the database, and new curves can easily be

implemented when needed. The second turbine model also takes the rotational speed of the turbine into account. Finally, the last model can be used together with a GCL model or a Hagg approximation. Here the individual locations of the turbines are used in the calculation of mechanical power.

2.1.3 Generator Models

The mechanical power is converted to electric power in the generator. EeFarm II includes five different generator models. The generic generator model defines the electric parameters and converts the mechanical power into an electric power using a fixed efficiency coefficient. This model is appropriate to use together with pre-calculated P(V)-curves. The other four models are more detailed models of an induction generator, a DFIG, an induction generator with full-power converter and a synchronous generator with full-power converter. These models require more detailed data and use of look-up tables with pre-calculated values in order to be modelled in a correct way. It might be a risk to get these parameters from manufacturers. Hence the generic model will be used in most cases since it only requires the P(V)-curve. However, using detailed generator models give opportunities to deeper investigate different designs.

2.2 Electric Grid Components

2.2.1 Transformer and Inductor Models

The EeFarm II model library contains two transformer models and one inductor model. The two transformer models are one standard load-flow model and one ideal transformer without losses, failure rate and price. The transformer models are based on one 10-kVA transformer, which parameters are transformed into p.u., and then recalculated to the actual size of the transformer. Consequently there is a risk that the parameters are not fully accurate, since these may not be scalable. However, it is possible to use values from a real transformer if they are available in order to obtain a more precise result. Today no data for an inductor exists in the database.

2.2.2 Cable Models

Two dc cable models and one ac cable model are included in the library. One dc model is to be used for single-pole dc transmission, and the other model for bi-polar transmission. Both dc cables are modelled as a temperature-dependent resistance. The conductor temperature must be given as an input to the cable model.

The ac cable is modelled with a π -scheme. This model can be used up to approximately 200 km. The current model in the library does not take the conductor temperature into consideration as the dc-cable model does.

The database contains a large number of different cables, which can be used initially. As earlier described, it is possible in a later stage to add new cables when needed. The

availability of the cables is not dependent of the cable length. This must be implemented in a later version of EeFarm II. Finally, when calculating the cable cost, it is possible to also include the cable laying cost, which is available in the database.

2.2.3 Power Electronic Models

EeFarm II library has models of different power-electronic components, such as rectifiers, inverters, chopper and STATCOM. The rectifier and inverter models exist with either thyristors or transistors switches, and the STATCOM with transistor switches only.

Different models of transistor switches exist and three of them have been implemented in EeFarm II: one model from the manufacturer Infineon, one model from TUD and one model developed by Kazmierkowski. The rectifier models have all the same signal input, but there is a small difference between the inverter models. The three rectifier/inverter models also result in different amount of losses. During the validation phase these models have been updated in order to work with the same set of data from the database and to give approximately the same result. Still the losses of all three models seem to be a bit high. Both parameter values and costs must be updated each time a new system is set up since these values improve all the time.

When it comes to the dc chopper model it is hard to estimate the cost for such a device since it does not exist yet. Still the model is important to be used in studies treating future dc solutions.

The STATCOM model is based on the TUD transistor model only. Depending on which of the three transistor models that is found to be most reliable, this model must be updated with that transistor model.

2.2.4 Miscellaneous

EeFarm II model library also contains additional components, which are necessary to set up a system are for example joints, sources, calculation tools, scopes and plot outs. These components are very straightforward to use.

2.3 Usability

Setting up new systems with the EeFarm II model library in MatLab/Simulink is very easy. Additional components can be selected from the built in Simulink library and used in order to perform extended design and analysis. All blocks representing different components in the system are first dragged and dropped into the new model and then interconnected with signal wires. This part of the work is very easy and takes little time.

The second step in the built-up phase is to link the database to the different components. The current version of EeFarm II contains two databases: one for transformers and one for the rest of the components. Since large systems contain a high number of components it can take some time to link data from the database to each component. However, the EeFarm II models are using data structures that simplify the work if many identical components are used, e.g. a wind turbine. The definition phase is made by setting up a text file which is executed when the calculation starts.

The last step is to analyze the output data from the system. This post process can be done using MatLab or data can be exported and used in other softwares, e.g. Microsoft Excel or SigmaPlot.

The following list is suggestions of improvements:

- a component should only be defined once, and then linked if used as a part in other components;
- only one of the three transistor models should be implemented in the final version;
- the availability of cables should be dependent of the cable length;
- the conductor resistance of both ac and dc cables should be dependent of the temperature; and
- possibility to control the reactive power of the turbines in such way that zero reactive power exchange in the point of common coupling is achieved.
- Analyzing the output data from systems build in EeFarm II would be more user friendly if each component was assigned with an output converter directly in the EeFarm II library. It would be preferable if this improvement were implemented with the same data structure that is already used in EeFarm II. The user could then get direct access to output data from each component after a simulation, without making any additional, time-consuming work in the model. One disadvantage with this solution could be the huge amount of data that would be generated during a simulation.

3 Case Study Lillgrund

3.1 Validating EeFarm II by modelling Lillgrund

The individual component models that are included in EeFarm II were validated in detail by VRD in parallel with the work of developing the models at ECN in the Netherlands. The purpose of validating all component models in such an early phase of the project was simply to make sure that each component were modelled in the right way. When the development of all components were finished, the software itself also had to be validated in order to see that the models of the different components could be connected to each other in EeFarm II models and that the simulation results were reliable. To validate EeFarm II, a model of the existing wind farm Lillgrund was built. The reason for choosing this particular wind farm is that the components in the wind farm and the output from it are well documented at Vattenfall.

Lillgrund offshore wind farm comprises 48 turbines, connected in five 33 kV radials with nine or ten turbines in each radial. The turbines have a rated power of 2.3 MW, which gives a total installed power of 110 MW. The total length of the cables in the internal 33 kV grid is 22 km, where copper cables with three different cross sectional areas are used; 95 mm², 185 mm² and 240 mm² depending on the location of the cable. The smallest cable is used furthest out on the radials and the biggest cable is used closer to the platform, to which all radials are connected. On the platform, a 33/138 kV transformer is placed. The platform is located 7 km from shore and a 145 kV, 400 mm² copper cable is used to connect the platform with the network on land. In Figure 1 below, the location of the 48 turbines is plotted.

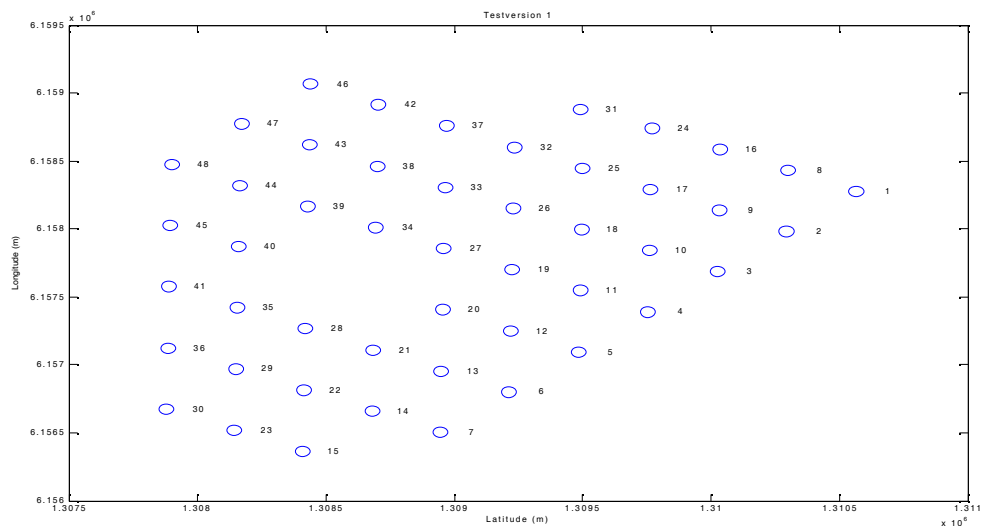


Figure 1. Map of all turbine coordinates in Lillgrund.

EeFarm II is a software for Simulink, where the user connects different components to each other when building a model. In Figure 2 and Figure 3, three different parts from the Lillgrund model in Simulink are illustrated. Figure 2 shows how the power curve originating from the wind data and coordinate for each turbine is connected to a generator, a transformer and in the end also a cable. The reason that the power curve is connected directly to a generator is that the output from the wind data is electrical power and not mechanical power. Therefore, it is not necessary to use a model of a turbine. All components of a single turbine are put together into one subsystem consisting of one block only. These turbine blocks can be seen for radial A in the lower picture in Figure 2.

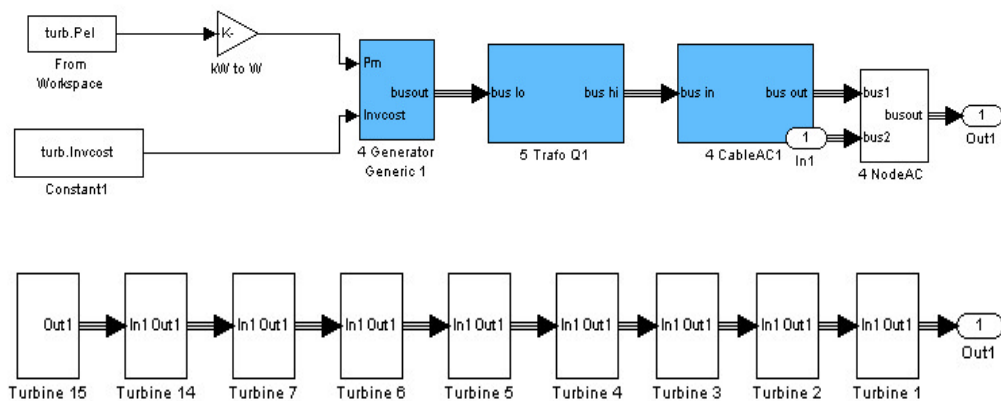


Figure 2. The components of a turbine can be seen in the top picture, while the picture at the bottom shows all turbines in Radial A connected to each other.

The blocks in each radial are also put together into new subsystems, which can be seen in the Figure 3. Here the five radials are connected to the platform, which in turn is connected to the export cable to shore. The transformer block and the cables from the radials are also put together into a subsystem, while the export cable is used exactly as it is in the library. That is the reason why the export cable is blue in Figure 3, while all other blocks, which are subsystems created of many other components, are white.

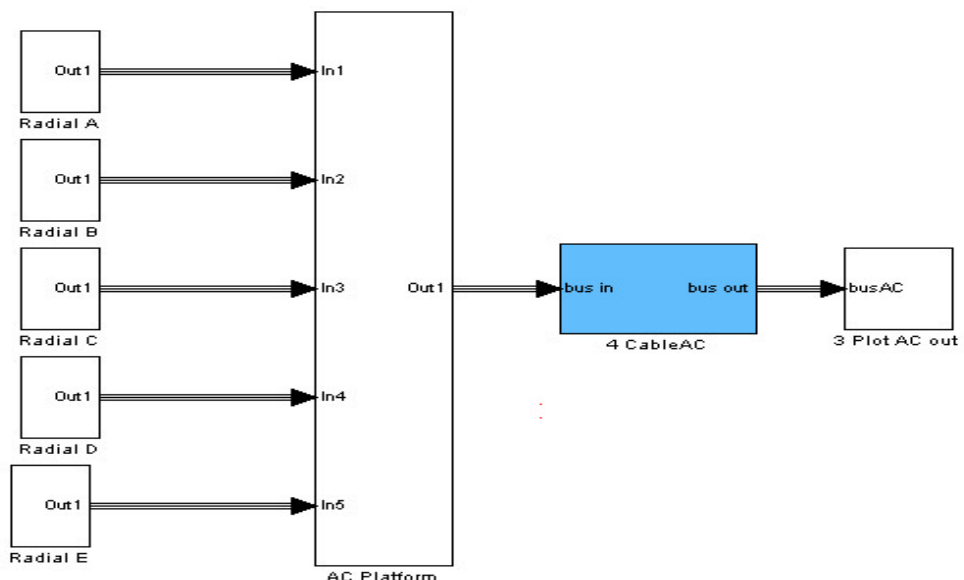


Figure 3. The model of Lillgrund as it is seen in EeFarm II. To the left, the radials are connected to the platform, which in turn is connected to the export cable.

3.2 Lillgrund characteristics

Lillgrund have some characteristics more or less specific for this farm and they are listed below. The validation of EeFarm II will investigate how the software takes these characteristics into account during the calculations.

- No reactive power is allowed to be exchanged between the wind farm and the network on land at the PCC in Bunkeflo. The export cable from the platform produces approximately 10 MVar of reactive power but still; no reactors are installed in Lillgrund. The reason for this is that the full power converters in the wind turbines together with the 33/138 kV transformer are able to consume all reactive power produced by the wind farm.
- The annual energy yield from Lillgrund is estimated to 330 GWh and the annual electrical energy losses are about 3.3 GWh while the highest allowed losses from the farm was estimated to 10 GWh by Vattenfall when designing the farm [6]. These 10 GWh corresponds to energy losses of 3% of the energy yield.
- For the economical evaluation of EeFarm II, the real investment cost of Lillgrund will be compared to the total investment cost calculated by EeFarm II. The total investment cost for the farm was calculated to 157 M€ in [6]. In EeFarm II, the Levelised Production Cost (LPC) can also be calculated in addition to the total investment cost. The LPC is the cost per delivered kWh over the whole lifetime of the wind farm, with all costs and revenues, like O&M costs, taken into account. These costs and revenues are discounted with the appropriate interest rate and inflation rate when calculating the LPC.
- In EeFarm II, it is also possible to perform reliability analyses, where the total ENS-value can be calculated. ENS means Energy Not Supplied and it is an index of how much energy a generator is supposed to supply to the network, but that for some reasons, like unexpected failures, is not supplied to the network during one year. For Lillgrund, a reliability analysis was performed in [6]. However, the result from that analysis may show deviations from the actual ENS-value from the farm because of uncertainty in the used input data and also a bug in the used software that was found after the thesis was finished.

Only AC cables are used at Lillgrund, but with EeFarm II it is also possible to compare different technologies with each other. For example, an AC solution of a wind farm can be compared to a DC solution. Thus, in the evaluation of EeFarm II,

the original layout of Lillgrund will be compared to a DC solution to see how these two solutions differ from each other when it comes to electrical energy losses and investment cost. In this case, the 33/138 kV transformer will be replaced by a rectifier on the offshore platform and an inverter on land, and the AC cable will of course be replaced by a DC-cable. The internal grid is still AC. Apart from the comparison between an AC and a DC solution for the original layout of the farm, the length of the export cable will also be altered in order to see for which length a DC solution become more advantageous than an AC solution.

3.3 Results

3.3.1 Reactive power

In Lillgrund, Vattenfall is not allowed to export any reactive power to the 130 kV network on land. The amount of 10 MVar reactive power that is produced in the wind farm is also consumed in the farm, by the transformer and the full power converters in the turbines. It is not possible to make the reactive power produced or consumed by the turbines dependent on the point of operation, it is only possible to specify a fixed value in EeFarm II at this date. Therefore, the reactive power after the export cable should be around 10 MVar. In Figure 4, the total amount of reactive power from EeFarm II, in different sections of the wind farm is shown.

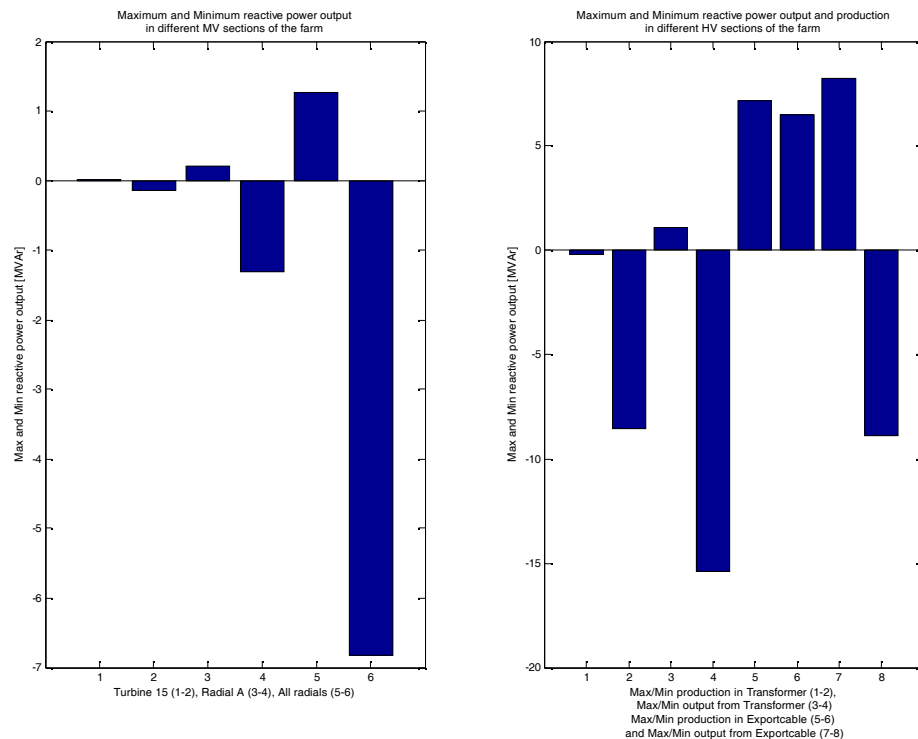


Figure 4. Reactive power in different sections of the farm.

As can be seen in the left diagram, all radials put together (bar 5 and 6) has a maximum reactive power output of about 1 MVar and a minimum reactive power output of almost -7 MVar. In the right diagram, it can be seen that the transformer never produces any reactive power but always consume between approximately 0 MVar and 8 MVar of reactive power. Since the reactive power output from the radials in some cases are as low as -7 MVar, the total reactive power output from the transformer is at some times as low as -15 MVar which can be seen in bar 4 of the right diagram. Bar 5-6 is the maximum and minimum reactive production in the export cable and bar 7-8 is the total output of reactive power from the wind farm to the net on land. As can be seen in bar 7-8, the total flow of reactive power in the export cable varies between approximately +8 MVar to -8 MVar, which is equal to an export/import of reactive power to/from the PCC. The network owner at land does not allow this export/import of reactive power.

3.3.2 Energy yield, power outputs and energy losses

With EeFarm II, it is possible to calculate and illustrate the power flow in each section of the wind farm and it is also possible to calculate how much each cable is utilized. Below, the maximum power flow and maximum cable utilization in Radial A, but also in the export cable, is shown.

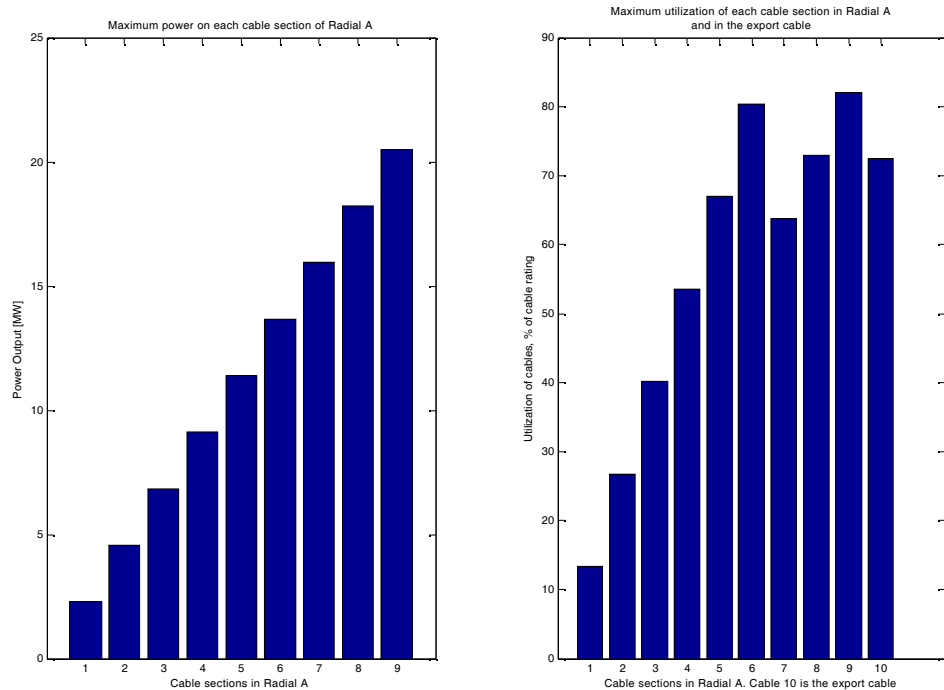


Figure 5. Power output from each turbine in Radial A and maximum utilization of the cables in Radial A and in the export cable.

Vattenfall estimated the annual energy yield from Lillgrund to be 330 GWh when designing the farm. With EeFarm II, the annual energy output is calculated to be 334.7 GWh, which only deviates 1.4% from the estimation made by Vattenfall. In Figure 6, the maximum power losses from different sections of the wind farm are shown. It can be seen that the highest power losses are in the transformer.

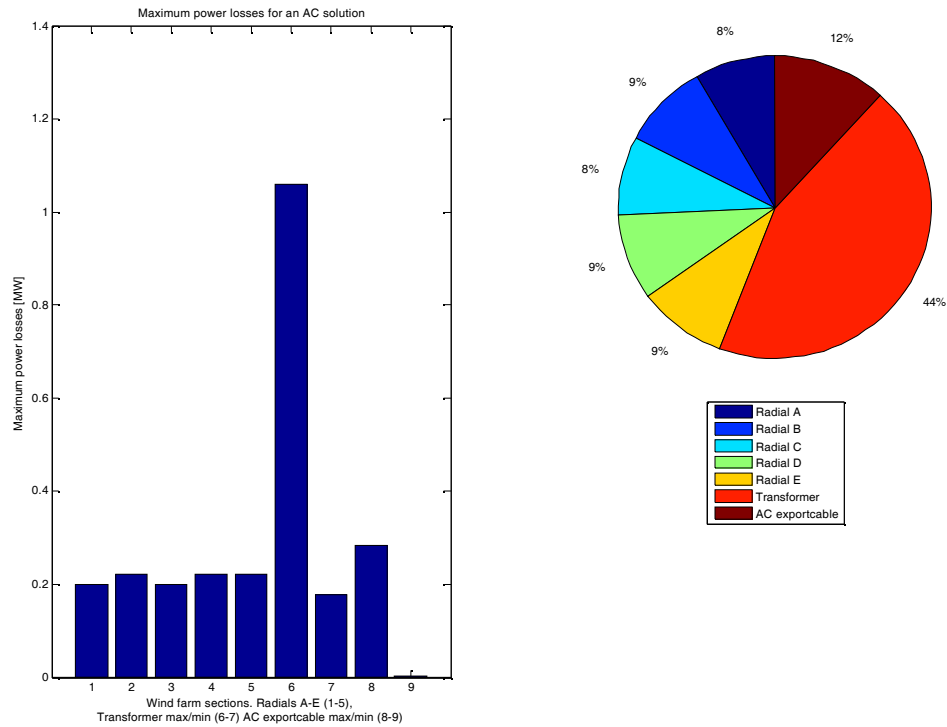


Figure 6. Maximum power losses in different sections of the wind farm for the AC case.

The total energy losses of Lillgrund when the farm is modelled in EeFarm II are 7.7 GWh. This value should be compared to 3.3 GWh and 10 GWh, which was the highest allowed amount of energy losses in the demands from Vattenfall [6]. As can be seen in Figure 6, the transformer losses are 44% of all losses. These rather high losses may depend on the transformer model parameters used in EeFarm II, since these parameters are scaled from a small 10 kV transformer. The cable losses are relatively low due to both a low utilization of the cables and a rather short cable length. The calculated losses of 3.3 GWh were not based on such detailed wind data as was used during the validation work of EeFarm II. Only coarse estimates of wind speed and wind directions were used then, which might be one reason for the difference in energy losses. In the thesis, a software using iterations was used, which might also lead to some differences in the results compared to EeFarm II. In the validation of EeFarm II, detailed data of turbine coordinates, wind statistics and power output for the wind data for each turbine was accessible. 7.7 GWh is 2.3% of the total energy

yield from the wind farm, which is lower than the 3.0% that Vattenfall used as an upper, acceptable limit of the energy losses in their demands.

3.3.3 Investment costs for the AC solution

No O&M costs were included in the initial economical calculations when validating EeFarm II. As for the losses, it is possible to calculate and illustrate the investment cost for each component and section in EeFarm II. The investment costs for different sections of the farm in the original AC solution is shown in Figure 7.

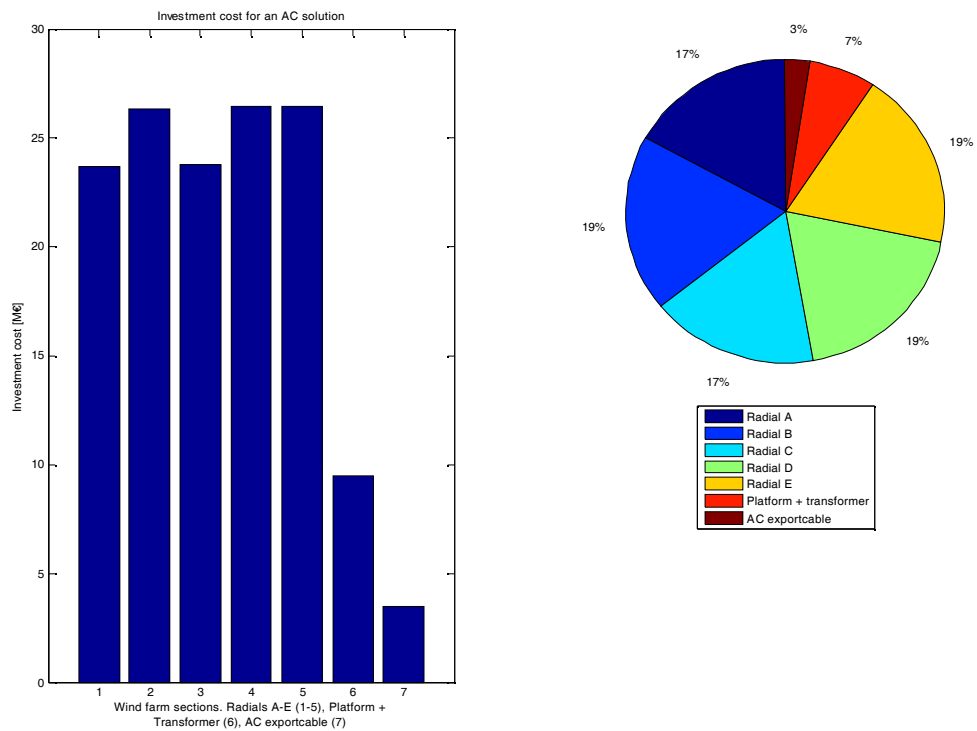


Figure 7. Investment cost of different sections of the wind farm for the AC case.

In [6], the total investment cost for the whole wind farm was 157 M€, while the total investment cost from EeFarm II is 160 M€. The reason for the slightly higher investment cost from EeFarm II is most likely the fact that the thesis was finished in spring 2008, while the simulations in EeFarm II was performed during spring 2009. Therefore, some costs used in EeFarm II differ from the ones in [6].

The LPC is 4.5 c€/kWh when not including any O&M costs. When using an O&M cost of 18.5 €/MWh, the LPC is raised to 6.02 c€/kWh. Both these LPC-values should be seen as reasonable.

3.3.4 Reliability

In EeFarm II, the reliability analysis is based on the fraction of time that each component is out of operation. The user sets these values in EeFarm. In this validation, reliability data from [6] were used. No outages due to O&M operations have been taken into account for when validating EeFarm II, in order to get a reliability study similar to the one in [6], where outages due to O&M were not included. The ENS value calculated by EeFarm II with these data is 4.6 GWh per year. The ENS value in [6] was 17.4 GWh. However, there was a bug in the software used in that project, which affected the reliability calculations and this bug was not found until after the project was finished. Therefore it is hard to compare the two results.

3.3.5 AC compared to a DC solution

When comparing an AC solution of Lillgrund with a DC solution, the original AC layout of the wind farm was compared to a DC solution where only the AC export cable was changed into a DC export cable with the same length. The transformer was also changed, into a rectifier, and an inverter on land also had to be used. The maximum power losses from different sections for this solution are shown in Figure 8.

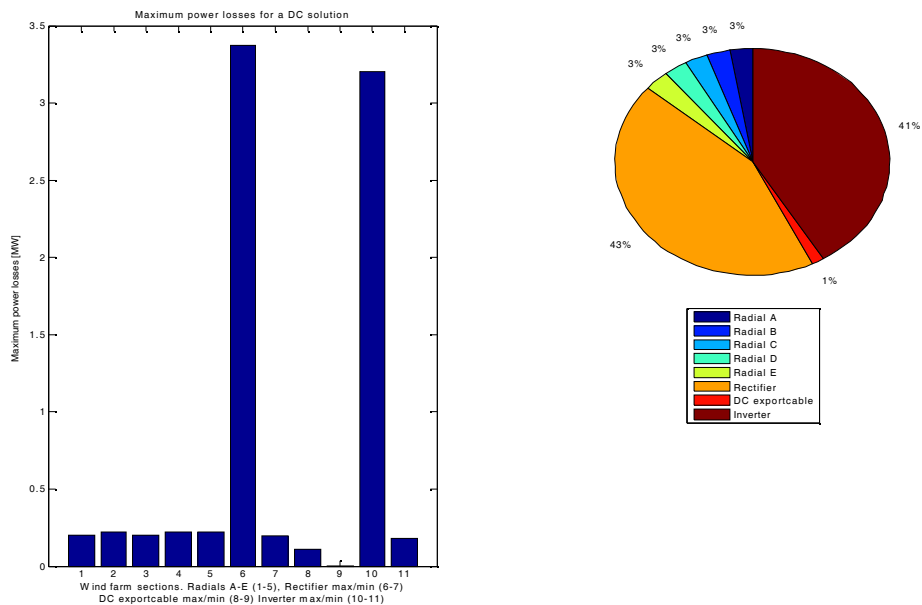


Figure 8. Losses in different sections of the wind farm for the DC case.

It is interesting to see that the maximum losses in the DC export cable are 0.44 MW while the maximum losses in the AC export cable is 0.28 MW. One reason for this might be that the AC cable has a rated power of 149 MVA, while the DC cable has a rated power of 128 MW. The total annual energy losses from this DC solution are 24.2

GWh per year, which is substantial higher than the 7.7 GWh from the AC alternative. For such a short distance as in Lillgrund, the DC option can never be more efficient than the AC option due to losses in the inverter and the rectifier. However, the losses in the rectifier and in the inverter are too high. They should be around 1.7% per station **Error! Reference source not found.** and not around 3 % as in this case. In EeFarm, three different inverter and rectifier models are included. The losses from all these models have been studied and they are given in the table below.

Table 1. Rectifier and inverter losses for the three different models in EeFarm II.

Model	Rectifier losses		Inverter losses	
	Absolute value [MW]	Percent of installed power	Absolute value [MW]	Percent of installed power
Infineon	3.45	3.36	3.18	3.10
Kaz	3.07	2.97	2.80	2.71
TUD	3.32	3.23	3.05	2.97

The investment costs for different sections of the farm for the DC case is shown in Figure 9.

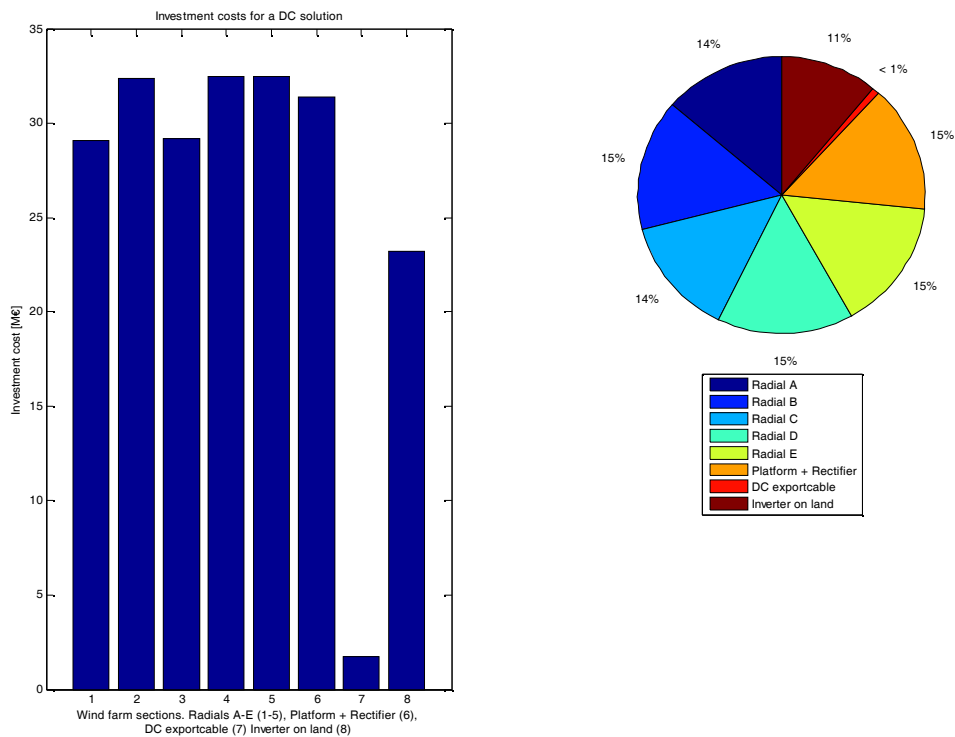


Figure 9. Investment costs in different sections of the wind farm for the DC case.

The total investment cost for the DC case is 211 M€, which is 54 M€ higher compared to the AC solution. The cost for a DC solution should be higher than an AC solution,

but just as for the other parameters, which determine the DC losses, the investment cost for DC components are extrapolated from just a few other components and this fact is probably affecting the accuracy of the total investment cost calculated by EeFarm II. In the AC model, more or less tailor-made components with known costs have been used, but for the DC solution the rectifier, inverter and the cables are standard components that are not designed for fitting to the Lillgrund wind farm. The exact cost for a DC platform is not known either. Instead, the same platform cost as in the AC solution is used. The LPC for the DC solution was 6.0 c€/kWh without any O&M costs included.

4 Conclusions

Working with MatLab/Simulink is very convenient since it is possible to build advanced systems utilizing both a GUI and text files for programming. The available models in EeFarm II for components within the turbine and in the electric grid cover the range of studies from simple and generic overviews to detailed and specific investigations. This makes it very easy to start building simple systems with a low level of required data in order to get a rough estimate. These systems can easily be improved and more details can be added along the way to improve the accuracy of the calculations. In order to obtain relevant results it is necessary to go through the database and update and check it with the latest values from manufacturers before each new project.

Modelling Lillgrund in EeFarm II was not that hard, since the software is easy to use. However, the process of evaluating the software was a bit more challenging, since some shortcomings with EeFarm II were found. These are listed below.

- The magnitude of the AC losses from the simulations were reasonable in general, except for the transformer where the losses were as high as 1 MW. This might depend on the lack of information when modelling the transformer component. In the latest version of component library (2009-06-17) a 10 kV transformer is scaled when using a transformer in a model.
- When it comes to the reactive power, it is not possible to control the reactive power flow to/from the wind farm in EeFarm II today. The reactive power is in reality controlled by the full power converters in the turbines. The magnitude of the reactive power consumption in the transformer and the reactive power production in the export cable seem to be reasonable, but the magnitude of the reactive power from the radials is unrealistic at the moment.
- When it comes to the DC solution, the rectifier models and the inverter models gave too high losses compared to what could be realistic. The losses in these components were almost two times higher in EeFarm II compared to figures from ABB (approximately 3% compared to 1.7%). In addition to this,

the rectifier always had somewhat higher losses than the inverter. No reasons for this were found.

- At this moment, no electrical or economical parameters are included for reactors in the parameter database in EeFarm II, even if a model of the component is available in the component library. In reality this means that it is impossible to make any realistic simulations of long export cables, which in turn makes it impossible to make any realistic comparisons between AC and DC solutions. Therefore it is not possible today to find a breakpoint where it is more feasible to use a DC solution instead of an AC solution.

The following list is suggestions of improvements:

- a component should only be defined once, and then linked if used as a part in other components;
- only one of the three transistor models should be implemented in the final version;
- the availability of cables should be dependent of the cable length;
- the conductor resistance of both ac and dc cables should be dependent of the temperature; and
- possibility to control the reactive power of the turbines in such way that zero reactive power exchange in the point of common coupling is achieved.
- Analyzing the output data from systems build in EeFarm II would be more user friendly if each component was assigned with an output converter directly in the EeFarm II library. It would be preferable if this improvement were implemented with the same data structure that is already used in EeFarm II. The user could then get direct access to output data from each component after a simulation, without making any additional, time-consuming work in the model. One disadvantage with this solution could be the huge amount of data that would be generated during a simulation.

5 References

- [1] Pierik, J., M. Damen, P. Bauer and S. de Haan (2001): Electrical and control aspects of Offshore wind farms, Phase 1: Steady state electrical design and economic modeling, Vol. 1: Project results. Report ECN-CX-01-083, ECN Wind Energy.
- [2] Lillgrund wind farm, Vattenfall. [Online]. Available: http://www.vattenfall.com/www/vf_com/vf_com/Gemeinsame_Inhalte/DOCUMENT/360168vatt/5965811xou/902656oper/903724wind/P0289268.pdf

- [3] MatLab/Simulink, The MathWorks [Online]. Available: <http://www.mathworks.com/>
- [4] J.T.G Pierik, U. Axelsson, E. Eriksson and D. Salomonsson, “EeFarm II – Model description and evaluation,” EN, Tech. Rep., Jul 2009.
- [5] WindPRO, EMD International [Online]. Available: <http://www.emd.dk/WindPRO/Frontpage>
- [6] Eriksson E. (2008), Wind farm layout – investment and reliability analysis,VRD
- [7] Jonsson, T., Power System ABB. E-mail

B Wind farm wake program input for EeFarm II

The input of a wind farm wake program for EeFarm II consists of (n+3) ASCII files, with n the number of turbines:

- for each turbine a file with the electric power per wind speed and direction bin, named t001.txt, t002.txt etc.;
- a file with the probability of each wind speed and direction bin in the turbine power files, named freq.txt;
- a file with the coordinates of each turbine, to calculate the lengths of the cables connecting the turbines and the transformer platform(s), named coord.txt;
- a file with the power curve used for the wind farm wake calculation, pv.txt.

Example of a turbine specific file t001.txt with turbine electric power per wind speed and direction bin (kW):

```
80 238 474 802 1234 1773 2379 2948 3334 3515 3577 3594 3599 3600 3600 3600 3600 3600 3600 3600 3600
80 238 474 802 1234 1773 2379 2948 3334 3515 3577 3594 3599 3600 3600 3600 3600 3600 3600 3600 3600
80 238 474 802 1234 1773 2379 2948 3334 3515 3577 3594 3599 3600 3600 3600 3600 3600 3600 3600 3600
80 238 474 802 1234 1773 2379 2948 3334 3515 3577 3594 3599 3600 3600 3600 3600 3600 3600 3600 3600
0 131 281 489 773 1129 1558 2095 2649 3178 3471 3578 3596 3600 3600 3600 3600 3600 3600 3600 3600
0 160 326 578 923 1306 1759 2369 2954 3383 3551 3588 3598 3600 3600 3600 3600 3600 3600 3600 3600
0 179 369 631 976 1414 1933 2528 3053 3402 3547 3587 3598 3600 3600 3600 3600 3600 3600 3600 3600
80 239 475 803 1236 1776 2382 2950 3335 3515 3577 3594 3599 3600 3600 3600 3600 3600 3600 3600 3600
80 238 474 802 1234 1773 2379 2948 3334 3515 3577 3594 3599 3600 3600 3600 3600 3600 3600 3600 3600
80 238 474 802 1234 1773 2379 2948 3334 3515 3577 3594 3599 3600 3600 3600 3600 3600 3600 3600 3600
80 238 474 802 1234 1773 2379 2948 3334 3515 3577 3594 3599 3600 3600 3600 3600 3600 3600 3600 3600
80 238 474 802 1234 1773 2379 2948 3334 3515 3577 3594 3599 3600 3600 3600 3600 3600 3600 3600 3600
80 238 474 802 1234 1773 2379 2948 3334 3515 3577 3594 3599 3600 3600 3600 3600 3600 3600 3600 3600
```

Example of a corresponding wind speed and wind direction probability file freq.txt (fraction of time):

```
0.003748 0.004339 0.004741 0.004951 0.004979 0.004846 0.004579 0.004212 0.003777 0.003307 0.002829 0.002367
0.001939 0.001555 0.001222 0.000941 0.000710 0.000526 0.000382 0.000272 0.000190 0.000131
0.004573 0.005146 0.005431 0.005443 0.005221 0.004816 0.004286 0.003689 0.003076 0.002489 0.001955 0.001493
0.001109 0.000801 0.000564 0.000386 0.000258 0.000168 0.000106 0.000066 0.000040 0.000023
0.004620 0.005142 0.005353 0.005281 0.004972 0.004492 0.003905 0.003276 0.002656 0.002083 0.001583 0.001167
0.000834 0.000579 0.000390 0.000255 0.000162 0.000100 0.000060 0.000035 0.000020 0.000011
0.004322 0.005034 0.005541 0.005837 0.005929 0.005837 0.005586 0.005211 0.004745 0.004224 0.003680 0.003139
0.002625 0.002152 0.001731 0.001367 0.001059 0.000806 0.000602 0.000442 0.000319 0.000226
0.006696 0.007495 0.007858 0.007816 0.007430 0.006785 0.005971 0.005076 0.004176 0.003329 0.002574 0.001932
0.001409 0.000998 0.000688 0.000461 0.000301 0.000191 0.000118 0.000071 0.000042 0.000024
0.005140 0.005768 0.006068 0.006059 0.005787 0.005311 0.004701 0.004022 0.003331 0.002676 0.002086 0.001579
0.001162 0.000832 0.000579 0.000393 0.000259 0.000167 0.000104 0.000064 0.000038 0.000022
0.007716 0.008822 0.009492 0.009735 0.009588 0.009113 0.008387 0.007492 0.006506 0.005501 0.004533 0.003643
0.002857 0.002189 0.001638 0.001198 0.000857 0.000599 0.000410 0.000274 0.000180 0.000115
0.006408 0.007586 0.008518 0.009187 0.009589 0.009734 0.009643 0.009343 0.008870 0.008261 0.007557 0.006795
0.006010 0.005231 0.004483 0.003784 0.003147 0.002579 0.002083 0.001659 0.001303 0.001010
0.004913 0.005842 0.006596 0.007160 0.007529 0.007708 0.007708 0.007547 0.007247 0.006834 0.006336 0.005780
0.005192 0.004594 0.004006 0.003444 0.002920 0.002442 0.002016 0.001642 0.001320 0.001048
0.003559 0.004225 0.004760 0.005154 0.005405 0.005515 0.005495 0.005359 0.005123 0.004808 0.004435 0.004024
0.003593 0.003159 0.002736 0.002336 0.001966 0.001631 0.001335 0.001078 0.000859 0.000676
0.003425 0.004000 0.004418 0.004673 0.004768 0.004718 0.004542 0.004264 0.003910 0.003507 0.003081 0.002652
0.002238 0.001854 0.001507 0.001203 0.000943 0.000727 0.000550 0.000410 0.000300 0.000216
0.005405 0.006050 0.006343 0.006309 0.005998 0.005477 0.004820 0.004098 0.003371 0.002687 0.002078 0.001559
0.001137 0.000806 0.000555 0.000372 0.000243 0.000154 0.000095 0.000057 0.000034 0.000019
```

Example of a turbine location file coord.txt: turbine number, latitude (m), longitude (m):

```
1 529096 5858788
2 529709 5858383
3 530323 5857978
4 530936 5857572
5 531549 5857167
6 532163 5856762
7 532776 5856356
8 533389 5855951
9 534003 5855546
10 534616 5855140
11 535229 5854735
12 535843 5854330
13 536456 5853925
14 537069 5853519
15 537682 5853114
16 538296 5852709
17 538909 5852303
18 539522 5851898
```

```
19 540136 5851493
20 540749 5851088
21 541362 5850682
22 541976 5850277
23 542589 5849872
24 529052 5858047
```

Example of a turbine power curve, pv.txt: windspeed (m/s), electric power (kW):

```
0 0
1 0
2 0
3 0
4 80
5 238
6 474
7 802
8 1234
9 1773
10 2379
11 2948
12 3334
13 3515
14 3577
15 3594
16 3599
17 3600
18 3600
19 3600
20 3600
21 3600
22 3600
23 3600
24 3600
25 3600
```


C EeFarm II questions and answers

1. *How does EeFarm II handle the case with two or more components connected to the same output bus*

In EeFarm-II a node is used to connect the output busses of two components. For a description see section 3.6. There is no feedback from a downstream component to an upstream as in an electrical network. To express it differently: each model operates as a voltage and current source. No iteration is included to ensure exact voltage and current values because the deviation in the losses caused by this omission is expected to be insignificant.

Each downstream component receives the output of the upstream component. If dividing the output is required, a splitter model should be used.

2. *What is the independent variable in EeFarm II that corresponds with the integrators in Simulink and how are the time step and tmax determined?*

EeFarm II is a steady state model, it does not include a single integrator. Simulink considers the time the independent variable. In EeFarm II a fixed step size is chosen (0.1 s) and either $t_{max} = 30$ s (if no FyndFarm or FluxFarm input is used) or a t_{max} determined by the FyndFarm or FluxFarm input. The time vector is used to read the FyndFarm or FluxFarm data or the P(V) tables. It is important to use a fixed step simulation and a corresponding t_{max} to make use of the full range of the input data. In the blocks that write the output data to workspace, a sample time equal to the fixed time step has to be chosen to maintain the correspondence between the input data (for instance FyndFarm bins) and the probability data in the preprocessor.

3. *How does EeFarm II determine the order in which to calculate the components?*

Simulink decides the calculation order of the blocks in a model. For the evaluation of each block the input voltage and current have to be known, except for the turbine blocks. Therefore, Simulink will start the evaluation at the turbine blocks and will proceed in the direction of the grid connection.

4. *How does EeFarm II calculate components connected in parallel?*

Component connected in parallel meet at the end in an AC or DC node. Each parallel string is evaluated starting at the common or non common first block of the string. At the node the voltages are averaged and the current is determined from the active and reactive power balance. Averaging the voltage introduces an error but it will be small due to the relatively small voltage deviations in the farm (a few percent in total).

5. *How does setting the turbine voltage effect the voltage at the point of grid connection of the farm?*

Since the turbine voltage is prescribed and not the grid voltage, the voltage amplitude at the point of grid connection of the farm will decrease with increasing power if the connection is mainly resistive. In reality, the voltage amplitude at the point of grid connection is more or less independent of the wind farm power and the turbine voltage amplitude will increase with increasing farm power. Since the voltage amplitude increase or decrease is relatively small (typically a few percent), the effect on the currents and the losses will also be relatively small.

6. *Why was the turbine voltage chosen to be constant instead of the voltage at the point of grid connection of the farm?*

By setting the turbine voltage the calculation is simple and straight forward. If the voltage at the point of grid connection of the farm is set, iteration is required.

7. *What are the differences between EeFarm II and commonly used load flow programs?*

Load flow programs only handle AC components and solve a matrix representation of the system. EeFarm II adopts a number of simplifications to calculate the voltages, currents and electric losses in systems with a combination of AC and DC components with sufficient accuracy. Secondly, it calculates the losses for each wind speed and wind direction bin and each turbine in the farm to have an relatively accurate estimate of the wind farm energy production and production costs.

8. *How does EeFarm II handle the wind farm losses during the periods of zero power production (no load losses)?*

EeFarm II calculates the total wind farm losses for each wind speed and wind direction bin, including the no load losses below cut-in and above cut-out wind speed. Based on the probability values from the wind speed distribution, the average annual energy production including the no load losses are calculated.

9. *How does EeFarm II handle long AC cables connecting the wind farm to shore?*

The capacitive current increases linearly with the length of an AC cable and can be a significant part of the total cable current. Although the active current over the length of the cable is more or less constant, since the cable losses are small, the capacitive current over the length of the cable decreases to zero. The point of zero capacitive current depends on the way the reactive power of the cable is consumed. If the capacitive current is consumed equally at both ends, the capacitive current will be zero at the middle. If the capacitive current is consumed only at one end, the capacitive current will be zero at the other end. Since the EeFarm II cable model is a lumped parameter model (it only contains two capacitors), long cables have to be represented in EeFarm II by a number of identical cable blocks in series. Otherwise, the cable losses would be over estimated.

D Electrical modelling aspects

D.1 Conventions

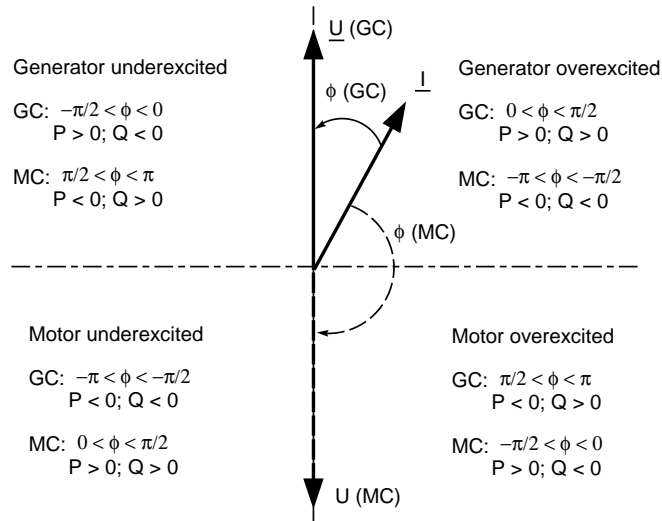


Figure 151: Voltage and current phasors in generator and motor convention systems (from [8])

Figure 151 shows the voltage and current phasors for the generator and motor convention system advised for synchronous generator description. For generator convention, the voltage phasor is in the direction of the positive y-axis (imaginary axis). For motor convention, the voltage phasor is in the direction of the negative y-axis. Together with the mode of operation (motor or generator and over or underexcited) this determines the value of the angle between the current and the voltage phasor and the sign of power and reactive power.

$$\phi = \angle(U) - \angle(I)$$

For generators, generator convention is chosen. For all other components, motor convention is chosen. Most common sign are:

	Operation mode	P	Q	
Generator	generator, underexcited	$P_{out} > 0$	$Q_{out} < 0$	requires Q
All other	motor, inductive	$P_{out} - P_{in} < 0$	$Q_{out} - Q_{in} < 0$	requires Q
All other	motor, capacitive	$P_{out} - P_{in} < 0$	$Q_{out} - Q_{in} > 0$	produces Q

$$P = \sqrt{3} \operatorname{Re}(\underline{U}_{line} \underline{I}_{phase}^*)$$

$$Q = \sqrt{3} \operatorname{Im}(\underline{U}_{line} \underline{I}_{phase}^*)$$

The voltages and currents in the grid component (cable, transformer) are complex variables. The generator models use dq-variables (Park transformation). Based on figure 151 with the voltage in the direction of the imaginary (Y-) axis, the relation with the dq-variables is:

$$\begin{aligned} u_q &= 0 \\ u_d &= |\underline{U}_{line}| \\ \underline{u} &= u_q + j * u_d \end{aligned}$$

The voltage at the generator terminals is always assumed to be in the d-direction!??

Effect of the phasor definition on the definition of Q

The phasor definition determines the equation for the reactive power, as can be demonstrated as follows (motor convention, underexcited):

$$\begin{aligned}
 \vec{u} &= j\omega L i \\
 u_q + j u_d &= j\omega L (i_q + j i_d) \\
 u_q &= -\omega L i_d \\
 u_d &= \omega L i_q \\
 u_q &= u \\
 u_d &= 0 \\
 Q &= u_d i_q - u_q i_d = \\
 &= -u \cdot -\frac{u}{\omega L} > 0 \\
 u_q &= 0 \\
 u_d &= u \\
 Q &= u_d i_q - u_q i_d = \\
 &= u \cdot \frac{u}{\omega L} > 0
 \end{aligned}$$

Alternatively:

$$\begin{aligned}
 \vec{u} &= j\omega L i \\
 u_d + j u_q &= j\omega L (i_d + j i_q) \\
 u_q &= \omega L i_d \\
 u_d &= -\omega L i_q \\
 u_q &= u \\
 u_d &= 0 \\
 Q &= u_d i_q - u_q i_d = \\
 &= -u \cdot \frac{u}{\omega L} < 0 \\
 u_q &= 0 \\
 u_d &= u \\
 Q &= u_d i_q - u_q i_d = \\
 &= u \cdot -\frac{u}{\omega L} < 0
 \end{aligned}$$

Since in motor convention, the underexcited reactive power should be positive, the equation for Q in the second case should be $Q = -u_d i_q + u_q i_d$. The phasor definition has no effect on the equation for the active power.

D.2 Reactive power of shore cable

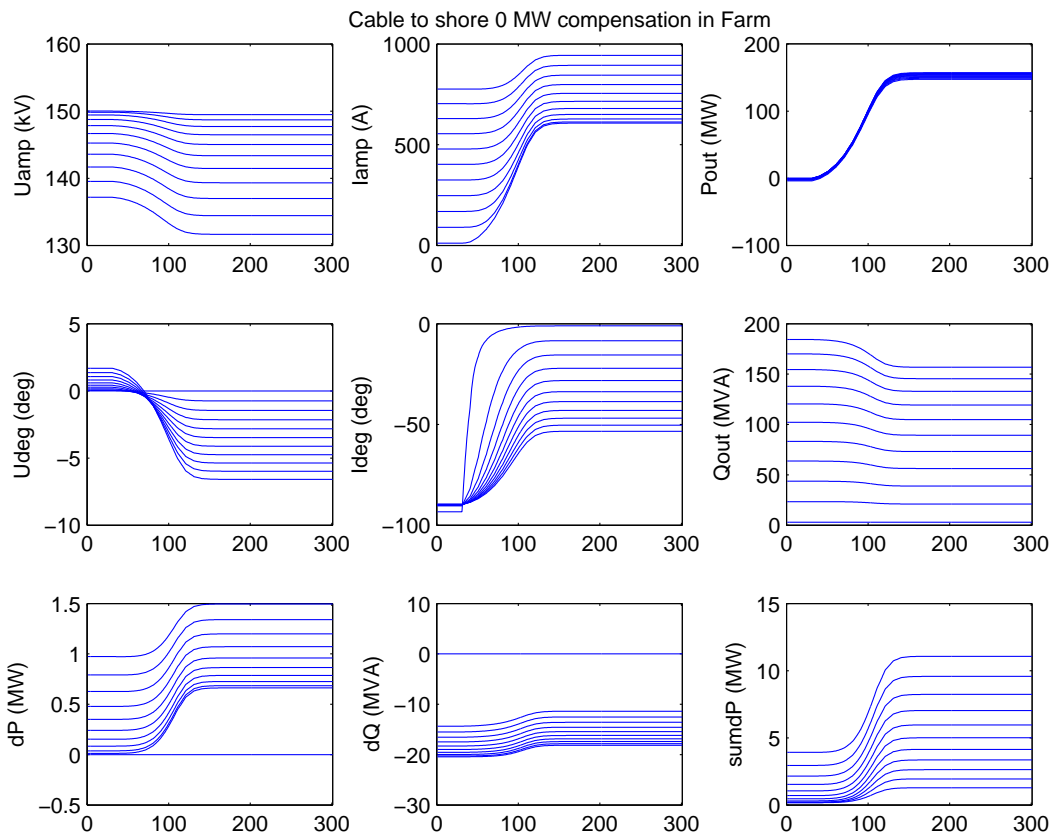


Figure 152: Cable to shore, 10 sections, zero inductive compensation in farm

Figure 152 gives the bussignals of a 150 kV cables to shore of 89 km, which is calculated as 10 sections, to distribute the resistance and capacitance over the length of the cable. Each line represents the output of a cable section. The horizontal axis is the wind speed, so equivalent to the transported power. The voltage of the wind farm is constant, so the voltage decreases in the direction of shore. The current increases in the direction of shore, since in this result all reactive current is supplied by the grid. This leads to a violation of the current limit of the cable (734A) in the sections closest to shore at maximum wind farm power. At the cable section connected to the wind farm platform, the current is zero at zero power.

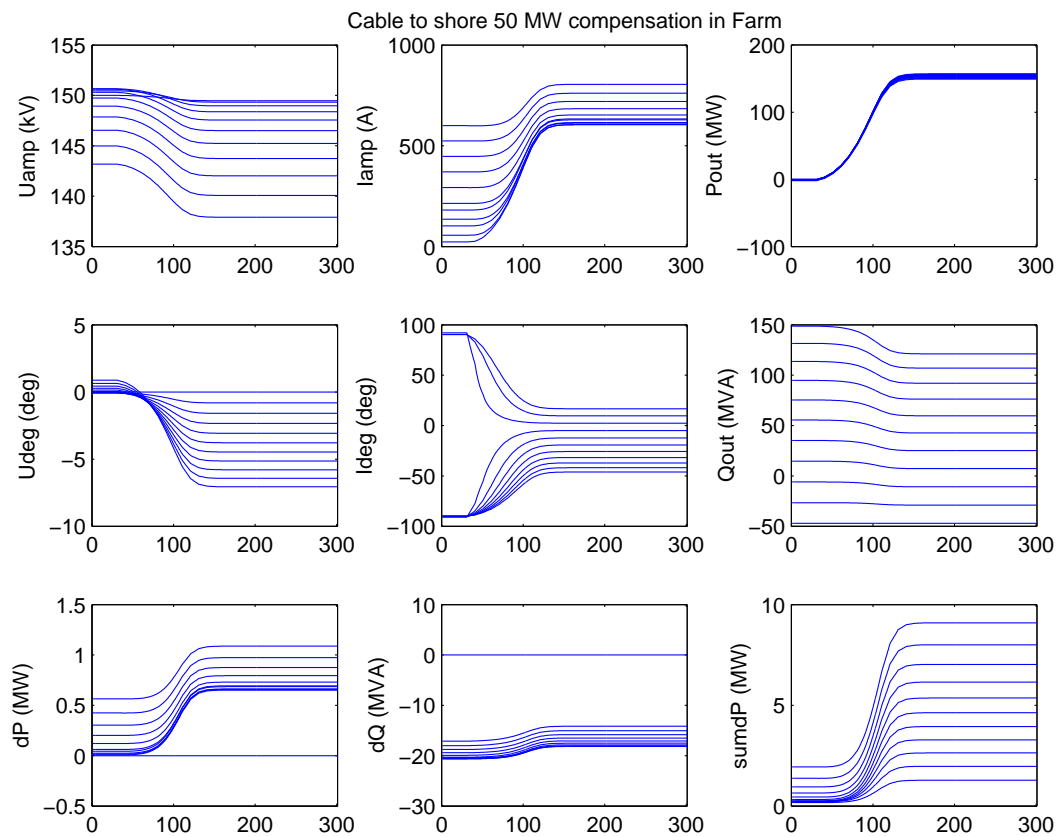


Figure 153: *Cable to shore, 10 sections, 50 MVA inductive compensation in farm*

Figure 153 gives the bussignals of the same cable to shore, with about half the reactive power (50 MVA) supplied by the wind farm. Now the current limit of the cable is not violated. This modus operandi also reduces the losses. At the half way cable section the current is zero at zero power.

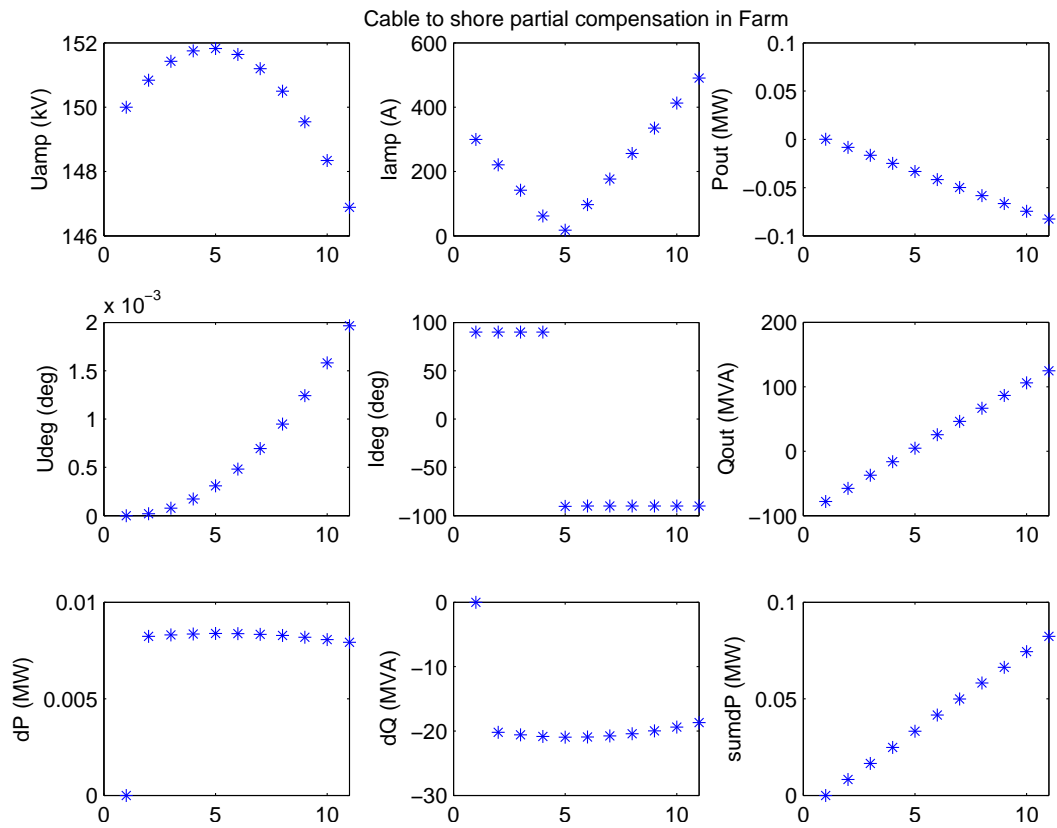


Figure 154: Cable to shore, 10 sections, partial inductive compensation in farm

Figure 154 shows the bussignals of the same cable to shore at the end of each cable section for zero power production of the wind farm and partial compensation. The horizontal axis is the cable section number, counting from farm to shore.

D.3 Effect of temperature on cable resistance

The effect of the conductor temperature on the cable resistance is represented by:

$$R_T = R_{20}(1 + \alpha_{20}(T - 20)) \quad (8)$$

with R_T the conductor resistance at temperature T and α_{20} the temperature coefficient: 0.00403 K^{-1} for aluminum and 0.00393 K^{-1} for copper [3]. Figure 155 shows the effect for a typical 32 kV and 150 kV cable.

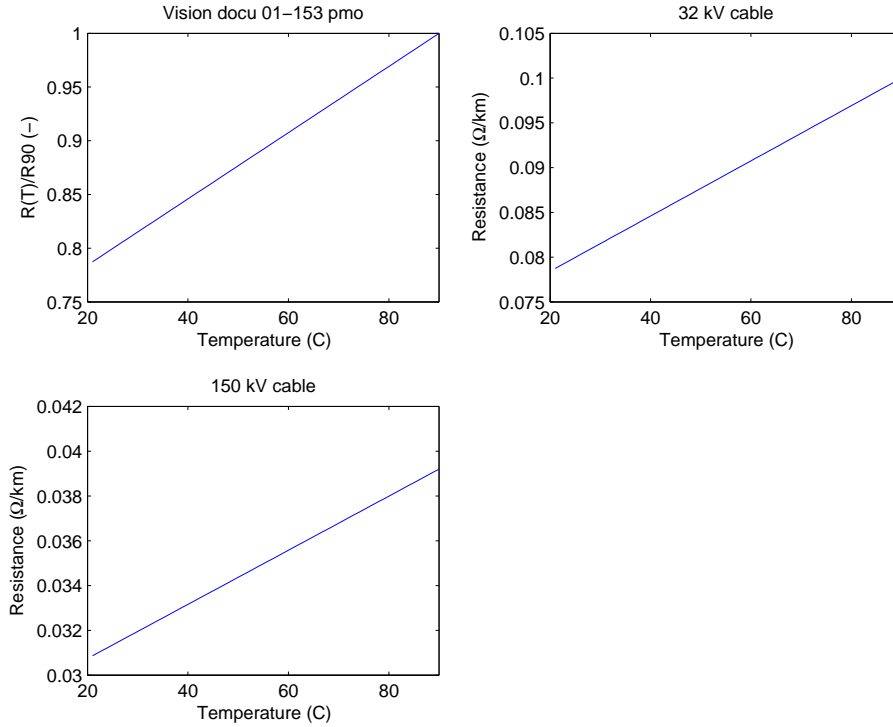


Figure 155: *Effect of cable temperature [3]*

IEC 60287-3 [6] recommends to use as an approximate cable temperature in economic optimization of power cables:

$$T_{av} = \frac{(T_{max} - T_{amb})}{3} + T_{amb} \quad (9)$$

In EeFarm II a the following approximation is implemented as an alternative. From:

$$\begin{aligned} Q &= k_Q(T - T_{amb}) \\ P_{loss} &= R_{20}(1 + \alpha_{20}(T - 20))I^2 \end{aligned}$$

the value of the heat transfer coefficient k_Q can be determined if we assume that the maximum conductor temperature is reached at maximum losses and the ambient temperature is 20° :

$$k_Q = \frac{R_{20}(1 + \alpha_{20}(T_{max} - 20))}{T_{max} - 20} I_{max}^2 \quad (10)$$

This establishes a nonlinear relation between the current and the conductor temperature. Since the current into the cable section is known, the temperature dependent resistance can be calculated directly. In EeFarm I an iterative method was used, based on a given value of the heat transfer coefficient, which was estimated.

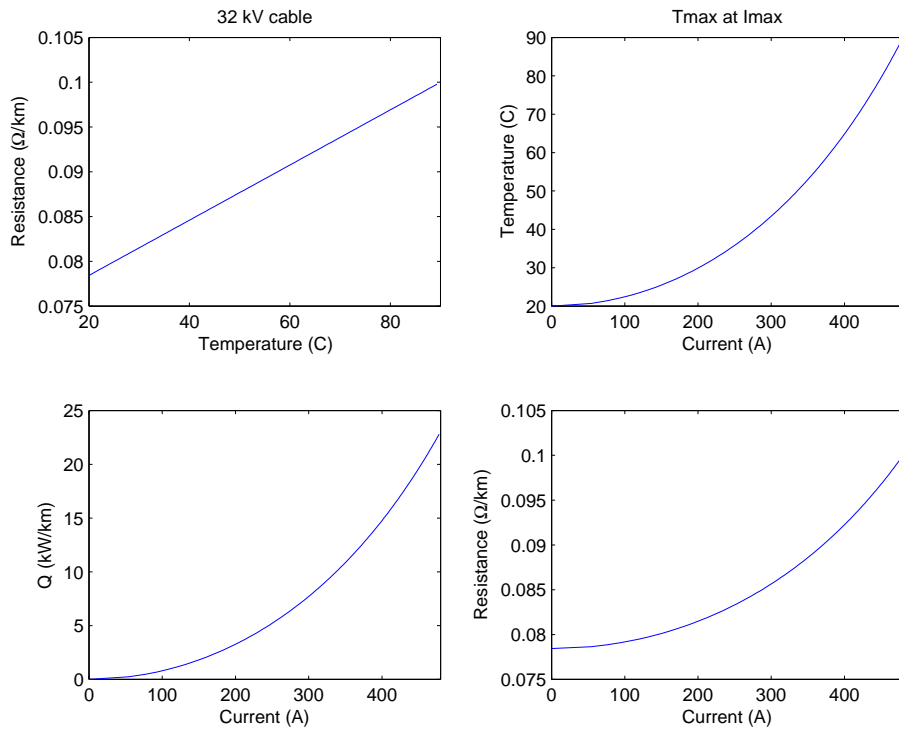


Figure 156: Cable current, heat transfer (losses), temperature and resistance

E EeFarm 1 database

E.1 Transformer data

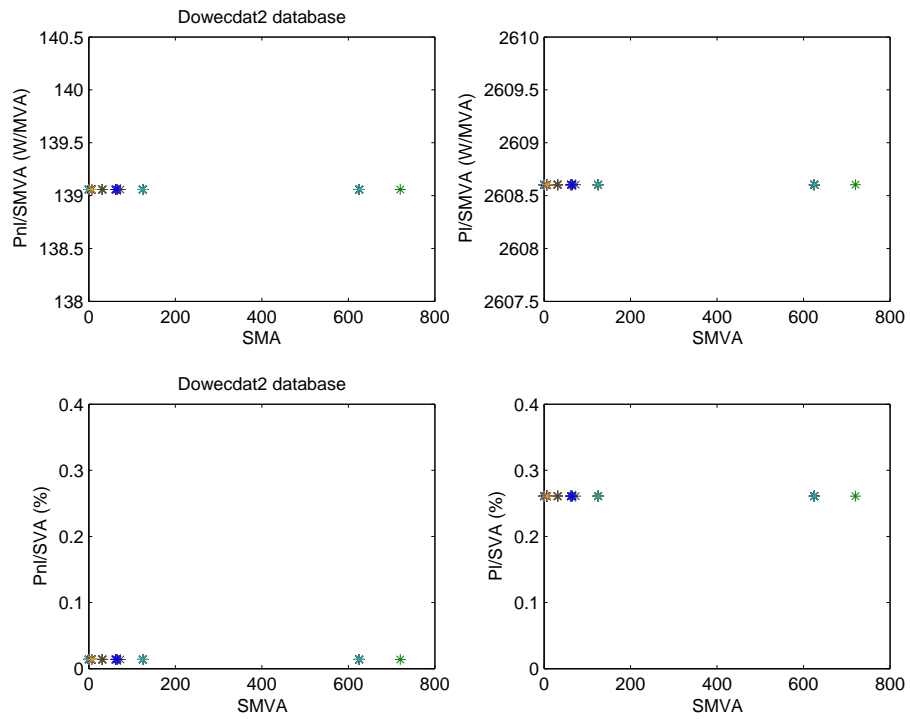


Figure 157: Normalised transformer losses in database

E.2 PWM converter data

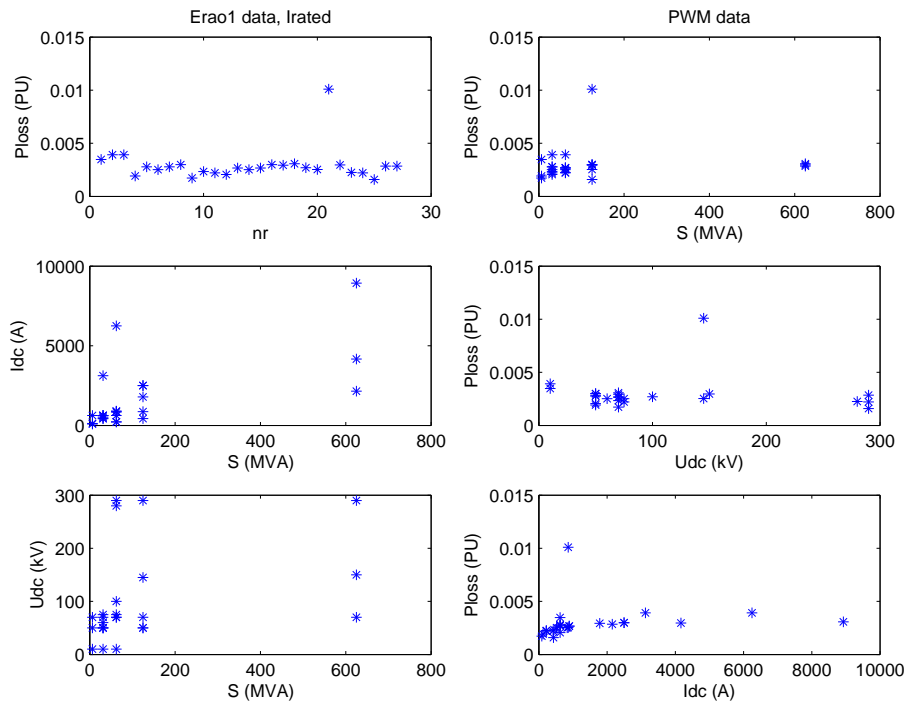


Figure 158: PWM data

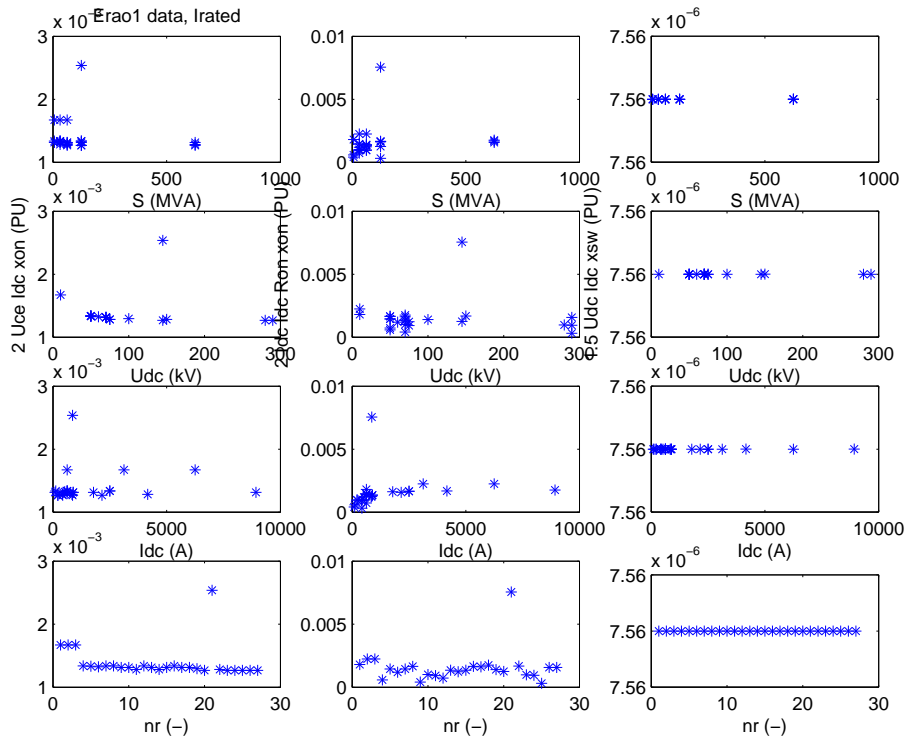


Figure 159: PWM data

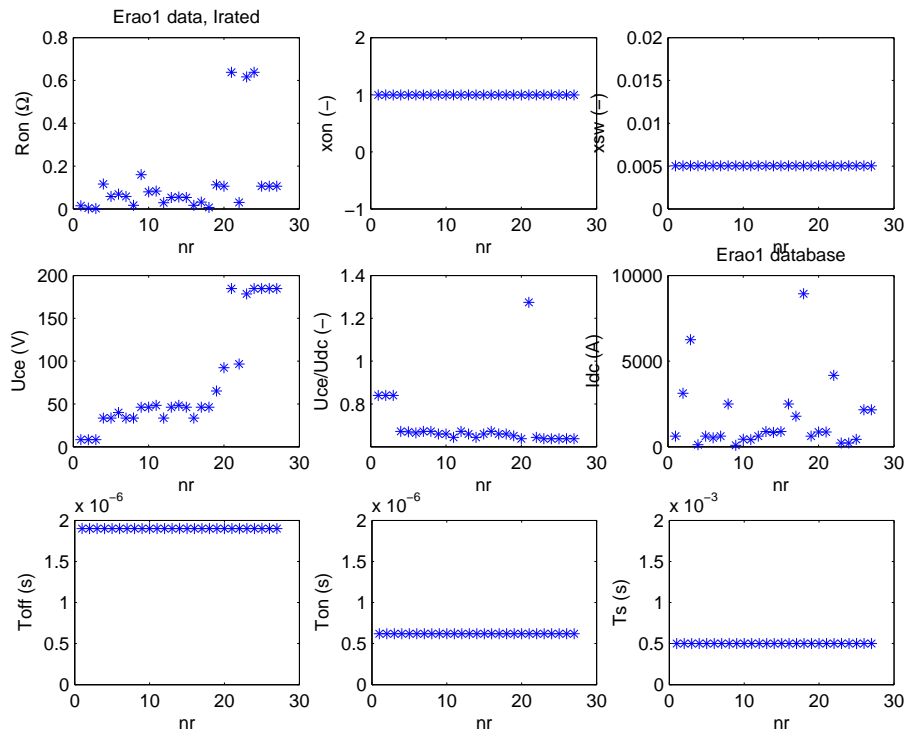


Figure 160: *PWM data*

E.3 THY converter data

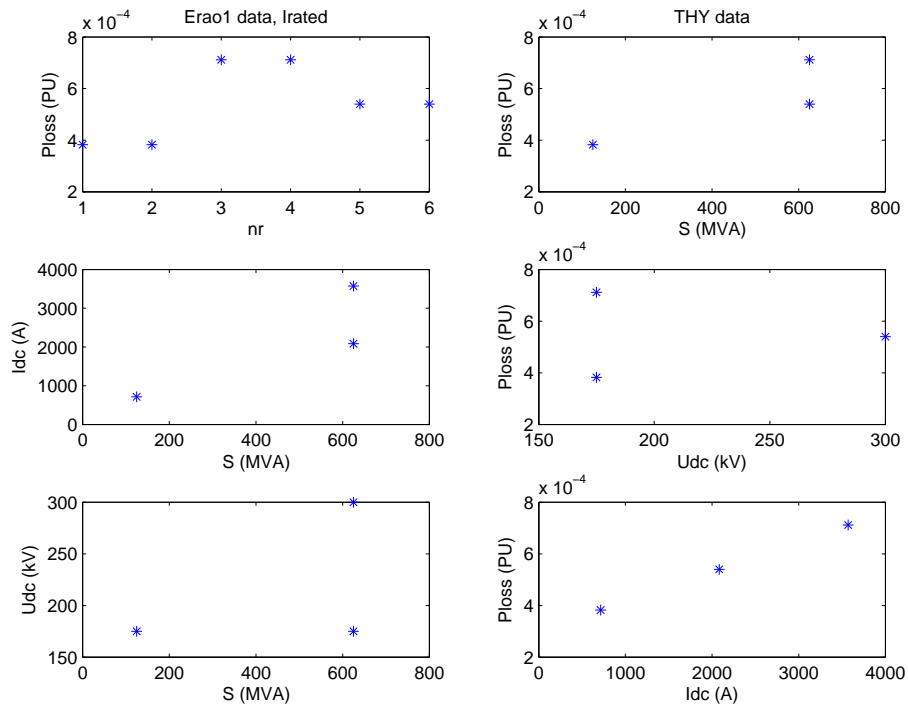


Figure 161: *THY data*

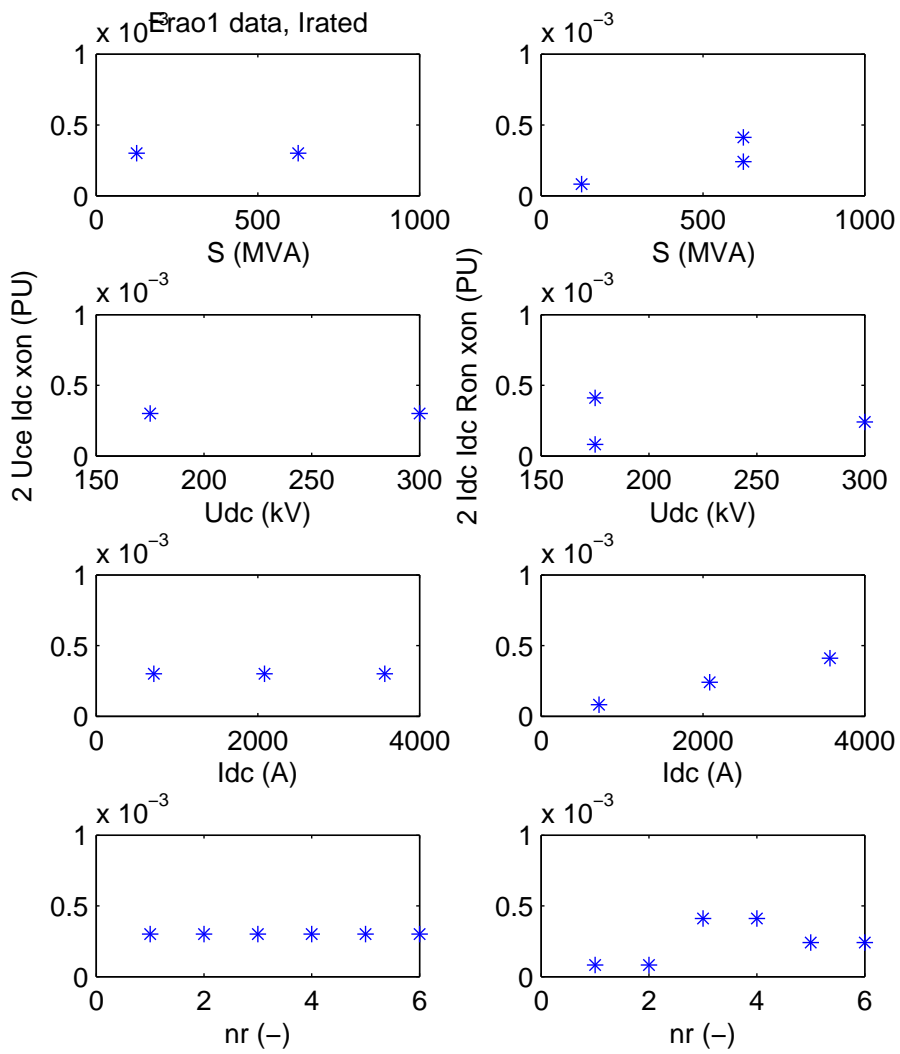


Figure 162: THY data

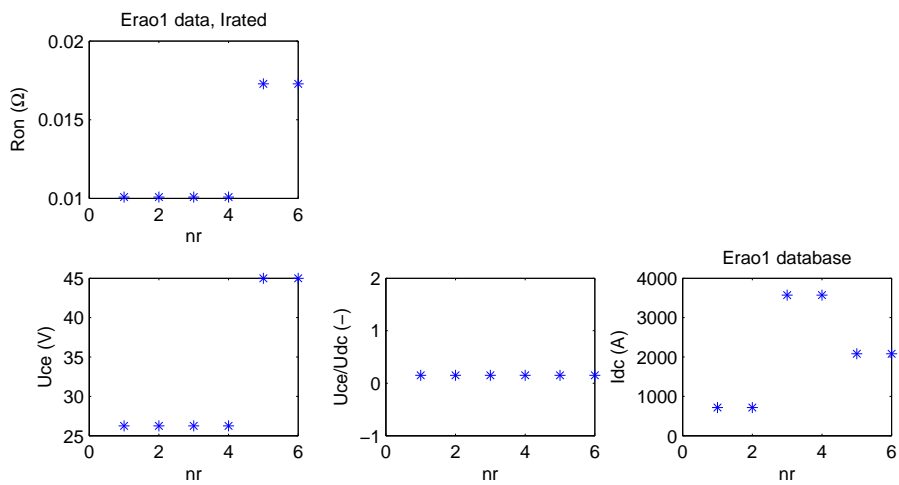


Figure 163: THY data

E.4 AC cable data

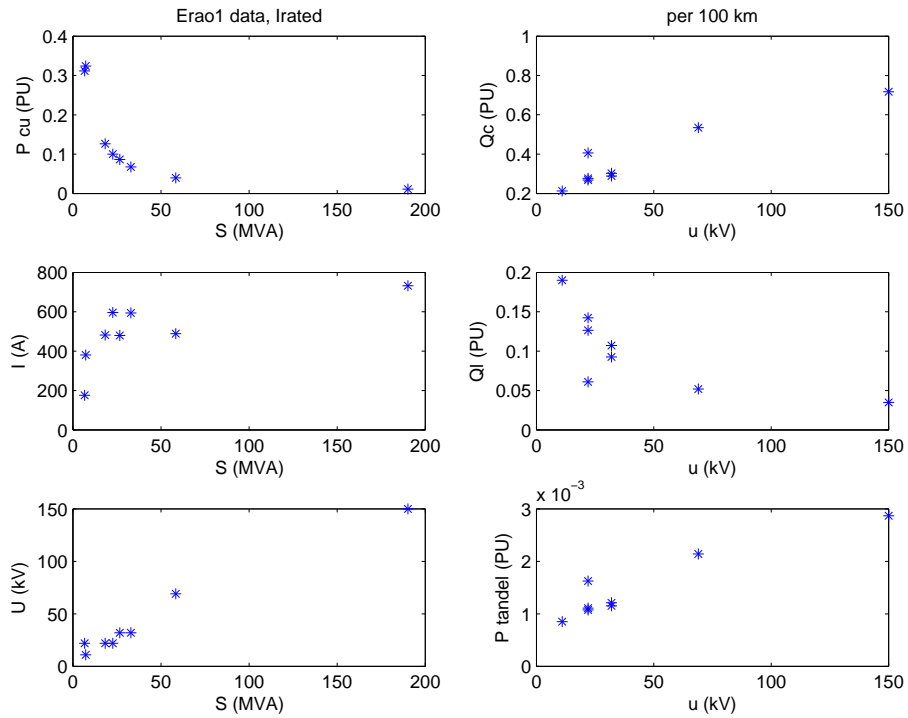


Figure 164: AC cable data

E.5 DC cable data

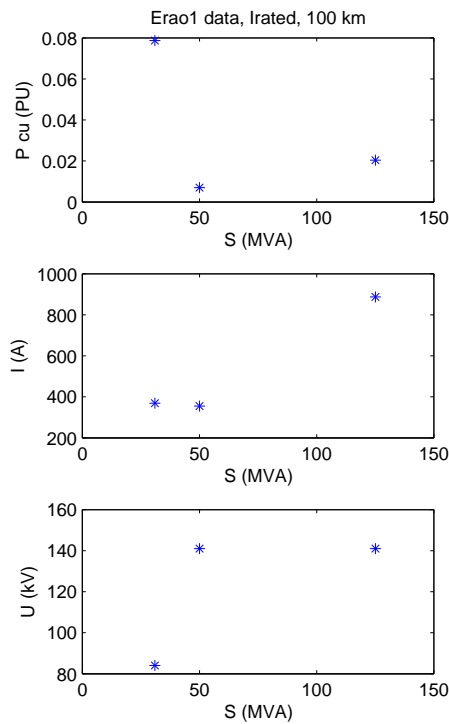


Figure 165: DC cable data

F Differences between the EeFarm and EeFarm-II program

EeFarm has been completely reprogrammed to escape the extreme user unfriendliness. The following improvements or changes have implemented:

- Simulink Component Library;
- Simulink component masks to enable multiple occurrences of the same component with different parameters;
- the component parameters are loaded into the block as a single structure;
- the calculation of the cable length in the wind farm from FluxFarm or FyndFarm turbine coordinates has been added;
- a simple connection of component model blocks by a standardised AC or DC bus signal has been used;
- the estimation of wind speed deficit by built in GCL model or Hagg approximation has been added;
- generator models for an induction machine, a DFIG, a FCIG and a FCSM have been added;
- a cable model with variable temperature but without iteration has been added;
- identical parallel cables are specified explicitly in EeFarm 2 (in EeFarm this was specified by a parameter);
- an AC and a DC node block has been added (was not a separate entity in EeFarm);
- an AC and a DC splitter block has been added (was not a separate entity in EeFarm);
- the PWM rectifier and converter models have been improved (the original TUD PWM converter model caused a problem at small or zero power factor);
- the effect of component reliability on power production has been included;

G Summary Erao 1 (EeFarm model version 1)

The ERAO project "Electrical and Control Aspects of Offshore Wind Farms" has two main objectives, which will be achieved in consecutive project phases. The aim of Phase 1 "Steady state electrical design, power performance and economic modeling" is to investigate the electrical concepts for the interconnection of offshore wind turbines and the transportation of the electric power to the high voltage grid. Phase 1 has now been completed. Technical and economic aspects have been taken into account in the evaluation of concepts based on AC as well as DC connections. Electrical designs of more than ten different electrical architectures have been made and the operational characteristics have been determined. A quasi-steady state model has been developed for the evaluation of these architectures and a case study with two wind farm sizes (100 and 500 MW) and two distances to shore (20 and 60 km) has been performed. This report describes the results.

The project started with an inventory of architectures to collect the electric power from individual wind turbines in an offshore wind farm and transmit this power to an on-shore high-voltage grid node. The inventory included constant, individual variable speed, cluster variable speed and park variable speed options using AC as well as mixed AC-DC-AC modes. Steady state electrical models have been developed for all electrical components in the architectures to calculate load flow and electrical losses. Based on these models, the *EEFARM* computer program (Electrical and Economical wind FARM Model) has been made, which includes a database of electrical and economic parameters of the components. The *EEFARM* program has been used in a case study to compare 13 electrical architectures. The electrical parameters voltage, current, active and reactive power have been calculated in all system nodes. Based on the aerodynamic performance of the chosen wind turbine, the electrical losses have been calculated over the entire range of operation of the wind farm. From budget prices obtained from manufacturers, the investment costs of the electrical systems and the contribution to the costs per kWh have been determined.

In the constant speed concepts C1 and C2 the wind turbines in the farm are connected by AC and the cable to shore is AC as well. These systems have the smallest number of main components, only transformers and cables. The case study has shown that these systems, C1 (string layout) and C2 (star layout), have the lowest contribution of the electrical system to the price per kWh for farm sizes 100 and 500 MW and 20 and 60 km distance to shore. Electrical system prices of 19.7 and 24.9 MEuro (100 MW, 20 km), 36.9 and 42.1 MEuro (100 MW, 60 km), 91.7 and 109.5 MEuro (500 MW, 20 km) and 132.9, 150.7 MEuro (500 MW, 60 km) have been determined. For the 100 and 500 MW farm at 20 km and the 500 MW farm at 60 km, the C1 system also has the lowest electrical losses.

In those cases where a DC connection to shore is preferred (longer distance to shore or avoidance of grid stability problems), the park variable speed configuration PV1, which includes a HVDC Light connection to shore, appears to be the best alternative under the assumptions of the case study. For the investigated distances and park sizes this currently increases the investment costs and contribution of the electrical system to the price per kWh by a factor 2 or more.

The *EEFARM* computer program represents a flexible and fast tool to evaluate the electrical infrastructure of offshore windfarms. The program has been validated by the Vakgoep Energievoorziening of TU Delft against the results from a PSS/E model. Kema prepared a summary of the grid integration aspects to be taken into account for the connection of wind farms to the high voltage grid.

In the second phase of the ERAO project the electrical interaction in an offshore wind farm and the control of the most promising concepts will be investigated. For this purpose, a dynamic model of an offshore wind farm will be developed, with emphasis on the modeling of the electrical system. In a case study the control of a farm will be designed. Park control is expected to be an important aspect of large multimegawatt offshore wind farms in order to minimise negative effects on the high voltage grid and assist in frequency and reactive power management.